Antibodies directed against AMPA and $GABA_B$ receptors in neurological disorders and identification of novel antigen targets

Anjan K Nibber

A thesis submitted for the Degree of Philosophy
University of Oxford

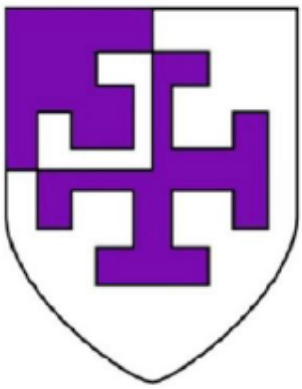

St. Cross College

University of Oxford

Trinity Term 2014

To Pramjit and Trajinder

Antibodies directed against AMPA and $GABA_B$ receptors in neurological disorders and identification of novel antigen targets

Anjan K Nibber, St. Cross College, University of Oxford

A thesis submitted for the degree of Doctor of Philosophy

Trinity Term 2014

Abstract

Antibodies directed against AMPAR and $GABA_BR$ subunits have been implicated in forms of limbic encephalitis (LE), a disease characterised by memory loss and seizures. Patients with LE show clinical improvement with immunomodulatory treatment, suggesting that the associated antibodies are pathogenic. To explore further the AMPAR and $GABA_BR$ antibodies, an in house cell based assay (CBA) was established for screening and potential pathogenicity was explored using a series of *in vitro* experiments.

Human embryonic kidney (HEK) cells transfected with AMPAR and $GABA_BR$ subunits and primary neuronal cultures were used to detect antibodies in patient sera and CSF. In total, 15/1361 (1.1%) AMPAR antibody positive samples and 24/1438 (1.7%) $GABA_BR$ antibody positive samples were identified.

The predominant antibody subclass for AMPAR and $GABA_BR$ antibodies was shown to be IgG1. Interestingly, on transfected cells, only AMPAR antibodies showed complement deposition, and therefore had the potential to activate the classical pathway of the complement cascade. Application of IgG purified from AMPAR antibody positive patients, but not $GABA_BR$ antibody positive patients caused a down regulation of the receptor from the cell surface of transfected HEK cells and primary hippocampal cultures. Electrophysiological analysis showed changes in Up state duration and spike rate in the entorhinal cortex following application of purified $GABA_BR$ antibody IgG on brain slices. These findings suggest that $GABA_BR$ antibodies are having a direct short-term effect on $GABA_BRs$, and by extension cortical networks.

Finally, we attempted to study whether or not viral infection could be a trigger for antibody production to known and novel antigen targets in a cohort of Japanese encephalitis viral (JEV) samples. A JEV cohort of 44 children was screened for antibodies to neuronal surface proteins by CBA. Twenty-seven percent of patients had antibodies to known neuronal surface antigens, with NMDAR and CASPR2 as the most common antigen targets. Interestingly, screening the cohort on primary neuronal cultures revealed that 65.9% of children with JEV have neuronal surface antibodies. The identification of the novel antigen target was attempted using immunoprecipitation and mass spectrometry techniques. In total, 4 neuronal surface proteins were identified that could be potential targets in JEV patients.

In summary, antibodies directed against previously described antigenic targets were explored further for pathogenic potential, and a cohort of patients with a viral infection with potential novel antigen targets was investigated.

ACKNOWLEDGEMENTS

First and foremost, I would like to thank my supervisor Dr. Bethan Lang, for the careful supervision, constant direction and support during the course of my DPhil project. Your enthusiasm for science has been truly inspiring. Thank you for recognizing my potential, even when I often could not see it myself; it was a pleasure being your student.

Dr. Philippa Pettingill, I have learned a great deal from your meticulous scientific approach, clear thinking, and analytical perception. Thank you for being there during the long days, early mornings, late nights and weekends. Words cannot express how much I appreciate you believing in me, always encouraging me and for always making sure there was milk in the fridge for tea. It was nice to have a friend who could relate to the ups and downs that often characterise one's doctorate in science.

It has been a pleasure working in the Neurosciences Group, and for that, I would like to thank Professor Angela Vincent for her expert guidance and for welcoming me into her lab. A heartfelt thanks to Dr. Patrick Waters for his insightful comments and expertise with the molecular biology components of the project. Thank you for taking me under your wing when I was just a starry-eyed young researcher. And additionally, I would like to thank Dr. Sarosh Irani and Dr. Holger Kramer, for their assistance with the clinical and mass spectrometry components of the JEV project.

Many others generously gave their support, reviewed papers, and offered advice including: Dr. Leslie Jacobson, Mrs. Linda Clover, Dr. Mark Woodhall, Dr. Ester Coutinho and Dr. Tanja Brenner. I would also like to thank Dr. Edward Mann, Dr. Simon Tuohy and Mr. Julian Bartram in DPAG who welcomed me into their lab to learn electrophysiology.

Finally, this thesis would not have been completed if not for the support and love of my family. Pranvit, Adesh and Rasna, thank you for always making me laugh and humouring me when I was missing home, when I called during dinnertime, or if I wanted to put in an extensive list of must-dos for my trips home. Mumma and Daddyji, thank you for staying by my side from beginning to end, providing guidance and support and reminding me at key moments why I was doing this.

ABBREVIATIONS

Abs	Antibodies
AChR	Acetylcholine receptor
aCSF	Artificial spinocerebral fluid
AED	Anti epileptic drugs
AMPAR	Amino-3-hydroxy-5-methyl-4-isoxazolepproprionic acid receptor
AQP4	Aquaporin-4
ATD	Amino terminal domain
BBB	Blood brain barrier
BSA	Bovine serum albumin
CASPR2	Contactin-associated protein like 2
CBA	Cell based assay
CHO cells	Chinese hamster ovary cells
CNS	Central nervous system
CSF	Cerebrospinal fluid
DAF	Decay accelerating factor
DAPI	4',6'-diamidino-2-phenylindole
DC	Disease control
DG	Dentate gyrus
Div	Days *in vitro*
DMEM	Dulbecco's Modified Eagle Medium
EAE	Experimental autoimmune encephalomyelitis
EAMG	Experimental autoimmune myasthenia gravis
EC	Entorhinal cortex
EGFP	Enhanced green fluorescent protein
ELISA	Enzyme linked immunosorbent assay
EMG	Electromyography
EPC	Epilepsia partialis continua
EPT	End-point titration
Fab	Fragment antibody region
FBDS	Faciobrachial dystonic seizures
FCS	Fetal calf serum
FIPA	Fluorescent immunoprecipitation assay
GABAAR	Gamma-aminobutryric acid receptor A
GABABR	Gamma-aminobutryric acid receptor B
GCL	Granular cell layer
GFP	Green fluorescent protein
GlyR	Glycine receptor
HBSS	Hank's balanced salt solution
HC	Healthy control
HEK cells	Human embryonic kidney cells

HRP	Horse-radish peroxidase
HSE	Herpres-simplex encephalitis
HSV	Herpes-simplex virus
ICV	Intracerebroventricular injection
IgG	Immunoglobulin G
iGluR	ionotrophic glutamate receptor
IHC	Immunohistochemistry
JEV	Japanese encephalitis virus
LE	Limbic encephalitis
LEMS	Lamber Eaton Myasthenic Syndrome
LGI1	Leucine glioma inactivated protein
LTP	Long term potentiaton
LV	Lateral ventricle
MAC	Membrane attack complex
MAP-2	Microtuble-associated protein-2
Mcx	Mouse cortex extract
MEM	Minimum Essential Medium
MHC	Major histocompatibility complex
MG	Myasthenia gravis
MIRL	Membrane inhibitor of reactive lysis
mGluR	metabotrophic glutamate receptor
ML	Molecular layer
mRS	Modified Rankin Score
MuSK	Muscle specific kinase
MWt	Molecular weight
NB^+ media	Neurobasal media
NGS	Normal goat serum
NMDAR	N-methyl-d-asparate receptor
NMJ	Neuromuscular junction
NMT	Neuromyotonia
NO	Nitric Oxide
OMS	Opsoclonus myoclonus syndrome
PBS-T	Phosphate buffer containing tween-20
PCD	Paraneoplastic cerebellar degeneration
PCR	Polymerase chain reaction
PEI	Polyethylimine
PERM	Progressive encephalomyelitis with rigidity and myoclonus
PEX	Plasma exchange
PIC	Protease inhibitor cocktail
PLL	Poly-l-lysine
PNH	Peripheral nerve hyperexcitability
PSA	Penicillin/streptomycin/amphotericin
PSD	Post synaptic density

PTX	Phosphate buffer containing triton-X
RIA	Radio-immuno assay
SCLC	Small cell lung carcinoma
SEM	Standard error of the mean
SLE	Systemic lupus erythematosus
SPS	Stiff person's syndrome
TFR	Transferrin receptor
UDS	Up/Down states
VGCC	Voltage gated calcium channel
VGKC	Voltage gated potassium channel
WBC	White blood cell

TABLE OF CONTENTS

CHAPTER 1: INTRODUCTION.....1

1.1: Introduction to the immune system and antibodies 1
1.1.1: The immune system 1
1.1.2: Antibodies 1
1.1.3: Structure of the IgG molecule and properties 2

1.2: Antibody-mediated autoimmune disorders 5
1.2.1: Introduction 5
1.2.2: Koch's postulates 5

1.3: Autoimmune disorders of the PNS 7
1.3.1: Myasthenia Gravis 7
1.3.2: Potential pathogenic mechanisms of AChR antibodies 10
1.3.3: Animal models of MG 14
1.3.4: Lambert Eaton myasthenic syndrome (LEMS) 15

1.4: Autoimmune diseases of the CNS and intracellular neuronal targets 16
1.4.1: Introduction 16
1.4.2: Intracellular neuronal targets 17

1.5: Autoimmune disorders of the CNS and extracellular neuronal targets 19
1.5.1: Introduction 19
1.5.2: VGKC complex antibodies 19
1.5.3: NMDAR antibodies 22
1.5.4: Glycine receptor (GlyR) antibodies 24
1.5.5: Dipeptidyl-peptidase-like protein -6 (DPPX) antibodies 24
1.5.6: Metabotropic glutamate receptor antibodies (mGluR) 25
1.5.7: $GABA_AR$ antibodies 26

1.6 AMPAR and their role in autoimmune disorders 27
1.6.1: AMPAR structure, interacting proteins and expression 27
1.6.2: AMPAR function 30
1.6.3: AMPAR subunit: knockout models 30
1.6.4: Antibodies in Rasmussen's encephalits 31
1.6.5: Role of antibodies directed against AMPAR in neurological disorders 36

1.7 $GABA_BR$ and their role in autoimmune CNS disorders 38
1.7.1: $GABA_BR$ structure and expression 38
1.7.2: $GABA_BR$: Function and knockout models 40
1.7.3: Role of antibodies directed against $GABA_BR$ in neurological disorders 42

1.8: Section 1 objectives 44

CHAPTER 2: METHODS 46

2.1: Plasmid constructs and commercial antibodies 46
2.1.1: Plasmid constructs 46

2.1.2: Commercial antibodies 46
2.1.3: Transformation of E. Coli competent cells 46
2.1.4: DNA Sequencing 47

2.2: Tissue Culture 47
2.2.1: HEK cells 47
2.2.2: Transfection of HEK cells 48

2.3: Immunofluorescence on transfected HEK cells 49
2.3.1: Cell based assay (CBA) 49
2.3.2: Subclasses 52
2.3.3: Complement fixation 52
2.3.4: Preadsorption experiments 52
2.3.5: Euroimmun slides 53

2.4:VGKC-complex radioimmunoprecipitation assay (RIA) 53

2.5: Cell surface protein isolation 54

2.6: Gel electrophoresis and western blotting 55
2.6.1: Sample extraction 55
2.6.2: Sample preparation and western blotting 55

2.7: IgG Purification 56

2.8: Primary cultures 56
2.8.1: Dissections 56
2.8.2: Staining primary cultures 57

2.9: Internalisation studies 57
2.9.1: Internalisation using CBA 58
2.9.2: Internalisation using primary neuronal cultures 58

2.10: Immunohistochemistry: 59
2.10.1: Section preparation: 59
2.10.2: Staining 59

2.11: Electrophysiology 59
2.11.1: Preparation of brain slices 59
2.11.2: Cell recordings 60
2.11.3: Data Acquisition 60

2.12: Immunoprecipitation for mass spectroscopy 61

2.13: Mass Spectrometry (MS) 61
2.13.1 In-gel trypsin digestion 61
2.13.2: LC-MS/MS analysis 62
2.13.3 Data processing and database searching 63

2.14: Statistical analysis 63

SECTION 1: ANTIBODIES DIRECTED AGAINST AMPAR AND $GABA_BR$ IN NEUROLOGICAL DISEASES 64

CHAPTER 3: DETECTION OF ANTIBODIES DIRECTED AGAINST AMPA AND $GABA_B$ RECEPTORS 64

PART A: DEVELOPMENT OF AMPAR AND $GABA_BR$ CBAS 65

3.1: Specificity of commercial antibodies 65
3.1.1: Specificity of AMPAR commercial antibodies 65
3.1.2: Specificity of $GABA_BR$ commercial antibodies 65

3.2: Cell surface expression of AMPAR and $GABA_BR$ subunits 68
3.2.1: Cell surface expression of AMPAR subunits 68
3.2.2: Cell surface expression of $GABA_BR$ subunits 69

3.3: Optimization of cDNA amount 72

PART B: SCREENING OF RE SAMPLES BY CBA 74

3.4: Rasmussen encephalitis, healthy control and disease control cohorts 74
3.4.1: Rasmussen encephalitis (RE) cohort 74
3.4.2: Healthy control and disease cohorts 75

3.5: RE CBA Results 75

PART C: SCREENING OF DIAGNOSTIC SAMPLES ON AMPAR CBA 79

3.6: Screening of diagnostic samples on AMPAR CBA 79
3.6.1: Presence of antibodies to GluA2 and GluA1+2 79
3.6.2: GluA2 antibodies and clinical correlation 85
3.6.3: Clinical features of AMPAR antibody positive patients 87

PART D: SCREENING OF DIAGNOSTIC SAMPLES ON $GABA_BR$ CBA 90

3.7: Screening of diagnostic samples on GABABR CBA 90
3.7.1: Screening of diagnostic samples 90
3.7.2: Clinical features of $GABA_BR$ antibody positive patients 95
3.7.3: Screening of a SCLC cohort 98

PART E: SCREENING OF ADDITIONAL COHORTS AND COMPARISON OF IN HOUSE DIAGNOSTIC CBA AND COMMERCIALLY AVAILABLE SLIDES 101

3.8.1: Additional cohorts screened on the assays 101

3.8.2: In house versus commercial assays 102

3.9 Summary and Discussion 104
3.9.1: Establishment of CBAs 104

3.9.2: Antibodies in Rasmussen Encephalitis 105
3.9.3: Antibody AMPAR and $GABA_BR$ subunit reactivity 107
3.9.4: Clinical features of AMPAR and $GABA_BR$ antibody positive patients 108
3.9.5: CSF antibody levels and clinical correlation 112

CHAPTER 4: CHARACTERISATION OF THE POTENTIAL PATHOGENIC ROLE OF ANTI-AMPAR AND $GABA_BR$ ANTIBODIES *IN VITRO* 114

4.1: Detection of antibody binding using rat brain sections 115
4.1.1: Binding of AMPAR antibodies to rat brain sections 115
4.1.2: Binding of $GABA_BR$ antibodies to rat brain sections 118

4.2: Detection of antibody binding using rat primary neuronal cultures 120
4.2.1: Reactivity of RE sera/CSF to primary neuronal cultures 120
4.2.2: Reactivity of AMPAR antibody positive patients to primary cultures 123
4.2.3: Reactivity of $GABA_BR$ antibody positive patients to primary neuronal cultures 128

4.4: AMPAR and $GABA_BR$ antibodies and complement activation 132

4.5: Internalisation of AMPAR and $GABA_BR$ 135
4.5.1: Internalisation of AMPAR using transfected HEK cells 135
4.5.2: Internalisation of $GABA_BR$ by patient sera using transfected HEK cells 141
4.5.3: Internalisation of AMPAR and $GABA_BR$ in primary neuronal cultures 145

4.6: Measuring surface expressed protein levels via biotinylation and western blot 147

4.7: Summary and Discussion 150
4.7.1: Reactivity to neuronal cultures and brain sections 150
4.7.2: AMPAR and $GABA_BR$ antibody subclasses and complement activation 153
4.7.3: Investigation internalisation of the receptor from the surface 155
4.7.4: Limitation and summary 159

CHAPTER 5: DIRECT MODULATION OF $GABA_BR$ ANTIBODIES ON UP AND DOWN STATES (UDS) OF THE ENTORHINAL CORTEX *IN VITRO*.....161

5.1 Clinical details and reactivity to CBA and primary cultures 162
5.1.1: Patient clinical details 162
5.1.2: Reactivity to transfected HEK cells and primary cultures 162

5.2: Presence of Up states in slices containing the EC 165

5.3: Effects of HC IgG on Up state duration and spike rate 168
5.3.1: Effect of IgG on Up state duration 168
5.3.2: Effect of IgG on spike rate 169

5.4: Effects of preadsorbed IgG on Up states 172

5.5: $GABA_{B2}R$ antibodies and $GABA_{B1}R$ agonist binding 175

5.6: $GABA_{B2}R$ antibodies and $GABA_{B1}R$ antagonist binding 177

5.7: Summary and Discussion 180
5.7.1: $GABA_BR$ antibodies are having a hypoexcitable effect 180
5.7.2 Antibodies and direct modulation of receptors 183
5.7.3 Limitations and future directions 184

SECTION 2: IDENTIFICATION OF NOVEL ANTIGENS IN JAPANESE ENCEPHALITIS VIRUS (JEV) SAMPLES.....186

CHAPTER 6: SCREENING OF JAPANESE VIRAL ENCEPHALITIS (JEV) COHORT AND IDENTIFICATION OF NOVEL ANTIGEN TARGETS.....186

6.1: Introduction 186
6.1.1 Autoimmune and infectious encephalitis 186
6.1.2: HSV infection and NMDAR antibodies 188
6.1.3: Japanese Encephalitis Virus (JEV) 190
6.1.4: Clinical Manifestations 191
6.1.5: Pathogenesis 191
6.1.6: JEV as an antibody mediated disease 192
6.1.7: Objectives 193

6.2: Methods 194

6.3: Results 194
6.3.1: Screening of JEV samples on CBAs 194
6.3.2: Testing on available CBAs 195
6.3.3: Clinical details of the JEV cohort 208
6.3.4: Antigen discovery using a positive control model system 212
6.3.5: Novel antigen targets in JEV samples 222
6.3.6: Potential antigen targets 227

6.4 Summary and Discussion 232
6.4.1 Viral encephalitis and autoimmune mediated encephalitis 232
6.4.2: Antibodies in JEV 232
6.4.3: Presence of novel targets in JEV sera 233
6.4.4: Preliminary investigations identifying a novel target 234
6.4.5: Limitation and future experiments 235
6.4.6: Conclusions 237

CHAPTER 7: GENERAL DISCUSSION 238

7.1: Introduction 238

7.2: Section 1 general discussion 238

7.3 Section 2 general discussion 241

7.4: Global questions and conclusion 243

REFERENCES: 245

APPENDICES: 260

LIST OF FIGURES

Figure 1.1: Structure of an IgG molecule....4
Figure 1.2: Pathogenic mechanisms of AChR antibodies....9
Figure 1.3: Summary of the classical pathway of complement activation....13
Figure 1.4: Crystal structure of homotetrameric GluA2....29
Figure 1.5: Structure of $GABA_BR$....40
Figure 2.1: Scoring system used for the in house diagnostic AMPAR CBA....50
Figure 2.2: Scoring system used for the in house diagnostic $GABA_BR$ CBA....51
Figure 3.1: Commercial antibodies showed specificity for the AMPAR subunit epitope to which the antibodies were raised against....66
Figure 3.2 Anti-$GABA_{B2}R$, but not anti-$GABA_{B1}R$ commercial antibodies recognised the specific epitope it was raised against....67
Figure 3.4: Western blots of cell surface $GABA_BR$ protein fractions isolated using EZ-EZ-Link® Sulfo-NHS-SS-Biotin....71
Figure 3.5: Optimal DNA amount for AMPAR (GluA1, GluA2 and GluA1+2) CBA....73
Figure 3.7: RE patients antibodies target a conformational epitope....78
Figure 3.8: Reactivity of AMPAR antibody positive patients to CBA....81
Figure 3.9: Comparative CBA scores of GluA1+ and GluA2 antibody positive sera....82
Figure 3.10: A comparison of end-point titrations between GluA1+2 antibody positive and GluA2 antibody positive patients....84
Figure 3.12: A comparison of GluA2 antibody levels in paired sera (blue) and CSF (red) taken from a patient with suspected LE with time....86
Figure 3.13: $GABA_BR$ antibody positive sera and CSF showed strong reactivity to the surface of $GABA_{B1+2}R$ transfected cells....91
Figure 3.15: A comparison of end-point titrations between $GABA_{B2}R$ antibody positive and $GABA_{B1+2}R$ antibody positive patients....94
Figure 3.16: A summary of the CBA scores of the $GABA_BR$ antibody positives according to the cohort they were identified from....100
Figure 3.17: Binding of $GABA_BR$ antibody positive patient (upper panel) and HC sera was (bottom panel) compared on the in house CBA and commercial Euroimmun slides....103
Figure 4.1: Immunolabeling of GluA2 antibody positive CSF to rat brain sections....117
Figure 4.2: Immunolabeling of $GABA_BR$ antibody positive CSF to rat brain sections....119
Figure 4.3: RE sera shows reactivity to the surface of live hippocampal neurons....122
Figure 4.4: AMPAR antibody sera and CSF show intense reactivity to primary hippocampal cultures in comparison to HC sera....124
Figure 4.5: Antibodies directed against the GluA1+2 subunits are specific to a conformationally expressed epitope....125
Figure 4.6: GluA2 antibodies are specific for the GluA2 subunit and show an abolition of binding following preadsorption with GluA2 transfected HEK cells....127
Figure 4.7: 14/24, $GABA_BR$ antibody positive patients bind to the surface of hippocampal neurons *in vitro*....129
Figure 4.8: AMPAR and $GABA_BR$ antibodies are predominantly IgG1....131
Figure 4.9: AMPAR-antibodies have the potential to activate complement....134
Figure 4.10: Reduction in AMPAR antibody staining to AMPAR transfected HEK cells....137
Figure 4.11: Comparison of AMPAR (GluA2) antibody IgG surface binding of two patients after incubation in GluA2 transfected HEK cells....138

Figure 4.12: Assessment of GluA2 levels in transfected HEK cells after treatment with HC and GluA2 IgG: Reduction of surface expression of GluA2 140
Figure 4.13: $GABA_BR$ antibodies do not cause receptor internalisation; No change in $GABA_BR$ IgG binding to $GABA_{B1+2}R$ transfected HEK cells over time. 142
Figure 4.14: Comparison of $GABA_BR$ antibody IgG surface binding of two patients after incubation in $GABA_{B1+2}R$ transfected HEK cells 143
Figure 4.15: Incubation of patient IgG with GluA2 of $GABA_BR2$ transfected cell had no effect on transfection over time 144
Figure 4.16: Surface IgG binding to hippocampal neurons after the application of IgG purified from a HC patient, a $GABA_BR$ antibody and an AMPAR antibody positive patient.....146
Figure 4.17: AMPAR IgG reduces the expression of the AMPAR on the surface of cortical neurons compared to cells incubated in $GABA_BR$ or HC IgG 148
Figure 4.18: $GABA_BR$ IgG does not cause a reduction of $GABA_BR$ expression on the surface of cortical neurons 149
Figure 5.1: IgG purified from a $GABA_BR$ antibody patient showed strong reactivity to transfected HEK cells and primary neuronal cultures 164
Figure 5.2: Up and Down state transitions are noted in LIII MEC neurons 167
Figure 5.3: Effects of IgG on various Up state characteristics were analysed using the following protocol, approximately 45 minutes in length 167
Figure 5.4: The effect of HC and Test IgG on Up state duration % and spike rate % ...170
Figure 5.5: Representative image of the effect of Test and HC IgG on Up states 171
Figure 5.6: Preadsorption of $GABA_BR$ positive Test IgG abolishes binding to transfected HEK cells and primary neuronal cultures 173
Figure 5.7: Representative images of the effects of $GABA_BR$-IgG on Up states in the entorhinal cortex following antibody absorption with $GABA_BR$ transfected HEK cells 174
Figure 5.8: Representative image of the effect of baclofen on Up states in the EC 176
Figure 5.9: Application of the $GABA_BR$ antagonist CGP55845 increases Up state duration. IgG does not affect $GABA_{B1}R$ function 178
Figure 6.1: Twelve patients in the JEV cohort were positive to a known antigen target, as determined via CBA 196
Figure 6.2: Binding of JEV sera to NMDAR and CASPR2 transfected HEK cells.....199
Figure 6.3: Relationship between antibody end-point titre and antigen specificity.....200
Figure 6.4: VGKC RIA titres for the 9 positive patients 200
Figure 6.6: JEV sera with $GABA_AR$ and NMDAR antibodies bound to the surface of hippocampal neurons 204
Figure 6.7: Samples from patients with positive CBA or VGKC RIA and neuron immunoreactivity 206
Figure 6.8: JEV samples bound to the surface of live hippocampal neurons.....207
Figure 6.9 Clinical outcome of JEV patients based on neuron immunoreactivity.....211
Figure 6.10: CASPR2 and $GABA_BR$ antibody positive samples used for the establishment of a positive control “model system” show strong reactivity to primary neurons before and after incubation.....214
Figure 6.11: Western blot of the immunoprecipitated material from cortical and hippocampal neurons confirmed the presence of the CASPR2 (A), $GABA_{B2}R$ (B) and the NR1 subunit of the NMDAR (C) 216
Figure 6.12: Fractionation of immunoprecipitates on Tris Acetate Gels: “model system” 218
Figure 6.13: Protein hits when looking at individual fractions for the CASPR2 antibody positive immunoprecipitates obtained via mass spectrometry 220

Figure 6.16: Mass Spectrometry hits when looking at individual fractions 5 and 6 for the JEV4 (NMDAR antibody positive) immunoprecipitate 225
Figure 6.17: The structure of Plexin-A2 228
Figure 6.18: Predictor of intracellular, extracellular and transmembrane regions of the melatonin-related receptor protein 229
Figure 6.19: Predictor of intracellular, extracellular and transmembrane regions of Alpha-2-MRAP 230
Figure 6.20: Predictor of intracellular, extracellular and transmembrane regions of Teneurin-4 231

LIST OF TABLES

Table 1.1: Summary of IgG subclasses....3
Table 3.1: Summary of RE samples....74
Table 3.2: Clinical details of GluA2+3 antibody positive patients....77
Table 3.3: Summary of diagnostic AMPAR antibody positive samples....88
Table 3.4: Summary of the clinical details of the AMPAR antibody positive patients identified....89
Table 3.5: Summary of diagnostic $GABA_BR$ antibody positive samples....96
Table 3.6: Summary of the clinical details of the $GABA_BR$ antibody positive patients identified....97
Table 3.7: Summary of the SCLC $GABA_BR$ antibody positive samples....99
Table 3.7: Summary of the samples screened on the AMPAR and $GABA_BR$ CBAs....101
Table 4.2: Summary of the relative AMPAR and $GABA_BR$ levels (shown as % intensity to loading control) when neurons are treated with AMPAR, $GABA_BR$ or HC IgG ..149
Table 5.1: Summary of the effects different material superfused on slices had on Up state characteristics....179
Table 6.1: Summary of JEV cohort....195
Table 6.2: Summary of the JEV positive samples as determined by CBA and VGKC RIA 197
Table 6.3: Summary of the CBA confirmed antibody positive samples....209
Table 6.4: Summary of the patients used for the positive control “model system” immunoprecipitation experiments....212
Table 6.4: List of proteins with extracellular regions, identified using mass spectrometry following immunoprecipitation of hippocampal neurons with JEV sera....226

CHAPTER 1: Introduction

1.1: Introduction to the immune system and antibodies

1.1.1: The immune system

The immune system is the body's main line of defense against harmful pathogens and can be divided into the innate and adaptive immune systems. In evolutionary terms, innate immunity developed first and is independent of prior exposure to the pathogen, therefore providing the body with protection in a nonspecific manner. Adaptive immunity however, is specific to a given antigen, and therefore requires initial exposure to a pathogen; the host is then able to mount a stronger response upon re-exposure. The adaptive response relies on both B-and T-lymphocytes. Fundamental to the proper functioning of the immune system is the ability to differentiate between self (host) and non-self (foreign) molecules. Impairment of the immune system to differentiate between host and foreign can result in autoimmune disorders, in which tolerance is lost and an immune response is mounted against the antigens expressed on host cells.

1.1.2: Antibodies

The specificity of the adaptive immune response is the result of antibodies, which are produced by plasma cells (differentiated B cells). There are five classes (isotypes) of antibodies, which together are referred to as immunoglobulins. Immunoglobulins are distinguished based on the type of heavy chain they contain: IgA (alpha) IgG (gamma), IgD (delta), IgE (epsilon) and IgM (mu). Each of the isotypes have different functions, vary in their sera concentration and their ability to interact with effector molecules (see Schroeder and Cavacini, 2010 for review). IgM accounts for approximately 10% of the immunoglobulin pool found in sera and is a pentamer, with ten antigenic sites, resulting

in the high avidity of the molecule. IgM is particularly important in the early response to infection. IgD accounts for approximately 1% of immunoglobulins found in sera, is monomeric and like IgM plays an important role in the initial phases of the immune response. Most antigens are T-cell dependent and therefore require T-cells for maximal antibody production. Following phagocytosis and presentation of the antigen to T cells, cytokines are released activating B-cells. This T-cell dependent activation causes B-cells to produce IgA, IgE and IgG molecules. IgA represents approximately 15% of the serum immunoglobulin levels, is found predominantly on mucosal surfaces, and is the antibody class important in protecting these membranes from infection. IgA is subdivided into IgA1 and IgA2 subclasses, and is generally expressed as a dimer. IgE is found at very low levels in the serum, is monomeric in structure and plays a critical role in immediate hypersensitive reactions, such as allergies and asthma. IgG is the most abundant isotype found in the blood (70-75%), and for the remainder of this thesis will be the major focus.

1.1.3: Structure of the IgG molecule and properties

IgG is a monomer and is made up of 2 identical light and 2 identical heavy chains. The bonding of heavy chains and light chains via disulfide bonds at the hinge region gives the molecule its distinct Y-shaped structure (Figure 1.1). The light and heavy chains are further subdivided into variable (V) and constant (C) regions. The V region on the light and heavy chain "arms" make up the hypervariable regions (also known as complementarity determining regions (CDR)), which bind the specific epitope(s) of the antigen, and is therefore the region that determines antigen specificity. Each IgG molecule has two antigen binding sites. The Fc fragment, composed of two constant regions at the base of the heavy chains (carboxyl-terminal) has important functional implications, such as activation of the complement cascade (discussed in 1.3.2).

Cleavage of the IgG molecule with the enzyme papain yields two Fab fragments and an Fc fragment. Pepsin, cleaves below hinge region, resulting in the formation of a $F(ab')_2$ fragment and a pFc' fragment (Figure 1.1). IgG is subdivided into four subclasses; IgG1, IgG2, IgG3 and IgG4. Within the subdivisions, there are differences noted in abundance in the serum, with IgG1>IgG2>1gG3=IgG4. In addition, the isotypes vary in their ability to bind the Fc receptors on other immune cells (e.g. phagocytes), their ability to cross the placenta, and ability to fix complement (Table 1.1)

Table 1.1: Summary of IgG subclasses

IgG subclass	Binds to Fc receptor on immune cells	Ability to cross placenta	Complement activator
IgG1	High affinity	Yes	Yes (second highest)
IgG2	Low affinity	No	Yes (third highest)
IgG3	High affinity	Yes	Yes (Highest)
IgG4	Intermediate affinity	Yes	No

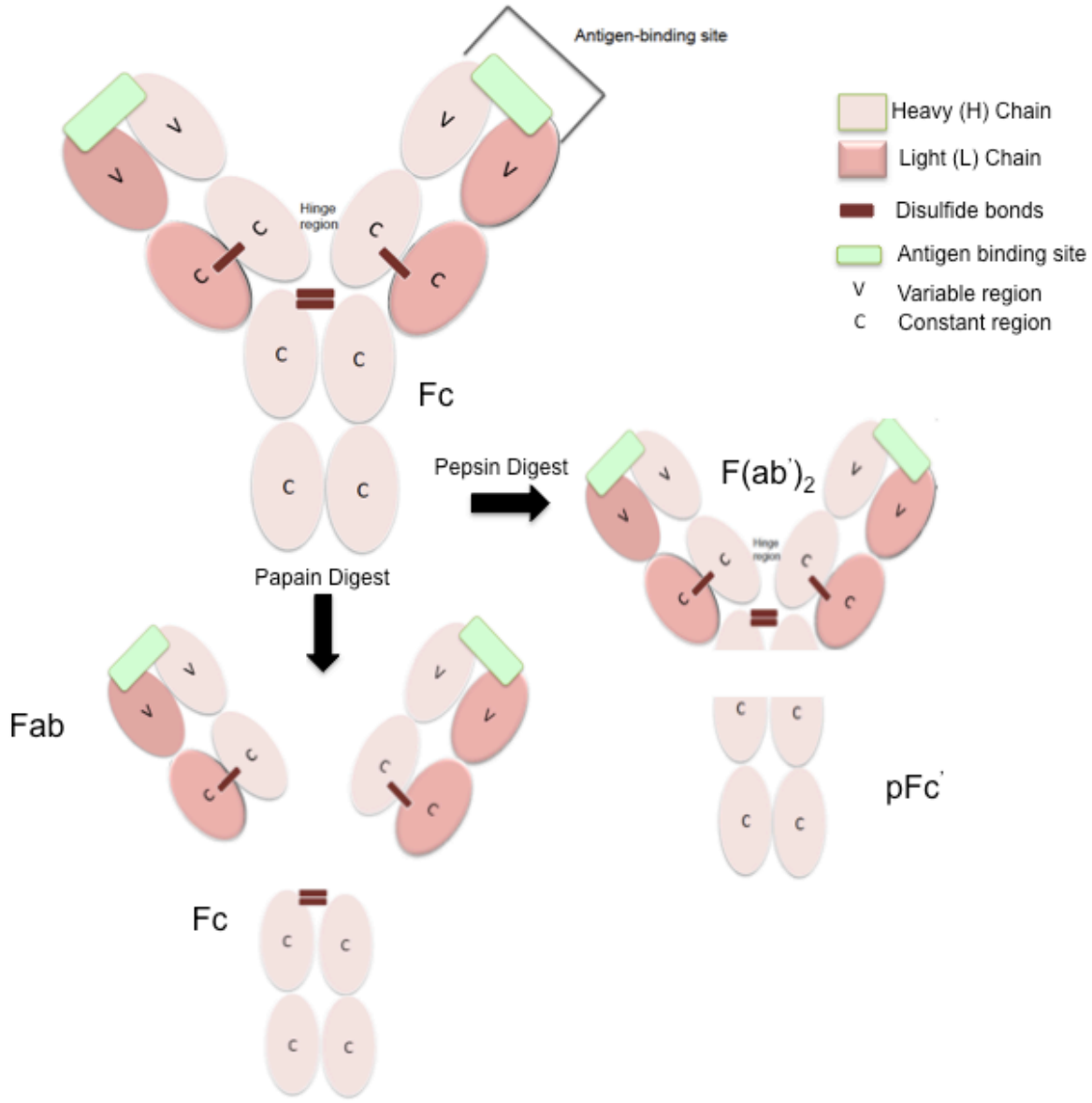

Figure 1.1: Structure of an IgG molecule

IgG molecules are made up of two heavy (H) and two light (L) chains connected via disulfide bonds. The H and L chains are subdivided into variable (V) and constant (C) regions. The structure can be broken down into the antigen binding sites at the amino terminus and Fc fragment and the carboxyl terminal. Two Fab and one Fc fragment are formed when IgG is cleaved with the enzyme papain. Digestion with pepsin results in the formation of one $F(ab')_2$ and one pFc' fragment.

1.2: Antibody-mediated autoimmune disorders

1.2.1: Introduction

The term "*horror autotoxicus"* was first coined by immunologist Paul Ehrlich in the 1890s to describe the "body's aversion to immunological self-destruction". That is, the immune system's ability to recognise and mount a response against foreign material, but not mount an inappropriate response against the host's "self". However, we now know that this concept does not always hold true, and autoreactive antibodies are associated with auto allergenic responses and diseases (both systemic and organ specific), though the status of whether or not these antibodies are directly pathogenic varies. In systemic autoimmune disorders, multiple organs are targeted by the immune response as is the case in systemic lupus erythematous (SLE). In autoimmune responses that are organ specific, such as in Graves' syndrome (where the thyroid is affected), the target antigen is expressed on one organ.

1.2.2: Koch's postulates

Bacteriologist Robert Koch explored the causal relationship between microbes and disease in the 19th century. The autoimmune aetiology of human diseases modeled after Koch's postulates was established in 1957 by Witebsky (Witebsky *et al.,* 1957). The criteria revised by Rose and Bonna (1993) are outlined below:

1). The autoimmune response should be recognised in the form of autoantibodies or self-reactive T-cells

2). The corresponding antigen should be identified

3). An analogous autoimmune response should be induced in an experimental animal

4). The immunised animal should develop a similar autoimmune disease

The criteria originally proposed for microbial pathogenicity are stringent, with an all-or-nothing response being required. The immunisation of an animal with the pathogen should always result in the development of the disease. Witebsky's criteria on the other hand are more lenient, highlighting the acceptance that a variety of additional factors may contribute to the development of an autoimmune disease independent of the antibodies and or cell-mediated factors. For example, SLE patients have deficiencies in Cq1, which result in problems with the activation of the complement cascade. There can also be human leukocyte antigen (HLA) susceptibilities to autoimmune diseases such as in myasthenia gravis (MG) and multiple sclerosis (MS) patients.

The identification of the corresponding antigen is clearly of great interest, and in certain cases may be used as a diagnostic criterion. Identification of antibodies to a specific antigen allows for measurement of antibody levels and can be used as a diagnostic tool. The identification of the target may also give clues to the pathogenic mechanisms of the antibodies. However, this is not to say that the presence of circulating antibodies are always definitely pathogenic, causing or contributing to the disease. For example, antibodies to intracellularly expressed neuronal proteins (Hu, Yo, CRMP5 and Ma2) have been described in patients with paraneoplastic neurological disorders. However, the localisation of these proteins, within the cell or even the nucleus, makes them inaccessible to circulating antibodies. These antibodies are likely to be produced secondary to a T-cell mediated immune response, and are unlikely to be causing the disease. As such, in these patients, there is little correlation between antibody levels and clinical outcome. However, these antibodies are important markers of underlying malignancies (see Dalmau and Rosenfeld, 2008 for review and discussion in 1.4.2).

The last two criteria in Witebsky's postulates, involving acute and passive transfer have been used to explore the peripheral neurological autoimmune disease MG,

which has formed the paradigm by which numerous other autoimmune diseases have been based on. However, the successful use of passive transfer to explore autoimmune diseases cannot necessarily be translated to every disease, as various additional factors such as microenvironment and genetic susceptibility may be involved in evoking an immune response against the antigen.

1.3: Autoimmune disorders of the PNS

Pathogenic autoantibodies have been well established as having a role in peripheral nervous system (PNS) diseases. Two well-documented autoimmune diseases of the PNS include MG and Lambert-Eaton myasthenic syndrome (LEMS).

1.3.1: Myasthenia Gravis

Myasthenia Gravis (MG) is one of the best-understood autoantibody-mediated neurological disorders. MG affects 1 in 10,000 in the UK and is marked by fatigable muscle weakness. Extra-ocular muscles are commonly the first affected muscles, and patients often present with ptosis (drooping of the eyelid or eyelids) and can suffer from double vision. The ocular muscles can be the only group affected (ocular MG), however, in the majority of cases other groups of muscles are affected resulting in generalized MG. Patients can experience head dropping, difficulties swallowing and impaired facial movements as bulbar muscles are often affected. Proximal limb muscles are more commonly affected than distal limbs. If respiratory muscles are affected, assisted ventilation is often required. Symptoms can develop at any age, though interestingly, two peaks where a majority of patients develop MG have been identified. The first is age 20-30 years whereby the majority of patients are female (3:1 predominance). The second is later during the 60-70s, with a male predominance (2:1; for review see Buckley, 2008).

Antibodies directed against the nicotinic acetylcholine receptor (AChR) in MG were serendipitously discovered after rabbits immunised with AChR developed symptoms characteristic of the disease (Patrick *et al.,* 1973). Antibodies against AChR are detected in approximately 85% of patients with generalized MG. These antibodies are predominately of the IgG1 and IgG3 subclass, and can be detected using iodinated (^{125}I-alpha-bungarotoxin) radioimmunoprecipitation assay (Lindstrom *et al.,* 1976). An additional 5% of patients have antibodies against muscle-specific kinase (MuSK), which are predominantly IgG4 subclass antibodies. Antibodies to low-density lipoprotein receptor-related protein 5 (LRP4) and agrin have also been reported. Tumours of the thymus gland (thymoma) are present in approximately 10-15% of these patients. A retrospective study showed patients were more likely to become asymptomatic and improve following thymectomy in comparison to those MG patients that did not undergo thymectomies (Gronseth and Barohn, 2000). Patients show clinical improvement once started on immunotherapy such as plasma exchange (PEX) or corticosteroids (Newsom-Davis *et al.,* 1978).

The AChR is critical for normal neuromuscular transmission, and a loss of function and reduction of this receptor from the neuromuscular junction (NMJ), could result in muscle weakness. Three mechanisms have been postulated as AChR antibodies have been shown to: 1) block the channel directly 2) cause internalisation of the receptor from the surface of the synapse via endocytosis and 3) cause cell lysis and damage through activation of the complement cascade. The three pathogenic mechanisms are shown in Figure 1.2 and discussed below in section 1.3.2.

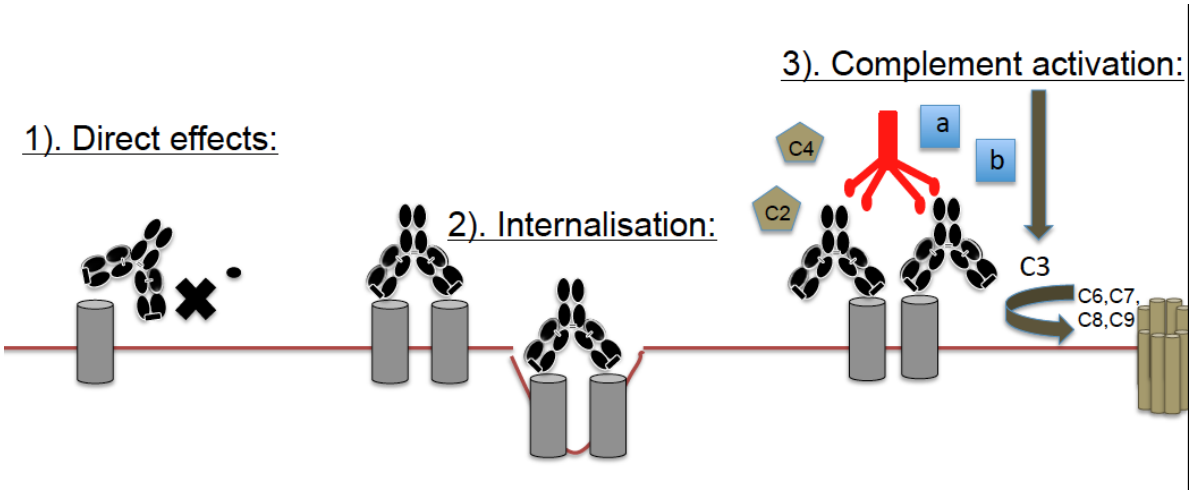

Figure 1.2: Pathogenic mechanisms of AChR antibodies

AChR antibodies have been shown to mediate their effects via three pathogenic mechanisms: 1). Direct effects: Antibody binding can mimic agonist and antagonist effects. AChR antibodies have been shown to have a direct blocking effect on the postsynaptically localized AChR 2). Internalisation: Cross-linking of receptors by IgG molecules results in endocytosis of these receptors causing a reduction in the surface expression 3). Complement activation: Antibody-antigen binding can initiate the classical pathway of the complement system. This results in the formation of membrane attack complex (MAC) resulting in lysis of cells

1.3.2: Potential pathogenic mechanisms of AChR antibodies

1). Direct effects on the target

Some AChR antibodies have been shown to directly block the foetal form (γ-subunit) of the AChR through binding to the agonist site, causing a reduction in sodium ion influx (Riemersma et al., 1996). Direct blocking of foetal form of the AChR is thought to contribute to arthrogryposis, which results in joint contractures leading to foetal paralysis whilst in utero. In addition to activating or blocking the antigen target, antibodies could also potentially alter the structure, preventing binding of agonists and antagonists.

2). Internalisation of the receptor

The loss of AChR has been shown to be the result of antibody-mediated crosslinking, causing internalisation of the receptor from the cell surface and consequential increased degradation of the receptor. Crosslinking is achieved by the divalent nature of the IgG molecules, which allows the IgG to bind two adjacent antigen targets. This divalency is integral, as cleavage of the antibodies into monovalent Fab fragments did not cause internalisation of AChR. However, when crosslinking between Fab fragments was restored using anti-Fab antibodies, internalisation was again observed (Drachman et al., 1978).

3). Activation of the complement cascade

The complement cascade is an intricate process of the innate immune system, which in addition to eliminating microbes, is important in orchestrating inflammatory processes (see Ricklin et al., 2010 for review). Three separate pathways exist: the classical, the lectin and the alternative pathway. The classical pathway is antibody-dependent and is initiated by the binding of IgM or IgG molecules to the antigen. Following this binding, the complement protein C1q binds the Fc region of the antibodies. IgG1 and IgG3 are more potent activators of complement than IgG2, while

IgG4 cannot activate the complement cascade due to modulation of the Fc region (a serine to proline substitution at 331; Tao et al., 1993).

Binding of C1q to the antigen-antibody complex causes C1q to become an active enzyme. This results in the activation of the proteases C1r and C1s, which cleave C4 and subsequently C2 into fragments (C4a/b and C2a/b). When C2 and C4 fragments combine they form the proteolytic enzyme (C3 convertase), which cleaves C3 into a non-proteolytic C3a fragment and a proteolytic C3b fragment, which initiates amplification and downstream effector functions. The formation of C3 convertases is also noted in the lectin and alternative pathway and all three pathways converge at this point.

C3b has two roles. First, it joins with the C2 and C4 fragments to form an enzyme (C5 convertase) that cleaves C5 into C5a and C5b. C5b combines with C6, C7, C8 and several molecules of C9 to form the membrane attack complex (MAC). The MAC spans the entire cell membrane, disrupting the integrity of the cell and eventually leads to cell death via osmotic lysis. The second role of C3b is to insert itself in the cell membrane, marking the cell as a target for phagocytosis.

The complement cascade is also modulated by numerous regulators, which act to prevent the unwanted attack on host tissue that may result in autoimmune disease. For example, the C1 inhibitor prevents the proteolytic activity of C1s and C1r at the beginning of the classical pathway following the binding of antibodies to the antigen target. CD55, which is also known as the decay-accelerating factor (DAF), binds to C3 convertase and accelerates its disassembly. Finally, CD59 inhibits the assembly of MAC. The regulators are present at varying levels on different tissues and this results in a differential sensitivity to the action of complement.

Impairment of factors involved in the complement cascade can lead to a variety of diseases, as tissue may be more or less susceptible to complement lysis. For example, SLE is associated with C1q, C4 or C2 deficiencies (Pettigrew et al., 2009).

The role of complement is well established in the PNS, but in the CNS, the role is less understood. Complement factors are produced in the liver, though these factors can also be synthesized in the central nervous system (CNS) by activated glial cells (Frank, 2010).

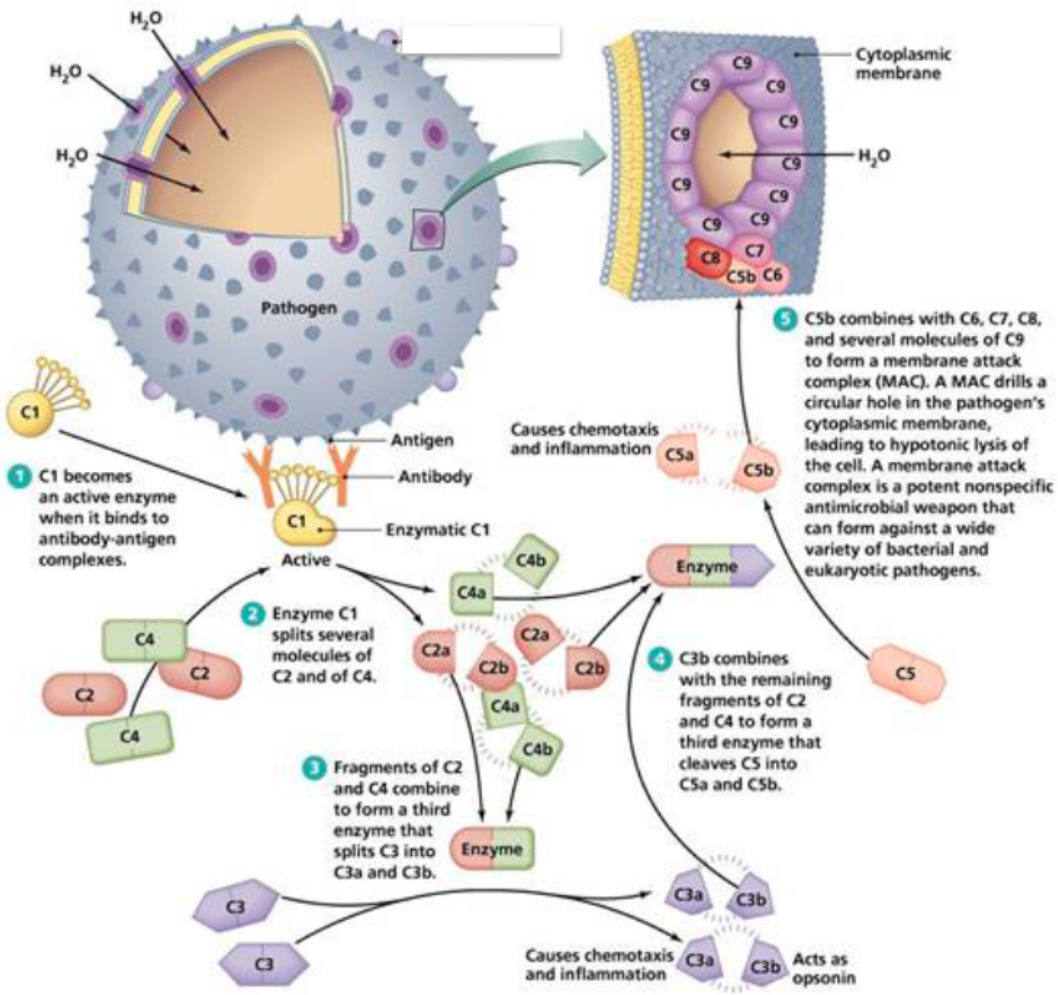

Figure 1.3: Summary of the classical pathway of complement activation

Antigen-antibody interaction (IgG1-3 or IgM) initiates the classical pathway. All complement pathways (lectin and alternative) converge at the activation of C3 convertase. Formation of the MAC leads to cell death and tissue destruction through osmotic lysis. Copyright Pearson education, 2006.

1.3.3: Animal models of MG

The first animal model of MG was serendipitously identified following the injection of AChR, derived from the electric fish *Torpedo* into rabbits, which then presented with symptoms reminiscent of MG (Patrick *et al.,* 1973). Subsequently, it was found that experimental autoimmune myasthenia gravis (EAMG) could be induced following the injection of purified AChR into susceptible mice strains (Berman and Patrick, 1980). The development of MG symptoms in the mice was dependent on strain susceptibility, as a combination of major histocompatibility complex (MHC) and genetic variations are necessary to create an "environment" whereby the antibodies become more pathogenic. Passive transfer of MG patient IgG to mice has shown histopathological features consistent with MG, namely a loss of AChR at the endplate and IgG and complement deposition (Fambrough *et al.,* 1973 and Engel *et al.,* 1977). Mice displayed muscle weakness and due to the loss of AChR at the NMJ, miniature endplate potentials were also reduced. These symptoms and pathogenic effects were enhanced by complement component C3, indicating the complement-dependent nature of the disease (Toyka *et al.,* 1975, 1977).

In about 10-15% of patients with MG who are AChR antibody-negative, antibodies are detected to a different protein, namely muscle specific kinase (MuSK), which is also found at the neuromuscular junction (Hoch *et al.,* 2001). The antibodies in MuSK positive MG patients are predominantly of the IgG4 subclass. Patients with MuSK antibodies show a reduction of AChR clusters at the NMJ end plate, and due to the lack of IgG1 and IgG3 subclass antibodies in these patients, complement deposition is not observed (Shiraishi *et al.,* 2005). MuSK is now known to be involved in clustering AChR through its binding with agrin. Injection of IgG purified from a MuSK antibody positive patient resulted in the induction of EAMG in mice, showing that these antibodies are also pathogenic (Bruges *et al.,* 1994). Furthermore Koneczny *et al.* (2014) showed that

purified MuSK IgG4 reduce agrin-induced AChR clustering. MuSK IgG4 antibodies also block LRP4 and MuSK interaction. Together these findings suggest MuSK antibodies have a pathogenic role distinct of AChR antibodies.

1.3.4: Lambert Eaton myasthenic syndrome (LEMS)

Like MG, Lambert Eaton myasthenic syndrome (LEMS) is an autoimmune disease of the NMJ. Patients suffer from proximal leg weakness, autonomic dysfunction and reduced tendon reflexes. The initial presentation of the disease can be confused with MG, though the clinical symptoms as the disease progresses and electrophysiological analysis show marked differences between these two autoimmune diseases. For instance, respiratory muscles are less affected in LEMS patients than MG patients. Approximately 50% of all LEMS patients have an underlying tumour, and this is almost always small cell lung carcinoma (SCLC) though cases of LEMS patients with thymomas, breast and prostate cancer have been described (Titulaer *et al.,* 2011). SCLC is a carcinoma of neuroendocrine origin, which expresses a number of synaptic receptors and proteins on their cell surface and is often associated with paraneoplastic neurological disorders (Benatar et al, 2001).

The discovery of pathogenic autoantibodies directed against the voltage-gated calcium channel (VGCC), has facilitated diagnosis, and has been key to understanding the pathophysiology of the disease. Approximately 40% of patients with LEMS have antibodies directed against VGCC, with the remainder being classified as 'seronegative' (Nakao *et al.,* 2002). The majority of VGCC antibody positive patients (approximately 85%) have antibodies directed against the P/Q-type VGCC. Loss of function of VGCC results in impaired AChR quantal release, while overall presynaptic AChR stores and postsynaptic response to AChR remains unaffected (Buckley, 2008).

The presence of antigens that mimic receptors expressed at the NMJ on the surface of tumour cells could be responsible for the presence of antibodies in patients with an underlying malignancy. However, this only explains half of the patients with LEMS. In addition, VGCC antibodies can develop in LEMS patients without tumours, which is most likely due to part of a more general autoimmune response. These antibodies can cause a down regulation of the receptors from the surface of the neuromuscular junction, as has been shown by biopsy studies of patients with these antibodies (Fukuda *et al.,* 2003).

As with MG, PEX and intravenous immunoglobulins (IVIG) generally results in clinical improvement of patients with LEMS, with the probability of relapses reduced if that patients are also concurrently taking immunosuppressants (Illa *et al.,* 2005).

1.4: Autoimmune diseases of the CNS and intracellular neuronal targets

1.4.1: Introduction

There is now an increased knowledge of the role of autoantibodies in CNS disorders, including a variety of encephalitides, cerebellar ataxia, and epilepsies. In these disorders, antibodies target neuronal cell-surface proteins, and these targets generally play crucial roles in synaptic transmission, excitability, inhibition and plasticity. In many of these autoimmune mediated disorders, there is an underlying malignancy, which express neuronal antigens. These disorders are known as paraneoplastic disorders, and the presence of a tumour may explain the development of the specific antibodies in the serum of these patients. Antibodies have been described against both intracellular and extracellular determinants in paraneoplastic cases. In addition, there is growing recognition that the antibodies associated with these diseases are pathogenic. Many patients with antibodies to extracellularly expressed neuronal antigen targets respond

well and can recover fully from their symptoms if started on immunomodulatory treatment. In contrast, when the antigen target is intracellular, patients show a more variable response to immunotherapy.

1.4.2: Intracellular neuronal targets

The first neuronal epitopes that were recognised in patients with neurological symptoms were intracellular and included Hu, Yo and Ma2 (see Lancaster *et al.,* 2012 for review). Due to the localisation, circulating antibodies in sera and CSF have limited accessibility to these proteins, and the question arises as to whether antibodies to these proteins are in fact pathogenic and contributing to the disease. Instead it has been suggested that these antibodies indicate a T-cell-mediated immune response (Dalmau *et al.,* 1991 and Giometto *et al.,* 1997).

Diseases in which antibodies to intracellular autoantigens occur do not fulfill Witebsky's criteria in general, as passive transfer experiments conclude that these intracellular antibodies are not primary contributors to the disease. For example, stiff-person syndrome (SPS) is a rare autoimmune disease characterised by severe spasms and has been associated with both glutamate decarboxylase 65 (GAD65) and amphiphysin antibodies with approximately 60-80% of SPS patients having antibodies to GAD65 (Costa *et al.,* 2002). However, passive transfer studies in mice have shown that the development of symptoms is most likely due to T-cell mediated mechanisms as transfer of T cells into mice lacking B cells developed encephalomyelitis, suggesting GAD65 antibodies may only contribute partially to symptoms (Burton *et al.,* 2008, 2009).

Tanaka *et al. (*1994, 1995) published 3 studies attempting to derive an animal model of paraneoplastic cerebellar degeneration (PCD) with anti-Yo antibodies. Attempts were not successful despite the use of 4 strains of mice bearing different MHC molecules. High anti-Yo antibodies were produced by the mice following intraperitoneal injection,

but none of the mice strains showed cerebellar ataxia, as is noted in patients with PCD. Furthermore, Purkinje cell loss, a hallmark of PCD was not observed following injection of PCD patient purified IgG into the brain, despite positive IgG staining of Purkinje cells. Additionally, injection with complement and lipopolysaccharide-activated human macrophages did not case an increase in cell loss. The overall conclusions of their studies were that Yo antibodies alone could not account for PCD symptoms and Purkinje cell loss and that the disease was to some part T-cell mediated.

Amphiphysin antibodies are less common, but tend to be strongly associated with patients with an underlying cancer (Murinson *et al.,* 2008). Interestingly, intrathecal application of anti-amphiphysin antibodies purified from a patient with SPS was found to induce SPS like symptoms in rats (Geis *et al.,* 2010). These antibodies were shown to be internalised and GABAergic synapses were found to be vulnerable to defective endocytosis as evidenced by defective loading of FM 1-43 (a dye used to label cell membranes). Electrophysiological alterations due to a decrease in GABAergic transmission also highlighted the pathogenic effect of these antibodies. While these antibodies have been shown to functionally disrupt inhibitory transmission, postmortem studies of patients with amphiphysin antibodies shows CD8-predominant T-cell infiltrates in the brain (Pittock *et al.,* 2005). It remains inconclusive whether or not disruptions of normal endocytotic activity, and/or T-cell mediated responses are more important to the development of the disease in these patients.

Response to immunotherapy in patients with antibodies to intracellular proteins tends to be poorer than in patients that recognise extracellular proteins. These findings suggest that intracellular antibodies are unlikely to be playing a causative role in the disease, though they may play a secondary role in disease propagation and are useful biomarkers.

1.5: Autoimmune disorders of the CNS and extracellular neuronal targets

1.5.1: Introduction

While it was initially hypothesized that autoantibodies to the voltage-gated potassium channel (VGKC) subunits, Kv1.1 and Kv1.2 gave rise to an array of distinctive diseases such as acquired neuromyotonia (NMT), Morvan's syndrome and limbic encephalitis (LE), it was later shown that the VGKC complex proteins; leucine rich, glioma-inactivated 1 (LGI1), contactin-associated protein-like 2 (CASPR2) and contactin 2, were the main antibody targets in most of these patients (Irani *et al.,* 2010 and Lai *et al.,* 2010).

1.5.2: VGKC complex antibodies

LGI1 is a glycoprotein secreted from presynaptic terminals that associates with synaptic VGKC subunits. LGI1 forms a crossbridge between the disintegrin and metalloproteinase domain-containing proteins 22 and 23 (ADAM 22/23), which are expressed post and presynaptically, respectively. CASPR2 has a large extracellular domain and acts as a cell-adhesion molecule, crucial for the localisation of VGKCs at neural juxtaparanodes. CASPR2 interacts with contactin 2, also an adhesion molecule with a large extracellular domain (though it forms a smaller component of the VGKC complex than CASPR2). While the VGKC radioimmunoassay (RIA) detects antibodies to the entire VGKC complex, CBAs allow for antibodies to specific VGKC complex proteins to be detected.

NMT, also known as Isaacs syndrome is characterised by spontaneously occurring muscle activity of the periphery, which results in myokymia (muscle quivering), painful muscle cramping, and autonomic irregularities. Approximately 20% of patients have an underlying tumour, usually in the form of a thymoma. Antibodies directed against the VGKC complex have been detected in approximately 40-60% of patients with NMT

(Shillito *et al.,* 1995). In addition, patients treated with PEX show reduced neuromyotonic discharges (Newsom-Davis *et al.,* 1993).

Morvan's syndrome is a rare but very interesting disease marked by peripheral nerve hyperexcitability, dysautonomia, and encephalopathy with marked insomnia. PNS symptoms may precede or follow the development of CNS symptoms.

Patients with limbic encephalitis (LE) suffer from symptoms associated with dysfunction of the limbic regions, such as short-term memory loss, confusion, seizures and psychological disturbance. Onconeurological markers of paraneoplastic markers have been discovered in patients with tumours. It is the most common syndrome associated with VGKC complex proteins and patients with these antibodies have a better prognosis than paraneoplastic LE patients (see Vincent *et al.,* 2011 for review).

Irani *et al.* (2010a) describe 96 patients that were positive on the VGKC RIA and tested for antibodies against LGI1 and CASPR2 by CBA. Fifty-five patients (57.3%) were found to be LGI1 antibody positive, and of these, 89% had LE. LGI1 antibodies were also found in 2/5 patients with Morvan's syndrome, 1/11 with NMT, 1/4 with epilepsy and 2/12 with other disorders. CASPR2 antibodies were identified in 19 patients (19.8%). Unlike the LGI1 antibodies, CASPR2 antibodies were less commonly found in patients with LE, with 52.6% of CASPR2 antibody patients having NMT or Morvan's syndrome.

LGI1 antibodies are found predominantly in patients with faciobrachial dystonic seizures (FBDS). FBDS comprises patients that have distinctive seizure semiology. In this study, 29 patients with FBDS were identified and 89% of these patients had antibodies to LGI1 (Irani *et al.,* 2011). Interestingly, FBDS can often precede LE, which was noted in 20/29 of the patients who initially presented with FBDS prior to the development of amnesia and confusion.

CASPR2 antibodies have been described in patients with PNS and CNS symptoms such as NMT, Morvan's syndrome and LE. Eight of 140 patients reported with having CASPR2 antibodies had symptoms such as encephalopathy (7/8), neuropathy or peripheral nerve hyperexcitability (PNH; 5) and one isolated case of PNH. These patients responded well to immunotherapy (Lancaster *et al.,* 2011). While none of these patients had an underlying malignancy, thymomas have been described in some patients in the literature. In Irani *et al.* (2012) 29 patients with Morvan's syndrome were tested for antibodies directed against VGKC complex antibodies. These patients were predominantly men and it was found that 24/27 patients had antibodies to CASPR2, LGI1 or both.

It is unclear why CASPR2 antibodies can cause such a variation in symptoms, but this may be due to the ubiquitous expression of the CASPR2 protein in many brain regions and its expression peripherally. The mechanism of action of these proteins may also contribute to the multifocal development of symptoms. Following incubation of IgG purified from CASPR2 and LGI1 antibody positive patients with primary neuronal cultures, there appears to be a reduction in the surface expression of the protein (Dr. Pettingill Thesis). In addition, preliminary investigations have shown that these antibodies are predominately IgG1 and IgG4, and also have the potential to activate complement on transfected HEK cells *in vitro* (noted by the deposition of C3b).

Genetic mutations and knock out mice can also give us information about the pathogenic mechanisms of these antibodies. LGI1 knockout mice show an array of seizure symptoms, and a majority of the mice in the litter die postnatally around 3 weeks of age. Mutations in the gene encoding LGI1 generally result in the impairment of LGI1 secretion, and these mutations are commonly found in patients with autosomal dominant lateral temporal epilepsy (ADLTE), a type of partial epilepsy (Ottman *et al.,* 2008). Mutations in the gene encoding CASPR2 (CNTNAP2) have also been implicated in

epilepsy, Tourette syndrome, obsessive-compulsive disorder and autism (Gregor *et al.,* 2011). Interestingly, many of the CASPR2 knockouts themselves do not exhibit any impairment of peripheral nerve conduction (Poliak *et al.,* 2003). As such, whether or not these symptoms found in patients with autoantibodies to these proteins are the direct result of potential complement activation or internalisation of the receptors, remains to be elucidated. It is possible that accessory or associated proteins may be down-regulated or impaired whilst LGI1 and CASPR2 are mediating their effects, and this may result in the development of the symptoms.

1.5.3: NMDAR antibodies

The N-methyl-D-aspartate receptor (NMDAR) is a member of the ionotropic glutamate receptor family (discussed below in 1.6.1). NMDARs are heterotetramers comprised of two obligatory NR1 subunits and two NR2 or NR3 subunits.

The first report of antibodies directed against the NMDAR was in 2007 by Dalmau *et al*. The authors reported 12 young females, whose cerebrospinal fluid (CSF) showed distinct staining to the neuropil of the hippocampus. Eleven of the patients had an ovarian teratoma, and the patients responded well to tumour resection and immunotherapy (Dalmau *et al.,* 2007). Since this original description over 500 patients have been reported, and it has become clear that males and children are also affected, and a tumour is not always associated with the disease (Irani *et al.,* 2010b). Characteristic symptoms of the encephalitis include presentation with prodromal flu-like symptoms, followed by an acute stage whereby patients present with prominent psychiatric symptoms, seizures, catatonia, abnormal movements and autonomic instability (Dalmau *et al.,* 2008, Titulaer *et al.,* 2013). The primary target of NMDAR encephalitis is the amino terminal region of the NR1 subunit, and deletion of amino acids in this region result in an abolition of binding (Dalmau *et al.,* 2008). While these

antibodies are also intrathecally produced, in general, these antibodies are always higher in the sera than in the CSF(Dale *et al.,* 2009 and Irani *et al.,* 2010).

NMDAR antibodies have been shown to cause a reversible reduction in the levels of surface expressed synaptic NMDAR levels (Dalmau *et al.,* 2008). In addition, these antibodies have been shown to cause a disruption in NMDAR-dependent synaptic currents, following incubation of neurons with NMDAR antibody positive CSF for 24 hours. Hippocampal pyramidal cells showed a reduction in NMDAR mediated currents, while amplitude and frequency of the currents were not affected, suggesting that presynaptic release of neurotransmitters is not altered by the patient's antibodies, and implying that this effect is due to a selective loss of NMDAR function. Furthermore, AMPAR mediated currents were unaffected, highlighting the specificity of these antibodies (Hughes *et al.,* 2010). In another study, IgG purified from NMDAR encephalitis patients (n=3) was shown to cause a reduction in long-term potentiation (LTP) when superfused on brain slices (Zhang *et al.,* 2012). In contrast, IgG from viral encephalitis patients did not have an effect.

While NMDAR antibodies have also been shown to activate the complement cascade *in vitro* (Irani *et al.,* 2010), there does not seem to be evidence of complement mediated tissue damage in brain tissue taken from NMDAR antibody patients as determined by C9neo deposition (Martinez-Hernandez *et al.,* 2011, Tuzun *et al.,* 2009, Bien *et al.,* 2012). As NMDAR are critical for plasticity, learning and memory, it is unsurprising that these antibodies produce effects similar to seen in mice in which the NMDAR has been genetically altered.

Patients with NMDAR encephalitis are often treated with an aggressive course of immunotherapy, and in the cases of patients with an ovarian teratoma, removal of the tumour is associated with an expedited recovery (Dalmau *et al.,* 2008). Untreated patients without tumours have been noted to relapse (Irani *et al.,* 2010b).

1.5.4: Glycine receptor (GlyR) antibodies

The GlyR is formed from a pentameric assembly consisting of α and β subunits. These antibodies were initially reported in patients with progressive encephalomyelitis with rigidity and myoclonus (PERM). Patients with PERM suffer from stiffness, rigidity, oculomotor dysfunction and an excessive startle response. The antibodies are directed against the α-1 subunit of the receptor, and the patients generally do not have an associated tumour. In addition, these patients responded well to immunotherapy (Hutchinson *et al.,* 2008). Follow up reports have also noted antibodies to additional subunits of the receptor. These patients show varying staining pattern on sections, corresponding to the expression of the subunits and a spectrum of clinical symptoms (Carvajal *et al.,* 2014).

Interestingly, these antibodies behave similarly to strychnine, a GlyR inhibitor. Administration of this drug results in symptoms such as rigidity, muscle spasms and an exaggerated startle response, all symptoms exhibited by patients with GlyR antibodies (Makarovsky *et al.,* 2008).

1.5.5: Dipeptidyl-peptidase-like protein -6 (DPPX) antibodies

Antibodies to DPPX have recently been described in 4 patients with prominent neuropsychiatric symptoms, 3 of which also had gastrointestinal dysfunction prior to the development of neurological symptoms such as agitation, myoclonus, and confusion (Boronat *et al.,* 2013). These patients all showed a distinct and similar staining pattern when serum or CSF was applied to rat brain sections. Mass spectrometric analysis from the immunoprecipitation of antibodies with primary hippocampal cultures revealed DPPX as the target. DPPX is a cell surface auxiliary subunit of the Kv4.2 potassium channel. Whilst only a small number of patients have been described with these antibodies, the patients responded well to immunotherapy, with relapses occurring when immunotherapy was decreased.

Recently, these antibodies have been detected in 3 patients with PERM and gastrointestinal symptoms. Intrathecal synthesis was found in all patients, with a good initial response to treatment (Balint *et al.,* 2014).

1.5.6: Metabotropic glutamate receptor antibodies (mGluR)

Antibodies directed against mGluR1 and mGluR5 have been described in patients with cerbellar ataxia and Ophelia syndrome, respectively. Smitt *et al.* (2003) described two patients with Hodgkin's lymphoma and paraneoplastic cerebellar ataxia with mGluR1 antibodies. Application of IgG purified from the serum of both patients to Chinese-hamster-ovary (CHO) cells transfected with mGluR1, resulted in the impairment of glutamate-stimulated formation of inositol phosphates. Injection of these antibodies into the cerebellar subarachnoid space of mice resulted in the animals displaying severe ataxia. In another report, application of mGluR1 antibodies to cerebellar slices resulted in long-term depression (LTD) of normal Purkinje cell basal activity (Coesmans *et al.,* 2003). Two further patients with cerebellar ataxia but without the lymphoma have also been described (Marignier *et al.,* 2010). mGluR1 is important for mediating fast, excitatory transmission in the cerebellum, and these findings were able to show how direct activation on a receptor could cause neurological impairment.

Ophelia syndrome is a rare syndrome whereby patients present with psychiatric symptoms and go on to develop memory and cognitive impairment. Patients with this syndrome and mGluR5 antibodies also have Hogkin's lymphoma, and show marked improvement when started on anti-tumour treatment (Lancaster *et al.,* 2011). Despite the high sequence homology between mGluR1 and mGluR5 no cross reactivity exists between the patients with Ophelia syndrome patients with mGluR5 antibodies and mGluR1 transfected cells. mGluR5 is predominately expressed in the hippocampus,

where it is critical for LTD (Faas *et al.,* 2002) and staining of sections shows strong immunolabeling of this region, which is consistent with the features of these patients.

1.5.7: $GABA_AR$ antibodies

$GABA_AR$ are pentameric in structure and comprised of α, β, and γ subunits. Eighteen patients with antibodies to the α-1 and β-3 subunits of the $GABA_AR$ have recently been described (Petit-Pedrol *et al.,* 2014). The patients that were identified could be split into two categories according to their antibody titres and by extension their clinical phenotype. High antibody titre patients suffered from severe encephalitis with seizures, whereas the low antibody titre patients (end point titre < 1:160) had a more diverse phenotype. When primary hippocampal neurons were exposed to IgG purified from a $GABA_AR$ antibody positive patient, it was noted that $GABA_AR$ were removed from the synapse. In turn, the loss of $GABA_AR$ inhibition is proposed to be responsible for development of status epilepticus (Gonzalez *et al.,* 2013).

A number of additional forms of encephalitis could have an underlying autoimmune aetiology. Two additional neuronal surface antigens; the AMPAR and $GABA_BR$ have been implicated in autoimmune neurological diseases, and are the focus of the remainder of this chapter and thesis.

1.6 AMPAR and their role in autoimmune disorders

1.6.1: AMPAR structure, interacting proteins and expression

L-glutamate is the main excitatory neurotransmitter of the human CNS. L-glutamate mediates its effects through metabotropic (mGluRs) and ionotropic receptors (iGluRs). There are three major types of iGluRs, with each defined and named after the different ligands they bind to; N-methyl-D-aspartate (NMDA), alpha-amino-3-hydroxy-5-methyl-isoxazole-4-propinonic acid (AMPA) and kainate (KA) receptors.

AMPAR are expressed as heterotetramers (dimer-dimer) of homologous subunits, GluA1-4, each approximately 894 amino acids in length (Nutt *et al.,* 1994). In general, GluA2 makes up one dimer-dimer pair and governs the permeability of these receptors to Na^{+}, K^{+} and Ca^{2+} ions. The post transcriptional modification of the GluA2 subunit results in a glutamine (Q) to an arginine (R) change within the pore of the channel, which makes the entry of larger cations (Ca^{2+}), energetically unfavorable. As GluA1/GluA2 and GluA2/GluA3 make up the majority of the AMPAR found at the synapse, and 99% of expressed GluA2 subunit are edited, in general AMPAR are considered to be impermeable to Ca^{2+}, a feature distinguishing it from the NMDAR.

Sobolevsky et al solved the crystal structure of the GluA2 subunit in 2009. The crystal structure and topology are shown in Figure 1.4A/B. Each AMPAR subunit has a large extracellular amino terminal domain (ATD), a ligand binding domain (LBD), a channel region composed of three transmembrane domains and a re-entrant p-loop and an intracellular carboxy-terminal domain (CTD).

Each subunit also has a “flip” and a “flop” variant, which is an interchangeable exon preceding the fourth transmembrane domain. Both forms are equally abundant in the brain, and the form expressed is region specific. For example, CA3 pyramidal neurons of the hippocampus only contain subunits with the “flip” variant, whereas in the dentate

gyrus the granular cells express more “flop” than “flip” (Hollmann and Heinman *et al.,* 1994). The efficacy of glutamate in activating variants of these receptors differs, with the “flip” channels being more efficient (Sommer *et al.,* 1990). The switch from “flop” to “flip” variants is important in LTP, and also could be important in synaptogenesis in early life. AMPAR receptors interact with a variety of other synaptic proteins such as SAP97 and GRIP1/2, which are important in AMPAR subunit trafficking (Huganir and Anngono, 2011). Through its interaction with the scaffolding protein postsynaptic density protein (PSD)-95 and stargazin, AMPAR interact with ADAM22 postsynaptically. LGI1 forms a trans-synaptic crossbridge between the postsynaptically localized ADAM 22 and the presynaptically localized ADAM 23. Modulation or loss of the LGI1-ADAM22 interaction has been shown to reduce AMPAR function, which could explain the epileptic phenotype of LGI1 KO mice (Ohkawa *et al.,* 2013). The interaction between AMPAR and stargazin is also important in regulating channel gating, modulating sensitivity to pharmacological agents and clustering of the receptor at the synapse (Diaz, 2010 and Cokic *et al.,* 2008).

AMPAR receptors are ubiquitously expressed, with the highest levels observed in the hippocampus, granular cell layer of the cerebellum and the cerebral cortex. Within the hippocampus, a majority of AMPARs are composed of GluA1/GluA2 (Wenthold *et al.,* 1996).

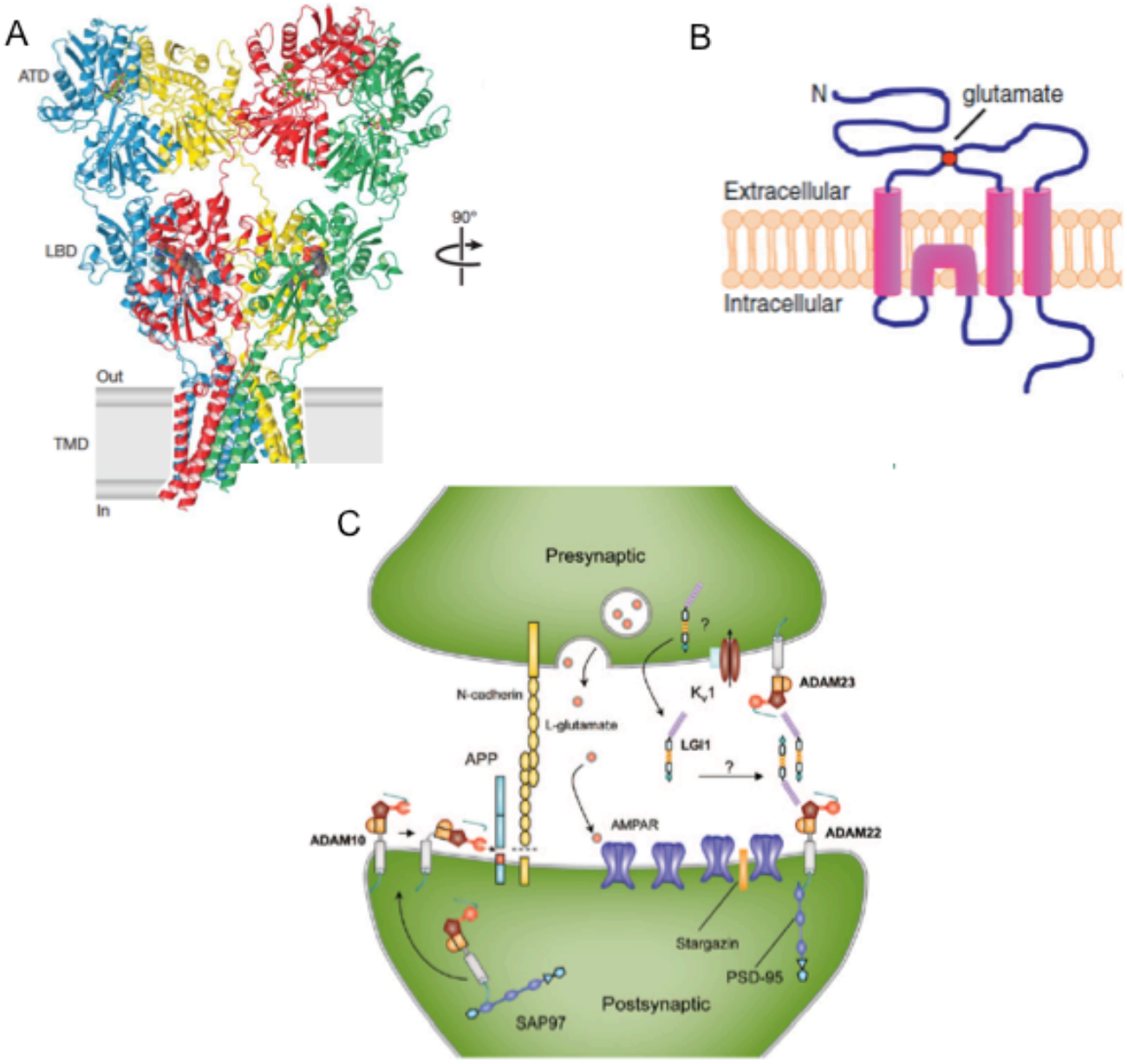

Figure 1.4: Crystal structure of homotetrameric GluA2

AMPAR subunits are comprises of 3 domains; the amino terminal domain (ATD), the ligand binding domain (LBD) and the transmembrane domain (TMB). Crystal structure published by Sobolevsky et al., 2009 (A). While the crystal structure shows homotetrameric assemblies of GluA2, AMPAR is a tetrameric channel assembled from two dimers of different subunits. Topological overview of AMPAR subunits showing the large ATD and LBD (B; Huganir and Anngono, 2011). The C-terminus of AMPAR subunits contain a PDZ interaction motif that allows clustering of the receptors and interaction with a variety of scaffolding proteins. AMPAR interact with ADAM 22 and ADAM 23, and LGI1 is important in forming this presynaptic crossbridge (Berranoch, 2012).

1.6.2: AMPAR function

AMPAR are a critical component of neuronal networking and are fundamental to a variety of brain functions. AMPAR only open following binding of L-glutamate, thus allowing Na^+ to enter through the pore. This depolarization is referred to as excitatory postsynaptic potential (EPSP) and summation leads to transmission of the synaptic signal. AMPAR are commonly expressed with NMDAR and both are important in LTP. Upon activation of AMPAR, membrane depolarization causes the NMDAR to become activated by relieving the magnesium block. This results in the influx of Ca^{2+} and subsequently the activation of Ca^{2+}-dependent intracellular signal transduction cascades, which subsequently increases the trafficking and insertion of AMPAR (predominantly GluA1/2) into the synapse, strengthening the stimulation. LTP is dependent on NMDAR for initiation and AMPAR for maintenance; changes in trafficking increase or decrease synaptic strength (Sprengel, 2006).

1.6.3: AMPAR subunit: knockout models

GluA1 deficient mice show normal development and life expectancy. In addition, the structure of neuronal synapses and dendrites and the expression of other AMPAR subunits remain unaltered (Zamanillo *et al.,* 1999 and Sanderson *et al.,* 2010). However, GluA1 knockout mice show impairments on spatial working memory tasks, while displaying normal behavior on spatial reference tasks. These findings suggest that short term memory processing is impaired in these mice (Sanderson *et al.,* 2010).

GluA2 knockout mice exhibit increased mortality, reduced exploration and impaired motor coordination (Jia *et al.,* 1996). When GluA2 is knocked out, AMPAR subunits continue to form as homomers or heterotetramers composed of combination of GluA1, GluA3 and GluA4. LTP in hippocampal slices taken from mice lacking this subunit has been shown to be enhanced, which is thought to be due to a increase in Ca^{2+} flux (Shepard, 2007).

Furthermore, there are differences noted between GluA2 knockout mice, and mice that show reduced editing. In Bursa *et al.* (1995) molecular engineering (which resulted in 25% of GluA2 mRNA remaining unedited) caused an increased Ca^{2+} permeability. The mice developed seizures and died prematurely. Changes in GluA2 Q/R editing are also evident in mice with ischemia. In 2006, Peng and colleagues showed that in circumstances of ischemia, a higher percentage of hippocampal neurons in the CA1 had unedited GluA2, increasing exotoxicity and subsequently cell death. However, the region specific ischemia could be recovered with the overexpression of the protein ADAR2 (responsible for the Q/R editing). The increase in editing resulted in a reduction in Ca^{2+} permeability and neuronal death (Peng *et al.,* 2006).

Finally, mutations in the gene encoding GluA4 (GRIA4) result in the development of absence seizures in mice. GluR4 knockout mice also show spike-wave discharges characteristic of absence seizures (Beyer *et al.,* 2008).

1.6.4: Antibodies in Rasmussen encephalits

1.6.4.1: Rasmussen encephalitis (RE)

Antibodies directed against the GluA3 subunit of AMPAR were amongst the first autoantibodies implicated in a neurological disease. Rasmussen encephalitis (RE) is an extremely rare but severe disease characterised by unihemispheric cortical atrophy, severe and frequent seizures and hemiparesis (Rasmussen *et al.,* 1958). One UK study reported an incidence of 1.7 cases per 10 million people aged 16 years and younger (Lamb *et al.,* 2013). Similarly, a recent German study reported an incidence of 2.8 cases per 10 million individuals of 18 years of age or younger (Bien *et al.,* 2013). No sex or ethnic predominance exists.

There are 3 predominant stages of disease: a prodromal phase, an acute phase and a residual phase. In the prodromal stage, patients exhibit infrequent seizures and mild hemiparesis. The acute stage marks the development of frequent seizures arising from one cerebral hemisphere. These patients can experience up to 70 seizures a day and are generally unresponsive to anti-epileptic drugs (AEDs). Fifty percent of patients develop epilepsy partialis continua (EPC), which is unilateral myoclonic twitching of the distal extremities that occur at very short intervals (no more than 10 seconds) for at least one hour (Thomas *et al.,* 1977). However, as the disease progresses different types of seizure semiologies are often observed, which may be due to different focal regions of the brain becoming affected. If patients are left untreated hemianopia, hemiparesis, cognitive decline and language deficits (dependent on the hemisphere affected) will result. The final stage is the residual phase during which time seizures become less frequent and patients have a stable neurological deficit (see Bien *et al.,* 2005). Less common presentations such as bilateral RE and RE in adulthood have also been reported (Tobias *et al.,* 2003 and Oguni *et al.,* 1991).

Multifocal inflammation within the affected hemisphere is progressive, and any area of the brain can be affected. The development of microglial and lymphocytic nodules as well as perivascular cuffing and neuronal death are all common pathological features noted during the acute stage of the disease (Bien *et al.,* 2002). End-state features noted include cortical cavitation, astrogliosis and continued neuronal death (for a full review see Varadkar *et al.,* 2014).

1.6.4.2: Role of AMPAR antibodies in RE

In 1994, scientists serendipitously found that rabbits injected with a GluA3 fusion protein developed seizures and had a cortical histopathology that resembled RE, namely

neuronal loss accompanied by microglial infiltrates (Rogers *et al.,* 1994, Bien *et al.,* 2002). Detection of antibodies in two patients during the active stage of the disease showed reactivity to GluA3-trpE fusion protein extracts, but no reactivity to other protein extracts (additional AMPAR subunits) via immunoblot. Two further patients with hemiparesis, or stable RE with no seizures showed no immunoreactivity to GluA3 protein extracts. However, 3 of the 4 patients showed reactivity to GluA3 transfected cells. Age and sex-matched epileptic controls or children with active CNS inflammation showed no reactivity via immunoblot or immunocytochemistry. Follow up studies documented that 3 of 4 patients treated with PEX recovered transiently from their seizures and showed neurological improvement (Rogers *et al.,* 1994). Due to the unilateral nature of the disease, it has been proposed that the blood brain barrier (BBB) becomes compromised at focal sites only on one hemisphere, resulting in unilateral focal seizures. This breakdown would result in an influx of anti-GluA3 antibodies that could result in the histopathology noted in these patients and which could result in more seizures, creating a vicious cycle (McNamara *et al.,* 1995). The contralateral side would be spared.

Follow up experiments concluded that the sera from the immunised rabbits had an agonist like effect on cultured cortical neurons. Synthetic antibodies generated to a peptide of the extracellular region (referred to as GluA3B) blocked the agonistic effect of the GluA3 antibodies, suggesting that this peptide region (amino acids 372-395) was the site of activation on the GluA3 subunit (Twyman *et al.,* 1995). Mimicking the effects of glutamate, antibody binding would cause an opening of the channel, and eventually lead to exocytoxic effects on the neurons (Gahring *et al.,* 1998). Complement dependent lysis was also noted in 3/5 brain samples taken from RE patients with active and progressive seizures. Complement factors (C4, C8 and MAC) were not observed

immunohistochemically in control patients with epilepsy or in two chronic RE patients (Whitney *et al.,* 1999).

Later studies examining the role of antibodies directed to GluA3 in RE have not reinforced these initial findings. Studies showed that GluA3 antibodies were present but not limited to RE and could be found in other focal epilepsies with or without an autoimmune aetiology (Mantegazza *et al.,* 2002, Wiendl *et al.,* 2001). Similarly, Watson *et al.* (2004) concluded that GluA3 antibodies were only infrequently found in RE and intractable epilepsy using tests such as immunoblot and immunoreactivity to rat brain sections. Use of ELISAs showed that RE sera showed the same immunoreactivity to the GluA3B epitope as a scrambled GluA3B peptide. Furthermore, it was found that none of the RE sera tested was able to elicit kainate receptor activation as had previously been reported, following incubation with GluA3 transfected oocytes. The application of anti-GluA3 IgG purified from a RE patient on dissociated neocortical neurons cultured from rats did not show any demonstrable effects (Frassoni *et al.,* 2001).

However, these negative results do not exclude a potential autoimmune role in this disease, as there are many limitations to the studies conducted. Testing of immunoreactivity to protein extracts via immunoblots and ELISA only investigates the binding of antibodies to denatured protein, and can therefore give skewed results. Binding of HC sera to GluA3 protein extracts and peptide sequences has also been shown, highlighting the fact that “false positive” results can occur from using these techniques. Furthermore, the absence of binding of some samples to denatured proteins may result from the inability of the antibodies to recognise epitopes that are no longer conformational. While relapses have been noted, there is marked neurological improvement of patient’s symptoms when started on immunomodulatory treatment. There still exists the possibility that other unidentified antigen targets may be the target of antibodies in this disease.

1.6.4.3: Other antibodies described in RE and a role for autoimmunity

Antibodies to the α-7 subunit of the AChR were found in two patients with RE, who responded well but transiently to PEX. Electrophysiological studies showed that the sera from these two patients were able to block the function of the α-7 AChR directly (Watson *et al.,* 2005), similar to AChR antibodies in arthrogryposis (Riemersma *et al.,* 1996).

Munc-18 is an intracellular neuronal protein essential for synaptic vesicle release and mutations in this gene result in early infantile epileptic encephalopathy. While antibodies to Munc-18 have been described in a few RE cases (Alvarez-Baron *et al.,* 2008 and Yang *et al.,* 2000), the intracellular localisation of the protein makes it an unlikely primary target, though it could be a biomarker of the disease.

Neither of these antibodies represents a feasible primary pathogenic role in RE.

1.6.4.4: T-cell mediated role

It is now well established that RE is predominantly a T-cell mediated disease. Histopathological analysis of RE tissue has shown that there is T-cell deposition (Farrell *et al.,* 1995), of which the majority of cells are CD8 positive (cytotoxic) and are granzyme B-positive. Spectra-typing of the T- cells from brain lesions has revealed that these cells have expanded from discrete antigenic precursor T- cells (Li *et al.,* 1997). Granzyme-B vesicles are cytotoxic granules and it is noted that these granules lie in close apposition to neurons and astrocytes, towards the cell membrane (Bien *et al.,* 2002). This cytotoxic T lymphocyte attack, could lead to the neuronal loss observed in RE patients, resulting in symptomology. Gharing *et al.* (2001) began preliminary investigations and suggested that the GluA3B region would become exposed upon cleavage of protein by granzyme B. In other words, proteolytic effects of granzyme B would be causing autoimmunity. A follow up to these studies has not been reported.

As such, knowing and understanding the antigenic target in this disease is important. It is possible that if a role for antibodies exists in RE, it may result from the development of antibodies triggered by the lysis of cells due to T-cell attack. For this hypothesis to hold true, intrathecal synthesis (rather than synthesis intraperitoneally) would need to occur and therefore it is important that CSF samples be tested.

1.6.5: Role of antibodies directed against AMPAR in neurological disorders

Antibodies to the GluA1 and GluA2 subunits of the AMPAR were first described by Lai *et al.,* (2009) in a subset of LE patients. Ten of 43 patients with clinically defined LE showed a distinct IHC pattern when applied to rat brain sections. CSF from these patients showed strong immunolabeling of the hippocampus, cerebral cortex and cerebellum in a manner distinct from NMDAR antibody positive patients. In addition, sera and CSF from these patients showed strong reactivity to the surface of hippocampal neurons. The target antigen was immunoprecipitated following incubation of patient sera with rat hippocampal neurons. When the precipitated material was analysed via mass spectrometry, it was revealed that the antibodies present in the sera bound to the GluA1 and GluA2 subunit of the AMPAR and immunoblotting confirmed the results showing that patients had antibodies to both subunits. Patient sera and CSF from patients with LE was tested for reactivity to HEK cells transfected with the single subunits and cotransfected cells. It was revealed that 6 patients had GluA2 antibodies, 3 had GluA1 antibodies and 1 patient had antibodies to both GluA1 and GluA2. None showed reactivity to GluA3 transfected HEK cells. Nine of the patients were female and the average age of all patients was 60 years old. Seven patients had tumours (3 thymoma; 2 breast cancer; 2 SCLC), and 4 of the patients had seizures. While patients responded well to immunotherapy (6 patients were also treated for their tumour), relapses were

common (5/9), with the time following relapse ranging from 2-10 months. Patients that continued to suffer from neurological symptoms following the removal of the GluA1/GluA2 antibodies, also had additional antibodies.

Subsequent studies have also documented AMPAR antibodies in two patients suffering from acute psychosis without seizures (Graus *et al*., 2011). Both patients were women aged 60 and 58 years old, with one of the patients having a thymoma, and treatment of patients with corticosteroids resulted in recovery.

In a recent publication by Gleichman *et al.* (2014) the antigen epitope was investigated. Patients with AMPAR antibodies were detected using a fusion protein (FP)-based western blotting test, and a CBA, in which HEK cells were transfected with deletion mutants of AMPAR subunits. CSF from patients in the original publication (Lai *et al.,* 2009), showed strong reactivity to HEK cells transfected with amino-terminal domain (ATD) constructs; more specifically the lower lobe of the ATD. A further 15 patients were identified using the immunoblots and CBA, though the antigen reactivity pattern was much broader, with the primary area of immunoreactivity was in the S2 region (lower region of the ligand binding domain). The newly identified cohort also had symptoms such as seizures and memory loss that were consistent to symptoms described in the original cohort. However unlike previous reports, there were an equal number of men and women and a greater age range (with 6 patients under the age of 30).

While these antibodies are very rare, the pathogenic potential has been documented. In the original publication *in vitro* experiments showed that the application of AMPAR antibody positive CSF (1:15) to primary hippocampal neurons for 6 days causes an internalisation of AMPAR subunits (noted by a reduction of GluA2/3 clusters colocalising with the postsynaptic marker PSD-95). If patient CSF was removed from cultures, and neurons were then exposed to control CSF, the GluA2/3 cluster number

increased again, showing that the internalisation effect is reversible. This effect is specific to the AMPAR as the NMDAR levels were unaffected (Lai *et al.,* 2009). Following incubation of cultured hippocampal neurons for up to 36 hours with IgG (100 μg/ml) purified from two patients, one from the original cohort (Lai *et al.,* 2009) and one a new patient (Gleichman *et al.,* 2014), mEPSCs were shown to be reduced in both cases. Despite these patients showing reactivity to different regions of the GluA2 subunit, IgG from both patients caused an increase in the inter-event interval and decreased peak amplitude in comparison to control IgG treated neurons, suggesting that antibodies from these patients caused a reduction in the AMPAR surface levels.

1.7 $GABA_BR$ and their role in autoimmune CNS disorders

1.7.1: $GABA_BR$ structure and expression

Gamma-aminobutyric acid (GABA) is a chief inhibitory neurotransmitter of the CNS, though dependent on the synapse, GABA can also have excitatory effects. GABA is able to mediate transmission through the ionotropic $GABA_AR$ and $GABA_CRs$ and the metabotropic $GABA_BRs$. The ionotropic group of GABARs mediate hyperpolarization, through chloride permeability.

On the other hand, the $GABA_BR$ are G-protein coupled receptors, and inhibit adenylate cyclase activity. These receptors are located both pre and postsynaptically, at glutamatergic and GABAergic synapses. In the brain these receptors are ubiquitously expressed with high levels in the hippocampus, cerebral cortex, hypothalamus, pituitary and cerebellum (Berranoch, 2011). $GABA_BR$ are also found at lower levels of expression in the heart, kidneys, pancreas, small intestine, thymus and mammary gland (Kaupmann *et al.,* 1998).

These receptors are comprised of two subunits $GABA_{B1}R$ and $GABA_{B2}R$, which form heterodimers through interactions of their intracellular C-terminus tails and extracellular ATDs. A schematic of the structure is shown in Figure 1.5. The $GABA_{B1}R$ subunit binds agonists such as GABA and baclofen and antagonists such as 3-aminopropyl (diethoxymethyl) phosphinic acid (CGP). Two isoforms of the $GABA_{B1}R$ subunit exist (B1a/ B1b), with a higher concentration of the $GABA_{B1a}R$ isoform at glutamatergic synapses, where they prevent the release of glutamate. Receptor isoform $GABA_{B1a}R$ is mostly expressed in the granular cell layer and molecular layer of the cerebellum, whereas isoform $GABA_{B1b}R$ is found predominately in the Purkinje cells. $GABA_{B2}R$ isoform mediates downstream signaling, as it couples the receptor with the effector G protein. Binding of agonists or antagonists causes a conformational change in the extracellular regions of the subunits causing the activation of down-stream signaling (for a full review see Berranoch, 2011). Synaptic inhibition via activation is mediated through the presynaptic VGCC and post-synaptic potassium channels (Wang, 2000).

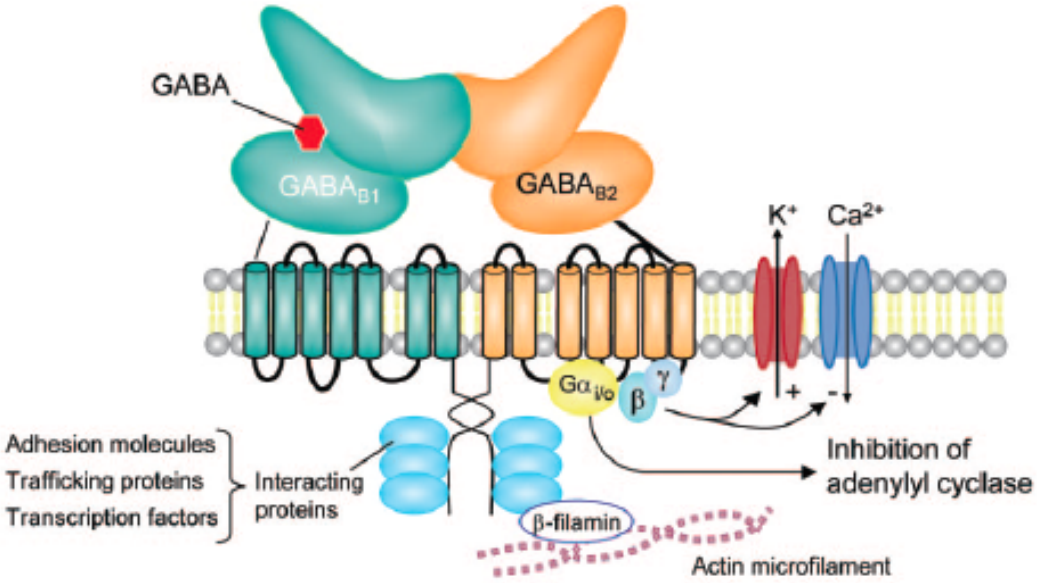

Figure 1.5: Structure of GABA$_B$R

GABA$_B$R are heterodimers formed by GABA$_{B1}$R and GABA$_{B2}$R subunits. Each subunit has a large extracellular domain and a central core domain made up of 7 transmembrane helices. The GABA$_{B1}$R subunit binds agonists and antagonists, while the GABA$_{B2}$R subunit is important in mediating downstream effects thought to be predominately through modulation of presynaptic VGCC and postsynaptic K$^+$ channels. Image taken from Benarroch, 2011.

1.7.2: GABA$_B$R: Function and knockout models

Spontaneous epileptic seizures are noted in all GABA$_{B1}$R -/- (knockout) mouse strains, though strain differences in viability have been reported. Using electroencephalogram (EEG) telemetry, Schuler *et al.* (2001) showed that adult mice were hyperactive and displayed abnormal periods of hyperexcitability and spontaneous seizures (both absence and tonic clonic seizures were noted). The GABA$_B$R agonist baclofen, which reduced EPSC amplitude in wild-type mice, showed no effect in mutant mice. In addition, baclofen and the GABA$_B$R antagonist CGP5626A had no effect on outward current. In another report, GABA$_{B1}$R knockout mice were found to be normal at

birth, but by post-natal day 21 the presence of spontaneous generalized seizures, provoked by mild stimuli was noted, resulting in premature death (Prosser *et al.,* 2001). Interestingly, in this same study it was noted that $GABA_{B1}R$ +/- did not develop seizures, despite a 40% reduction in subunit expression. Interestingly, $GABA_{B2}R$ expression is down regulated in $GABA_{B1}R$ knockout mice, making it difficult to discern whether or not the phenotype is purely due to the loss of one subunit. While it is suggested that $GABA_{B2}R$ subunits are not functional in isolation, it is proposed that the symptoms noted in these knockout animals is due to an overall loss of $GABA_BR$ (Prosser *et al.,* 2001).

Higher working functions rely on persistent neuronal activity (Major and Tank, 2004), which is the sustained change in action potential discharge that outlasts a stimulus. Network mechanisms in specific brain regions generate persistent neural activity. While asleep, neurons remain active and cortical neurons fluctuate between active Up states, and quiescent Down states (Massimini *et al.,* 2004). During the Down states, cortical neurons are hyperpolarized for a few milliseconds, and during the active state, the membrane potential is restored back to firing threshold and Up states occur. The oscillations between Up and Down states (UDS) are initiated, maintained and terminated intrinsically (Timofeev *et al.,* 2000). In the entorhinal cortex, UDS are maintained in brain slices *in vitro* (Cunningham *et al.,* 2006), and controlled by GABA receptors (Mann *et al.,* 2009). Application of increased concentrations of the $GABA_AR$ antagonist gabazine resulted in decreased Up state activity eventually leading to epileptiform activity. In contrast, application of the $GABA_BR$ antagonist CGP55845 resulted in increased Up state duration, suggesting $GABA_BRs$ are critical for Up to Down state transitioning. The roles of $GABA_{B1}$ receptor isoforms B1a and B1b have been dissociated further (Craig *et al.,* 2013). Both $GABA_AR$ and $GABA_BR$ are important in the maintenance and termination of UDS, and modulation of these receptors could disrupt this cortical network, leading to encephalopathic and epileptiform activity.

1.7.3: Role of antibodies directed against $GABA_BR$ in neurological disorders

Antibodies to the $GABA_BR$ were first described by Dalmau and colleagues in 2010. Fifteen patients with LE who presented with seizures were noted to have a distinct immunostaining pattern (different from patients with antibodies to VGKC complex or NMDAR) when applied to brain sections. In particular, high immunoreactivity was observed in the hippocampus, the cerebellum, the cerebral cortex and thalamus, with sparing of the corpus callosum.

Serum from two patients with this unique staining pattern were used to immunoprecipitate proteins from cultured rat hippocampal neurons. Using mass spectrometry, the $GABA_BR$ was identified as the target in these patients. A CBA was established by transfecting HEK cells with either $GABA_{B1}R$, $GABA_{B2}R$ or both subunits. Screening revealed that all 15 patients had antibodies to the $GABA_{B1}R$ subunit, with one additional patient having antibodies to the $GABA_{B2}R$ subunit as well. Three of these patients had antibodies that were only detectable in the CSF. Antibodies were predominately of the IgG1 subclass. Seven of 15 patients had lung tumours (5 of which had SCLC), and 9 of the 10 patients that were started on immunotherapy showed a positive neurological outcome.

Boronat *et al.* (2011) described an additional 17 patients with LE (143 samples tested). Fifteen/17 of these patients had SCLC. GAD antibodies were identified in two patients with $GABA_BR$ antibodies. These two patients with GAD antibodies also had a SCLC, suggesting that at least in these patients the presence of both GAD and $GABA_BR$ antibodies is dependent on the presence of a tumour. $GABA_BR$ antibodies were not routinely found in GAD antibody associated diseases such as SPS or cerebellar ataxia. Antibodies were detected in both sera and CSF taken from 5 patients. Only one patient with both antibodies was identified in a nonparaneoplastic case of reversible cerebellar ataxia (Boronat *et al.,* 2011).

While $GABA_BR$ antibodies have predominately been described in patients with an LE phenotype, a recent publication described a case series of 20 patients with encephalitis, but with additional symptoms noted in 3 patients (Hoftberger *et al.,* 2013). Here, 17 patients presented with symptoms typical of LE; seizures, memory and cognitive impairment. In addition, one patient presented with status epilepticus (SE), one patient with ataxia, and one patient presented with opsoclonus-myoclonus syndrome (OMS). The patients that presented with ataxia and OMS went on to develop LE. Here, 50% (10/20) of patients had SCLC, and 15 of 19 (6 with SCLC) patients that were started on immunotherapy showed recovery from their symptoms. Seven of the 8 patients that died had SCLC. Of note was the absence of $GABA_BR$ antibodies in a cohort of 116 SCLC samples without neurological symptoms.

The prevalence of $GABA_BR$ antibodies was investigated by Jeffrey *et al.* (2013). Patients were detected from 3 groups of patients. Group 1: Screening of 3939 samples with suspected autoimmune encephalitis (17 positive patients). Group 2: Screening of 49 patients that showed a distinct staining pattern on rat brain sections (5 positive patients). Group 3: Screening of 384 SCLC patients (5 positive patients). In all of the Group 3 patients identified, additional antibodies were also detected. Group 3 patients also had the lowest titres (end point titration of 1:256), and the neurological symptoms were more varied than those in Group 1 that presented with a typical LE phenotype.

The good response to treatment that many of the patients show is suggestive that these circulating $GABA_BR$ antibodies are pathogenic. However, preliminary investigations suggest that these antibodies do not cause an internalisation of the receptor, as has been observed with NMDAR and AMPAR antibodies (results not shown; Lancaster *et al.,* 2010). As such, these antibodies may be mediating their pathogenic effects through the activation of the complement cascade, or through direct modulation of the receptor. Alternatively, these antibodies may be “bystander”

antibodies that are produced because of the expression of $GABA_BR$ on the surface of tumour cells (in paraneoplastic cases), but are not having a primary causative role. The presence of neuronal surface expressed co-immunogens such as N-type VGCC antibodies (Jeffrey *et al.,* 2013) may be contributing to the disease.

1.8: Section 1 objectives

Over the last 15 years, the presence and relevance of autoantibodies in CNS disorders has become increasingly recognised. Antibodies directed against the AMPAR and $GABA_BR$ have only been newly described and the symptoms associated with and the potential pathogenic mechanisms of these antibodies needs to be explored in greater detail. As such, the aim of this thesis was:

1). To establish a cell based assay (CBA) that can be utilised for the detection of AMPAR and $GABA_BR$ antibodies. This technique would be beneficial for screening of patient samples, as the receptors are expressed conformationally at the surface of the cell.

2). To evaluate the frequency of these antibodies in both selective cohorts and also samples with suspected autoimmune aetiology sent to our laboratory for diagnostic testing. Select cohorts include Rasmussen encephalitis, small cell lung carcinoma, opsoclonus myoclonus syndrome and new onset epilepsy samples.

3). To begin preliminary investigations into the potential pathogenic mechanisms of these antibodies by:

- Immunolabeling of rat brain sections with patient sera and CSF to investigate the regional specificity
- Investigate reactivity of AMPAR and $GABA_BR$ antibodies to primary neuronal cultures

- Explore by CBA and reactivity to primary cultures, whether AMPAR and $GABA_BR$ antibodies have the potential to cause receptor loss from the cell-surface via internalisation and/or activation of the complement cascade
- Finally, explore the direct effects of $GABA_BR$ on cortical networks in the entorhinal cortex using whole cell electrophysiological recordings

CHAPTER 2: METHODS

2.1: Plasmid constructs and commercial antibodies

2.1.1: Plasmid constructs

Plasmid constructs encoding the human sequences of GluA1, GluA2 and $GABA_{B1}R$ were cloned by Dr. Patrick Waters. The GluA3 construct used in these experiments was synthesized by Dr. Robert Watson and Dr. Bethan Lang (Watson *et al.,* 2004). The $GABA_{B2}R$ construct was a gift from Dr. Christian Probst (Euroimmun). A list of all of the constructs used for the establishment of the CBAs, and the vectors each of the plasmids are cloned in are listed in Appendices Table 1.

All other constructs used; CASPR2 (pEGFP-N1), LGI1-CASPR2 tail (pcDNA3.1), and the NMDAR subunits NR1 and NR2B (pcDNA3.1) have been described previously (Leite et al. 2008; Irani et al. 2010a). Combined heteropentameric $GABA_AR$ (α1, β2, γ2-subunits plasmids (all pcDNA3.1)) were cloned by Dr. Bethan Lang, Dr. David Beeson, Dr. Philippa Pettingill and Dr. Patrick Waters (Pettingill *et al.,* 2014; under submission).

2.1.2: Commercial antibodies

Primary and secondary antibodies used in this thesis are listed in the Appendices; Table 2 and Table 3, respectively.

2.1.3: Transformation of E. Coli competent cells

1 μl of DNA was added to 50 μl of E. Coli JM109 competent cells (Promega; L2001), and incubated for 10 minutes on ice. Cells were placed in a 42°C incubator for one minute to ensure heat shock transformation, and then placed back on ice for 2 minutes. 400 μl Luria-Bertani Broth (LB; 10 g/L Tryptone, 5 g/L Yeast Extract, 5 g/L NaCl; Promega) was added to the cells, and incubated in a 37°C shaking incubator for

one hour. 100 μl of the bacterial suspension was spread onto LB agar plates supplemented with the appropriate antibiotic at a 1:1000 dilution. Colonies were grown for 16-18 hours in the 37°C incubator.

Starter cultures were prepared by inoculating 5 ml of LB with one colony from the agar plates and grown for 3-5 hours at 37°C. When grown, the inoculum was transferred to a larger volume (400-600 mls of LB) for larger scale DNA preparations. DNA was purified using Promega Maxiprep kit (A2393)

2.1.4: DNA Sequencing

All DNA sequencing was carried out by the WIMM DNA sequencing service, Department of Biochemistry, University of Oxford using a 48 capillary AB1-3730 DNA analyser. All sequences were viewed and analysed using the sequencing program ChromasPro (Technelsyium).

2.2: Tissue Culture

For sterility, all tissue culture procedures were carried out in a UniMAT-BS Class II microbiology fume hood. Phosphate Buffer Saline (PBS), distilled water, pipette tips, and any other glass material were autoclaved prior to use. All media was purchased from Lifetechnologies (Thermo Fisher Scientific) and chemicals from Sigma Chemical Company unless otherwise stated.

2.2.1: HEK cells

Human Embryonic Kidney Cells 293T (HEK293) were cultured in Dulbecco's Modified Eagle's Medium (DMEM) containing Fetal Calf Serum (FCS,10 %v/v) and Penicillin/Streptomycin/Amphotericin B (PSA,1 %v/v) in T175cm^2 flasks (Corning) at

37°C in 5% CO_2. Cell lines were passaged at 80-90% confluency. In order to subculture monolayer cell cultures, old media was aspirated and 0.5 %v/v of trypsin in PBS was added to the flasks and incubated at 37°C for 5 minutes. Flasks were tapped to dislodge any cells that remained attached to the plastic surface. New media was added to deactivate the trypsin after which cells were spun at 1200 rpm (revolutions per minute) for 5 minutes (Thermo Heraeus Labfuge 400). The supernatant was removed, new media was added and the solution was resuspended by pipetting up and down. Cells were then diluted appropriately with new media and added to a new flask. All HEK cells were maintained and grown in a humidified 37°C, 5% CO_2 incubator, and the same HEK cells were passaged no more then 20 times.

2.2.2: Transfection of HEK cells

6-well plates (GIBCO) containing coverslips, and flasks were coated with poly-L-lysine solution (PLL 1 %v/v in PBS) prior to plating out. After removing the PLL solution and allowing coverslips to dry, approximately 3.5-5 x 10^5 HEK cells/well were plated out in 2-3 mls of media. Approximately 1.2 x 10^6 HEK cells were seeded out in a T175 cm^2 flask. After allowing the HEK cells to reach 40-50% confluency, the cells were transfected with plasmids containing the DNA of interest using polyethylenimine (PEI). Typically, for 6 well plates, 3 μg of DNA, 50 μl of DMEM and 1.5 μl of PEI per well were mixed and incubated for 5 minutes, after which approximately 50 μl was added to each well. For transfections involving T175 cm^2 flasks, 60 μg of DNA, 30 μl of PEI and 1 ml of DMEM were used per flask.

2.3: Immunofluorescence on transfected HEK cells

2.3.1: Cell based assay (CBA)

Transfected cells, grown on PLL-coated coverslips, were placed in 24 well plates containing serum (1:20 or 1:100) or CSF (neat-1:10) diluted in 250 μl of DMEM, supplemented with bovine serum albumin (BSA) (1 %v/v) and 4-(2-hydroxyethyl)-1-piperazineethanesulfonic acid (HEPES 2.3 g/500ml DMEM). After a one hour incubation at room temperature (RT), the supernatant was aspirated and coverslips were washed 3 times in 250 μl DMEM+HEPES. Cells were fixed for 10 minutes with 250 μL of 4% formaldehyde in PBS, washed 3 times in PBS to remove the formaldehyde solution and then incubated for 45 minutes in the dark at RT with 250 μl of secondary antibody (goat anti-human IgG (H+L chain), Alexa Fluor 488 or 568) diluted 1:750 in DMEM+HEPES+BSA. The coverslips were washed 4 times in PBS, mounted on glass slides using fluorescent mount media, containing 4', 6-diamidino-2-phenylindole (DAPI; 1:1000), and left to dry. Cells were viewed under an immunofluorescent microscope and binding was scored from 0-4 (0= no binding, 1= very weak binding, 2= moderate binding, 3=strong binding, 4=very strong binding), with the cut off for positivity as 1 for all the assays (Figure 2.1 and 2.2).. The imaging software Image J (Wayne Rasband, National Institutes of Health, USA) was used to quantify the number and positivity of positively labelled fluorescent cells.

Positive samples were serially diluted (1/3 dilution) and end-point titres were obtained (dilution at which binding could no longer be detected).

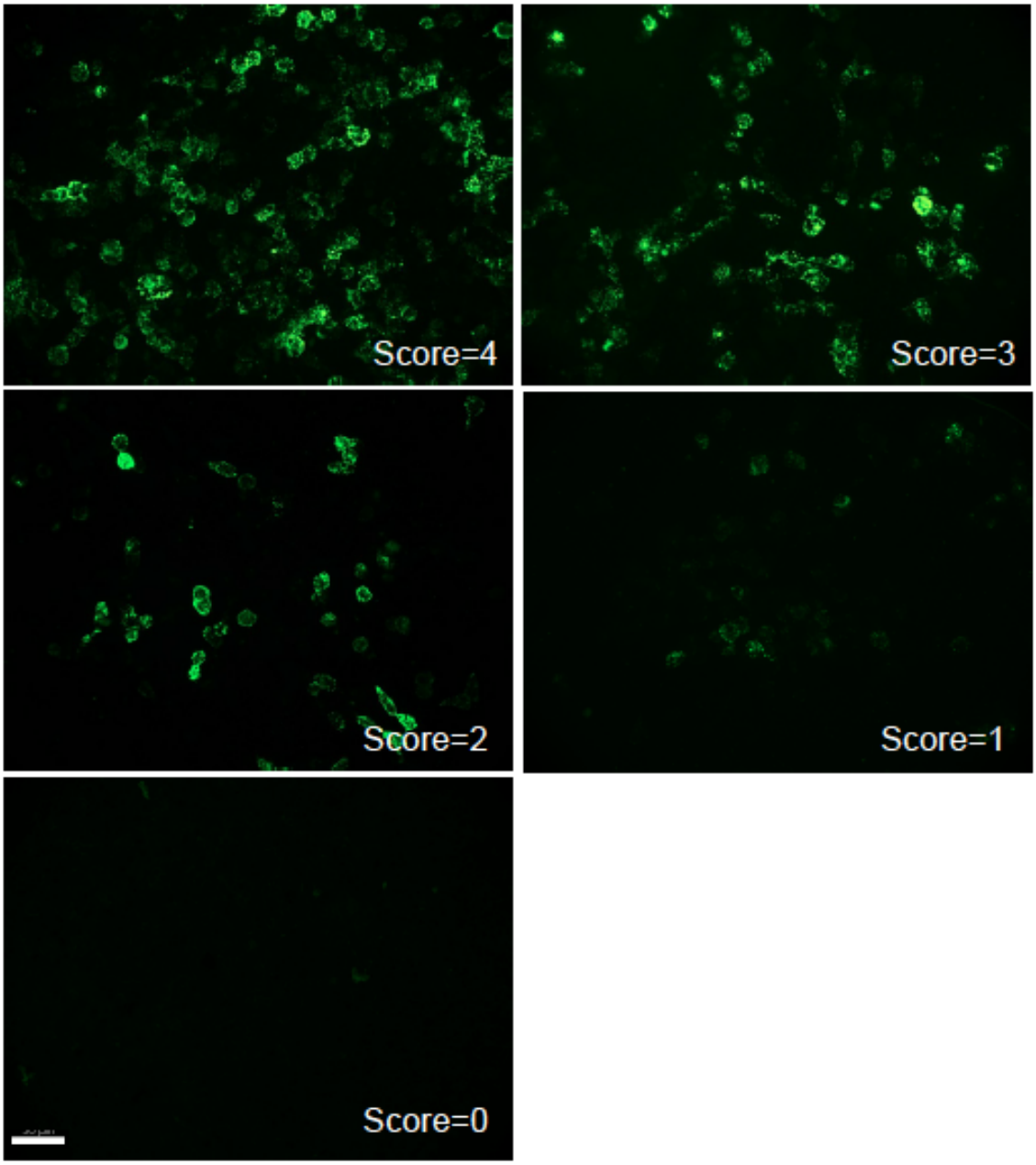

Figure 2.1: Scoring system used for the in house diagnostic AMPAR CBA

Representative staining of AMPAR antibody positive patients with scores ranging from 1-4 on GluA1+2 transfected HEK cells. Healthy control samples did not show reactivity to transfected cells (Score=0). Scale bar =50 µm

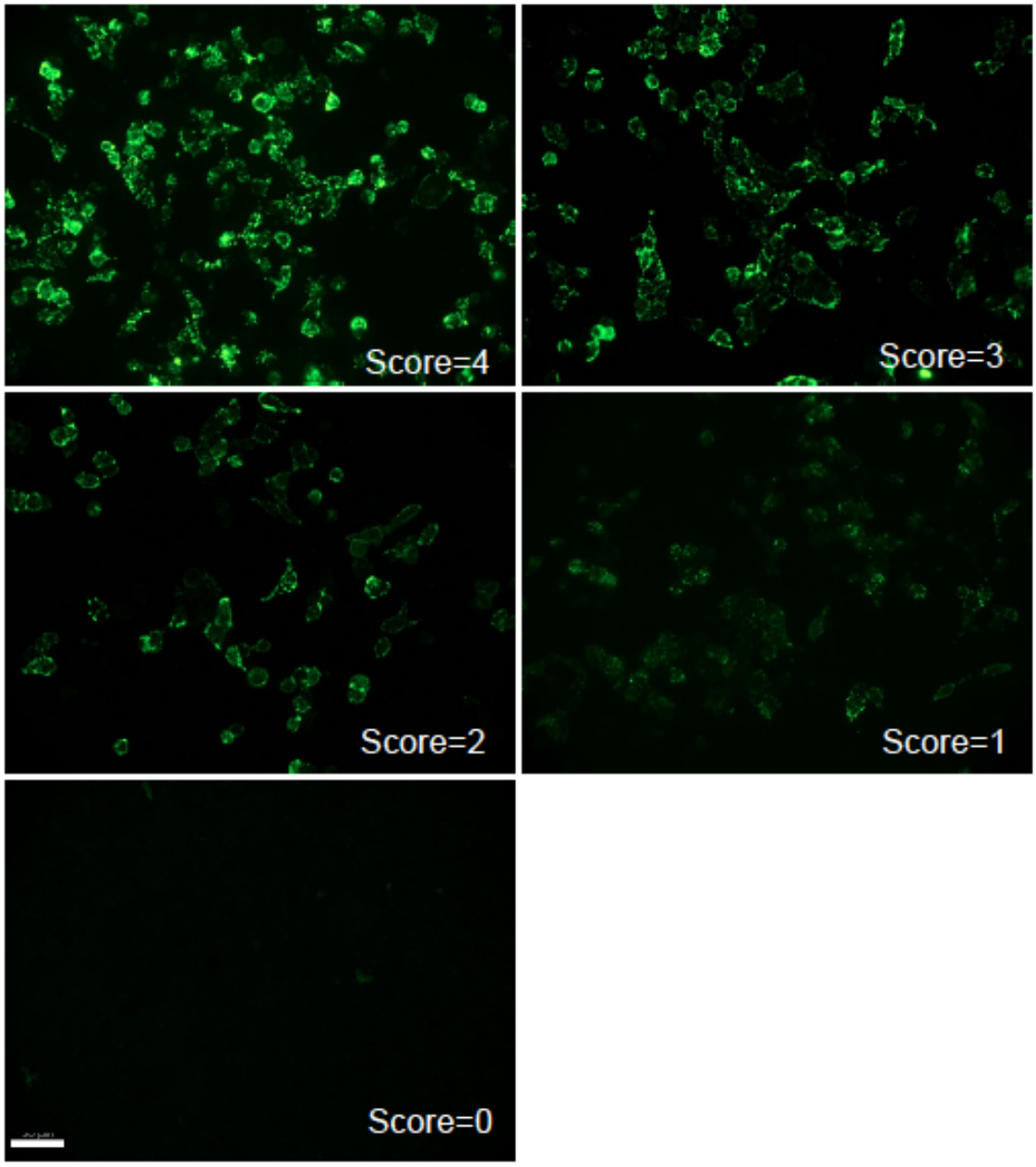

Figure 2.2: Scoring system used for the in house diagnostic $GABA_BR$ CBA

Representative staining of $GABA_BR$ antibody positive patients with scores ranging from 1-4 on $GABA_{B1+2}R$ transfected HEK cells. Healthy control samples did not show reactivity to transfected cells (Score=0). Scale bar =50 µm

2.3.2: Subclasses

IgG subclass specificity was determined by CBA. Sera was incubated with transfected HEK cells, washed and fixed as described in 2.3.1. However, instead of the addition of secondary anti-human IgG, the cells were incubated with commercial mouse antibodies directed against epitopes specific to IgG1-4 (Binding Site, UK) at a 1:50 dilution in DMEM+HEPES+BSA for one hour. To visualize binding, coverslips were incubated with a secondary antibody (goat-anti mouse IgG Alexa Fluor 568) at a 1:750 dilution in DMEM+HEPES. All incubations were carried out at RT and binding was scored using the same system as with the CBA.

2.3.3: Complement fixation

For detection of deposited complement on transfected cells, patient sera was heat inactivated at 57°C for 30 minutes, prior to incubation (1:20 or 1:100 for 37°C for 30 minutes) with HEK cells transfected with either AMPAR or $GABA_BR$ subunits. Fresh human sera (used as a source of complement), was incubated with HEK cells at 4°C for 30 minutes in order to reduce nonspecific complement activation prior to application to the transfected cells. Coverslips were subsequently fixed and incubated with an anti-complement antibody (rabbit anti C3c; 1:250 (DAKO)) for 45 minutes washed and incubated with a secondary antibody (goat-anti rabbit Alexa Fluor 568 IgG (1:750)) for 30 minutes. Coverslips were washed and mounted and binding was scored using the same system as with the CBA.

2.3.4: Preadsorption experiments

HEK cells were grown and transfected in T175 cm^2 flasks as above. Approximately 36 hours following transfection, cells were removed by scraping and re-suspended in DMEM+HEPES. Based on the antibody end-point titres of the given sample, the number of cells required to absorb out the antibody was determined. Approximately $1x10^7$cells/ml were pelleted and incubated (while rotating) with 250 µl of

sera (1:10) in DMEM+HEPES for approximately one hour. To ensure full absorption samples were sequentially transferred from one pellet of cells to the next, resuspending the cells in each mixture, typically at least 5 times, and the supernatant was collected each time by centrifugation (1300rpm, 4 minutes). Absorbed samples were tested on the CBA at the optimal dilution for the assay (1:20 and 1:100 for AMPAR and $GABA_BR$, respectively). In some instances, absorbed samples were also tested at a 1:100 dilution on primary neuronal cultures.

2.3.5: Euroimmun slides

Samples were tested on Euroimmun commercial slides (Euroimmun, Lubek, Germany) as per instructor's manual. Briefly, slides included biochips of formalin fixed HEK cells transfected with AMPAR (GluA1 or GluA2), LGI1, CASPR2 and $GABA_{B1}R$. NMDAR transfected cells are acetone fixed. Patient sera were diluted 1:10 in PBS-Tween, and CSF was tested undiluted. Diluted samples were incubated with cells for 30 minutes at RT after which slides were washed with PBS-Tween for 5 minutes. Bound primary antibody was visualised using the same secondary antibody as the in house CBA; goat anti-human Alexa Fluor 488 (1:750). Binding was visualised using an immunofluorescence microscope as outlined in 2.3.1.

2.4:VGKC-complex radioimmunoprecipitation assay (RIA)

Testing for VGKC-complex antibodies was accomplished using a radioimmunoassay (as described previously Vincent *et al.,* 2004) . Dr. Bethan Lang completed all VGKC-RIAs described in this thesis. Briefly, VGKC-complexes were extracted from rabbit whole brain membranes and solubilised in 2% digitonin (Calbiochem, USA) in DTX buffer (100mM NaCl, 20 mM Tris, 5 mM KCl adjusted to pH

7.12). Solubilisation was carried out in a 37°C water bath for 30 minutes. The membranes were centrifuged at 13,000rpm for 10 minutes. The supernatant was collected and subsequently diluted 2:1 in PTX (0.02 M phosphate buffer, 0.1% Triton X100, pH 7.2), after which complexes were labelled with ^{125}I-α DTX at 1 x 10^6 counts per minute (cpm) per ml of extract. 50 µl of labelled extract was incubated with 1µl and 5 µl of each sample being tested, and the total volume was made up to 50 µl with PTX. Samples were incubated overnight at 4°C. Secondary antibodies (50 µl of goat anti-human IgG (Binding Site, UK)) were added to each reaction the following morning. After 90 minutes, 500 µl of PTX was added to each reaction and the antibody-antigen complex was immunoprecipitated by centrifugation at 13,000rpm for 5 minutes. The supernatant was discarded and the pellet washed twice in PTX (500 µl), after which the pellets were counted using a Cobra 2 gamma counter (Perkin Elmer).

2.5: Cell surface protein isolation

Proteins expressed at the cell surface were isolated using a biotinylation kit (Thermo scientific 21445). Briefly, HEK cells were transfected in T75 cm^2 flasks. The cells were biotin labelled with a thiol cleavable biotinylation reagent (EZ-Link® Sulfo-NHS-SS-Biotin) for 30 minutes at 4°C. Cells were then harvested, and lysed on ice for 30 minutes, vortexing every 5 minutes. Biotin-labelled cell surface expressed proteins were captured, via incubation with neutravidin agarose beads for one hour at RT. Unbound proteins (intracellular proteins) were collected in the flow through. Bound proteins were eluted in sodium dodecyl sulphate ((SDS)-Page sample buffer; Invitrogen)) with 50 mM DTT and analysed via western blots.

2.6: Gel electrophoresis and western blotting

2.6.1: Sample extraction

Media was aspirated from transfected HEK cells and extraction buffer (1% Triton X-100, 10 mM Tris pH 8.0, 100 mM NaCl, 1 mM EDTA) supplemented with protease inhibitor cocktail (PIC, 1:1000), was added to the cells (500 µl for 6-well plates and 3 mls for T175 cm^2 flasks). Cells were rotated at 4°C for one hour prior to centrifugation at 13,000rpm for 10 minutes, and supernatants stored at -20°C until use.

2.6.2: Sample preparation and western blotting

Samples were diluted in SDS-loading buffer (1:4) and sample reducing agent (1:10; NuPAGE Invitrogen) and boiled for 10 minutes at 95°C. Samples were centrifuged at 13,000g for 2 minutes to remove insoluble material and supernatants were collected for analysis. 4-12% NuPAGE BisTris or 3-8% NuPage Tris-Acetate polyacrylamide gels were used in experiments with 1X MES buffer or 1X Tris-Acetate running buffer, respectively (all Invitrogen). Lanes were loaded with 10-20 µl of sample, or 5-10 µl of the molecular weight markers Seeblue plus prestained marker or HiMark™ protein standards (both Invitrogen). Gels were run for approximately 90 minutes at 150 mV. Gels were carefully removed and protein was subsequently transferred to nitrocellulose paper for approximately 90 minutes at 30 mV in 1X transfer buffer (Invitrogen).

Nitrocellulose membranes were washed three times in PBS containing 0.1% Tween (PBST) prior to incubation with the blocking agent (5% milk powder (Marvel)) for one hour at RT. Membranes were washed in PBST and incubated with primary antibodies (see Appendix Table 2 for dilutions) overnight at 4°C. The membranes were washed 3 times for 5 minutes in PBST before HRP-conjugated anti-species IgG (1:2000) were incubated with membranes for 45 minutes at RT. Membranes were washed a final 3

times for 5 minutes in PBST and incubated with ECL (Pierce 32106) for one minute. The membranes are exposed to photographic film (Amersham) and the signal visualised.

2.7: IgG Purification

IgG was purified from patient plasma/sera (dependent on volumes available) using Protein G-coupled Sepharose beads (Sigma). Plasma/sera was heat inactivated for 30 minutes at 56°C, filtered to remove particulate matter, diluted in Hartmann's solution (1:4), and incubated at approximately 0.5 mls of Protein G-Sepharose beads per 1 ml of patient plasma/sera overnight at 4°C. The following morning, the plasma and beads were run slowly (approximately 0.2 mls/minute) through a glass column to separate the beads, and the flow through was collected. Beads were washed extensively with Hartmann's solution until no further protein was detected in the flow-through. The IgG was serially eluted from the beads in 0.1 M glycine (pH 2.3) solution, and fractions (1ml) were collected and neutralised immediately in 100 µl of 1 M Tris (pH 8) on ice. The protein content in each of the fraction was determined. Fractions containing protein were pooled and dialysed (Snakeskin dialysis tubing; 10,000kDa ThermoScientific 88243) against Hartmann's solutions (5 x 500 ml, changed every 30 minutes) at RT. IgG was collected, filtered and aliquots were stored at 4°C until use.

2.8: Primary cultures

2.8.1: Dissections

All hippocampal and cortical culturing procedures were carried out using postnatal day 0 (P0) Sprague-Dawley rat pups. Briefly, rat pups were decapitated and brains were removed from the skull quickly and placed on ice cold Hank's Balanced Salt Solution (HBSS; Gibco Life Technologies). From each brain the hippocampi and

cortices were dissected out, the meninges were removed and tissue was added to 2.5% trypsin in HBSS for 15 minutes at 37°C. The trypsin-HBSS solution was removed from the cells and MEM (Gibco), supplemented with FCS (10%) and PSA (1%), was added to inactive the trypsin. Cells were centrifuged at 1000 rpm for 5 minutes and then titrated with a 1000 µl and 200 µl pipettes. MEM was added to cells and adjusted to give a concentration of approximately $2.5x10^5$ cells/ well (approximately one hippocampi per well). MEM was replaced with neurobasal media (NB, supplemented with B27, 200 mM L-glutamine and PSA), approximately 3 hours following seeding out.

2.8.2: Staining primary cultures

Hippocampal neurons were grown on glass coverslips and staining was generally carried out on 14-18 days *in vitro* (div) neurons. Staining of cortical neurons was carried out on 10-13 div cultures. Patient sera (1:100 in NB +1%BSA) was incubated with live hippocampal neurons for one hour. Neurons were washed and fixed with 3% formaldehyde for 10 minutes and then incubated with a secondary antibody (goat anti-human IgG Alex Fluor 488; 1:1000) for 45 minutes in the dark. Neurons were permeabilised for 15 minutes in 0.25% Triton-X100 in PBS (PBST), followed by incubation with microtubule-associated protein 2 (MAP2; a neuronal marker) at 1:1000 for one hour. Finally, cells were incubated with anti-mouse Alexa Fluor 568 (1:1000) for 45 minutes, in the dark and mounted and visualized as outlined in the CBA protocol. All incubations were carried out at RT.

2.9: Internalisation studies

Surface expression of AMPAR and $GABA_BR$ on transfected HEK cells and primary neuronal cultures in the presence of autoantibodies was compared over time.

2.9.1: Internalisation using CBA

HEK cells (in 6-well plates) expressing AMPAR or $GABA_{B1+2}R$ were grown on glass coverslips for 36 hours, after which coverslips were incubated with heat inactivated sera diluted in DMEM+HEPES (1:100-1:500) for one hour at 37°C. The supernatant was subsequently removed and coverslips were washed 3 times in DMEM+HEPES. At this stage, new DMEM+FCS was added to the cells, and coverslips were returned to the incubator or stained with secondary antibodies (goat anti-human IgG Alexa Fluor 488) for 45 minutes prior to fixing and mounting. Coverslips were stained at 3, 12 and 24 hours for a comparison of surface IgG binding over time. These results were compared to coverslips treated identically with control sera or media alone. Coverslips were scored by 2 independent observers. Representative images were also taken of each coverslip (at least 3 random areas on each coverslip) and the cell number counted using ImageJ using the built-in cell counter plugin (Analyse/Cell Counter).

2.9.2: Internalisation using primary neuronal cultures

Hippocampal neurons (14 div) were cultured and stained as described in 2.8.2. As commercial antibodies directed against the extracellular regions of AMPAR and $GABA_BR$ were not available, binding of patient-specific IgG was used as a measure of protein expression.

The Cell Surface Protein Isolation Kit (89881, Thermo Scientific) and method described above (see 2.5) were utilised to examine changes in protein level in primary neuronal cultures. Cortical neurons were cultured in T175 flasks and were incubated with media containing diluted IgG (adjusted to 100 µg/ml per T175 flask) for 3 days. After 72 hours, the media was removed and cells were washed in PBS prior to incubation with the EZ- EZ-Link® Sulfo-NHS-SS-Biotin. The method was followed as per manufacturer's instructions, with the exception of the final elution step, which was

adjusted to 100 µl in SDS-loading buffer (Invitrogen). Samples were then loaded on 4-8% Bis-Tris gels and probed with commercial antibodies and protein levels were examined. The relative amounts of the surface expressed transferrin receptor (TFR) were used as a loading control.

2.10: Immunohistochemistry:

2.10.1: Section preparation:

Rats were anaesthetised according to British Home Office regulations and perfused with ice-cold PBS, before removal of the brain, which were snap frozen in isopentane on ice. When required the frozen brain was mounted in tissue tek embedding medium, and brain sections were cryostat (ThermoScientific) sectioned (12 µm). Sections were collected on X-tra adhesive glass slides (Sigma), wrapped in aluminium foil and stored with silica gel beads at -20°C until use.

2.10.2: Staining

Sections were thawed for 30 minutes prior to use, and blocked in 10% normal goat serum (NGS) in PBS (45 minutes) and incubated with patient sera (1:400-1:800) or CSF (1:10), diluted in 5% NGS n PBS overnight at 4°C. Sections were washed 3 times in PBS (each wash lasting 5 minutes) and incubated with a goat-anti human Alexa Fluor 488 (1:2000) for one hour at RT. Slides were washed and binding was visualized as outlined in the CBA protocol (section 2.3.1).

2.11: Electrophysiology

2.11.1: Preparation of brain slices

Postnatal day 14-21 B57BL/6 mice were anesthetized using isoflourane and decapitated, according to British Home Office regulations. Brains were removed and

placed in ice cold artificial CSF (aCSF; 126 mM NaCl, 3 mM KCl, 1.25 NaH2PO4, 1 mM MgSO4, 1.2 mM CaCl2, 26 mM NaHCO3, and 10 mM glucose, pH 7.2–7.4.) with the NMDAR antagonist kynurenic acid. Horizontal brain sections, 350 µm thick, containing the entorhinal cortex (EC) and hippocampus were cut using a microtome and slices were incubated in an interface chamber between carbongen gas (95% O_2 and 5% CO_2) and aCSF at RT for one hour prior to recording.

2.11.2: Cell recordings

Slices were mounted on glass coverslips (coated with 0.1% PLL) and placed in the recording chambers. Slices were superfused with aCSF (bubbled in 95% O_2 and 5% CO_2), and the chamber maintained at a constant temperature of 32°C. Whole-cell patch recordings were completed using a Molecular Devices Axon Multiclamp 700B amplifier. Borosilicate glass containing internal solution (110 mM potassium gluconate, 40 mM HEPES, 2 mM Mg-ATP, 0.3 mM NaGTP and 4 mM NaCl, adjusted to pH 7.2 with KOH) was used for whole-cell patching of pyramidal cells in layer III of the entorhinal cortex. A stimulation electrode was placed approximately 200 µM away from the recording cell and stimulated at an amplitude of 150 mA every 30 seconds (stimulation settings were altered for certain slices).

2.11.3: Data Acquisition

Data was acquired as previously described (Mann *et al.,* 2009). Briefly, all data was filtered and acquired using a Molecular Devices Axon Multiclamp 700B amplifier. Signals were recorded using the Axon pClamp 9 acquisition software, and UDS analysis was accomplished using Igor Pro (Wavemetrics). Dr. Edward Mann programmed all custom-made procedures.

2.12: Immunoprecipitation for mass spectroscopy

Cortical and hippocampal neurons were dissected as described in 2.8.1, and cultured in T175cm^2 and T75cm^2 flasks, respectively. Neurons were incubated with patient or healthy control serum (1:100) in NB medium supplemented with 25mM HEPES for 30 minutes at 37°C. Neurons were subsequently washed in NB and solubilised in solubilisation buffer (10 mM Tris pH 7.5, 100 mM NaCl, 1 mM EDTA, 2% digitonin containing protease inhibitors) and the extracts harvested by centrifugation (13,000 x g, 10 minutes, 4°C). The supernatants were incubated with approximately 20 µl of Protein-G Sepharose beads overnight at 4°C. Approximately 16 hours later, beads were washed in solubilisation buffer 4 times. SDS sample buffer (20 µl, 4X) containing 1X sample reducing agent (Invitrogen) was added to the beads and bound IgG-protein complexes. Samples were heated at 95°C for 5 minutes in order to elute the bound IgG-protein complexes. Supernatants were collected and stored at -20°C until further processing for mass spectrometry.

2.13: Mass Spectrometry (MS)

2.13.1 In-gel trypsin digestion

Samples were loaded on a 3-8% Tris-Acetate poly acrylamide gel and ran for approximately 90 minutes at 150mV. In order to visualize protein content, the gels were incubated with Coomassie blue stain (ThermoScientific #24590) for approximately 20 minutes and destained in nuclease-free H_2O to resolve staining (5 x 30 minute washes). Gels were cut into 1-3mm^3 gel pieces and placed into 1.5 ml eppendorfs. The gel pieces were rinsed twice in 600 µl of wash solution (50% methanol, 5% acetic acid) and left overnight at RT. The following morning, the wash solution was removed and gel pieces were dehydrated in acetonitrile (200 µl, concentration) for 5 minutes. The wash was

removed and gel pieces were dried for 3 minutes in a vacuum centrifuge. Proteins were reduced via incubation with DTT (10 mM, 90 µl for 30 minutes) and alkylated with iodoacetamide (100 mM, 90 µl for 30 minutes), after which the supernatant was removed and pieces were again dried using the vacuum centrifuge. Gel pieces were washed with ammonium bicarbonate (100 mM, 600 µl, for 10 minutes), after which the supernatant was removed and dehydration performed with acetonitrile and evaporation as outlined above. The gel samples were then rehydrated on ice with freshly prepared trypsin solution (60 µl, 20 ng/µl sequencing grade trypsin [Promega] in 50 mM ammonium bicarbonate). Finally, after rehydration, excess trypsin supernatant was removed and 20 µl of 50 mM ammonium bicarbonate was added. Finally, gel pieces were digested at 37ºC for 18 hours. A series of extractions were preformed on the gel pieces sequentially using 60µl of 50 mM ammonium bicarbonate, 50% acetonitrile, 5% formic acid and 85% acetonitrile. The combined extracts were evaporated in a vacuum centrifuge and were dissolved in 5% acetonitrile, 0.1% formic acid (20 µL) on an ultrasonic bath and transferred into liquid chromatography-mass spectrometry (LC-MS) sample vials.

2.13.2: LC-MS/MS analysis

For the analysis of in-gel digested protein material, liquid chromatography (LC) was performed using an Ultimate 3000 nano-HPLC (high performance liquid chromatography) system (Dionex, Sunnyvale, CA, USA) comprising a WPS-3000 micro auto sampler, a FLM-3000 flow manager and column compartment, a UVD-3000 UV detector, an LPG-3600 dual-gradient micro-pump, and an SRD-3600 solvent rack controlled by Hystar (Bruker Daltonics, Billerica, MA, USA) and DCMS link 2.0 software. Samples were concentrated on a trapping column Dionex (Sunnyvale, CA, USA), 300 µm i.d., 0.1 cm) at a flow rate of 20 µl/min. For the separation with a C18 Pepmap column (75 µm i.d., 15 cm, Dionex), a flow rate of 250 nl/min was used as generated by

a cap-flow splitter cartridge (1/1000). Peptides were eluted by the application of a 30 min multi-step gradient using solvents A (98% H2O, 2% acetonitrile, 0.1% formic acid) and B (80% acetonitrile, 20% water, 0.1% formic acid). The liquid chromatography was interfaced directly with a 3D high capacity ion trap mass spectrometer (amazon; Bruker Daltonics) utilizing 10 µm i.d. distal coated SilicaTips (New Objective, Woburn, MA, USA) and nano-ESI mode. SPS parameter settings on the ion trap were tuned for a target mass of 850 *m/z*, compound stability 100% and a smart ICC target of 250,000. MS/MS analysis was initiated on a contact closure signal triggered by HyStar software (version 3.2). Up to five precursor ions were selected per cycle with active exclusion (0.5 min) in collision-induced dissociation (CID) mode. CID fragmentation was achieved using helium gas and a 30%–200% collision energy sweep with amplitude 1.0 (ions are ejected from the trap as soon as they fragment).

2.13.3 Data processing and database searching

Raw LC-MS/MS data were processed and Mascot compatible files were created using DataAnalysis 4.0 software (Bruker Daltonics). Database searches were performed using the Mascot algorithm (version 2.4) and the UniProt_SwissProt database with mammalian taxonomy restriction (v2012.09.07, number of entries 537,505, after taxonomy filter: 66,032).

2.14: Statistical analysis

The statistical analysis utilised in each experiment is outlined in the appropriate sections. All statistics were performed using GraphPad Prism version 6 for Mac.

Section 1: Antibodies directed against AMPAR and $GABA_BR$ in neurological diseases

CHAPTER 3: Detection of antibodies directed against AMPA and $GABA_B$ receptors

Detection of antibodies directed against integral membrane neuronal proteins that have extracellular domains or that have part of their structure available on the extracellular surface for antibody binding, has been made possible through the use of cell based assays (CBAs). The main advantage of using this technique is the visualisation of antibody binding to conformationally expressed receptors at the surface of the cell. The HEK293T cell line has used as an expression vehicle for recombinant proteins for many years. Although HEKs are epithelial in origin, the cell line has been optimised to carry out the post-translational folding and processing required for generating native proteins at a high level. In order for the CBAs to be used for diagnostic evaluation, the assay must fulfill two criteria; they must be sensitive enough to pick up low levels of antibody, and specific enough that they pick up only antibodies directed against the protein the HEK cells are transfected with. As such, the first aim of this project was to set up and optimise CBAs that could be used to detect antibodies directed against the AMPAR and $GABA_BR$. Following this, the second aim was to screen sera and CSF from Rasmussen encephalitis (RE) patients and samples with CNS symptoms suspected of having an autoimmune aetiology for antibodies directed against AMPAR and $GABA_BR$ and compare to control cohorts. The prevalence of antibodies to these receptors was evaluated.

PART A: Development of AMPAR and $GABA_BR$ CBAs

3.1: Specificity of commercial antibodies

3.1.1: Specificity of AMPAR commercial antibodies

Antibodies that were raised against the extracellular amino terminal of the AMPAR subunits (see Appendix Table 2; rabbit anti-GluA1 (AGC-004), goat anti-GluA2 (N-19), rabbit anti-GluA3 (sc-7613)) were tested for reactivity to live HEK cells transfected with the specific corresponding subunits. However, binding was not detected when any of the antibodies were incubated with live (un-fixed) HEK cells transfected with the GluA1, GluA2 and GluA3 cDNA. However, all of the commercial antibodies bound to permabilised HEK cells transfected with the corresponding DNA, showing specificity of these commercial antibodies for the antigen target they were raised against (Figure 3.1). In particular, the pan anti-GluA2/3 antibody showed no cross reactivity with GluA1 transfected cells.

As AMPAR are expressed as heterotetramers (with GluA2 generally being coexpressed), antibody binding to live HEK cells transfected with two AMPAR subunits was carried out. Again no reactivity was observed (Figure 3.1: bottom panel).

3.1.2: Specificity of $GABA_BR$ commercial antibodies

Similar experiments were also used to determine commercial antibody specificity for specific $GABA_BR$ subunits. No commercial antibodies directed against extracellular regions of the subunits were available to test on live cells. Commercial antibodies raised against intracellular epitopes of the $GABA_{B1}R$ and $GABA_{B2}R$ subunits (see Appendix Table 2; mouse anti-$GABA_{B1}R$ (ab550551) and mouse anti-$GABA_{B2}R$ (ab5934)) were used to detect specificity to permeabilised $GABA_{B1}R$ or $GABA_{B2}R$ transfected HEK cells. Only the anti-$GABA_{B2}R$ commercial antibodies showed specificity to permeabilised $GABA_{B2}R$ transfected cells (Figure 3.2).

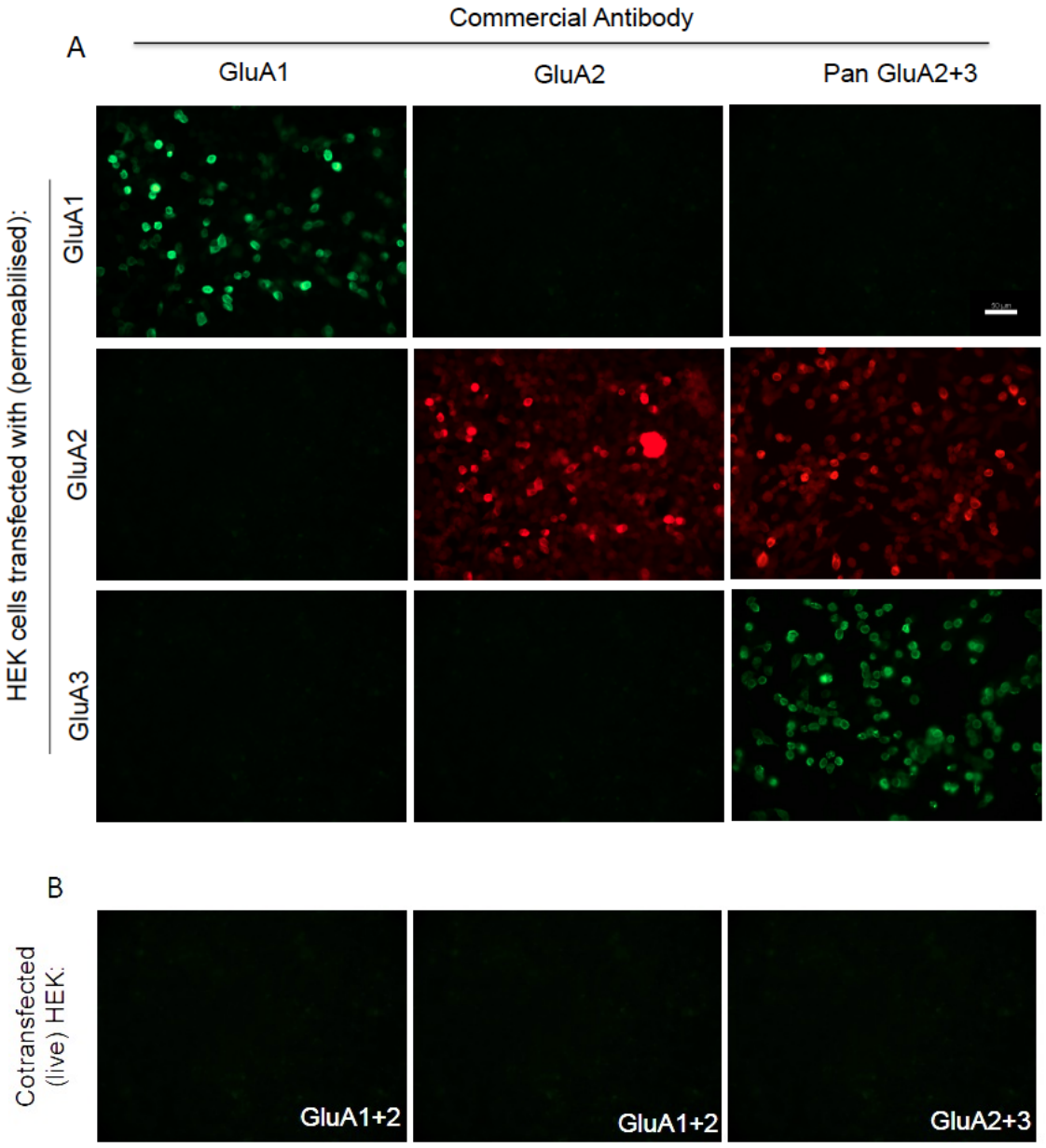

Figure 3.1: Commercial antibodies showed specificity for the AMPAR subunit epitope to which the antibodies were raised against

Permeabilised HEK cells transfected with either GluA1 (upper panel), GluA2 (middle panel), or GluA3 (bottom panel) were probed with commercial antibodies rabbit anti-GluA1 (ab1504; 1:250), goat anti-GluA2 (sc-N19; 1:50) and a rabbit pan anti-GluA2/3 (ab1506; 1:100), and visualized with goat anti-rabbit IgG Alexa Fluor 488 (green) or goat anti-mouse IgG Alexa Fluor 568 (A). Commercial antibodies did not show binding to live transfected cells co-transfected with GluA1+2 or GluA2+3 (B). Images 400x magnification. Scale bar= 50 µm.

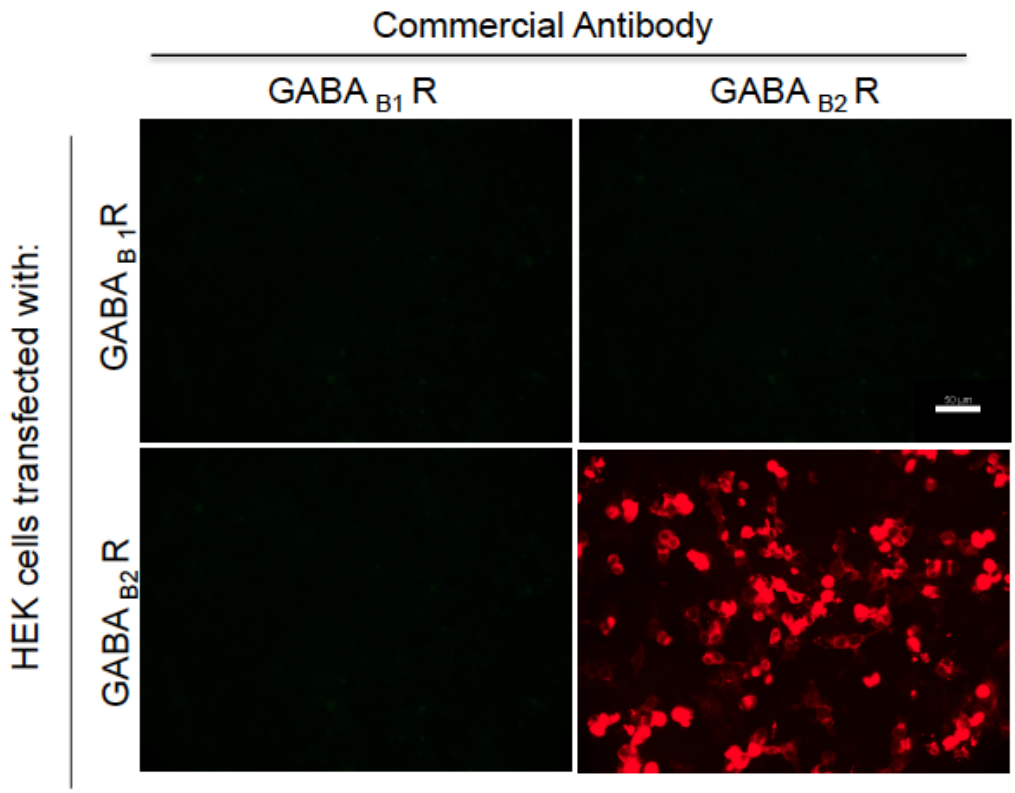

Figure 3.2 Anti-$GABA_{B2}R$, but not anti-$GABA_{B1}R$ commercial antibodies recognised the specific epitope it was raised against

Permeabilised HEK cells transfected with $GABA_{B1}R$ (upper panel) and $GABA_{B2}R$ (bottom panel), were probed with commercial antibodies specific for anti-$GABA_{B1}R$ (ab55051; 1:50) and $GABA_{B2}R$ (ab5394; 1:50) and visualized with goat anti-mouse IgG Alexa Fluor 568 (red). Images 400x magnification. Scale bar= 50 µm.

3.2: Cell surface expression of AMPAR and $GABA_BR$ subunits

Receptors are more likely to be antigenic targets if they are accessible to circulating autoantibodies. That is, part of the antigen target needs to be extracellularly expressed. While the commercial antibodies showed specificity for the protein subunit of the antigen they were raised against, and as they appeared to be unable to bind to live cells, this did not confirm whether or not the proteins were being expressed at the cell surface. To resolve this issue, a cell surface protein isolation kit (ThermoScientific 89881) was utilised to capture surface expressed proteins and protein expression was confirmed via western blotting. Briefly, HEK cells were transfected with the cDNA encoding the AMPAR or $GABA_BR$ subunits and cell surface expressed proteins were labelled with a thiol-cleaveable biotin enzyme. Running the lysed fraction through a neutravidin column captured biotin-labelled extracellular proteins. Extracellular fractions were analysed via western blot using commercials antibodies (see Appendix Table 2 and 3) to probe for AMPAR and $GABA_BR$ subunits.

3.2.1: Cell surface expression of AMPAR subunits

While AMPAR are physiologically expressed as heterotetramers (Nutt *et al.,* 1994), western blot analysis revealed that all AMPAR subunits could be extracellularly expressed as homomers (Figure 3.3). As GluA2 is generally co expressed with the other AMPAR subunits forming "dimer-dimer" pairs, co-transfection (1:1) with GluA1 at 60 µg and 120 µg of DNA per T175 cm^2 flask was carried out. Immunoblotting revealed that co-transfection did not increase surface expression of either GluA1 or GluA3 with increasing concentrations of GluA2 (Figure 3.3A/B). Both GluA2 and GluA3 receptors were detected using the pan anti-GluA2/3 commercial antibody (B). Transferrin receptor (TFR) was used as an extracellular loading control.

3.2.2: Cell surface expression of $GABA_BR$ subunits

In accordance with previous reports (Berranoch, 2011), cell surface protein isolation showed that $GABA_{B1}R$ is not expressed at the cell surface on its own (Figure 3.4). As such, HEK cells were co-transfected with cDNA encoding $GABA_{B1}R$ and $GABA_{B2}R$ at equimolar ratios. Western blot analysis of biotinylated co-transfected cells showed that in the presence of $GABA_{B2}R$, $GABA_{B1}R$ is expressed at the surface (Figure 3.4A). On the other hand, $GABA_{B2}$ was expressed at the surface of HEK cells in the absence of $GABA_{B1}$ (Figure 3.4B).

A

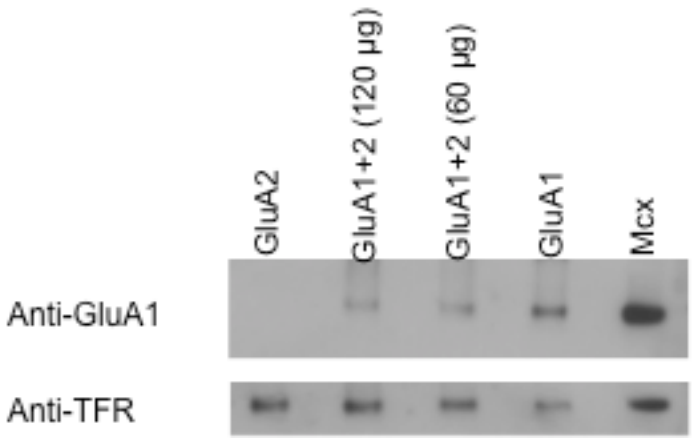

B

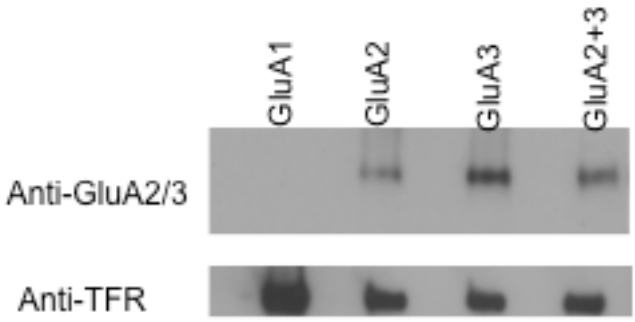

Figure 3.3: Western blots of cell surface GluA1, GluA2 and GluA3 protein fractions isolated using EZ- EZ-Link® Sulfo-NHS-SS-Biotin. All AMPAR subunits were expressed at the surface of the cell as homomers or heterotetramers

HEK cells were cultured in T175 cm^2 flasks and mono-transfected with GluA1 (60 µg DNA/flask), GluA2 (60 µg) or GluA3 (60 µg). HEK cells were also cotransfected with GluA1+2 (60-120 µg) or GluA2+3 (60 µg) and surface expressed proteins were collected as per manufactures instructions (ThermoScientific 89881). Fractions were loaded and run on 4-10% Bis Tris gels, transferred to nitrocellulose membranes and blotted with specific anti-AMPAR subunit antibodies.

Western blots of the fractions are shown. The blots were probed with specific antibodies (1:1000) to GluA1 (A) or pan GluA2/3 (B). As loading controls all blots were probed with anti-transferrin receptor (TFR) antibodies (1:1000). Mouse cortex extract (Mcx) was used as a positive control.

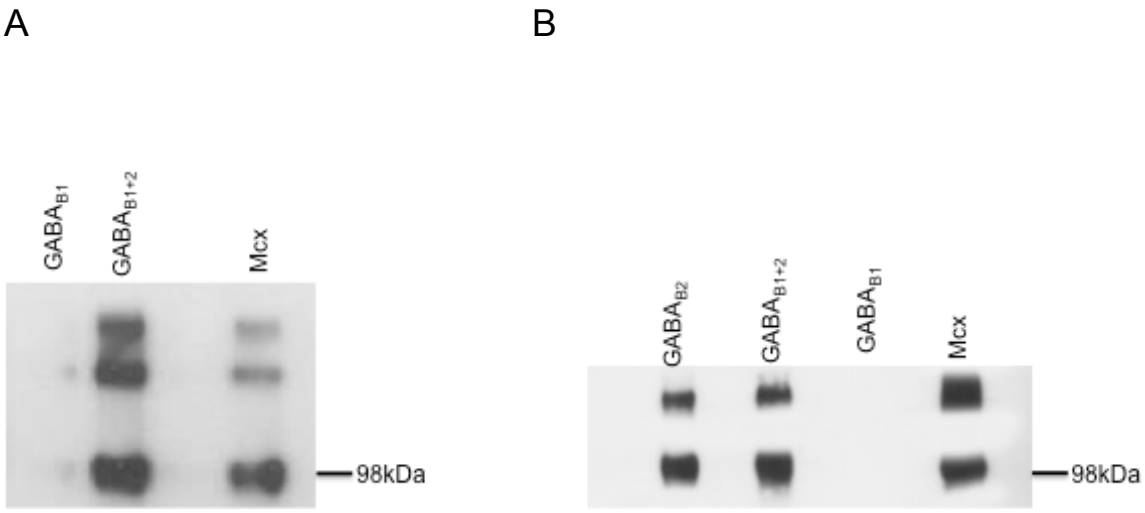

Figure 3.4: Western blots of cell surface GABA$_B$R protein fractions isolated using EZ- EZ-Link® Sulfo-NHS-SS-Biotin

HEK cells were cultured in T175 flasks and transfected with GABA$_{B1}$R alone (60 µg DNA/T75 flask), GABA$_{B2}$R (60 µg) alone or GABA$_{B1+2}$R (120 µg), biotinylated and surface expressed proteins collected as manufacturer's instructions (ThermoScientific 89881). Fractions were loaded and run on 4-10% Bis Tris gels, transferred to nitrocellulose membranes and blotted with specific anti-GABA$_B$R subunit antibodies.

Western blot of fractions are shown. GABA$_{B1}$R is not expressed at the surface unless cotransfected with the GABA$_{B2}$R subunit (A). However, GABA$_{B2}$R is expressed at the surface on its own (B), and the commercial antibody showed no cross reactivity with the GABA$_{B1}$R. Mouse cortex extract (Mcx) was used as a positive control.

3.3: Optimization of cDNA amount

To standardise the optimal cDNA amount for single and co-transfected assays per well of a 6-well plate, HEK cells (3x 10^5- 5x 10^5) were transfected with cDNA at varying amounts. The volume of PEI (normally used as 1.5 µl per 3 µg of cDNA) was adjusted according to the amount of DNA. Cells were subsequently permeabilised and probed with anti-GluA1 or anti-GluA2/3 commercial antibodies. The number of GluA1 and GluA2 transfected cells were counted using Image J program and plotted as a ratio to the number of total cells, determined by staining with DAPI. The number of GluA1 and GluA2 transfected cells was highest with a total amount of 3 µg or 6 µg for both the mono- and co-transfected assays (Figure 3.5A/B; $p<0.0001$). Transfection of cells with 1.5 µg or 9 µg resulted in poor transfection rates, with cells appearing unhealthy at 9 µg (data not shown). As 3 µg of DNA with 1.5 µl of PEI is routinely used in the lab, this total amount of DNA was used for both mono and co-transfected (1.5 µg of each subunit for the co-transfected assay) assays in subsequent experiments and screening of patient sera.

The optimal DNA amount per well of a 6-well plate was also optimised for the GluA2+3 co-transfection and $GABA_{B1+2}R$ transfection and again, 3 µg of DNA (1.5 µg of each subunit) yielded the highest transfection.

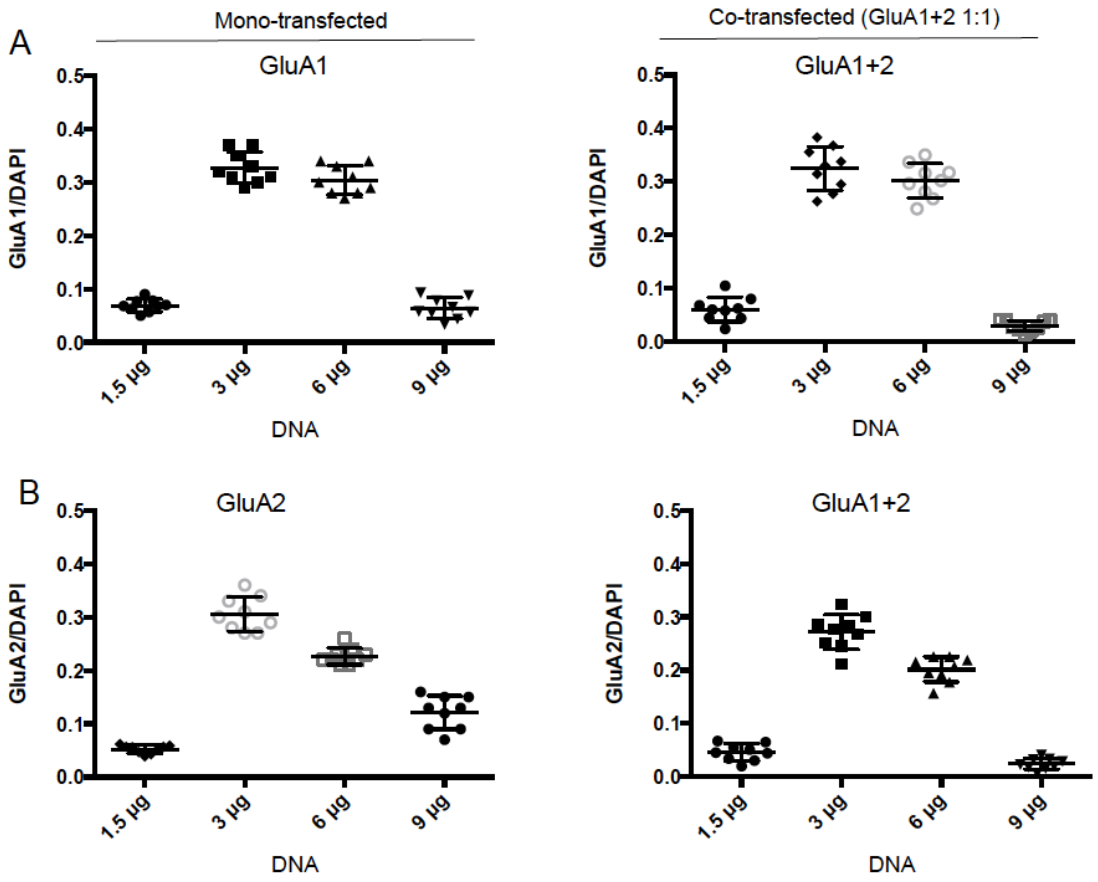

Figure 3.5: Optimal DNA amount for AMPAR (GluA1, GluA2 and GluA1+2) CBA

A comparison of the GluA1 (A) and GluA2 (B) transfections (shown as a ratio to DAPI), versus total DNA amount (µg) when cells are mono-transfected (left column) or co-transfected at equimolar ratios (right column). Cells were counted using image j.

Data analysed using a one-way ANOVA. Wells containing 3x 10^5- 5x 10^5 cells were transfected with DNA (1.5 µg, 3 µg, 6 µg or 9 µg). The ratio of GluA1/DAPI and GluA2/DAPI was highest when HEK cells were mono- or cotransfected with 3 µg and 6 µg of DNA A). GluA1: 3 µg & 6 µg >1.5 µg & 9 µg ($p<0.0001$). B) GluA2: 3 µg & 6 µg> 1.5 µg & 9 µg ($p<0.001$).

PART B: Screening of RE samples by CBA

Antibodies directed against the GluA3 subunit of AMPAR were amongst the first autoantibodies implicated in a neurological disease. As antibodies directed against the GluA3 subunit were first described in Rasmussen encephalitis (Rogers *et al.*, 1994), a cohort of RE samples was screened on the newly established CBAs.

3.4: Rasmussen encephalitis, healthy control and disease control cohorts

3.4.1: Rasmussen encephalitis (RE) cohort

Thirty-six biopsy or MRI confirmed RE patients were used in the study, of which 10 patients had paired serum and CSF samples available for analysis. In addition, 4/36 patients had unpaired CSFs, and clinical details from these patients were not available. A historical cohort of RE sera (n=27, Watson *et al.,* 2004) was also tested for antibodies against antigenic targets in the lab. A summary of all patients (n=63) tested is outlined in Table 3.1.

Table 3.1: Summary of RE samples

Patient Group	Number (N)	Gender (F:M)	Median age at "acute" state presentation Range (yrs)
Historical Samples (Watson *et al.*, 2004)	N= 27 Children: 19 Adults: 8	19:8	Children: 7.5 (1-18) Adults: 30.5 (19-40)
Newly reported	N=36 Children:24 Adults:8 NK: 4*	18:14 NK: 4	Children: 8.4 (3-16) Adults: 40.5 (19-55)

* Not Known (NK): CSF available from 4 patients. Clinical details not available from these patients.

3.4.2: Healthy control and disease cohorts

Samples from 30 adult healthy controls (HC) were screened on the assay. As RE is predominantly a pediatric disease characterised by seizures, binding by CBA was compared to children with epilepsy but not diagnosed with RE (n=106); designated as disease controls (DC), and from sera taken from HC children (n=112, Dutch cohort Wright *et al.,* 2014 in preparation).

3.5: RE CBA Results

When HEK cells were co-transfected with GluA2+3, 2/59 sera samples showed reactivity (Figure 3.6A). End-point titrations analysis demonstrated that the samples had antibody titres of 1:540 and 1:180. Additionally, RE samples also did not show any reactivity to untransfected HEK cells or to those transfected with single AMPAR subunits (GluA1, GluA2 or GluA3 alone), or co-transfected GluA1+2 cells. None of the 14 CSF samples showed any reactivity to the GluA2+3 transfected cells. Clinical details of the two GluA2+3 antibody positive patients are shown in Table 3.2. Of all the samples in the cohort, only one sample (1102) had serial samples collected. Only the latter samples (collected 2 years after onset of the acute stage) showed binding on the CBA (Table 3.2).

All samples, test and control, were negative for NMDAR, LGI1, CASPR2, $GABA_AR$ and $GABA_BR$ antibodies determined by CBA (Figure 3.6C). Samples also tested negative on the VGKC RIA (data not shown). CBAs carried out as described in Irani et al., 2010a and 2010b, and Pettingill et al., 2014 (under submission). Similarly, none of the HC (n=142) or DC (n=106) samples showed reactivity to the GluA2+3 CBA (Figure 3.6B).

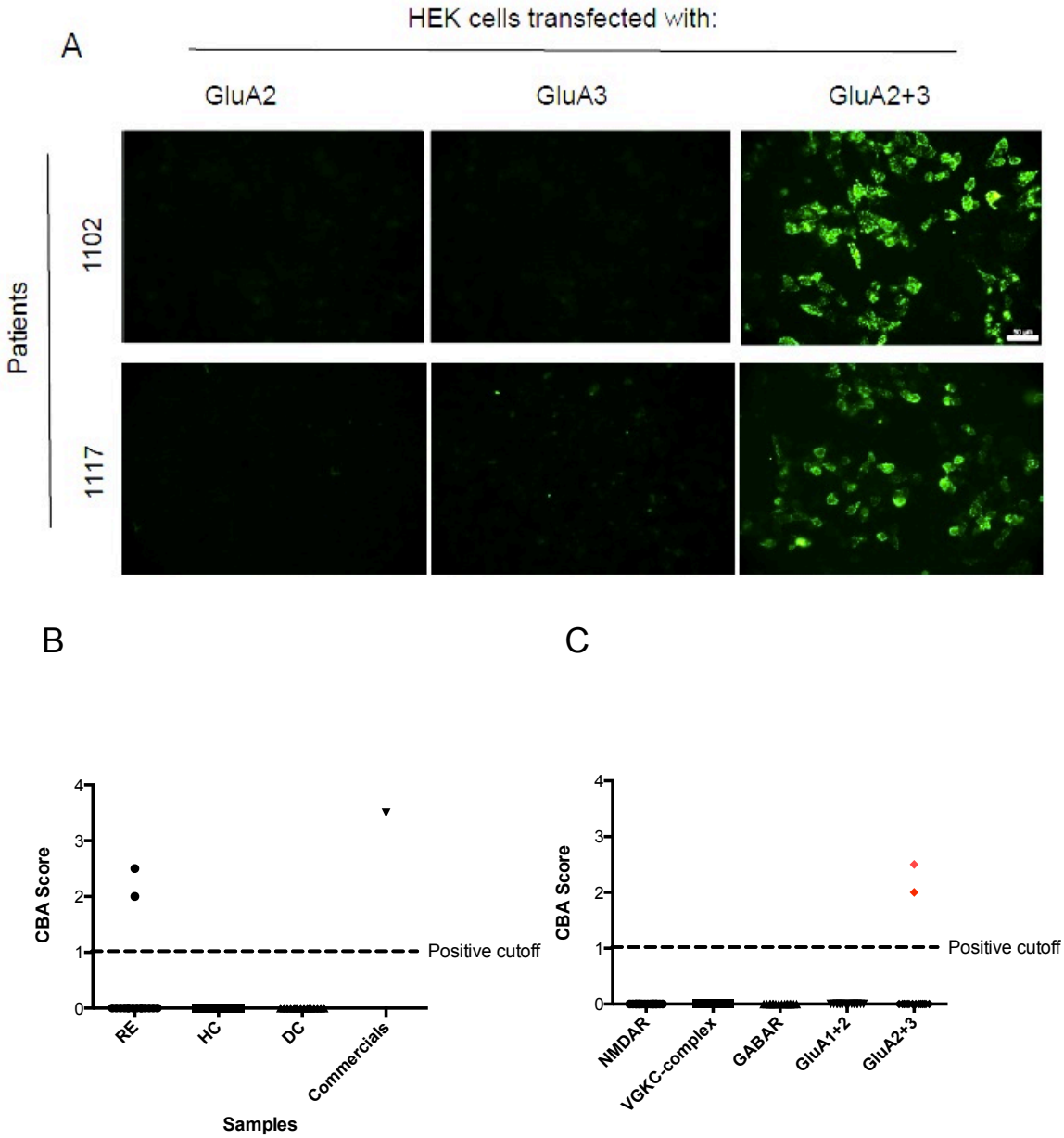

Figure 3.6: Antibodies directed against GluA2+3 are present in two sera samples from patients with RE

Sera (1:20) and CSF (neat) were incubated with HEK cells monotransfected with GluA1, GluA2, and GluA3 or cotransfected with GluA1+2 or GluA2+3. Two of 59 serum samples showed reactivity to HEK cells co transfected with GluA2+3. Sera showed no reactivity to HEK cells transfected with GluA2 or GluA3 alone. Patient binding detected using goat-anti human Alexa Fluor 488. Images 400X magnification. Scale bar=50 µm (A). All pediatric and adult HC samples (n=142) and disease control (DC) samples (n=106) were negative on the GluA2+3 CBA. Commercial antibodies (pan anti-GluA2/3) were used as a positive control (B). All CSFs (n=14) tested were negative on the assay. (C) RE sera showed no reactivity to HEK cells transfected with NMDAR, VGKC complex (LGI1 and CASPR2), GABAR ($GABA_AR$ and $GABA_BR$) or GluA1+2.

Table 3.2: Clinical details of GluA2+3 antibody positive patients

Sample Number	Gender	Age at "acute stage" onset	Date of sample collection (years after acute stage)	GluA2+3 CBA Score (titre)
1102	Male	10	1	Neg
1102	Male	10	2	2.5 (1:540)
1117	Female	7	6	2 (1:180)

To further explore the binding of these antibodies to a conformational epitope, preadsorption experiments were carried out. Samples were preadsorbed against GluA2, and GluA3 mono-transfected HEK cells and then re-tested on HEK cells expressing GluA2+3. The CBA score was unaffected when samples were preadsorbed against GluA2 or GluA3 alone. However, binding was completely abolished when cells had been preadsorbed with cotransfected GluA2+3 cells (Figure 3.7).

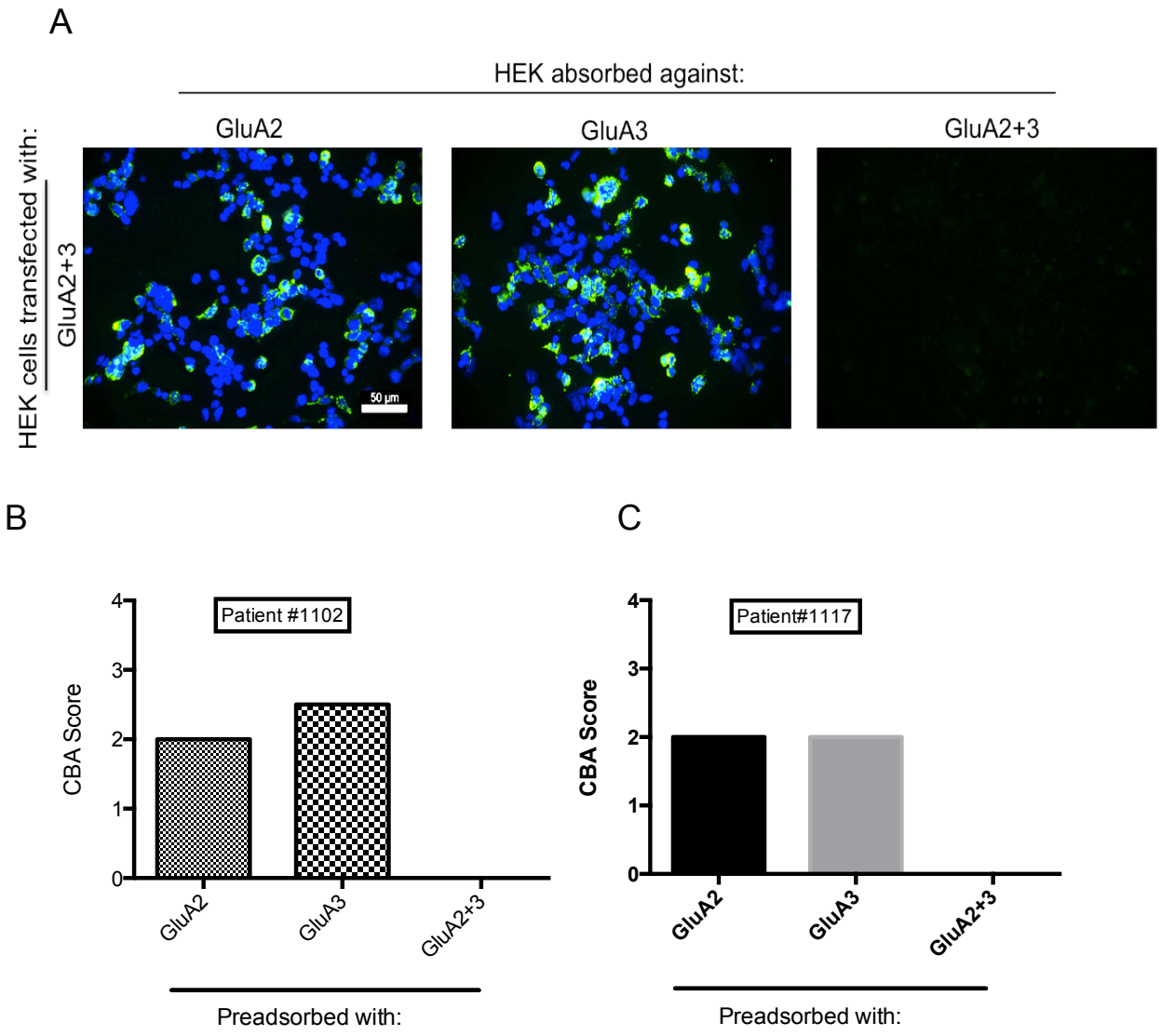

Figure 3.7: RE patients antibodies target a conformational epitope

Antibodies were absorbed by incubating serum with a resuspension of HEK cells (n=1.2x10^7) mono-transfected with GluA2, GluA3 or cotransfected with GluA2+3. Absorbed samples were then retested on the GluA2+3 CBA for reactivity.

When RE samples were preadsorbed against HEK cells transfected with GluA2 or GluA3 subunits alone, the binding on the GluA2+3 CBA was unaffected. However, preadsorption against GluA2+3 cells resulted in complete abolition of binding. These results indicate that the antibodies do not recognise GluA2 or GluA3 subunits alone, but an epitope present when both subunits are co-expressed (A). Images 400X magnification. Scale bar= 50 µm. CBA scores of the two antibody positive patients following preadsorption (B and C).

PART C: Screening of diagnostic samples on AMPAR CBA

Lai and colleagues documented 10 patients with antibodies directed against the GluA1 or GluA2 subunits of the AMPAR in 2009. At the time this project was undertaken, only 6 further patients had been described (Graus *et al.,* 2010, Bataller *et al.,* 2010, Wei *et al.,* 2013). As such, one of the aims of this chapter was to investigate the prevalence of patients with AMPAR antibodies using the newly set up AMPAR CBA, and the sensitivity and specificity of the assay was explored further.

3.6: Screening of diagnostic samples on AMPAR CBA

3.6.1: Presence of antibodies to GluA2 and GluA1+2

To investigate the prevalence of antibodies to the AMPAR in sera that were sent for testing (suspected LE and other CNS disorders of autoimmune origin), all samples received over an 18-month period were tested on the AMPAR CBA as a trial diagnostic screen. A total of 1298 samples were screened on the GluA1, GluA2 and on the co-transfected GluA1+2 assays. Thirteen out of 1298 (1%) of diagnostic samples were positive for AMPAR antibodies. From this initial screening, two distinct populations of samples became apparent. Five out of 13 patients bound to the co-transfected GluA1+2 assay, but were negative or showed very weak reactivity to HEK cells when transfected with GluA1 or GluA2 alone. That is, reactivity was increased when GluA1 and GluA2 were co-transfected at equimolar ratios (Figure 3.8: upper panel). It is likely that the patient's antibodies are targeting a conformational epitope only present when heterotetramers are formed.

A second population of 8 samples also bound to the co-transfected GluA1+2 assay. However, upon further examination, it was revealed that these samples were specific for the GluA2 subunit (Figure 3.8: middle panel), with no binding present when

incubated with GluA1 transfected cells alone. A schematic showing GluA1+2 and GluA2 antibody binding to HEK cells transfected with combinations of AMPAR subunits is shown in Figure 3.9. GluA2 antibodies were still identified using the co-transfected assay, though the CBA score on the co-transfected assay was always slightly lower than on the GluA2 assay alone (not statistically significant, p=0.145, Mann-Whitney). Patients with GluA1+2 antibodies showed no reactivity to GluA3 or GluA2+3 transfected cells. In addition, GluA2 antibody positive patients only showed reactivity to the GluA2+3 assay, and not the monotransfected GluA3 assay. These findings show that GluA2 antibodies are only detected if HEK cells are either mono or cotransfected with GluA2. The detection of GluA2 antibodies using either co-transfected GluA1+2 or GluA2+3, suggests that the epitope the GluA2 antibodies are recognizing are still present when dimer-dimer pairs of the subunits are formed. Finally, as no samples were found that only bound to the monotransfected cells without binding to the GluA1+2 co-transfected assay, the co-transfection assay was used for screening purposes.

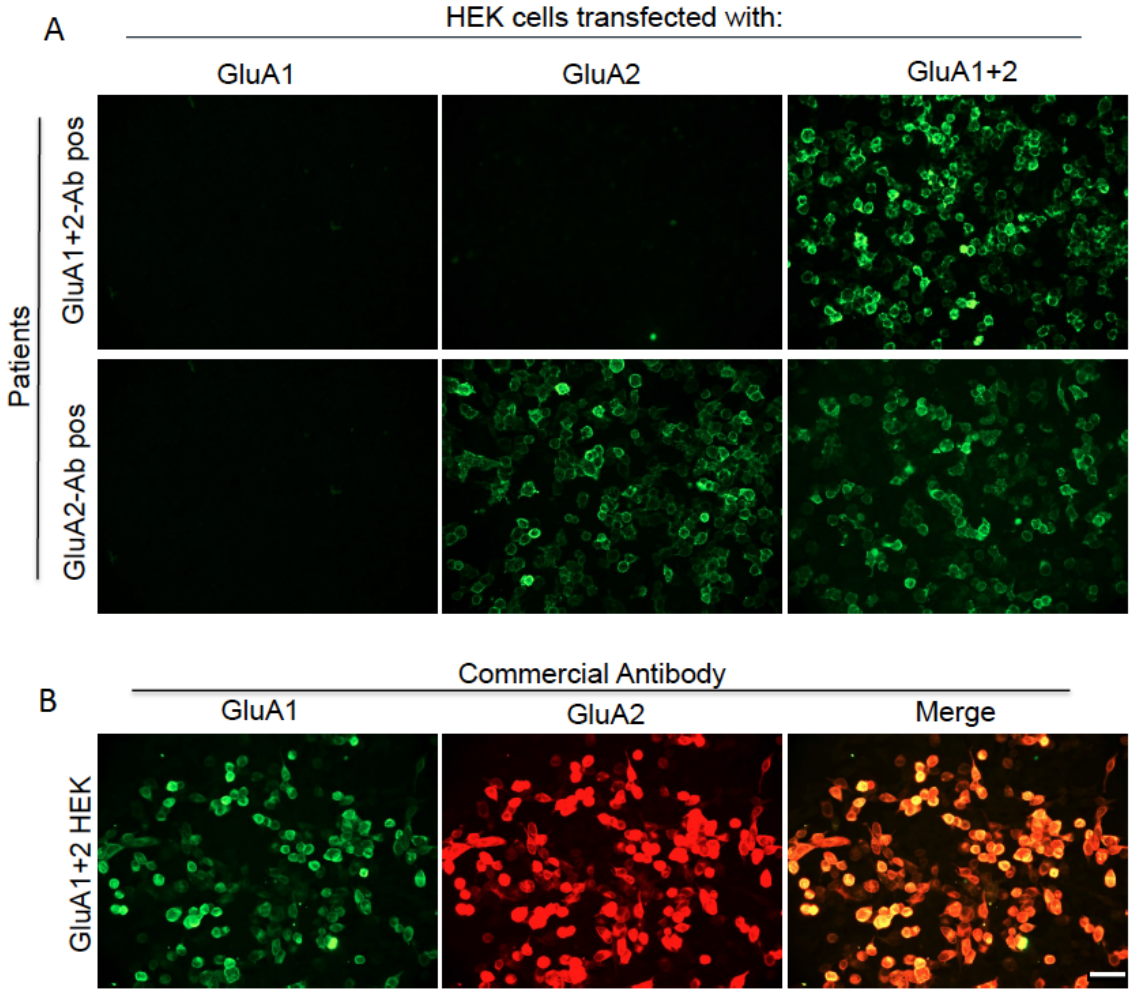

Figure 3.8: Reactivity of AMPAR antibody positive patients to CBA

Sera (1:20) were incubated with HEK cells mono-transfected with GluA1, GluA2 or co-transfected GluA1+2. Patient binding was detected using a goat-anti human IgG Alexa Fluor 488 (green).

A). Patients with GluA1+2 antibodies only showed reactivity to HEK cells transfected with GluA1+2. No binding was noted to cells transfected with GluA1 or GluA2 alone (upper panel). GluA2 antibody positive sera was specific for the GluA2 subunit but could still be detected using the co-transfected assay (bottom panel).

B). HEK cells cotransfected with GluA1 and GluA2, were permeabilised and commercial antibodies (anti-GluA1 or anti-GluA2) were used as positive controls, and visualised using goat anti-rabbit Alexa Fluor 488 (green) and donkey anti-goat Alexa Fluor 568 (red; bottom panel). Representative examples shown. Images 400x magnification. Scale bar =50 μm.

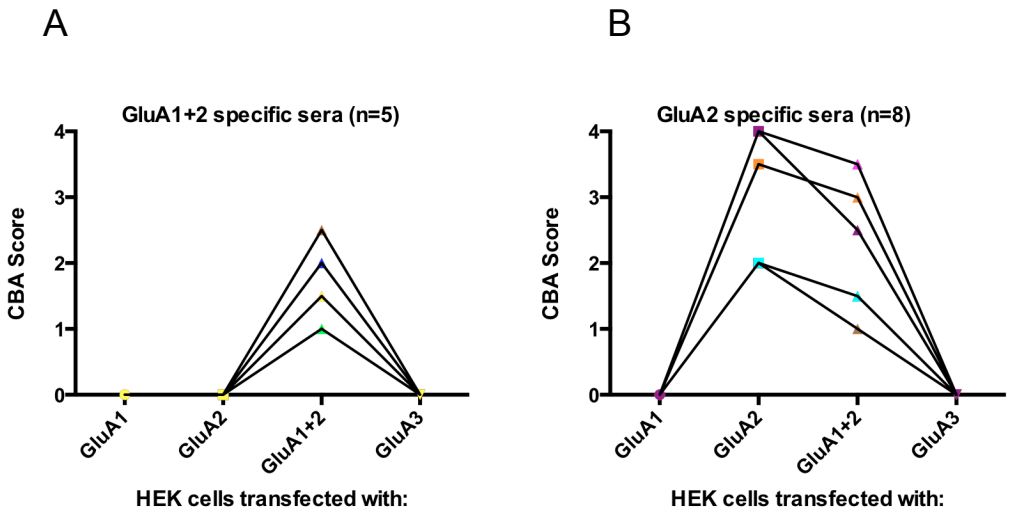

Figure 3.9: Comparative CBA scores of GluA1+ and GluA2 antibody positive sera

Samples that were positive on the GluA1+2 co-transfected assay were tested for positivity to HEK cells mono-transfected with GluA1, GluA2 and GluA3.

GluA1+2 antibody positive patients (n=5) showed specificity to GluA1+2 transfected and could not be detected using any other assays (A). GluA2 antibody positive patients (n=8) did not show reactivity to either GluA1 or GluA3 subunits, but could still be detected using the cotransfected GluA1+2 assay, though CBA scores were slightly lower but not significantly different (p=0.145, Mann-Whitney) (B).

A direct comparison of end-point titres between these two subsets of patient groups revealed that patients with GluA1+2 antibodies had significantly lower antibody titres than patients with GluA2 specific antibodies (Figure 3.10, p= 0.014, Mann-Whitney).

Finally, end-point titrations for GluA2 antibody and GluA1+2 antibody positive patients were compared on assays with varying total amounts of DNA (representative samples shown in Figure 3.11 A and B, respectively). The optimal DNA amount to run samples on the CBA was confirmed to be 3 µg. Furthermore, GluA2 antibody positive sera showed similar end-point titres on both the GluA2 and GluA1+2 CBAs, showing that the co-transfected assay is sensitive for picking up antibodies to single subunits.

While, it has been shown that the end-point titrations correlate with the CBA score (patients with higher antibody levels have a higher CBA score), the CBA is subjective. It should also be noted, that much of the additional optimisation of the assays was completed retrospectively, when sera with different CBA values became available.

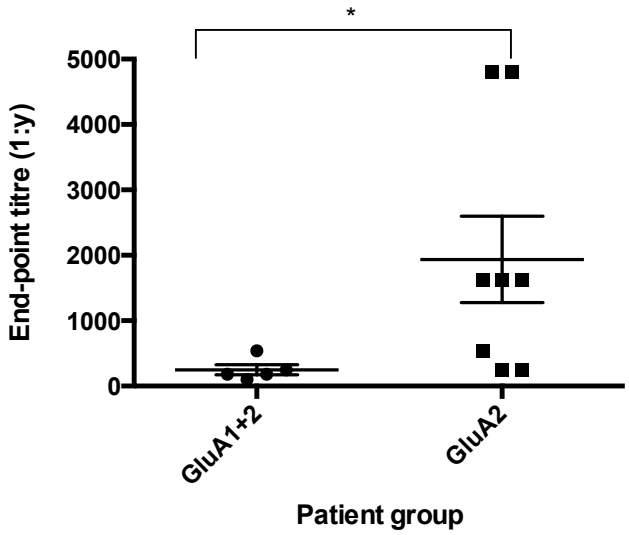

Figure 3.10: A comparison of end-point titrations between GluA1+2 antibody positive and GluA2 antibody positive patients

GluA1+2 and GluA2 antibody sera (1:20) were serially titrated on GluA1+2 HEK cells until binding could no longer be visualised (end-point titre). GluA1+2 patients had antibody levels that were significantly lower than patients with GluA2 antibodies (p=0.014, Mann-Whitney).

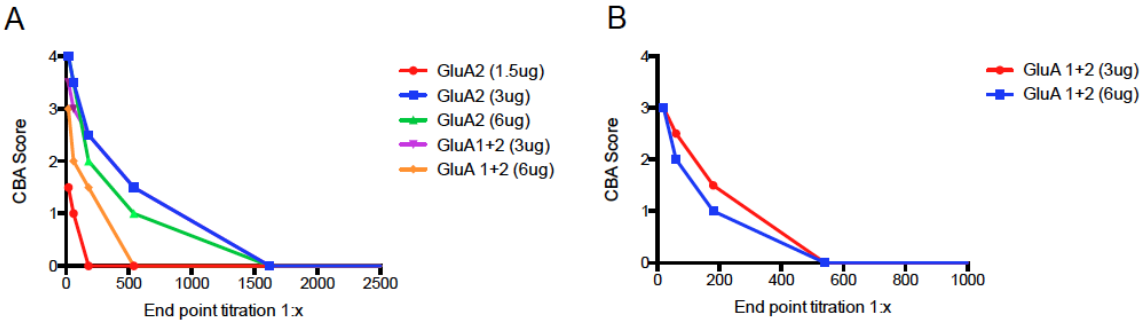

Figure 3.11: A comparison of end-point titrations of a GluA2 antibody positive (A) and GluA1+2 antibody positive (B) patient on AMPAR assays with varying DNA amounts

End-point titres of GluA2 antibody positive patients (representative A#7) were highest on CBAs (mono and co-transfected) using 3 µg of DNA (A). CBA scores were slightly higher when GluA1+2 antibody patients (representative A#13) were titrated out on the co-transfected GluA1+2 assay using 3 µg of DNA (B).

3.6.2: GluA2 antibodies and clinical correlation

Patients that were followed up in the original Lai *et al.* (2009) publication showed clinical improvement that correlated with antibody titre. These patients responded well to immunotherapy, though relapses were noted. When matched serum and CSF are available, it is possible to make comparisons in the antibody levels in the serum and CSF and therefore investigate whether or not antibodies gain access through the brain via a disruption of the BBB, or whether the antibodies themselves are being synthesized in the brain (intrathecal synthesis).

Unfortunately, only one of the AMPAR antibody positive samples detected through the diagnostic screen had serial paired sera and CSF taken at 4 time points throughout his hospitalization and follow-up. A comparison of antibody levels between paired sera and CSF were made in this patient and analysed in the context of the patient's clinical outcome. This patient was GluA2 antibody positive. Figure 3.12A shows the patient's GluA2 antibody levels in the sera and CSF with respect to time. Briefly, the sera antibody levels (demonstrated by end-point titre) increased from the time of admission to subsequent time points (14 days after starting treatment with methylprednisolone and 60 and 150 days from admission). The patient's antibodies in the sera titrated out to 1:1620 at 150 days, even after the patient had improved from his seizures (time point C). While the antibody levels in the sera did not correlate with the clinical course of the disease and response to treatment, analysis of the patient's CSF antibody titre during this time course revealed interesting changes. Following an initial increase of GluA2 antibodies in the CSF (that mirrored the levels in the serum between admission and treatment; time point B), the CSF antibody levels dropped dramatically, correlating with the patient's clinical improvement. A comparison of antibody index (comparison based on end point titre of CSF/Sera) showed the antibody levels were

higher in the CSF (Figure 3.12B), assuming a 1:400 gradient for IgG in serum versus CSF.

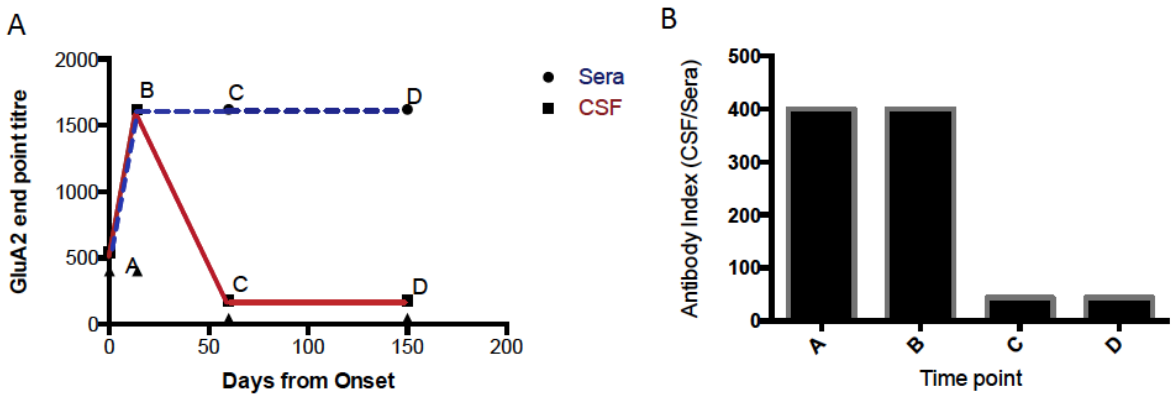

Figure 3.12: A comparison of GluA2 antibody levels in paired sera (blue) and CSF (red) taken from a patient with suspected LE with time

Sera (starting dilution of 1:20) and CSF (neat) were assayed on the GluA2 CBA and end-point titre was evaluated. Samples were taken at various time points. **A: On admission; B: 14 days after high-dose intravenous methylprednisolone; C: 60 days in hospital (patient has shown clinical improvement); D: 150 days from onset (patient has recovered)**

Comparison of end point titre for sera and CSF samples taken at the different time points (A). Comparison of antibody index (CSF/Sera titre when a 400-time titre is applied) over time (B).

3.6.3: Clinical features of AMPAR antibody positive patients

A questionaire was sent to 13 of the clinicians in charge of the AMPAR antibody positive patients. Questions included the major symptoms patients presented with, whether or not there was an underlying tumour, and if treated, the patient's reponse to treatment. Replies from 9/13 were obtained, and the clinical features of the AMPAR antibody positive patients identified are outlined in Table 3.3. Eight of the thirteen antibody positive patients were male.

The patients with GluA2 (n=8) antibodies had higher antibody levels (mean :1:1928 (p=0.014), median: 1:1620, range: 1:250-1:4800). The mean age of onset for this subset of patients was 51 years (median; 50, range; 20-86). These patients often presented with symptoms of limbic encephalitis, such as seizures and cognitive impairment (short-term memory loss, amnesia etc). Three patients that were started on immunomodulatory treatment (cyclophosphamide, plasma exchange, or high dose methyl prednisolone) showed clinical improvement and eleviation of their symptoms. Follow up samples were only available from one patient and is described in Figure 3.12. Two samples had matched CSF available and tested positive on the CBA. Both sera and CSF from these patients titrated out to 1:1620 (Table 3.4, see discussion).

The second subset of patients (n=5), those with antibodies to GluA1+2, had lower antibody titres (mean:1:250, median: 1:180, range: 1:100-1:540). The mean age of onset was younger in this subgroup of patients at 40.6 years (median; 40, range; 19-73). The presenting symptoms were more variable in this group (unconciousness, dementia of the Alzheimer's type, and cerebellar ataxia). A single patient in this group (A#13) presented with status epilepticus and had features similar to LE and MRI investigations showed the presence of brain lesions. Treatment data was available for this patient, and this patient made full recovery once started on mycophenelate mofetil

,with subsequent MRI scans showing the disappearance of lesions. No CSFs were available from this group.

Long-term follow up data was not available for any of the patients. As such, it was not possible to investigate whether or not the patients relapsed as had been described in earlier publications (Lai *et al.,* 2009). With the exception of patient (A#12) with an underlying lymphoma, none of the patients where clinical details were available had a tumour (1/9).

Table 3.3: Summary of diagnostic AMPAR antibody positive samples

Patient Group (N)	Mean age (Median; Range)	Sex F:M	Tumor	Mean titre (range)
GluA1+2 (5)	40.6 (40; 19-73)	2:3	1/5	1:250 (1:100-1:540)
GluA2 (8)	51 (50; 20-86)	3:5	0/8	1:1938 (1:250-1:4800)

Table 3.4: Summary of the clinical details of the AMPAR antibody positive patients identified

Patient	Sex/Age	Symptoms	Additional notes	Antibodies (end-point titre)	CSF (end-point titre)
A#1	F/71			GluA2 (1:250)	No
A#2	M/20	Short term memory loss, visual hallucinations, depression, anxious, movement disorder	Fully recovery after 3 months following treatment (cyclophosphamide)	GluA2 (1:540)	No
A#3	M/22	Status epilepticus		GluA2 (1:250)	No
A#4	F/86	NA		GluA2 (1:4800)	No
A#5	M/	NA		GluA2 (1:1620)	No
A#6	M/60	Suspected limbic encephalitis		GluA2 (1:4800)	No
A#7	F/48	Acute onset amnestic syndrome	Responded well to plasma exchange	GluA2 (1:1620)	Yes (1:1620)
A#8*	M/50	Tonic clonic seizures, Status epilepticus, limb rigidity, agitationm, ataxia	Complete recovery of seizures following treatment with methylprednisolone	GluA2 (1:1620)	Yes (1:1620)
A#9	F/19	Unconsciousness		GluA1+2 (1:100)	No
A#10	M/45	Dementia of the Alzheimer's type		GluA1+2 (1:180)	No
A#11	F/73	NA		GluA1+2 (1:180)	No
A#12	M/40	Cerebellar syndrome, weight loss	Lymphoma	GluA1+2 (1:250)	No
A#13	M/26	Seizures, generalized myoclonus and cognitive deterioration	Brain lesions on MRI that disappeared following treatment with mycophenilate mofetil	GluA1+2 (1:540)	No

*Serial paired sera/CSF samples collected. Highest antibody titres shown
NA; not available

PART D: Screening of diagnostic samples on $GABA_BR$ CBA

3.7: Screening of diagnostic samples on GABABR CBA

In order to identify whether or not diagnostic samples with a suspected neurological autoimmune aetiology had antibodies to $GABA_BRs$, full-length plasmids encoding the $GABA_{B1}R$ and $GABA_{B2}R$ subunits were transfected into HEK cells. As the $GABA_{B1}R$ subunit does not reach the surface of the cell on its own, the two subunits were co-transfected in equimolar ratios as previously described (section 3.2-3.3). All initial screening of samples was carried out on the co-transfected cell based assay.

3.7.1: Screening of diagnostic samples

Nine hundred and sixty four diagnostic samples were screened for these antibodies. A total of 14 patients (1.5%) were identified as positive, using the co-transfected assay. Paired CSF from two $GABA_BR$ antibody positive patients were available for analysis. The CSF also bound to the surface of $GABA_{B1+2}R$ co-transfected cells intensely. A representative image of a paired sera and CSF from a patient with $GABA_BR$ antibodies is shown in Figure 3.13A. A comparison of end-point titres in sera (1:6400 and 1:4800) and CSF (both 1:800) from these two patients is shown in Figure 3.13B/C. The antibodies present in the sera titrated out further than the CSF. An approximation using a 400 time increase (based on the ratio of albumin in the sera and CSF) shows that the antibody levels in the CSF are 50-times and 66-times higher than in the sera (Figure 3.13C).

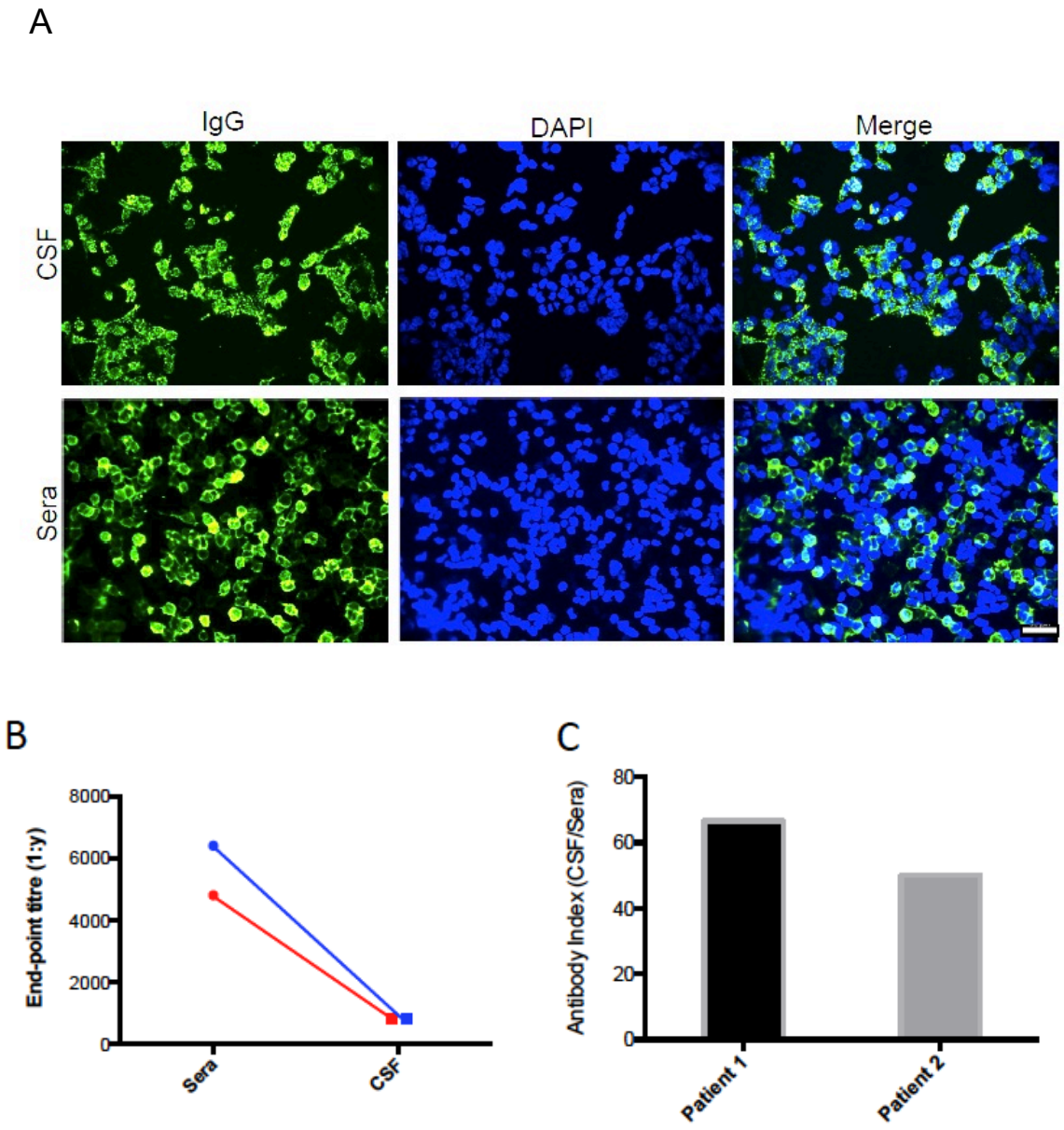

Figure 3.13: $GABA_BR$ antibody positive sera and CSF showed strong reactivity to the surface of $GABA_{B1+2}R$ transfected cells

CSF (neat) and sera (1:100) were incubated with $GABA_{B1+2}R$ transfected HEK cells

Representative staining of a $GABA_BR$ antibody paired serum and CSF (G#8.) Binding was detected using goat anti-human IgG Alexa Fluor 488 secondary antibody (green), and merged with DAPI (blue; to visualize the total number of cells). 400x magnification. Scale bar =50 μm (A). End point titrations for paired serum and CSF samples for two patients (G#8 and G#9). The overall antibody end-point titre was higher in the serum than the CSF (B). When the relative amounts of IgG are normalized (x400), the antibody levels in the CSFs are approximately 50-66-times higher than in the sera (C).

The $GABA_{B2}R$ subunit can be expressed at the cell surface on its own. Therefore monotransfected $GABA_{B2}R$ HEK cells can be used to study antibody binding to this subunit. Six of 14 patients bound to the $GABA_{B2}R$ transfected cells exclusively. This observation was supported by adsorption studies: when sera were preadsorbed against HEK cells transfected with $GABA_{B2}R$ and then placed back on the cotransfected $GABA_{B1+2}R$ CBA, binding was abolished (Figure 3.14). As the $GABA_{B1}R$ is not expressed on the cell surface by itself preadsorption experiments were carried to determine if these patients had antibodies exclusively to the $GABA_{B1}R$ subunit. Preadsorbing the sera revealed that a further 8 patients had $GABA_{B2}R$ and additional $GABA_{B1}R$ antibodies (Figure 3.14). Patients that tested positive on both the $GABA_{B2}R$ assay and the cotransfected $GABA_{B1+2}R$ assay are called $GABA_{B1+2}R$ positive from hereon.

However, if samples stained positively, this could either mean that they had antibodies that recognised an epitope on the $GABA_{B1}R$ subunit, or that these antibodies recognise a conformational epitope only present when the two $GABA_BR$ subunits are co-expressed together. Therefore, a permeabilised CBA to look at binding to intracellular $GABA_{B1}R$ was also investigated. Here, HEK cells that had been transfected with only $GABA_{B1}R$ DNA were permeabilised and sera was incubated. Unfortunately, permeabilising the cells results in high nonspecific background following incubation with sera, which was also noted with HC sera binding. Only patients with high antibody titres could be distinguished from nonspecific staining (data not shown). All of the high antibody titre patients were shown to have both $GABA_{B1}R$ and $GABA_{B2}R$ antibodies.

A comparison of the antibody titres of the two subpopulations is shown in Figure 3.15. $GABA_{B2}R$ antibody positive patients had end-point titres that were significantly lower than $GABA_{B1+2}R$ antibody positive patients ($p=0.0320$, Mann-Whitney). A summary of all the $GABA_BR$ patients is found in Table 3.5 and 3.6.

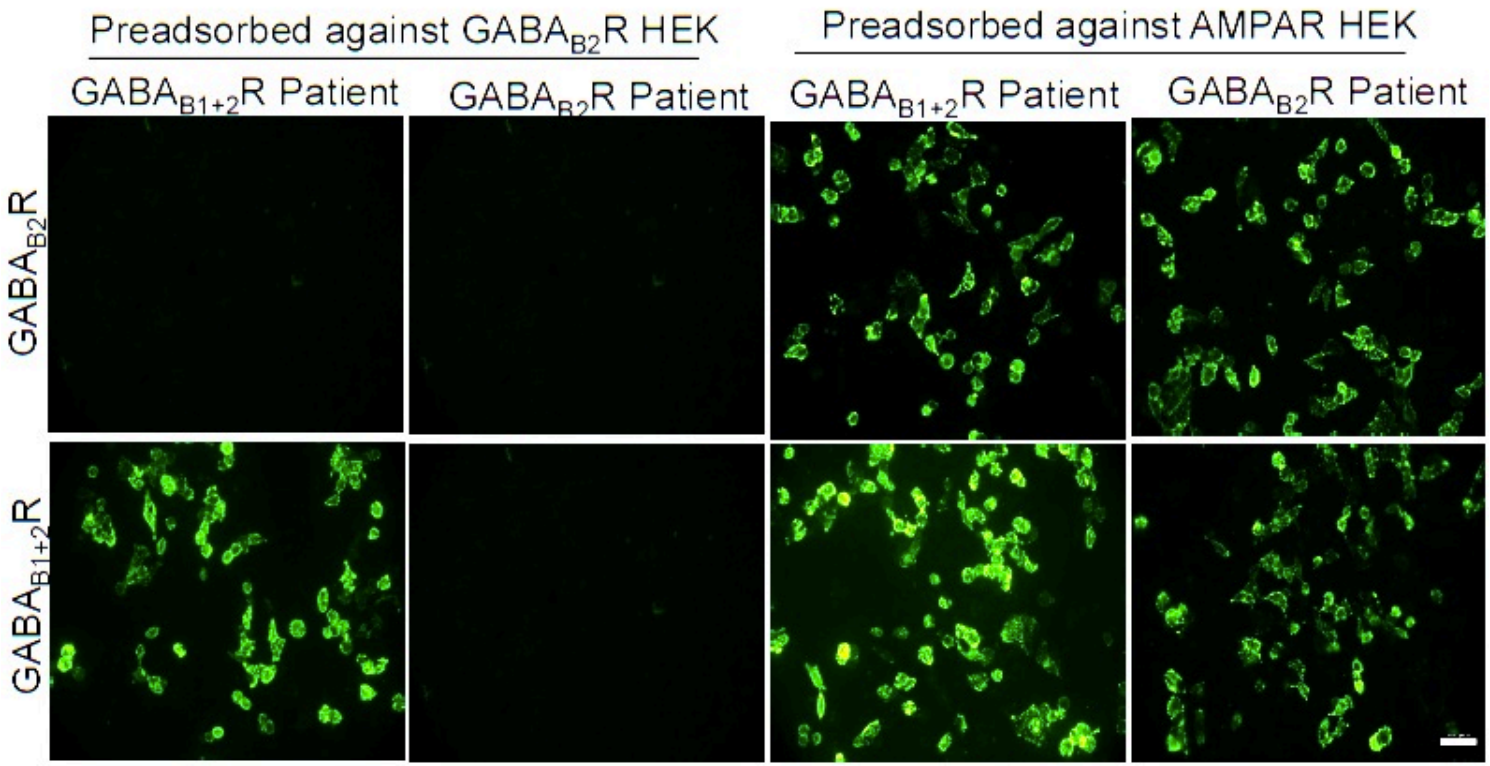

Figure 3.14: Two distinct populations of GABA$_B$R antibody positive samples exist

Antibodies were absorbed by incubating sera with a suspension of HEK cells (n= 1.2x10^7) mono-transfected with GABA$_{B2}$R or GluA2 transfected cells. Absorbed samples were then tested on the GABA$_{B2}$R and GABA$_{B1+2}$R CBA

Samples (n=14) were preadsorbed against GABA$_{B2}$R transfected HEK cells. If binding was diminished, then it was determined that these patients had GABA$_{B2}$R antibodies (this was noted in 6 patients whose binding was abolished following preadsorption, indicating a single specificity). However, 8 additional patients showed binding to the cotransfected assay following preadsorption with GABA$_{B2}$R HEK cells. Preadsorption against an unrelated antigen (AMPAR) was used as control.

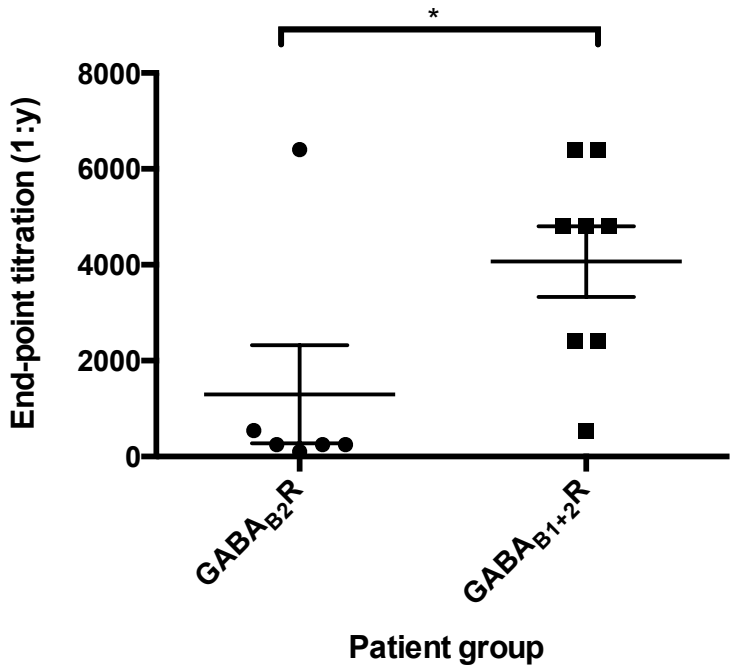

Figure 3.15: A comparison of end-point titrations between GABA$_{B2}$R antibody positive and GABA$_{B1+2}$R antibody positive patients

GABA$_{B2}$R and GABA$_{B1+2}$R antibody sera (1:100) were serially titrated on GABA$_{B1+2}$R HEK cells until binding could no longer be visualised (end-point titration).

GABA$_{B2}$R patients had antibody levels that were significantly lower than patients with GABA$_{B1/2}$R antibodies (p=0.0320, Mann-Whitney).

3.7.2: Clinical features of $GABA_BR$ antibody positive patients

Clinicians taking care of the $GABA_BR$ antibody positive patients were contacted for further clinical details. Replies from 9/14 were obtained, and a summary of $GABA_BR$ antibody positive patients identified are outlined in Table 3.6. There were 9 males and 5 females in this group. The tumour status of six patients was documented, all of which had cancer of the lung (5/6 were SCLC).

A clinical summary of the 14 diagnostic patients is outlined in Table 3.5. The cohort could be split into $GABA_{B2}R$ antibody positive patients (G#1-G#6) and $GABA_{B1+2}R$ antibody patients (G#7-G#14). The mean age at onset of the $GABA_{B1+2}R$ antibody patients was 64.9 years (median; 69, range; 47-75). The $GABA_{B2}R$ antibody patients were slightly younger with a mean age at onset of 56.3 years (median; 54.5, range; 50-70).

While the distinguishing feature of the 15 patients described in Lancaster *et al.,* 2010 was seizures, in this study only 5 patients (all with $GABA_{B1+2}R$ antibodies) had seizures as a main presenting feature. However, symptoms associated with LE were not the only features noted in the patients identified. All the patients with $GABA_{B2}R$ antibodies (n=6) were diagnosed with LEMS or suspected LEMS (cases G#2-G#4 are historical samples with limited clinical details available). Of note was one patient (#G5), which was a SCLC patient that presented with an encephalopathy as the EEG showed brain slowing. This patient later went on to develop LEMS. Patients with high antibody titres ($GABA_{B1+2}R$ antibody) generally had symptoms of LE, whereas lower titre patients ($GABA_{B2}R$) had SCLC with PNS symptoms.

Table 3.5: Summary of diagnostic $GABA_BR$ antibody positive samples

Patient Group (N)	Mean age (Median; Range)	Sex F:M	Tumor	Mean titre (range)
$GABA_{B1+2}R$ (8)	64.9 (69; 47-75)	5:3	3/3*	1:1298 (1:100-1:6400)
$GABA_{B2}R$ (6)	56.3 (54.5; 50-70)	4:2	3/3*	1:250 (1:100-1:540)

* Clinical details obtained

Table 3.6: Summary of the clinical details of the $GABA_BR$ antibody positive patients identified

Patient	Sex/Age	Symptoms	Tumor	Additional notes	Antibodies	CSF Titres
G#1	F/53	LEMS	SCLC	SCLC	$GABA_{B2}R$ (1:100)	
G#2	F/56	Suspected LEMS	NA		$GABA_{B2}$ (1:250)	
G#3	F/70	Suspected LEMS	NA		$GABA_{B2}R$(1:250)	
G#4	F/53		NA		$GABA_{B2}R$(1:250)	
G#5	M/50	Presented with confusion, unsteadiness and proximal leg weakness, respiratory insufficiency, Electrophysiology consistent with LEMS	SCLC	EEG was encephalopathic. Neurophysiology was consistent with LEMS	$GABA_{B2}R$ (1:6400)	
G#6	M/56	LEMS	SCLC		$GABA_{B2}R$ (1:540)	
G#7	F/-	LE with seizures	Lung nodule		$GABA_{B1+2}R$ (1:6400)	
G#8*	M/71	TL seizures, memory loss. Increasing disorientation, confusion	SCLC	Immunoabsorption, steroids. Within 5 weeks: mRS0---5	$GABA_{B1+2}R$ (1:6400)	(1:800)
G#9	F/60	Disorientation for 3-4 weeks, weight loss, back pain. Series of focal R-sided seizures and SGTCS. Hallucinations	SCLC	Chemo-Tx+IVIG, later PEX. Within 2 months: mRS 3---5	$GABA_{B1+2}R$ (1:4800)	(1:800)
G#10	F/47	LE	NA		$GABA_{B1+2}R$ (1:2400)	
G#11	F/69	LE	NA		$GABA_{B1+2}R$ (1:4800)	
G#12	F/74	NA	NA		$GABA_{B1+2}R$ (1:2400)	
G#13	M/58	NA	NA		$GABA_{B1+2}R$ (1:540)	
G#14	M/75	NA	NA		$GABA_{B1+2}R$ (1:4800)	

NA; Not available; LEMS; Lambert-Eaton myasthenic syndrome, LE; limbic encephalitis, SCLC; small-cell lung carcinoma, IVIG; intravenous immunoglobulins, PEX; plasma exchange, mRS; modified Rankin Score

3.7.3: Screening of a SCLC cohort

As a majority of the patients picked up on the diagnostic assay had an underlying malignancy, generally SCLC, a consecutive cohort of 237 serum samples from patients who presented to an oncology clinic and whom SCLC was later confirmed were screened for $GABA_BR$ antibodies. Ten (4.2%) $GABA_BR$ antibody-positive patients were detected. The $GABA_BR$ antibody positive patients identified from this cohort are summarised in Table 3.7. As SCLC patients have been shown to have P/Q- and N- type VGCC antibodies as well as paraneoplastic markers (namely SOX and Hu), the cohort was additionally screened for these antibodies (by Dr. Bethan Lang and Dr. Paul Maddison). There was variability in $GABA_BR$ antibody levels as can be seen by the CBA scores (ranging from CBA score of 1-4). Unlike the diagnostic samples identified whereby $GABA_{B2}R$ antibody patients had lower antibody titres, low and high antibody titre patients could not be distinguished based on subunit specificity in this group. Three patients had antibodies specific to the $GABA_{B2}R$, but due to low numbers, no statistical significance between $GABA_{B2}R$ and $GABA_{B1+2}R$ antibody levels could be determined. Patients with low antibody titres (<1:540) generally did not have any neurological symptoms, whereas the higher antibody titre patients did.

Table 3.7: Summary of the SCLC $GABA_BR$ antibody positive samples

Number	$GABA_B$ (R1/R2)	$GABA_BR$ antibody titre	P/Q VGCC (pM)	N VGCC (pM)	VGKC	SOX	Hu	Neurological symptoms
G#15	$GABA_{B1}R$/ $GABA_{B2}R$	1:6400	139	146	-	+	-	LE
G#16	$GABA_{B1}R$/ $GABA_{B2}R$	1:6400	854	184	281 (CASPR2 +)	+	-	LEMS
G#17	$GABA_{B2}R$	1:1200	345	951	-	+	-	Ataxia, LEMS
G#18	$GABA_{B2}R$	1:540	-	-	-	-	+	Some confusion
G#19	$GABA_{B2}R$	1:540	-	-	-	+	-	none
G#20	$GABA_{B1}R$/ $GABA_{B2}R$	1:540	-	-	188	-	-	none
G#21	$GABA_{B1}R$/ $GABA_{B2}R$	1:250	-	-	-	n/d	n/d	none
G#22	$GABA_{B1+2}R$	1:250	-	-	-	-	-	none
G#23	$GABA_{B1+2}R$	1:100	-	-	-	-	+	none
G#24	$GABA_{B1+2}R$	1:100	-	181	-	+	-	none

-; negative, +; positive, n/d; not done; LE; limbic encephalitis, LEMS; Lambert-Eaton myasthenic syndrome

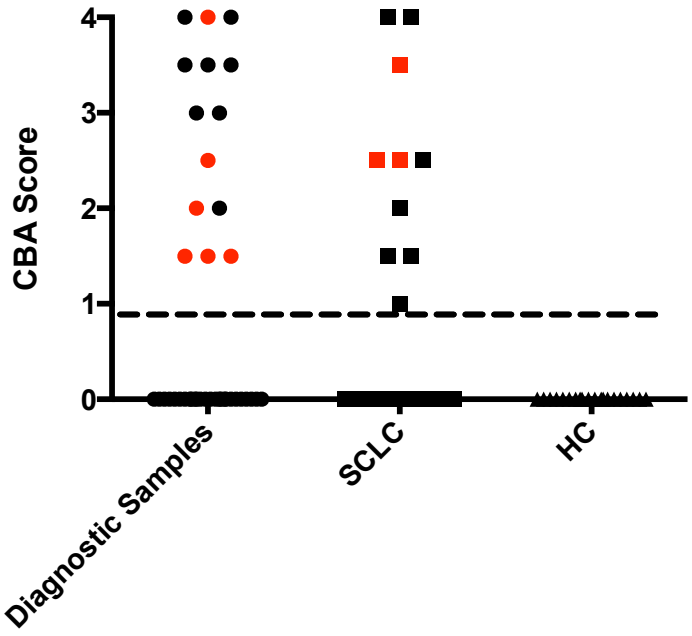

Figure 3.16: A summary of the CBA scores of the $GABA_BR$ antibody positives according to the cohort they were identified from

All samples (n=1201) were initially screened on $GABA_{B1+2}R$ transfected HEK cells. Twenty-four samples were found to be positive. All positive samples were tested on $GABA_{B2}R$ HEK cells, and preadsorption experiments were carried out to determine subunit specificity. All samples highlighted in red (n=9) had only $GABA_{B2}R$ antibodies.

PART E: Screening of additional cohorts and comparison of in house diagnostic CBA and commercially available slides

3.8.1: Additional cohorts screened on the assays

As patients with $GABA_BR$ antibodies have been described in patients with OMS (Hoftberger *et al.,* 2013), and a majority of these patients are children, a cohort of these samples was run on the newly established CBAs. In addition, a cohort of previously published NMDAR encephalitis patients (N=52, Irani *et al.* 2010), was also screened on the AMPAR assay (GluA1+2). A summary of all of the samples screened for particular assays are summarised in Table 3.7.

Table 3.7: Summary of the samples screened on the AMPAR and $GABA_BR$ CBAs

Sample Group	Number (N)	AMPAR-Ab (subunit specificity)	$GABA_BR$-Ab (subunit specificity)
Rasmussen's Encephalitis	63	2 (GluA2+3)	0
Opsoclonus-myoclonus syndrome (OMS)	26	0	0
Paediatric epilepsy (not RE)	106	0	Not tested
Healthy control children	112	0	Not tested
Diagnostic (suspected limbic encephalitis/ CNS disorder)	1298	13 (GluA1+2=5 , GluA2= 8)	14 ($GABA_{B2}R$= 6, $GABA_{B1+2}R$= 8) 964 samples tested
NMDAR-Ab positive cohort	52	0	Not Tested
SCLC	237	0	10 ($GABA_{B2}R$= 3, $GABA_{B1+2}R$= 7)
Healthy control adult	30	0	0

3.8.2: In house versus commercial assays

Binding of antibody positive sera was compared between the in house CBA and commercially available diagnostic slides (Euroimmun, see section 2.3.5). A total of 4 $GABA_BR$ antibody positive patients and 2 GluA2 antibody positive patients (data not shown) all with a CBA score of 4 were run on the commercial slides, and none showed reactivity. Representative staining of a $GABA_BR$ antibody positive patient (G#9) diagnosed with LE is shown in Figure 3.17. Interestingly, this strong positive (end-point titre 1:4800) was only weakly positive on $GABA_{B1}R$ and $GABA_{B1+2}R$ Euroimmun slides. In addition, the staining pattern was not very different to HC staining. These findings highlight the increased sensitivity of the in house CBA over the commercially available slides.

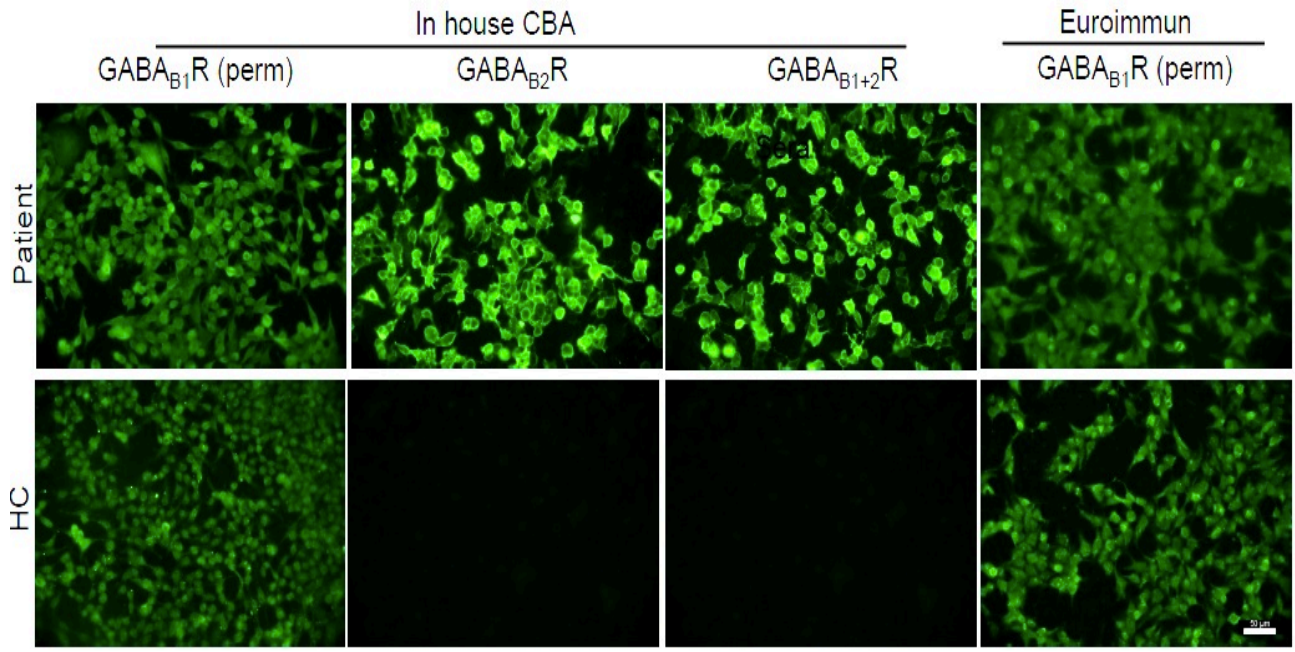

Figure 3.17: Binding of GABA$_B$R antibody positive patient (upper panel) and HC sera was (bottom panel) compared on the in house CBA and commercial Euroimmun slides

GABA$_B$R antibody positive patients showed specific staining on the in house CBA using live HEK cells transfected with either GABA$_{B2}$R or GABA$_{B1+2}$R. No difference was noted between the staining of patient or HC to permeabilised GABA$_{B1}$R transfected HEK cells on the in house CBA. Euroimmun slides (far right column) contain permeabilised HEK cells transfected with GABA$_{B1+2}$R. Again, no specific stain that could be differentiated from background staining (HC staining) was noted on these cells. Scale bar= 50 µm

3.9 Summary and Discussion

3.9.1: Establishment of CBAs

CBAs are one of the principal methods now adopted for detection of antibodies directed against surface antigenic targets. The major advantage of using this technique over others is the expression of the protein at the surface of a mammalian cell with the correct glycosylation and in a native state, as opposed to immunoblotting or ELISAs, whereby antibody binding to denatured protein is detected. In order for this technique to be considered valuable, the CBAs must be both sensitive and specific. The use of commercial antibodies raised against epitopes specific to proteins detected via indirect immunofluorescence can be used to answer the specificity. All of the commercial antibodies used in the thesis showed specificity for the subunit it was raised against. However, despite the use of antibodies that were raised against extracellular epitopes (anti-GluA1 AGC-004, anti-GluA2; N-19, anti-GluA3; SC-7613), none of the antibodies bound to the surface of live cells, though reactivity was noted with permeabilised cells. However, these commercial antibodies were raised against short linear peptides, which may not be accessible or conformationally available in the "mature" protein that is expressed on the surface. As such, there are limitations to the use of these antibodies to validate the CBA. However, these antibodies do seem to bind to the protein when the cell is permeabilised and in this case the commercial antibodies could be binding to a linearized intracellular form of the protein before it folds in to the conformationally active form for insertion into the membrane.

Despite this, immunoblotting using surface biotinylation did reveal that the proteins were surface expressed, which is necessary if the antibodies are to interact with the antigenic target and be detected by CBA. The use of commercial antibodies was made possible as fractions were denatured and the proteins are no longer in a

conformational expressed form. All of the AMPAR subunits and $GABA_{B2}R$ were expressed at the surface alone (homomers). While homotetramers have been shown to be functional *in vitro,* AMPAR subunits generally assemble as heterotetramers *in vivo*, with the GluA2 subunit forming one of the dimer-dimer pairs (Huganir, 2007). In addition, $GABA_{B1}R$ was shown to be present at the surface of cells only in the presence of $GABA_{B2}R$, as has previously been reported (Benarroch, 2012).

Transfection studies showed that the total optimal DNA amount required for the co-transfected assays for approximately 3-5x 10^5 HEK cells was 3 µg (1.5 µl PEI), at a 1:1 ratio of each of the subunits. Slightly lower expression levels were obtained at 6 µg, whilst higher levels caused cell death (lower overall DAPI count), which may have been due to higher levels of PEI. Retrospectively, sera end-point titres were shown to be highest when a total of 3 µg for the CBA was used. Finally, the In house CBA was shown to be more sensitive than commercially available Euroimmun slides.

3.9.2: Antibodies in Rasmussen Encephalitis

Previous reports have implicated antibodies to AMPAR subunits, particularly to GluA3, in the pathogenesis of the severe childhood epilepsy RE. Rogers *et al.* (1994) were the first to describe RE patients with GluA3 antibodies, detected by immunoblotting and ICC using permeabilised transfected HEK cells. Repeated PEX of one patient with GluA3 antibodies showed marked clinical improvement (reduction in seizures and improved neurological function). Interestingly, despite not being the main antigen target subsequently investigated, it should be noted that weak binding of two patients with RE was noted to transfected GluA2 cells via immunoblot. Subsequent publications have either only infrequently found these antibodies in RE (Watson *et al.,* 2004), or also found GluA3 antibodies in epilepsy patients without RE (Wiendl *et al.,* 2001 and Mantegazza *et al.,* 2002). However, immunoblotting and ELISAs were employed in these studies,

which as mentioned previously can detect antibody binding to denatured protein. Therefore a previously documented cohort (Watson et al., 2004) as well as 36 biopsy/MRI proven RE samples were rescreened for antibodies against the AMPAR subunits using a more native substrate.

Interestingly, only two RE sera bound to HEK cells when transfected with GluA2 and GluA3, but not GluA2 or GluA3 alone. Preadsorption studies showed that the antibodies recognise an extracellular conformational epitope, and that reactivity was not against either the GluA2 or GluA3 subunits alone. All samples also tested negative against other known CNS antigens available in the laboratory.

There was no apparent difference clinically between these two patients and the rest of the RE patients in this cohort. Longitudinal samples were only available from one patient. Samples from this patient were collected one and two years following onset of the acute stage of the disease (characterised by frequent seizures and neurological deterioration leading to hemianopia and hemiplegia (Bien *et al.,* 2005)). Interestingly, GluA2+3 antibodies were only found in the second sample, taken two years after onset of the acute stage. This finding is suggestive that these antibodies are not playing a primary causative role in the disease but may either be a marker of brain atrophy and disease progression or that these antibodies are playing a secondary pathogenic role after T-cell mediated damage has already occurred (Bien, *et al.,* 2002).

There have been a number of reports of the presence of antibodies in neurological diseases, which may not be contributing to the pathogenesis. For example, NMDAR, VGKC and GlyR antibodies have been described in patients with Creutzfeldt-Jakob disease (Grau-Rivera *et al.,* 2014, Mackay *et al.,* 2012, Angus-Leppan *et al.,* 2012), though these antibodies are more likely to be secondary to neuronal damage. The presence of antibodies directed against intracellular proteins such as Hu and Yo have also been documented in many paraneoplastic cases. However, given the

localisation of these proteins, it is unlikely that these antibodies themselves are pathogenic and contributing to the disease. However, in such a rare disorder as RE with relatively few samples, and even fewer with follow up samples it is difficult to determine whether or not these antibodies are indeed secondary contributors to the disease progression. Whether or not antibodies play a role in the early stages of this disease, when diagnosis is difficult also needs to be determined, as most samples assayed here were taken from patients after established disease. As such, whether or not these antibodies are diagnostically relevant remains to be elucidated.

3.9.3: AMPAR and $GABA_BR$ subunit antibody reactivity

The presence of antibodies specific to the GluA1, GluA2 and $GABA_{B1}R$ subunits in serum samples suspected of having LE, or having a neurological disease of autoimmune origin has been documented in previous studies (see sections 1.6 and 1.7). In this chapter, we identified AMPAR antibodies and $GABA_BR$ antibodies in 1% (13/1298 patients) and 1.45% (14/964 patients), respectively of the diagnostic samples screened. $GABA_BR$ antibodies were also identified in 4.2% (10/237) of SCLC samples screened on the assay.

Furthermore, we identified two subsets in either group of AMPAR and $GABA_BR$ antibody patients. We found that in 38% of AMPAR antibody patients (5/13), the antigen target seems to be against a conformational epitope that is only present when GluA1 and GluA2 are co-expressed, similar to the findings of the two GluA2+3 positive RE patients. This was an interesting finding as the majority of published cases of anti-AMPAR positive patients describe reactivity to only one AMPAR subunit (either GluA1 or GluA2). Those with antibodies to GluA1+2, had lower antibody titres (median: 1:180, range: 1:100-1:540). The second subset of AMPAR antibody patients identified had

antibodies specifically against the GluA2 subunit, with higher titres (p=0.14; median: 1:1620, range: 1:250-1:4800), but could still be detected on the co-transfected assays.

In this study, we also identified 9 patients (37.5%) with antibodies to only the $GABA_{B2}R$ subunit. These patients tended to have low antibody titres with 7/9 patients having titres lower than 1:540. Again, this was an interesting finding, as previous reports have suggested $GABA_{B1}R$ as the main antigen target, as all 15 patients originally described had antibodies to this subunit in a subset of LE patients (Lancaster *et al.,* 2010). Antibodies to the $GABA_{B2}R$ subunit alone have not been previously described. The second subset of $GABA_BR$ antibody patients had antibodies to both the $GABA_{B1}R$ and $GABA_{B2}R$ subunits, and these patients tended to have higher antibody levels than $GABA_{B2}R$ patients (p=0.032, Mann-Whitney).

3.9.4: Clinical features of AMPAR and $GABA_BR$ antibody positive patients

At the start of the thesis 16 patients had been described with AMPAR antibodies, of which 15 were older women (mean age: 60) and 14 were diagnosed with LE. Fifty percent of these patients had an underlying malignancy, which may be a contributing factor to the disease. The incidence of tumours is also high in $GABA_BR$ antibody patients, who often present with symptoms of LE such as seizures early on in disease (Lancaster *et al.,* 2010). More recent reports have identified $GABA_BR$ antibodies in patients with a more expanded phenotype (ataxia, status epilepticus, OMS), and not just seizures and symptoms following from impairment of the limbic region (Hoftberger *et al.,* 2013). Patients showed clinical improvement in both groups of patients when started on immunomodulatory treatment.

Interestingly, only one of the AMPAR positive patients for whom we had clinical details (n=9) had a tumour. This may indicate that the original clinical tumour associations may have been over-estimated. These reports were from laboratories involved in screening for paraneoplastic disorders and may explain why the clinical details of the antibody-positive patients is different the results found here where the incidence of tumours is much lower. The clinical symptoms of the patients identified also showed a much broader phenotype and were subgroup specific. Patients with GluA1+2 antibodies had more varied presenting symptoms (unconsciousness, amnesia, cerebellar ataxia, dementia). In addition, AMPAR antibodies were found in males (8/13), and in a younger and broader age range (19-86, median; 46.5) than originally described. A newly identified group of samples (n=15) by Gleichman *et al.* (2014) also had symptoms such as seizures and memory loss that were consistent to symptoms described in the original cohort, but there were an equal number of men and women and the a greater age range in this study (with 6 patients under the age of 30) reported. Long-term follow up data was not available for any of the AMPAR antibody patients described in this thesis. Therefore, it was not possible to investigate whether or not the patients relapsed as had been described in earlier publications (Lai *et al.,* 2009).

Patients with a higher antibody titre were mainly $GABA_{B1+2}R$ positive and had symptoms typical of LE, that were more consistent with early reports. Seven of 9 patients with $GABA_{B2}R$ antibodies had LEMS. This is an interesting finding as $GABA_BR$ are only weakly expressed in the periphery and are absent at the neuromuscular junction (Kaupmann *et al.,* 1998). Few reports describing a link between $GABA_BR$ antibodies and LEMS have been made (Onugoren *et al.,* 2014). $GABA_BR$ antibodies were also found in 6 SCLC patients without CNS and PNS symptoms. This finding was in contrast to Hoftberger *et al.* (2013), which documented that $GABA_BR$ antibodies were not found in SCLC cohort of 116 without neurological symptoms. $GABA_BR$ are present

on the surface of tumour cells (Lancaster *et al.,* 2010) and this may trigger the production of these antibodies and explain the presence of $GABA_BR$ antibodies in the sera of patients with PNS symptoms, or SCLC patients without neurological symptoms. Due to the limited expression of $GABA_BR$ in the PNS, and without access to the brain, these antibodies may simply be bystanders in these patients. Furthermore, 3 of the 10 patients from the SCLC cohort that had neurological symptoms had additional P/Q and N-type VGCC antibodies. Antibodies against P/Q and N-type VGCC and $GABA_BR$ were not present in patients with SCLC that did not develop peripheral or central neurological symptoms. This was interesting as N-type VGCC antibodies are generally found in a smaller proportion of LEMS patients (30%), as opposed to 90% of patients who have a P/Q –type VGCC-Abs (Motomura *et al.,* 2003). In our study, $GABA_BR$ antibodies have only been found in SCLC patients with neurological symptoms that had N-type VGCC antibodies in addition to P/Q-VGCC-antibodies. Based on these findings, it is possible that the VGCC antibodies are causing the disease. Whilst autoimmunity in patients with LEMS takes place in most patients before the tumour has been detected, in a few cases, patients may not present with neurological symptoms until years after the development of the tumour (Titulaer *et al.,* 2011). As follow up samples were not available from many of the samples in the SCLC cohort, the development of neurological symptoms cannot be explored further. Nevertheless, in the future, P/Q and N-type VGCC positives should be screened on the $GABA_BR$ assay as these look like patients, which would develop neurological impairment.

The presence of low antibody levels in patients with SCLC but the lack of neurological symptoms may also be a specificity issue of the diagnostic assay, i.e., the assay is picking up “false positives”. In cases of very weak staining patterns, the clinical symptoms of the patients should be carefully examined. The use of additional antibody

detection methods, such as binding to rat brain sections and primary neuronal cultures can be used to confirm these results (discussed further in Chapter 4).

3.9.5: CSF antibody levels and clinical correlation

Based on the distribution of the AMPAR and $GABA_BR$, it is unlikely that antibodies directed against these receptors are having a direct pathogenic effect in the periphery, despite the presence of these receptors on the surface of tumour cells. However, if these antibodies are able to cross the BBB and gain access to the brain, where these receptors are highly expressed, neurological symptoms can result. As such, clinical correlation and antibody titre in the sera and CSF from follow up samples was assessed.

Two of the patients with high levels of GluA2 antibodies in the sera (end-point titre 1:620), also had very high levels in the CSF (1:520 and 1:1620). For one of the patients that had serial paired sera and CSFs taken at various time points during his disease course, prior to treatment, the antibodies in the sera and CSF both titrated out to 1:1620. While, normalization of IgG levels using an albumin ratio, is required to determine whether or not these high antibody levels in the CSF are due to a breakdown of the BBB or intrathecal synthesis, a crude estimate of relative levels could be concluded by multiplying the CSF antibody levels by 400 (as the ratio of albumin in sera to CSF is 400:1). The relative antibody index (CSF/Sera) would suggest that prior to treatment the patient had 400 times the antibody level in the CSF than sera. This is either suggestive of intrathecal synthesis and/or following the seizures; there was a weakening of the BBB which allowed antibodies to enter the brain. This patient's clinical outcome improved as the GluA2 antibody levels in the CSF decreased (Figure 3.12), even as the antibodies in the sera remained high. One explanation is that the BBB was repaired following the patient's recovered from his seizures, preventing new synthesized GluA2 antibodies in the sera from accessing AMPAR in the CNS. These findings highlight the importance of testing for AMPAR antibodies in the CSF of these patients.

Intrathecal synthesis has also been reported in patients with NMDAR

encephalitis (Dalmau, 2008, Pruss *et al.,* 2010). However, unlike what was noted in our AMPAR patient, in the majority of cases the antibody levels in the sera are higher than in the CSF (Irani *et al.,* 2010 and Dale *et al.,* 2009). Irani *et al.* (2010) showed in NMDAR encephalitis that the mean antibody levels in the sera were approximately 13.5 times higher in the sera than the CSF.

Furthermore, two patients with LE that had high $GABA_BR$ antibody levels in the serum (end-point titre 1:4800 and 1:6400) also had paired CSF, which showed strong reactivity to transfected HEK cells. A comparison of end-point titre between the paired samples showed that antibody levels were higher in the serum than the CSF, which is consistent with other autoimmune encephalitis studies (Dale *et al.,* 2009 and Irani *et al.,* 2010). However, if normalized, it was revealed that antibodies were 50-60-fold higher in the CSF than in the serum (Figure 3.13). Again, this could be due to a disruption of the BBB, which allows antibodies in the periphery to gain access to the CNS. However, antibodies could also additionally be intrathecally produced. Unfortunately these findings and a direct correlation between antibody levels and disease severity cannot currently be assessed as CSF and /or follow up sera samples are unavailable for the majority of the patients investigated in this study so far. Therefore, it remains inconclusive whether or not these patients clinical outcome correlated better with an antibody titre in either the sera or CSF.

CHAPTER 4: Characterisation of the potential pathogenic role of anti-AMPAR and $GABA_BR$ antibodies *in vitro*

The identification of the antigenic target in a putative autoimmune disease is central to understanding the pathological mechanisms involved. The identification of the causative autoantibodies can be important for monitoring disease progression and the efficacy of treatment modality. Studies have shown that AChR antibodies in MG can mediate their pathogenic effects via three mechanisms: 1) direct blocking of AChR 2) internalisation of AChR and 3) antibody mediated activation of the complement cascade (see Section 1.3.2). However, there are also a variety of diseases, whereby autoreactive components are present and the antibodies themselves are an epiphenomenon such as the Yo and Hu-specific antibodies in PCD (Smitt *et al.,* 1995). Both Yo and Hu are intracellularly expressed, and their localisation makes them an unlikely target for circulating antibodies. The mere presence of an autoantibody does not necessarily mean that they play a pathogenic role in the disease.

Like MG, many patients (approximately 90%) with AMPAR and $GABA_BR$ antibodies show a substantial improvement when started on immunotherapies (Lai *et al.,* 2009 and Lancaster *et al.,* 2010), which correlated with a fall in antibody titre. Similarly, patient relapses were often associated with a rise in antibody levels. AMPAR antibodies have been shown to cause a reduction in the number of the receptors at the synapse due to internalisation of the receptor and modulation of receptor trafficking (Lai *et al.,* 2009). However, the pathogenic potential of $GABA_BR$ antibodies remains to be elucidated, although others have suggested that receptor internalisation is not the pathogenic mechanism (Lancaster *et al.,* 2010). A loss of receptor function would result in the development of many of the symptoms associated with AMPAR and $GABA_BR$ antibody positive patients (see Section 1.6.2 and 1.7.2.). These findings suggest that

these antibodies have a pathogenic role and the aim of this chapter was to explore this role in greater detail using a variety of different *in vitro* techniques.

4.1: Detection of antibody binding using rat brain sections

In order to investigate to which brain regions patient antibodies bind, the immunoreactivity of patient sera to sagittal rat brain sections was examined. Depending on regional and neuronal reactivity, this method can provide insight into the clinical features of the patients.

4.1.1: Binding of AMPAR antibodies to rat brain sections

Sera and CSF was available to study from patients with high antibody levels (GluA2 patients mean titre; 1938), whilst only sera were available from low antibody titres (GluA1+2 mean titre: 1:250) patients. With sera and CSF from patient A#8 (GluA2, titre 1:1620) strong immunoreactivity was observed in the cerebellum, hippocampus, cerebellar cortex and pituitary gland (CSF shown in Figure 4.1A). Within the hippocampus, specific areas were immunolabeled, including the CA3 region, the granular cell layer (GCL) of the dentate gyrus (DG), the outer molecular layer (OML) and hippocampal fissure (hif), whereas staining was spared in the inner molecular layer (InML), the CA1 region and radiatum (Rad; Figure 4.1B). In addition, both the GCL and molecular cell layer (ML) were intensely stained in the cerebellum (Figure 4.1C). Purkinje cell (PCL) staining was not noted in this patient, as has previously been reported (Lai *et al.,* 2009). A similar staining pattern was noted with all of the GluA2 antibody positive sera with an end point titre of >1:1620 (n=5/8 patients). GluA2 antibody positive patients with titres below 1:1620 did not show a specific staining pattern.

CSF was unavailable from the patients with GluA1+2 antibodies. Although immunostaining with GluA1+2 sera was attempted (n=5), the low antibody titres made it difficult to distinguish any specific stain from background levels (data not shown).

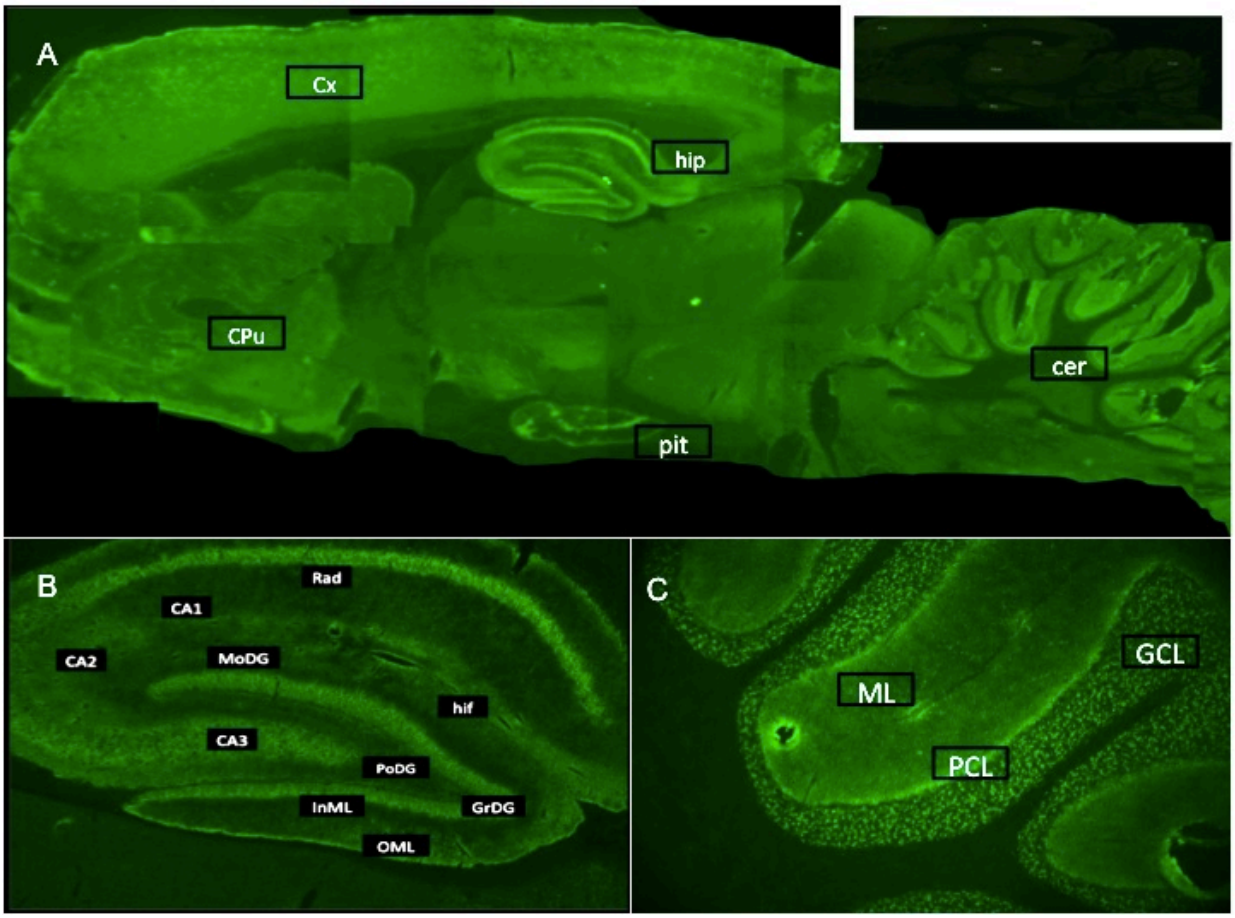

Figure 4.1: Immunolabeling of GluA2 antibody positive CSF to rat brain sections

Sagittal rat brain sections (12 µm) were incubated with sera (1:200-1:1000) or CSF (1:10) overnight at 4°C. Antibody binding was detected using a goat anti-human IgG Alex Fluor 488 (1:1000 green). Figure 4.1A shows whole brain (25x magnification), specific area of hippocampus shown in B (50x magnification), and cerebellum shown in C (50x magnification).

GluA2 antibodies (CSF from A#8) showed strong reactivity to the granular cell layer (GCL) in both the hippocampus (hip) of the dentate gyrus (GrDG; B) and the cerebellum (cer; C). The molecular layer (ML) of the cerebellum also showed increased stain, with sparing of the Purkinje cells layer (PCL) (C). Other brain regions that showed immunostaining include the cerebral cortex (Ctx), the caudate putamen (CPu) and the pituitary gland (pit; A). Inset in A shows HC staining.

4.1.2: Binding of $GABA_BR$ antibodies to rat brain sections

The $GABA_BR$ antibodies also reacted with the rat brain sections in an antibody concentration-dependent manner. In total 8/24 patients showed immunoreactivity to rat brain sections. Patients with $GABA_BR$ antibody titres below 1:4800 showed very little reactivity, which was indistinguishable from background staining seen with HC (similar staining seen in Figure 4.1A inset). However, both high titre $GABA_{B2}R$ (n=1 patient with titre of 1:6400) and $GABA_{B1+2}R$ showed similar staining patterns. As the receptor is ubiquitously expressed throughout the brain, immunoreacitivity was noted across the sagittal rat brain section, with areas of the highest immunoreactivity being the cortex, hippocampus, cerebellum (ML and GCL), thalamus and pituitary gland. The caudate putamen (CPu) was less intensely stained. Unlike AMPAR antibody immunoreactivity, $GABA_BR$ antibodies did not show specific immunoreactivity to the hippocampal layers (Figure 4.2). However, the OML was intensely labeled and the InML of the hippocampus was noted to be spared.

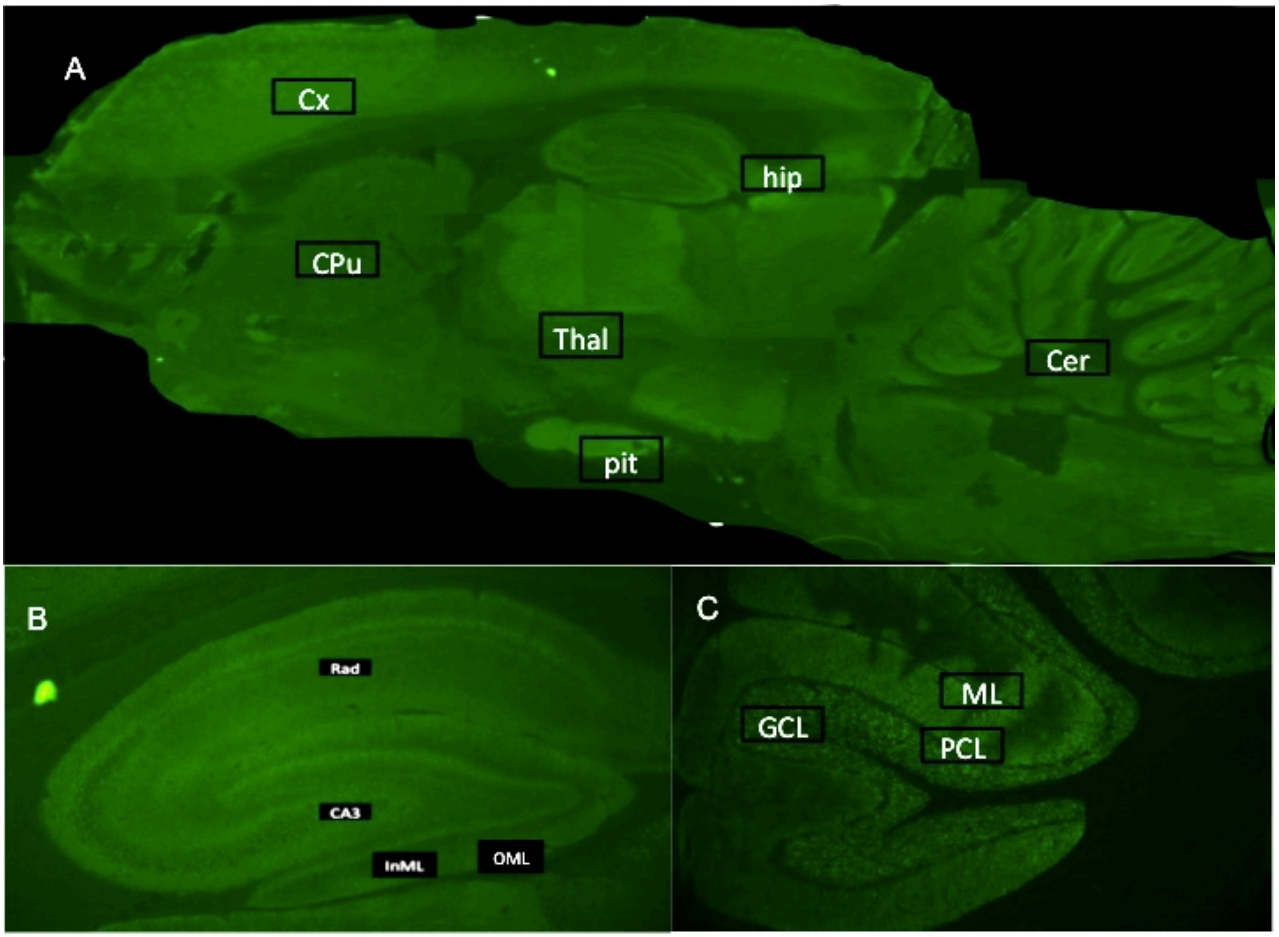

Figure 4.2: Immunolabeling of $GABA_BR$ antibody positive CSF to rat brain sections

Sagittal rat brain sections (12 µm) were incubated with sera (1:200-1:1000) or CSF (1:10) overnight at 4°C. Antibody binding was detected using a goat anti-human IgG Alex Fluor 488 (green). Figure 4.2A shows whole brain (25X magnification), specific areas of the hippocampus are shown in B (50x magnification) and cerebellum shown in C (50x magnification).

$GABA_BR$ antibodies (CSF from G#8) showed reactivity to the OML of the hippocampus (B). In addition strong reactivity to the granular cell layer (GCL) and molecular layer (ML) of the cerebellum were noted with sparing of the Purkinje cell layer (PCL) (C). Other brain regions that showed immunostaining include the cerebral cortex (Cx), the thalamus (thal), and the pituitary gland (pit).

4.2: Detection of antibody binding using rat primary neuronal cultures

The use of the CBA for the detection of antibodies in patient sera and CSF is clearly advantageous over other techniques such as ELISA and immunoblotting, as antibody binding to the extracellular domains of conformationally expressed protein is assessed. While the CBA is an excellent tool for the detection of antibodies, it is an artificial system, and the overly expressed protein levels may not be representative of the actual levels *in vivo.* Additionally, by using a CBA, only antibodies directed against the antigen being explored can be investigated, and antibodies to additional neuronal surface autoantigens will not be detected. As such, it is important to investigate binding to native cells, using primary neuronal cultures. As many of these patients present with features affecting limbic regions, hippocampal neurons were selected to test reactivity of patient's sera and CSF. Primary hippocampal neurons were prepared from P0 rat pups and cultured for 14 days (div14) on glass coverslips, before staining. In order to ensure that the extracellularly expressed proteins were being examined, binding was investigated using live (unpermeabilised) cultures.

4.2.1: Reactivity of RE sera/CSF to primary neuronal cultures

The cohort of 63 patients with RE proven or suspected (see Table 3.1) was screened on hippocampal cultures (as described in 2.8). As RE is a disease that also affects cortical regions, cortical neurons were also cultured from P0 rat pups and grown for 10 div on glass coverslips prior to staining. Only 2/63 patients bound to cortical neurons, neither of which were GluA2+3 antibody positive. In addition to the two GluA2+3 antibody positive patients, 8 additional patients that were negative on all CBAs, bound to hippocampal neurons (10/63; 15.8%; Table 4.1). Representative images showing the staining of GluA2+3 antibody positive sera and antigen unknown sera to live

hippocampal neurons are shown in Figure 4.3. One of the patients bound to both cortical and hippocampal neurons (case 4). Of the 10 samples that showed neuronal immunoreacitivity, 4 of the patients were adults. Unfortunately, none of the positive samples had paired CSF. Of the available CSFs (n=14), none of the samples showed binding to either cortical or hippocampal neurons.

Data on sample collection was available from 36/63 patients (57%), and 5/10 of the patients that showed neuron reactivity. The average date of sample collection from the 36 patients with this data available was 4.2 years. In contrast, the average time following the acute stage of neuron positive samples was shorter at 2.3 years. This data suggests the importance of collecting samples early on from the development of the acute stage.

Table 4.1: Summary of RE patients that bind to neuronal cultures

Case	Sex/Age at onset	Diagnosis	Binding to Primary Cultures	Antibodies Detected	Sample collection (after acute stage)
RE#1	F/14	RE	Hippocampal	None	NA
RE#2	M/15	RE	Hippocampal	None	NA
RE#3	F/22	RE	Hippocampal	None	NA
RE#4	F/33	Suspected RE	Hippocampal and cortical	None	NA
RE#5*	F/20	Suspected RE	Cortical	None	NA
RE#6	M/3	RE	Hippocampal	None	2 months
RE#7	M/5	RE	Hippocampal	None	1 year
RE#8	F/19	RE	Hippocampal	None	3 years
RE#9	M/10	RE	Hippocampal	GluA2+3	1 and 2 years
RE#10	F/7	RE	Hippocampal	GluA2+3	6 years

*Not enough sample available for testing on both cultures

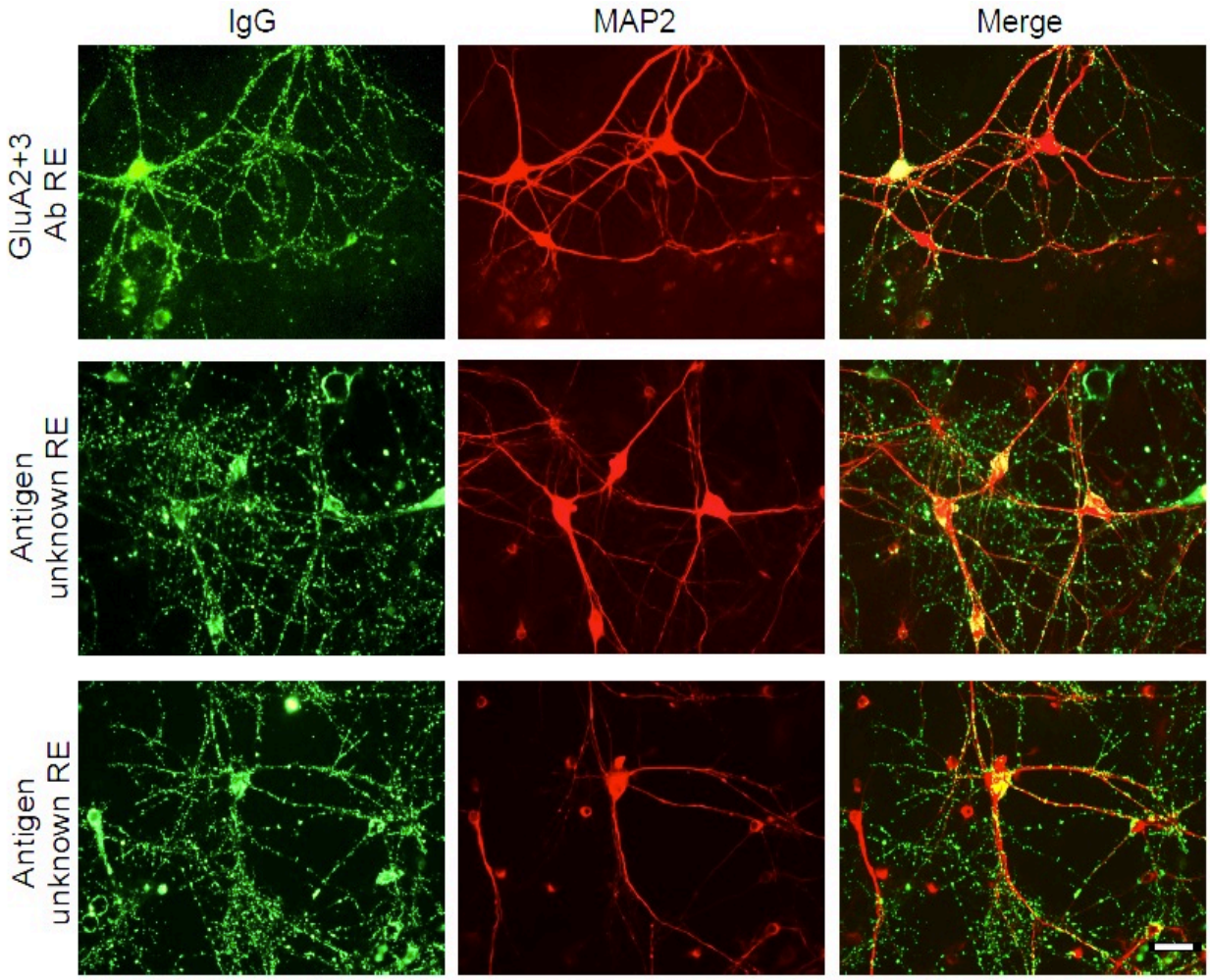

Figure 4.3: RE sera shows reactivity to the surface of live hippocampal neurons

Cultured hippocampal neurons (div 14) were incubated with patient sera (1:100) for one hour, and IgG binding visualized with a goat anti-human IgG Alexa Fluor 488 (green, 1:1000). Neurons were subsequently fixed, permeabilised and incubated with MAP2 (a neuronal marker detected in red).

GluA2+3 antibody positive patients showed reactivity to hippocampal neurons (RE#9; upper panel). An additional 8 samples with an unknown antigen bound strongly. Representative antigen unknown RE shown in the middle (RE#2) and bottom panel (RE#4). Images 400x magnification. Scale bar= 50 µm.

4.2.2: Reactivity of AMPAR antibody positive patients to primary cultures

In addition to the AMPAR antibody patients identified in the cohort of RE patients, antibodies to this receptor were also detected in samples sent for diagnostic testing (see Table 3.3. and 3.4). Two distinct types of AMPAR antibody positive samples were identified from this screening; patients with GluA1+2 antibodies (n=5) and patients with antibodies to GluA2 alone (n=8). All 13 AMPAR antibody positive patients showed reactivity to primary hippocampal neurons. Representative images of AMPAR antibody positive patient staining are shown in Figure 4.4A. Available CSF from two GluA2 antibody positive patients also showed staining to hippocampal cultures (Figure 4.4B). Sera from HC patients did not bind to the surface of neurons (Figure 4.4A: bottom panel).

As described in chapter 3, the patients with GluA1+2 antibodies showed reactivity to HEK cells co-transfected with GluA1 and GluA2. The presence of conformational epitopes only present when certain co-expressions of proteins is an interesting finding, as in a majority of autoimmune CNS disorders, the antibodies are directed against one subunit of the protein (Dalmau *et al.,* 2008, Lai *et al.,* 2009 and Irani *et al.,* 2010). In order to investigate this further, samples positive on the cotransfected assay were preadsorbed against singly transfected GluA1 and GluA2 HEK cells and then reapplied to the co-transfected assay and hippocampal neurons. Preadsorption against HEK cells transfected with single AMPAR subunits had no effect on the binding to the co-transfected assay suggesting that antibodies directed against GluA1 or GluA2 are not present in the sera of these patients (Figure 4.5). In addition, the abolition of reactivity to patient sera to hippocampal neurons following incubation with HEK cells transfected with GluA1+2, is suggestive that the antigenic target is dependent on conformational subunit assembly, and that no other antigen target is present in these patients.

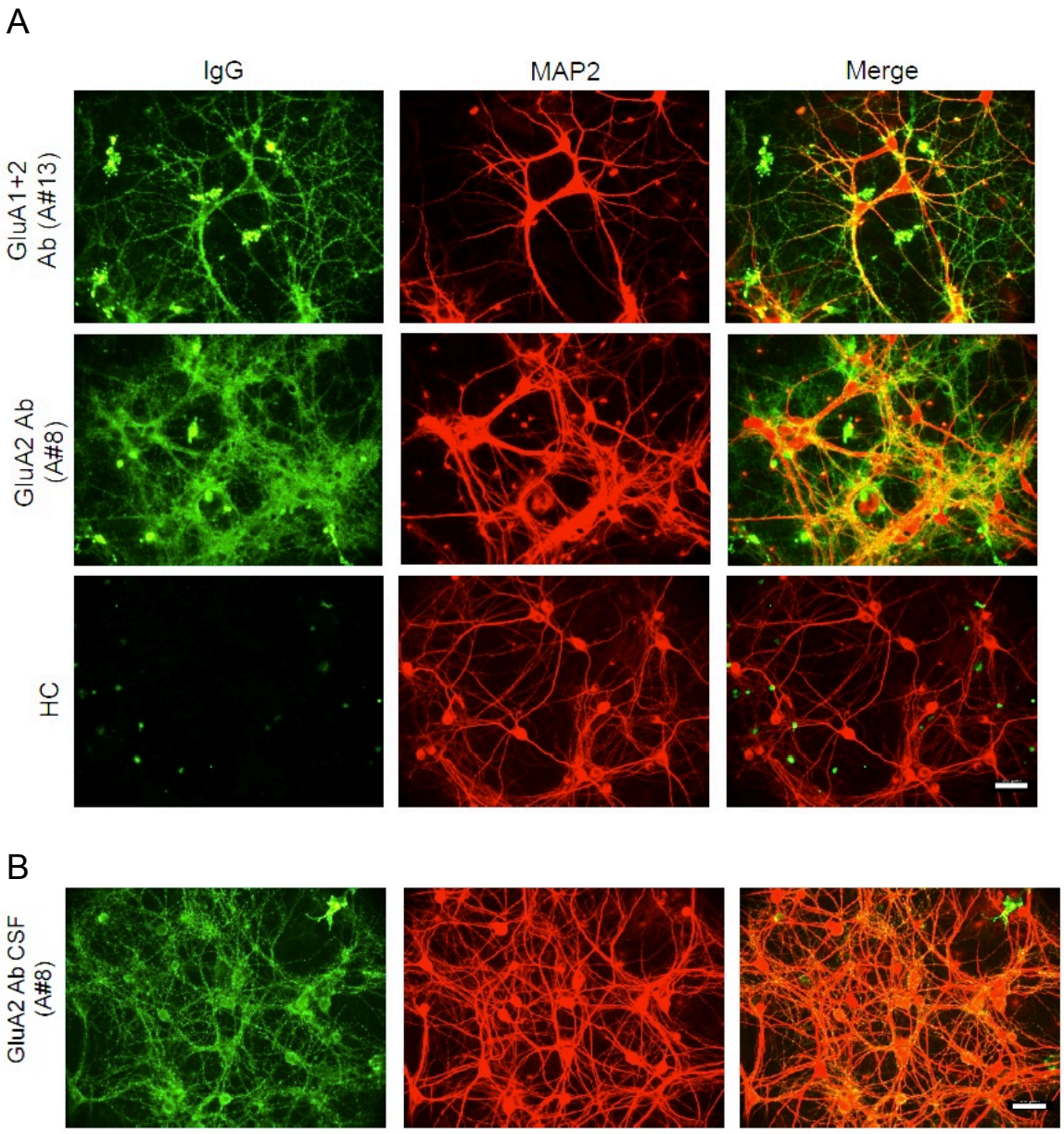

Figure 4.4: AMPAR antibody sera and CSF show intense reactivity to primary hippocampal cultures in comparison to HC sera

Cultured hippocampal neurons (div 14) were incubated with patient sera (1:100) for one hour, and IgG visualized with a goat anti-human IgG Alexa Fluor 488 (green; 1:1000). Neurons were subsequently fixed, permeabilised and incubated with MAP2 (red).

Representative images of a GluA1+2 (A#13; upper panel) and GluA2 (A#8; middle panel) antibody positive patients. Intense reactivity to the surface of hippocampal neurons was observed, whilst HC sera showed no reactivity (bottom panel; A). CSF from GluA2 antibody positive patients (A#8, 1:10) also bound to neurons (B). 400X magnification. Scale bar= 50 µm.

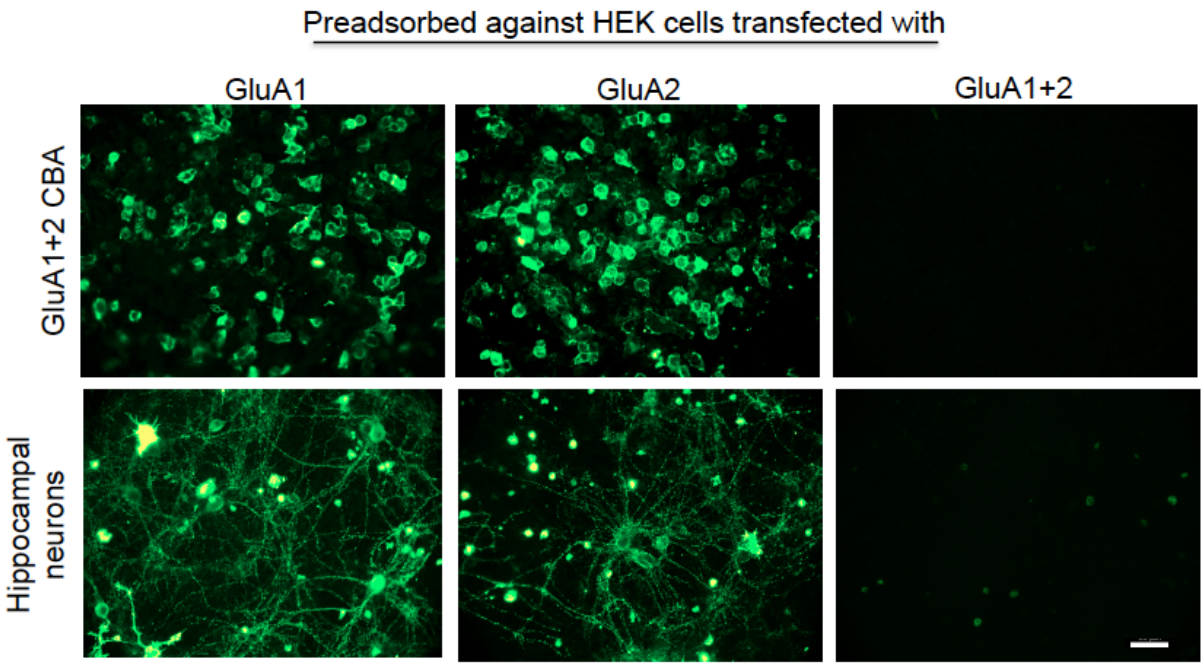

Figure 4.5: Antibodies directed against the GluA1+2 subunits are specific to a conformationally expressed epitope

Antibodies were absorbed by incubating sera (1:20) with a resuspension of HEK cells mono-transfected with GluA1 or GluA2 alone or cotransfected with GluA1 and GluA2. Absorbed samples were re-tested on the GluA1, GluA2 or GluA1+2 transfected HEK cells (upper) and on hippocampal neurons (lower) for reactivity.

When GluA1+2 positive sera (1:20; representative image of A#13 shown) is preadsorbed against HEK cells transfected with GluA1 or GluA2, sera still shows reactivity to GluA1+2 transfected HEK cells. However, when sera are preadsorbed against GluA1+2 co-transfected HEK cells, all reactivity is abrogated (upper panel). Furthermore, all reactivity to neuronal cultures is lost when sera are preadsorbed against GluA1+2 HEK cells, but not when preadsorbed against GluA1 or GluA2 transfected HEK cells (bottom panel). Binding visualized with a goat anti-human IgG Alexa Fluor 488 (green; 1:1000). Images 400x magnification. Scale bar =50 µm.

Similar preadsorption experiments were completed with GluA2 antibody positive sera. When sera was preadsorbed against GluA1 HEK cells, or untransfected HEK cells (control), the sera still showed binding to the GluA2 CBA and hippocampal neurons, suggesting that these patients do not have antibodies to GluA1. However, when sera is preadsorbed against HEK cells transfected with GluA2, there is complete ablation of IgG immunoreactivity to GluA2 transfected HEK cells and hippocampal neurons, suggesting that these patients have antibodies specific to the GluA2 subunit and no additional antibodies to extracellular proteins are present (Figure 4.6).

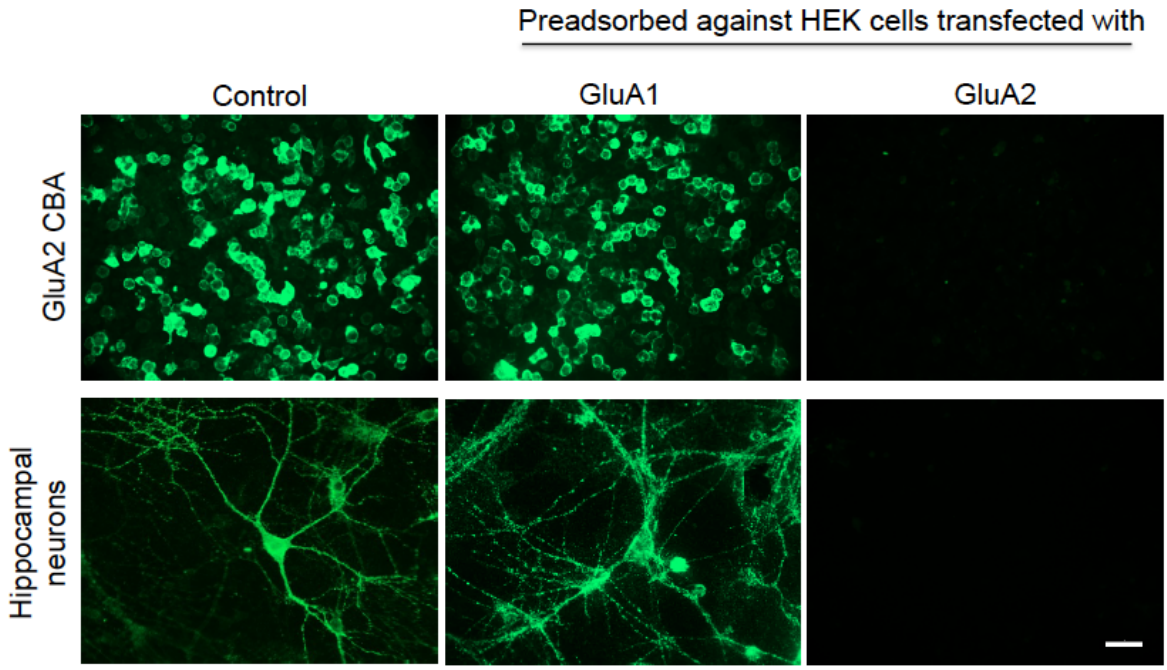

Figure 4.6: GluA2 antibodies are specific for the GluA2 subunit and show an abolition of binding following preadsorption with GluA2 transfected HEK cells

Antibodies were absorbed by incubating sera (1:20) with a resuspension of HEK cells mono-transfected with GluA1 or GluA2 or untransfected HEK cells (control). Absorbed samples were tested on the GluA1, GluA2 transfected HEK cells and hippocampal neurons for reactivity.

When GluA2 positive sera (1:20; representative image of A#8 shown) is preadsorbed against HEK cells transfected with GluA1, or untransfected HEK cells (control,) sera still shows reactivity to GluA2 transfected HEK cells and hippocampal neurons (left and middle column). Sera preadsorbed against GluA2 transfected HEK cells lost all reactivity once incubated with GluA2 HEK cells and did not bind to neurons (far right column). Binding visualized with anti-human IgG Alexa Fluor 488 (green; 1:1000). Images 400x magnification. Scale bar =50 µm.

4.2.3: Reactivity of $GABA_BR$ antibody positive patients to primary neuronal cultures

Only 14/24 sera with $GABA_BR$ antibodies bound to hippocampal neurons. Representative images of $GABA_BR$ antibody patients showing positive (G#5) and negative (G#13) immunoreactivity to hippocampal neurons is shown in Figure 4.7A.

Unlike the AMPAR antibody patients which all showed reactivity to primary hippocampal neurons, the binding of $GABA_BR$ antibody patients was more variable. Patients with a higher antibody titre were significantly more likely to bind to hippocampal neurons than patients with a lower CBA score ($p<0.001$, Mann-Whitney, Figure 4.7B). When $GABA_BR$ antibodies were preadsorbed and re-tested for reactivity to hippocampal neurons, binding was abolished in 14/14 sera tested (data not shown).

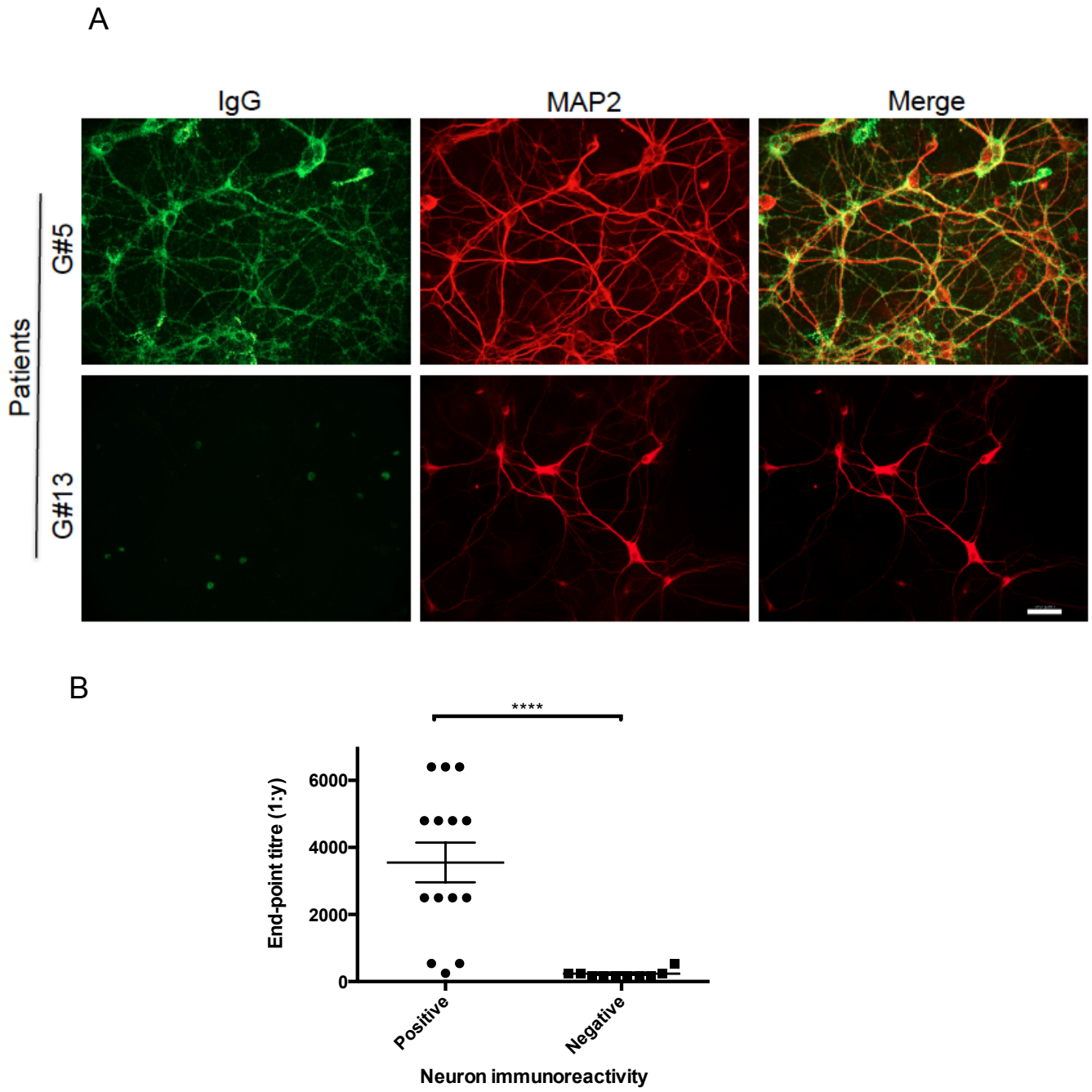

Figure 4.7: 14/24, $GABA_BR$ antibody positive patients bind to the surface of hippocampal neurons *in vitro*

Representative staining of a high (G#5 1:4800) and low antibody titre patient (G#13 1:250) on the surface of hippocampal neurons. Staining was detected using anti-human IgG Alexa Fluor 488 secondary antibody (green; 1:1000). Neurons were subsequently fixed, permeabilised and incubated with MAP2 (red). 400X magnification. Scale bar= 50µm (A).

A significant difference in end-point titre was noted between samples that showed positive and negative immunoreactivity to primary hippocampal neurons (p=<0.0001, Mann-Whitney; B)

4.3: AMPAR and $GABA_BR$ antibody subclasses

Neuronal death as a result of activation of the complement cascade is one potential mechanism that could be mediated by autoantibodies (see section 1.3.2). Only some of the human IgG subclasses are able to activate complement, namely IgG1 and IgG3. IgG2 is a less potent complement activator, while IgG4 has been shown to not activate the complement cascade (Table 1.1). In order to investigate the ability of AMPAR and $GABA_BR$ antibodies to activate the complement cascade, the IgG subclass specificity was first assessed by CBA. Secondary antibodies raised against the individual subclasses were utilised to detect antibody subclass specificity.

Due to a limited volume of sera, only 20 antibody positive patients were tested for IgG subclasses. Of the available sera, 11 had AMPAR antibodies (7 GluA2 antibody, 2 GluA1+2 antibody and 2 RE patients with GluA2+3 antibodies) and 9 patients had $GABA_BR$ antibodies (3 $GABA_{B2}R$ antibody and 6 $GABA_{B1+2}R$ antibody). A breakdown of patient number with antibodies to an IgG subclass is shown in Figure 4.8. Eight of 11 tested AMPAR antibody positive sera were positive for a specific IgG subclass. All 8 samples were IgG1 positive with one patient having additional IgG2 subclass antibodies, and a final patient having antibodies to both IgG2 and IgG3. Whilst two RE patients were positive for GluA2+3 antibodies, only one of the RE samples (RE#9 titre 1:540) had very low IgG1 antibody levels detected in the sera (CBA score=1).

IgG1 was also the most predominant IgG subclass present in $GABA_BR$ antibody patients. In total 7/9 $GABA_BR$ antibody patients were positive for an IgG subclass and 6/7 had IgG1. One patient with IgG2 and IgG3, but no IgG1 subclass antibodies was also present in this group of samples.

Three of the 11 AMPAR antibody sera and 2/9 $GABA_BR$ antibody sera showed no reactivity when incubated with specific IgG commercial antibodies. These samples were all low antibody titre patients (<1:540), and the lack of staining could be indicative

of the lack of specificity of the subclass CBA. IgG4 was absent in all of the samples tested. The CBA scores on individual IgG subclass assays are shown in Appendix Figure 1.

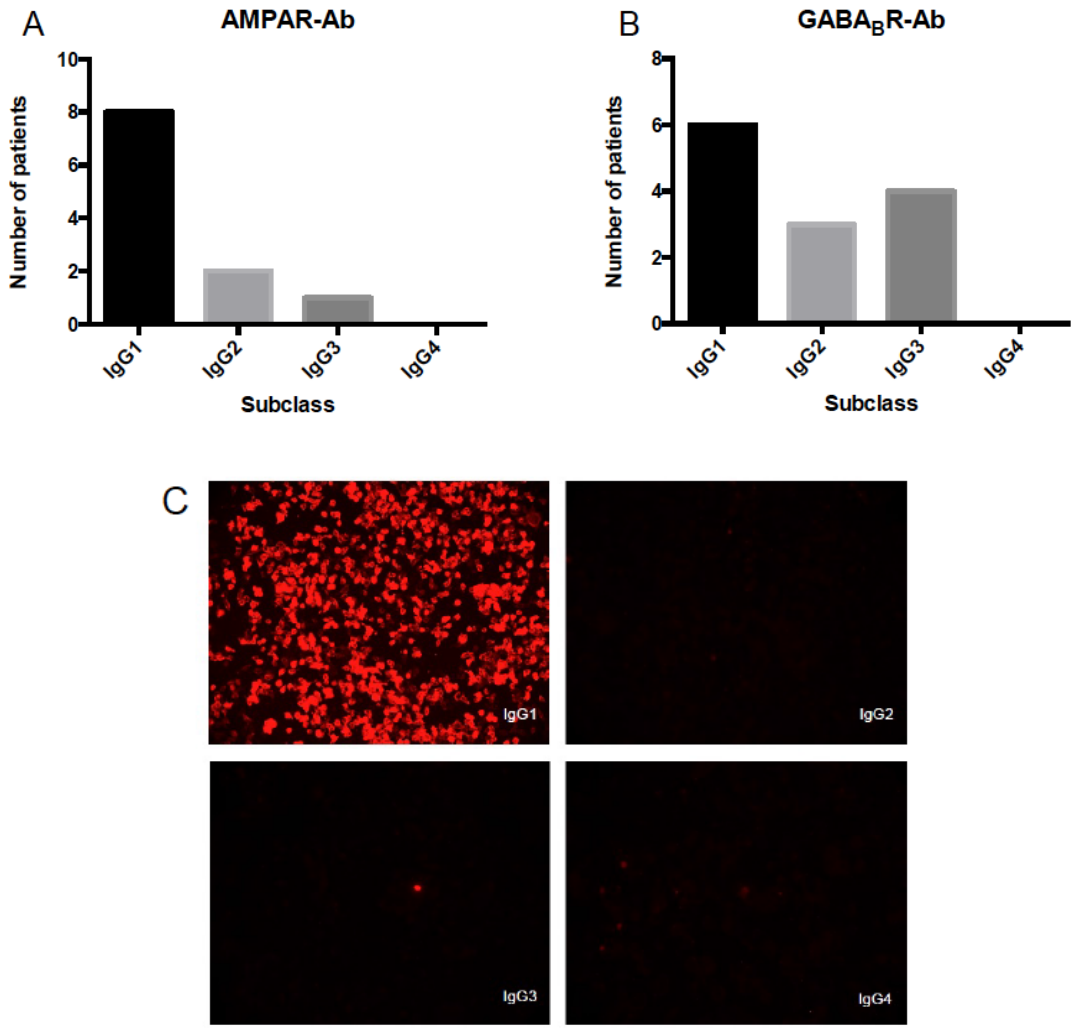

Figure 4.8: AMPAR and GABA$_B$R antibodies are predominantly IgG1

Non-saturating amounts of sera were incubated on AMPAR transfected HEK cells (1:50) or GABA$_{B1+2}$R transfected HEK cells (1:100). Subunit specific commercial antibodies against IgG1, 2,3 and 4 (1:20) were applied to the cells and IgG subunit specific binding visualised using a goat anti-mouse IgG Alexa Fluor 568.

AMPAR antibodies (n=8/11 positives) were predominantly IgG1 (A). GABA$_B$R patients (n=6/9 positives) were also predominantly IgG1 (B). A representative example of the CBA image for a typical AMPAR antibody positive patient (A#8) that was solely IgG1 positive is shown.

4.4: AMPAR and $GABA_BR$ antibodies and complement activation

As the majority of the samples were of the IgG1 subclass (with some patients having additional IgG3 antibodies), the sera have the potential to activate the complement cascade. To determine the feasibility, a complement activation assay was used. For these experiments, AMPAR and $GABA_BR$ antibody sera were heat inactivated to inactivate any complement components present in the patient sera and subsequently incubated with transfected HEK cells. After IgG binding, a fresh source of complement (fresh frozen serum from a healthy donor) was applied to the cells and staining with a commercial antibody anti-C3c using the CBA was carried out. Anti-C3c is a marker of C3b, which is an early stage component of the complement system (see section 1.3.2). Positive staining to components of the complement cascade is suggestive of complement activation.

Results are shown in Figure 4.9. Of the 11 AMPAR antibody positive sera tested, 5/11 (45%) AMPAR antibody sera deposited C3b binding on the cell surface (Figure 4.9A). Of note, all 5 patients had IgG1 antibodies and one patient had both IgG1 and IgG3 serum antibodies. Of the 9 $GABA_BR$ antibody sera, only one patient (11.1%) showed the potential to activate the complement cascade, albeit this was very weak (CBA score= 1, Figure 4.9B).

Whether or not AMPAR antibodies could activate complement was dependent on the overall antibody levels. Sera that showed C3b deposition had higher overall AMPAR antibody levels than the sera that showed no deposition (median of C3b positive; 1:1620, median of C3b negative; 1:215, $p=0.013$ Figure 4.9C). Two AMPAR antibody patients with low IgG1 levels (end-point titre 1:540) did not show complement activation, suggesting that while patients may have detectable levels of antibodies specific to a subclass, these antibodies may not be sufficient to cause complement deposition. Furthermore, neither of the RE sera showed the ability to fix complement, despite

detection of IgG1 in RE#9 sera (CBA score=1). C3b deposition was not noted in any of the 11 HC patients. Interestingly, with the exception of one patient, the $GABA_BR$ antibodies did not show any C3b binding. Representative staining of complement components is shown in Figure 4.9D.

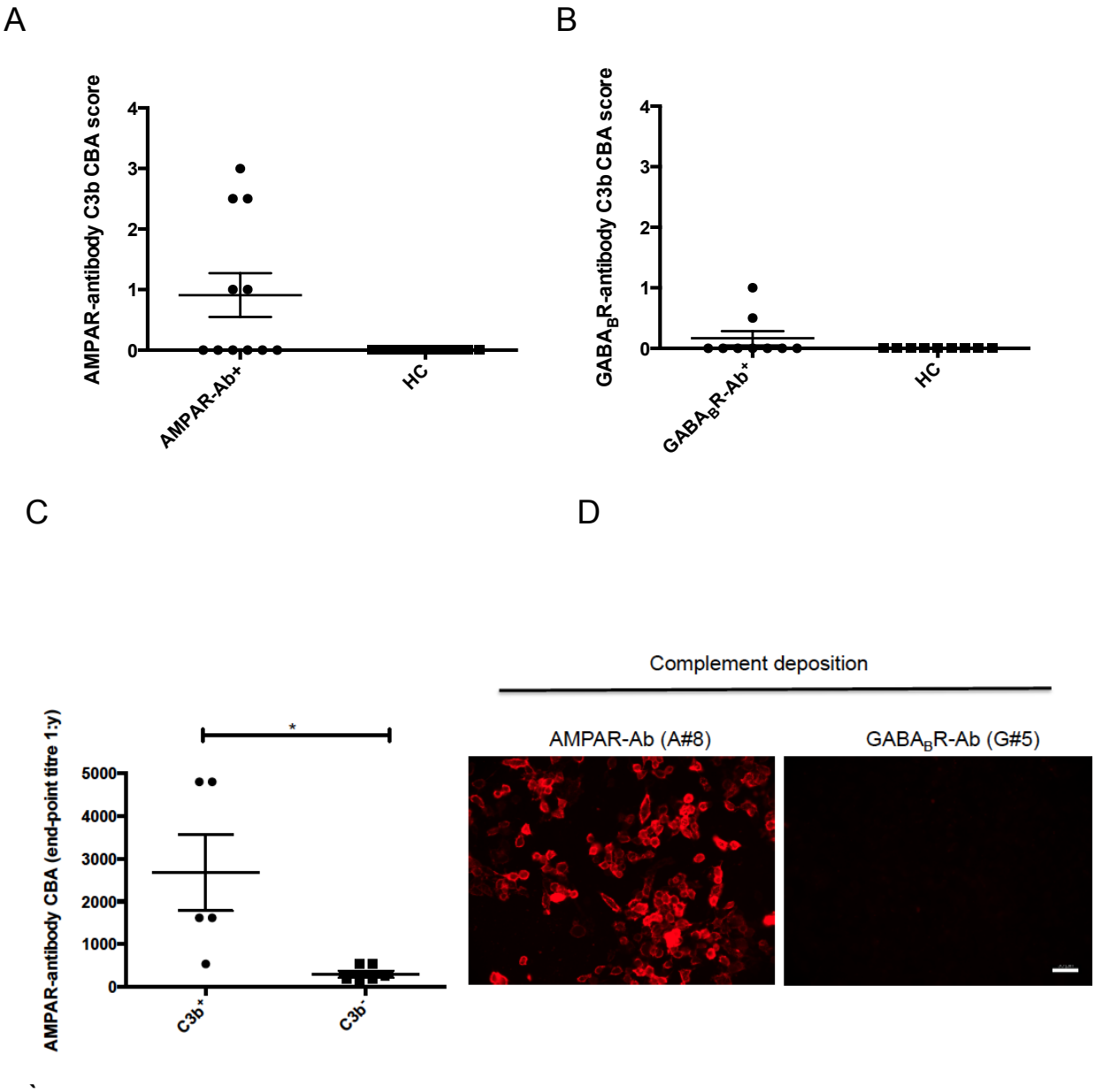

Figure 4.9: AMPAR-antibodies have the potential to activate complement

Five of 11 AMPAR antibody positive samples showed positive staining on the C3b CBA (A). Only one out of 9 GABA$_B$R antibody positive patients showed positive staining on the C3b CBA (B) Staining was compared to HC sera (n=11), and a CBA score of >1 was used as a positive cutoff. The potential of AMPAR antibodies to activate complement (C3b$^+$) was related to antibody end point titration (p=0.013, Mann-Whitney) (C). Representative image of C3b deposition a GluA2 antibody positive (A#7, titre; 1:1620) and lack of deposition noted with a GABA$_B$R antibody positive patient (G#5, titre; 1:6400) (D). Images 400x magnification. Scale bar= 50 µm

4.5: Internalisation of AMPAR and $GABA_BR$

Another potential antibody mechanism may be the internalisation of the target receptor from the cell surface. The internalisation of AChR and NMDAR via cross-linking of IgG molecules has been demonstrated in MG and anti-NMDAR encephalitis (Drachman *et al.,* 1978*,* Nagel *et al.,* 1988 and Hughes *et al.,* 2010). Previously, reduction in the number of AMPAR at the synapse of hippocampal neurons following the application of AMPAR antibody positive CSF for 6 days has been documented, which is likely to also be mediated by antibody cross linking (Lai *et al.,* 2009).

4.5.1: Internalisation of AMPAR using transfected HEK cells

Sufficient sera were only available from two patients with GluA2 antibodies. As such, further investigations were carried out from IgG purified from this subtype of AMPAR antibody patients. To explore whether antibodies directed against the AMPAR could cause receptor internalisation, GluA2 transfected HEK cells were incubated with purified IgG (from two GluA2 antibody positive patients and control sera) for one hour at 37°C. Cells were subsequently washed, and incubated with a secondary antibody (goat anti-human IgG Alexa Fluor 488) prior to fixing and mounting the coverslips. Surface IgG staining was compared over time (0, 3, 12 and 24 hours). The scoring system established for the diagnostic CBA was used to evaluate changes in IgG surface stain.

AMPAR antibodies showed a decrease in surface binding 3 hours following incubation, and immunofluorescent intensity continued to decline up to the 24-hour mark. Representative staining from one GluA2 antibody patient (A#8) is shown in Figure 4.10A. To ensure, internalisation was not occurring due to nonspecific effects of the antigen-antibody interaction, cells were fixed in 4% formaldehyde for 10 minutes prior to incubation with the primary antibody for one hour. After incubation with patient

antibodies, the cells were incubated for 3, 12, and 24 hours (Figure 4.10A; bottom panel). This process would prevent internalisation of the receptor. To analyse the effect of AMPAR antibody sera quantitatively, low magnification images were taken of coverslips and the number of total cells (determined by DAPI positivity) were compared to the number of cells that showed surface stain. No change in the number of total cells was observed over time, suggesting antibodies themselves are not causing cell death during this time (4.10B). In addition, the transfection also seemed to slow down cell growth, as an increase in cell number was not observed over time. The ratio of positive cells (stained green) to the total number of cells dropped (Figure 4.10C/D). This may be a result in internalisation or the dissociation of the IgG-antigen interaction over time.

Unfortunately insufficient sera volume from GluA1+2 antibody sera was available for testing. As such, whether or not antibodies from this subgroup of AMPAR patients can also cause internalisation of the receptor could not be answered in this thesis.

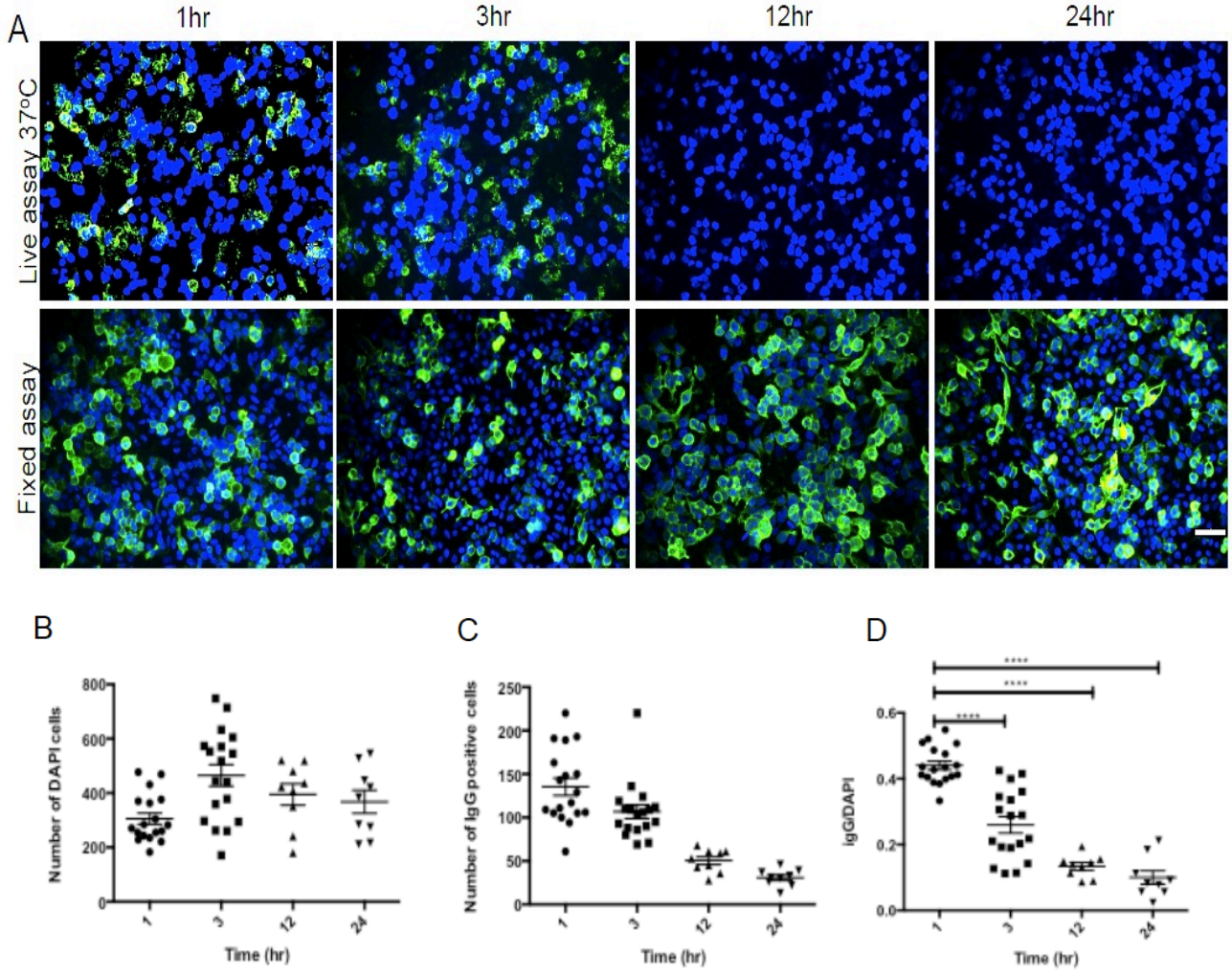

Figure 4.10: Reduction in AMPAR antibody staining to AMPAR transfected HEK cells

GluA2 transfected cells were stained with IgG purified from GluA2 antibody positive patients (100 µg/ml). IgG was removed after one hour and cells incubated in media for a further 3, 12 and 24 hours.

Binding of antibodies to the surface of cells was reduced over time (A; upper panel). Fixed cells showed no change in surface stain over time (A; bottom panel). Images 400x magnification. Scale bar = 50 µm. The total number of DAPI cells was not affected over the time course (B). The number of positively stained cells decreased over time (C), and the ratio of positively stained to total DAPI cells showed a reduction for both patients over time (D). Cells counted using Image J.

A comparison of CBA scores from the two GluA2 antibody sera at one hour and 24 hours in both the live and fixed assay were compared (Figure 4.11). Both patients showed a decline in surface stain over time ($p<0.001$, t-test unpaired). When cells were fixed, no significant change in cell surface staining was observed for either patient, suggesting that fixation prevents the antibody-antigen complex from being internalised.

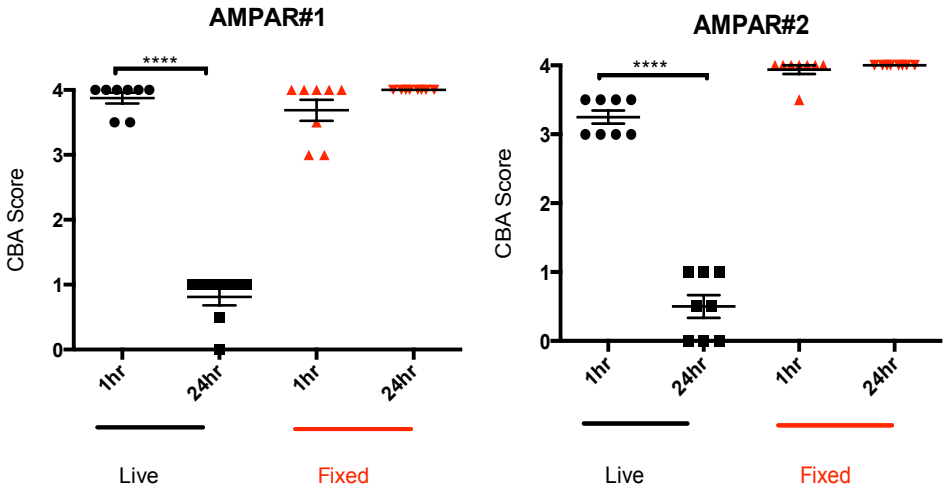

Figure 4.11: Comparison of AMPAR (GluA2) antibody IgG surface binding of two patients after incubation in GluA2 transfected HEK cells

Using the live assay (black), there was a significant reduction in surface IgG stain in both patients at 24 hours in comparison to one hour (p<0.0001, unpaired t-test). However, if prior to the initial incubation, HEK cells were fixed (red), surface IgG stain was not reduced in either patient.

As the commercial anti-AMPAR antibodies did not bind extracellularly, the surface expression of GluA2 following incubation of transfected cells with purified IgG for 24 hours was investigated by reprobing cells with GluA2 antibody IgG. As can be seen in comparison to control cells (incubated for one hour in HC IgG), surface binding was less intense on GluA2 IgG treated cells when reprobed, showing the relative drop in surface expressed GluA2 levels after 24 hours (Figure 4.12). In addition, while a reduction was noted after 3 hours, the binding continued to decrease suggesting that these antibodies also interfere with the turn around and recycling of these receptors in the cells, following endocytosis. We were unable to investigate the reversible effects as the IgG on the transfected HEK cells, as the cells could not be maintained for over 24 hours after incubation due to overgrowth and eventual cell death.

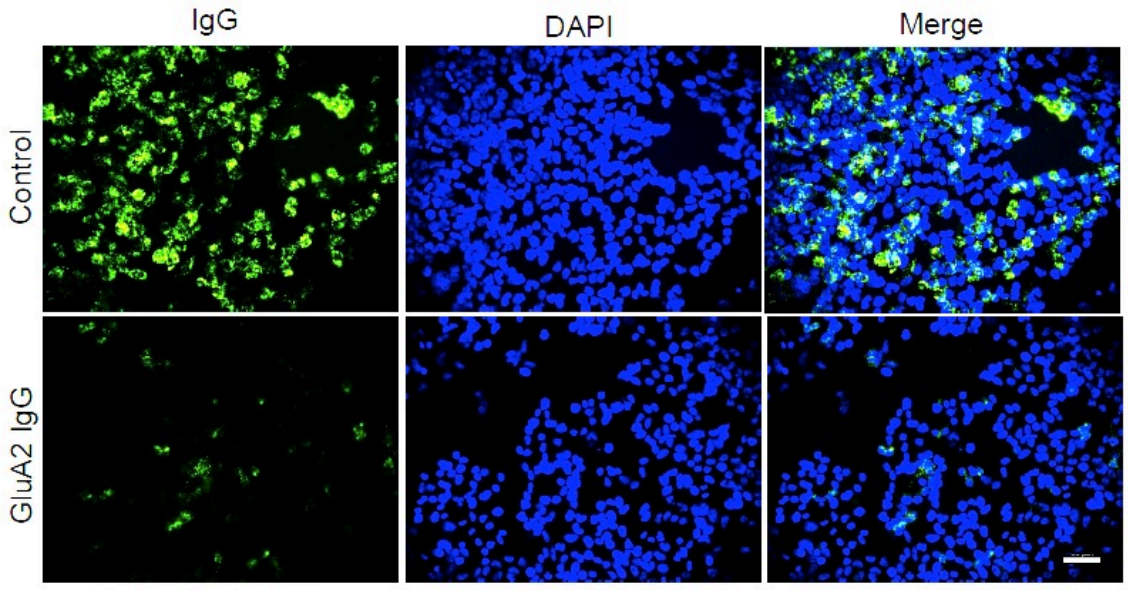

Figure 4.12: Assessment of GluA2 levels in transfected HEK cells after treatment with HC and GluA2 IgG: Reduction of surface expression of GluA2

GluA2 transfected cells were treated with either HC IgG (control; upper panel) or GluA2 antibody IgG (bottom panel) for one hour at 37°C. Cells were washed and incubated for a further 24 hours. After 24 hours cells were reprobed with GluA2 IgG (100 µg/ml) to determine residual AMPAR levels.

Surface IgG binding was significantly less intense in the GluA2 IgG treated cells than those treated with HC IgG, suggesting that GluA2 levels at the surface have been reduced by incubation with specific autoantibodies. Surface IgG staining was detected using a goat-anti human IgG Alexa Fluor (green). Merge with DAPI positive cells is shown (right column). 400x magnification. Scale bar= 50 µm

4.5.2: Internalisation of $GABA_BR$ by patient sera using transfected HEK cells

Similarly, IgG from two patients with $GABA_BR$ (one patient with $GABA_{B2}R$ (G#5) and one with $GABA_{B1+2}R$ (G#8)) antibodies were incubated with HEK cells transfected with $GABA_{B1+2}R$, and surface staining was assessed over time and compared to cells that were fixed prior to this initial 1 hour incubation. Unlike the results observed following incubation with AMPAR antibodies, $GABA_BR$ IgG immunoreactivity did not reduce over time, and hence $GABA_BR$ antibodies do not appear to cause an internalisation of the receptor (Figure 4.13).

A comparison of CBA score between the two patients on both the live and fixed assays are shown in Figure 4.14. No significant differences were observed between either patients and fixed cells. These results imply that the $GABA_BR$ antibodies, unlike those from patients with AMPAR antibodies may not cause a down regulation. Reprobing transfected HEK cells treated with $GABA_BR$ IgG with patient IgG did not show any changes in surface $GABA_BR$ expression, suggesting that the incubation in patient sera did not alter the levels of the specific $GABA_BR$ surface expression (data not shown).

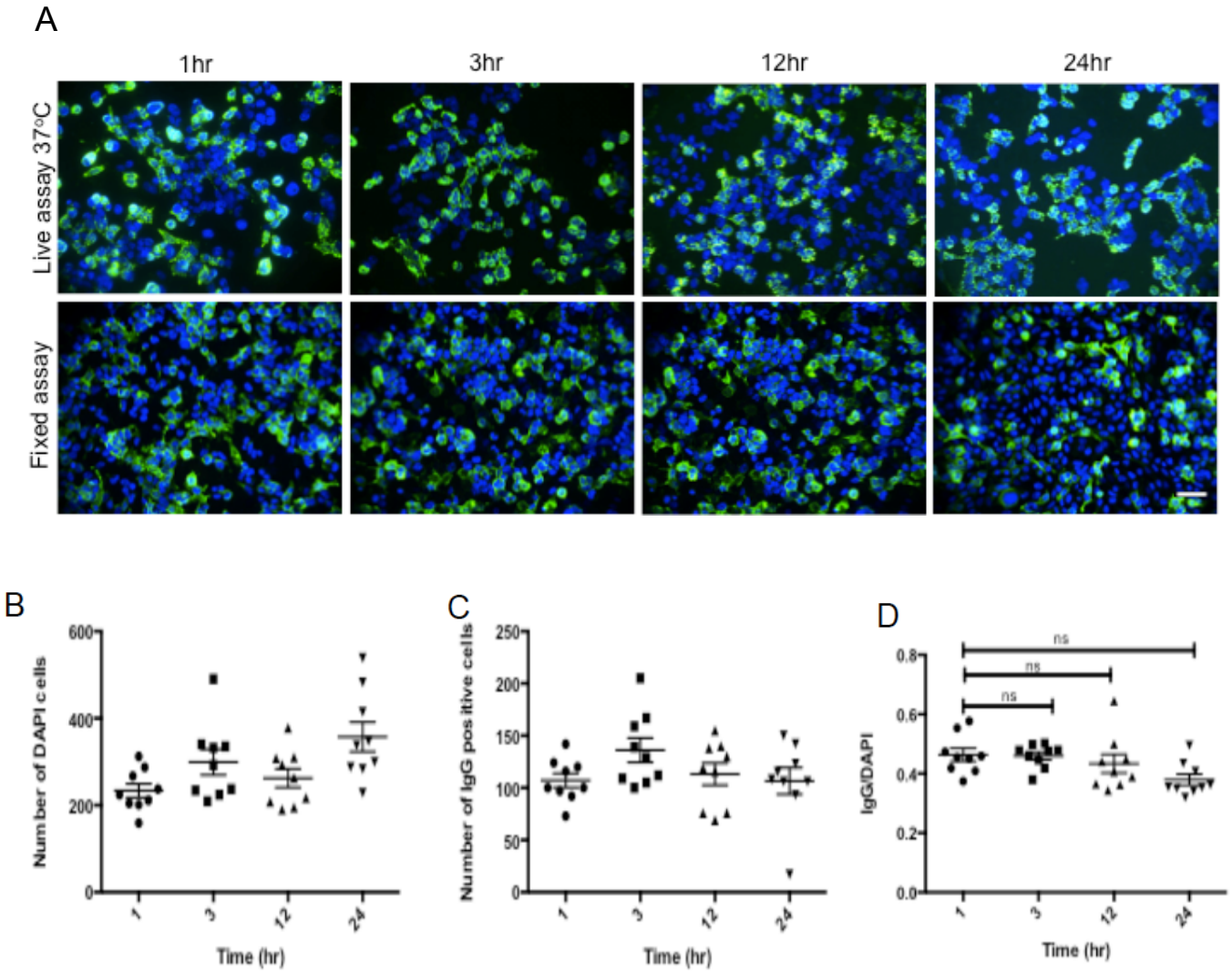

Figure 4.13: $GABA_BR$ antibodies do not cause receptor internalisation; No change in $GABA_BR$ IgG binding to $GABA_{B1+2}R$ transfected HEK cells over time.

$GABA_{B1+2}R$ transfected cells were stained with IgG purified from two $GABA_BR$ antibody positive patients (100 µg/ml). IgG was removed and cells incubated in media for a further 1, 3, 12 and 24 hours.

Binding of IgG to the surface of cells did not decrease with respect to time upper panel) and was similar to the levels in the fixed cells (bottom panel (A). The total number of DAPI cells (blue) was not affected over the time course (B). The number of positively stained cells (green; C) and the ratio of positively stained to total DAPI cells (D) did not change over time. 400x magnification. Scale bar = 50µm.

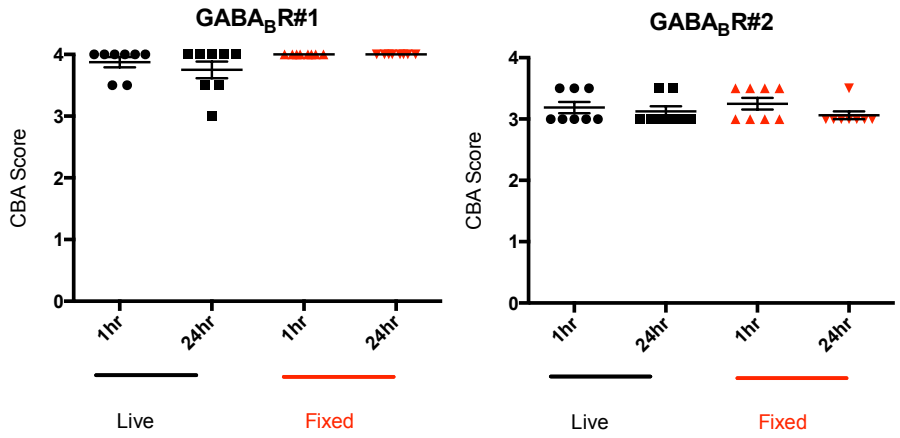

Figure 4.14: Comparison of GABA$_B$R antibody IgG surface binding of two patients after incubation in GABA$_{B1+2}$R transfected HEK cells

Using the live assay (black), there was not a significant reduction in surface IgG stain with either patient at 24 hours in comparison to one hour (p=0.7128, unpaired t-test). Similarly, if prior to the initial incubation, HEK cells were fixed, surface IgG stain was not reduced in either patient.

Finally, in order to confirm that surface staining over time was not changing due to a change in the number of transfected cells, and by extension, the cells expressing AMPAR or GABA$_B$R, the number of positively stained cells (using an anti-GluA2 and anti-GABA$_{B2}$R) were counted and compared to the total number of cells (DAPI positive). As can be seen, the ratio of transfected cells stayed constant for both assays over time following incubation with patient IgG (4.15A). Representative CBA images taken from HEK cells transfected with GABA$_{B2}$R are shown in Figure 4.15B. In all assays, cells were permeabilised as the commercial antigens were only against an intracellular epitope of the appropriate antigen.

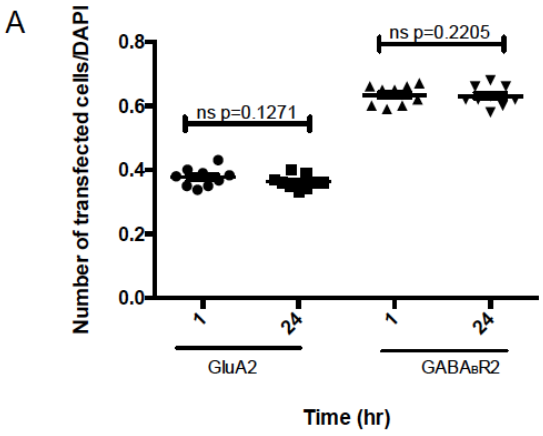

Figure 4.15: Incubation of patient IgG with GluA2 or $GABA_BR2$ transfected cells had no effect on transfection over time

GluA2 and $GABA_{B1+2}R$ cells were incubated with IgG purified from a GluA2 antibody positive and $GABA_{B2}R$ antibody positive patient for 1 hour. Following removal of IgG cells were either incubated for a further 23 hours or cells were fixed, permeabilised and incubated with specific commercial antibodies. The ratio of positively transfected cells to total cells (DAPI positive) did not change over the course of 24 hours for either type of transfection (A). Representative CBA image of $GABA_{B1+2}R$ transfected cells treated with IgG, and stained for anti-$GABA_{B2}R$ after 1 and 24 hours (B). Images 400x magnification. Scale bar =50 µm.

4.5.3: Internalisation of AMPAR and $GABA_BR$ in primary neuronal cultures

To investigate pathogenic effects in native cultures, which represent *in vivo* modulation more accurately, primary hippocampal neurons were also utilised. Primary hippocampal neurons were grown on coverslips and cultured for 14 div. Previously, it has been shown that neurons showed morphological changes with time if they were not maintained in their cultured growth media (Dr. Pettingill Thesis). As such, in order to maintain the overall integrity of the neurons, purified IgG was filtered and diluted (100 µg/ml) in the NB media and incubated with the neurons. Again, due to the limited amounts of sera/plasma available to purify IgG, two GluA2 antibody positive and two $GABA_BR$ antibody patients (one $GABA_{B2}R$ and one $GABA_{B1+2}R$) were used to study this mechanism on cultures. These patients were previously used in the HEK internalisation experiments and were incubated with the neurons for 1 hour at 37^oC. Cells were subsequently washed in NB media and incubated in conditioned media collected from cells of a similar, age for 24 hours. Staining was compared at 1 hour and 24 hours and MAP2 was used to visualize the neurons.

Representative images of GluA2 IgG, $GABA_{B2}R$ IgG and HC staining with primary neurons at 1 and 24 hours are shown in Figure 4.16. GluA2 levels were reduced after 24 hours, as shown by a reduction in surface staining at this time point. In comparison, surface binding did not change over time when neurons were incubated identically with $GABA_BR$ antibodies. As was previously noted, HC patients did not show positive neuron immunoreactivity.

When neurons were reprobed with GluA2 purified IgG after 24 hours, the GluA2 treated cultures showed reduced binding in comparison to the one hour stained neurons, suggestive of a reduction in overall AMPAR surface expression. The results were consistent with what was noted with changes in surface binding on the transfected HEK cells.

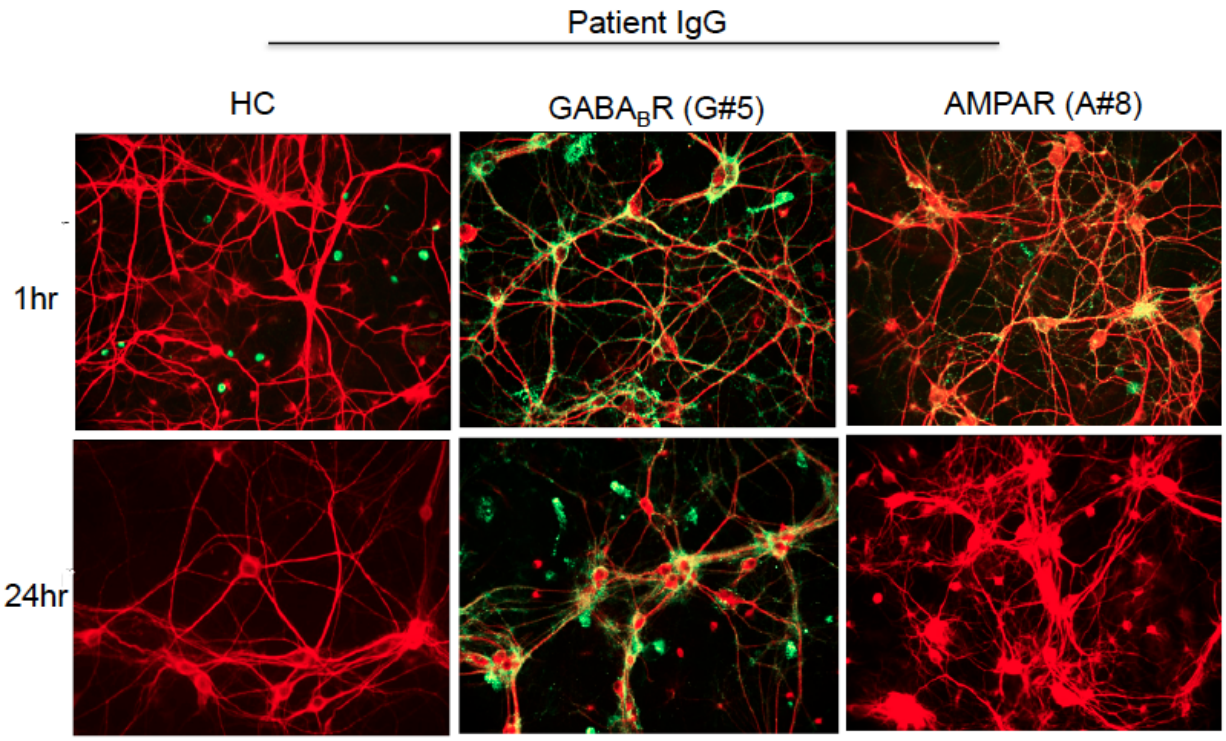

Figure 4.16: Surface IgG binding to hippocampal neurons after the application of IgG purified from a HC patient, a GABA$_B$R antibody and an AMPAR antibody positive patient

Hippocampal neurons (div 14) were incubated with IgG from HC, GABA$_B$R and AMPAR patients ((N=2) 100 µg/ml) and specific binding was visualised using a goat anti-human IgG Alexa Fluor 488 (green). Cells were subsequently fixed, permeabilised and stained for neuronal marker, MAP2 (red).

At one hour both the GABA$_B$R and AMPAR IgG showed strong immunoreactivity to cells (top panel). However, at 24 hours, the surface IgG stain of the AMPAR IgG treated neurons was significantly lower than those to GABA$_B$R IgG treated neurons, suggesting AMPAR antibodies reduced surface expression of the receptor (right column) where as those incubated in GABA$_B$R IgG did not (middle column). HC IgG did not show any immunoreactivity to the surface of hippocampal neurons at 1 hour or 24 hours (left column). Images 400x magnification

4.6: Measuring surface expressed protein levels via biotinylation and western blot

As discussed in Chapter 3, the commercial antibodies directed against both AMPAR and $GABA_BR$ (listed in Appendices Table 2) did not bind to the external surface of live transfected cells. As such, colocalisation studies using these particular autoantibodies to show a reduction in surface protein expression could not be carried out. However, these same commercial antibodies showed reactivity via immunoblot and to permeabilised cells, indicating reactivity to intracellular and/or linear epitopes. While surface IgG binding was used as a measure of surface protein expression, it is possible that staining is reduced over time in the AMPAR patients because of dissociation of the antibody from the antigen (AMPAR) complex over time. In order to evaluate whether or not this was a factor, cortical neurons were prepared from P0 rat pups and cultured for 10 div. Cortical neurons were selected as a greater number of neurons can be cultured from the dissections. From 7-10 div, neurons were chronically incubated with IgG purified from two GluA2 antibody patients (A#7 and A#8), two $GABA_BR$ antibody patients (G#5 and G#7) and three HCs (100 µg/ml). Following incubation for 72 hours, neurons were washed in media to remove IgG and incubated with a thiol-cleavable biotin enzyme. Neurons were subsequently lysed, and run through a neutravidin column capturing the biotinylated extracellular proteins. Beads were then eluted and fractions were analysed by western blot. Transferrin receptor (TFR), which is expressed at high levels on the surface of cells was used as an extracellular loading control.

Representative results of the western blot analysis after probing with anti-GluA2 (Figure 4.17) and anti-$GABA_{B2}R$ (Figure 4.18) are shown. Band intensity (shown as a % of TFR intensity) is shown in Table 4.2 (pooled data from 2 experiments). Less intense AMPAR bands were observed in fractions from neurons that had been treated with AMPAR IgG (6.9%; band size at 98kDa). However, GluA2 levels were comparable between HC (87.2%) and $GABA_BR$ (93%) IgG treated neurons, suggesting antibodies

purified from these patients are not having a nonspecific effect on AMPAR levels (Figure 4.17). On the other hand, surface expressed $GABA_BR$ levels were not reduced when neurons had been treated with $GABA_BR$ IgG (levels were comparable with HC and AMPAR IgG treated patients; Figure 4.18 and Table 4.2).

Taken together these results support the CBA and neuronal internalisation studies. AMPAR antibodies cause internalisation of the receptor from the cell surface, and changes are unlikely to be due to dissociation of the antigen and antibody complex.

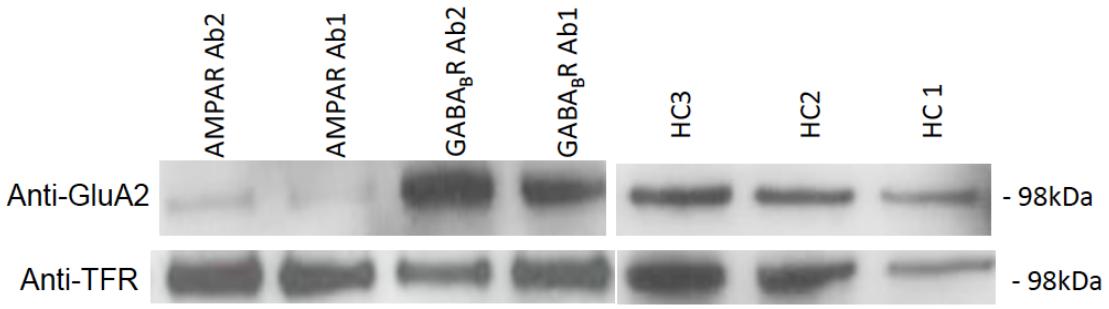

Figure 4.17: AMPAR IgG reduces the expression of the AMPAR on the surface of cortical neurons compared to cells incubated in $GABA_BR$ or HC IgG

Cortical neurons (10 div) were cultured and incubated with IgG purified from GluA2 antibody positive patients, HC or $GABA_BR$ antibody positive patients (100 µg/ml) for 3 days. When probed with an anti-GluA2 antibody, GluA2 surface levels were reduced in the fractions from GluA2 IgG treated neurons in comparison to fractions from cells treated with HC or $GABA_BR$ IgG. TFR was used as an extracellular loading control.

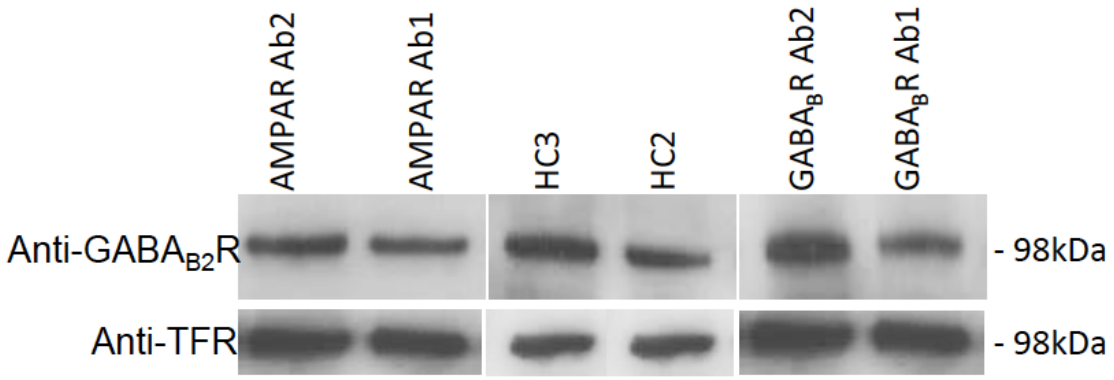

Figure 4.18: GABA$_B$R IgG does not cause a reduction of GABA$_B$R expression on the surface of cortical neurons

Cortical neurons (10 div) were cultured and incubated with IgG purified from GluA2 antibody positive patients, HC or GABA$_{B2}$R antibody positive patients (100 µg/ml) for 3 days. When probed with an anti-GABA2$_B$R antibody, no discernable changes in the surface levels of GABA$_{B2}$R in fractions treated with any of the IgGs were noted. TFR was used as an extracellular loading control.

Table 4.2: Summary of the relative AMPAR and GABA$_B$R levels (shown as % intensity to loading control) when neurons are treated with AMPAR, GABA$_B$R or HC IgG

IgG treated	AMPAR levels (% intensity to loading control)	GABA$_B$R levels (% intensity to loading control)
AMPAR	6.9%	74.7%
GABA$_B$R	93%	68.7%
HC	87.2%	105%

4.7: Summary and Discussion

In the previous chapter a CBA was established to detect the presence of autoantibodies to AMPAR and $GABA_BR$. In this chapter, the pathogenic potential of these autoantibodies was investigated. In addition this chapter introduced additional methods of antibody detection in patient sera and CSF, which included binding to primary neuronal cultures, and to rat brain sections. While the CBA is an excellent tool for detecting and measuring antibodies in sera and CSF, primary cultures have the advantage of looking at binding to receptors in a native conformation and where the protein levels are more representative of actual levels found *in vivo*. Immunohistochemistry allows for the detection of immunolabeling to various brain regions and may detect additional specificities that may not be easily cultured *in vitro.* In order for receptors to be potential targets, part of the antigen must be extracellularly expressed, where they can accessible to circulating antibodies. The binding of intracellularly expressed antigen, picked up by less specific techniques such as immunoblotting are most likely secondary targets and possibly an indication of T-cell mediated neuronal damage and cell death (see 1.4.2).

4.7.1: Reactivity to neuronal cultures and brain sections

Prior to the preparation of this thesis, AMPAR and $GABA_BR$ sera staining to rat brain sections had been described (Lai *et al.,* 2009 and Lancaster *et al.,* 2010). In these studies and in this thesis, AMPAR antibodies strongly immunolabeled the hippocampus (where distinct layers could be identified), the cortex, the pituitary gland and the GCL and ML of the cerebellum. Similarly, brain stem regions and the corpus callosum were not intensely immunolabeled. However, unlike previous reports the PCL was no more intensely labeled than other regions. The regions that showed intense staining correlate to the clinical features of the patients that were used in the IHC. These patients

generally had features more reminiscent of LE with seizures and cognitive impairments, and the hippocampus and cortical regions were intensely stained as has been previously reported (Lai *et al.,* 2009). Patient samples stained rat brain sections in an antibody titre dependent fashion. Lower antibody level samples (GluA1+2 antibody patients) did not produce staining patterns that were distinctive enough from HC staining. As such, staining of the different subtypes of AMPAR antibody (GluA2 vs. GluA1+2) could not be investigated.

$GABA_BR$ antibodies showed intense staining throughout the section, with regions of higher neuron density (the hippocampus, cortex, thalamus and cerebellum) being areas of more intense staining. As discussed in chapter 3 (section 3.7), with the exception of one patient, the $GABA_{B2}R$ antibody patients had low titres (<1:540). However the immunostaining of the high $GABA_{B2}R$ antibody positive patient was similar to the reactivity observed when $GABA_{B1+2}R$ antibodies were applied to sections, suggesting that these subtypes of patients stain similarly. As $GABA_BR$ are expressed as heterodimers, the lack of a distinct staining pattern between these two subsets of patients was not surprising. The lack of immunostaining to rat brain sections from patients with low titre antibodies has been described in patients with low-level $GABA_AR$ antibodies (titrate out <1:160, Petit-Pedrol *et al.,* 2014). The results suggest that this method of detection is less sensitive than the CBA and also highlights the importance of verifying the presence of antibodies using more than one method of detection.

Sera and CSF from AMPAR and $GABA_BR$ antibody positive patients showed reactivity to the surface of live hippocampal neurons. In contrast to the AMPAR antibody sera whereby all antibody-positive patients showed immunoreacitivity to hippocampal neurons, only high antibody titre $GABA_BR$ antibody sera showed binding ($p<0.0001$). While both AMPAR and $GABA_BR$ are highly expressed in the hippocampus (Benarroch, 2011), it is possible that the levels of $GABA_BR$ are not high enough to detect low levels

of $GABA_BR$ antibodies. This phenomenon has also been noted in the literature, whereby some $GABA_AR$ antibody positive patients were only detected using the live CBA, but not via cultured neurons or application to rat brain sections (Petit-Pedrol et al., 2013).

The GluA2+3 antibody positive RE patients showed reactivity to hippocampal neurons. These patients did not show binding to cortical neurons. This was an interesting finding as the disease primarily affects the cortex, though this may be due to the antigen having a higher density on cultured hippocampal neurons, thereby being more easily visualised. It is possible that the density of GluA2+3 is higher on the cultured hippocampal neurons than the cortical neurons, and therefore the antibodies are more likely to be detected by screening on this subtype of neurons (Huganir, 2007). Alternatively, the epitope the antibodies recognise may only be present on hippocampal neurons, explaining the negative results from screening on cortical neurons. Nevertheless, the remainder of the cohort was also screened on the cultures to determine whether or not there was presence of a novel antigenic target. Eight further patients (15.9% of the cohort) showed reactivity to the hippocampal neurons, and one patient showed binding to cortical neurons as well. These samples were negative on all in house diagnostic assays indicative of possible novel antigens in this subset of RE patients. Why autoantibodies are present in only some samples but not others is an interesting finding. It is possible that some samples may have antibodies to autoantigens expressed on a very small subset of neurons not present in our hippocampal or cortical cultures. The neuron positive samples had a much shorter duration of sample collection following the acute stage than neuron negative RE samples in the cohort (2.3 and 4.2 years, respectively). It is possible that reactivity to hippocampal cultures would have been observed in a greater number of patients if samples had been collected in a shorter period after diagnosis.

4.7.2: AMPAR and $GABA_BR$ antibody subclasses and complement activation

As has previously been described, AMPAR and $GABA_BR$ antibodies in patients with neurological disorders were found to be predominantly of the IgG1 subclass (n=14). IgG3 and IgG2 (n=5 in both) were the next predominant subclasses. IgG4 was absent in all samples tested. IgG1 and IgG3 are known potent activators of the complement cascade. AMPAR antibodies were shown to cause deposition of C3b (an early complement component) via CBA, in an antibody titre dependent manner (p=0.013, Mann-Whitney). Only patients with antibodies that titrated out further than 1:540 showed complement deposition, as shown by staining of C3b. Two additional AMPAR antibody patients that had low IgG1 levels (CBA score =1, end point titre 1:540) did not show deposition. The two GluA2+3 antibody-positive RE patients were tested for IgG subclasses and activation of the complement cascade. Only one of the RE samples (RE#9) had very low IgG1 antibodies (CBA score=1). However, neither of the samples showed the potential to fix complement, via C3b staining. Unfortunately insufficient volumes of sera from these two patients were available for testing whether or not GluA2+3 antibodies were pathogenic.

It is possible that the protocol is not sensitive enough to detect low levels of complement deposition, as sera from the patients with the lowest titres (median 1:215) were unable to fix complement. Leite *et al.* (2008) described the ability of some patient sera with antibodies to low to detect in the routine immunoprecipitation assay, to mount an immune response to the AChR. It is possible that an increased incubation period with the fresh source of complement could improve the sensitivity of the assay, and complement deposition could be observed. Blocking intrinsic complement regulators such as CD55 and CD59 (described in 1.3.2) in HEK cells prior to the application of patient antibodies could also lead to increased detection as has been described in

clustered AChR antibodies in MG (Jacob *et al.,* 2012). However, insufficient sera volumes were available to investigate this hypothesis further.

Despite IgG1 and IgG3 subclasses also being observed in $GABA_BR$ antibody sera, complement deposition was only observed in one patient with very low binding (CBA score 1). Again evaluation of brain tissue from these patients would need to be investigated before more definitive conclusions can be drawn.

The documentation of antibodies in CNS disorders and their ability to activate complement has been variable. While NMDAR antibodies have also been shown to activate the complement cascade *in vitro* (Irani *et al.,* 2010), there does not seem to be evidence of complement mediated tissue damage in brain tissue taken from NMDAR antibody patients as determined by C9neo deposition (Martinez-Hernandez *et al.,* 2011 and Bien *et al.,* 2012). Complement deposition in mice brains following injection with aquaporin 4 (AQP4) IgG and human complement has been demonstrated. Furthermore, the histopathology of brains taken from mice post injection was characteristic of what has been described in neuromyelitis optica patients (NMO) with AQP4 antibodies, in which NMO lesions with complement deposition and astrocytic death have been described (Saadoun *et al.,* 2010). As such, deposition of complement components in post mortem or biopsy brain tissue from AMPAR antibody encephalitis patients would need to be evaluated in order to determine whether or not these mechanisms could be responsible for pathogenic effects *in vivo*.

In both instances, as the prevalence of these antibodies are rare, and the patients respond to immunotherapy, investigating complement deposition in brain tissue would be difficult. *In vivo* experiments similar to those carried out by Saadoun *et al.* could be carried out and the effects of injecting AMPAR and $GABA_BR$ IgG in the presence of human complement in mice could be assessed. Complement mediated neuronal loss in certain regions of the brain could give rise to the symptoms observed in

AMPAR and $GABA_BR$ antibody patients. However, the clinical improvement of patient's symptoms with immunomodulatory therapies suggests that the diseases are at least slowly reversible. It is therefore unlikely that neuronal death due to complement activation plays a major primary role, as reversibility of phenotype following major atrophy is not likely.

4.7.3: Investigation internalisation of the receptor from the surface

4.7.3.1: Antibodies causing internalisation in the literature

The second pathogenic mechanism investigated in this chapter was internalisation of the receptor due to cross-linking by IgG molecules. Loss of AMPAR at the synapse following treatment of hippocampal neurons (6 div) with AMPAR CSF (1:15) has been documented (Lai *et al.,* 2009), and this effect was shown to be reversible. The reversibility of internalisation may explain the clinical improvement of patients better than complement mediated damage, although both mechanisms may play a part. More recently, AMPAR antibodies have been shown to cause a reduction in mEPSCs following incubation of rat cerebrocortical neurons with AMPAR IgG (100 µg/ml) purified from two patients for up to 36 hours. IgG from either patient group showed an increase in the inter-event interval and decreased peak amplitude in comparison to HC IgG treated neurons, suggestive of a loss of receptor from the surface of neurons (Gleichman *et al.,* 2014).

Antibody mediated internalisation of iGluRs is not restricted to the AMPAR. Antibodies directed against other members of the iGluR family have also shown similar results. For example, internalisation has also been described *in vitro* in anti-NMDAR encephalitis, whereby antibodies to the surface of live hippocampal neurons caused an internalisation of the receptor after incubation after 72 hours (Dalmau *et al.,* 2009). In

addition, Mikasova *et al.* (2012) showed that hippocampal neurons transfected with a NR2A construct N-terminally super-ecliptic pHluorin (SEP is a pH-sensitive eGFP molecule) labeled, showed a reduction in fluorescent intensity after incubating for 2 hours and a 50% reduction was noted after 20 hours, indicating rapid internalisation. These findings suggest that the whole tetrameric assembly of the NMDAR receptor is affected by NMDAR antibodies, despite the primary target being the NR1 subunit. Hughes *et al*. (2010) showed that incubation of hippocampal neurons with CSF for one day resulted in a reduction in NMDAR clusters at the synapse in an antibody titre dependent fashion, while the overall integrity of the synapse was maintained and other synaptic protein levels remain unaltered. Whole-cell recordings from brain slices have also shown long-term effects of NMDAR antibodies. Following incubation of neurons with NMDAR antibody positive CSF for 24 hours, hippocampal pyramidal cells showed a reduction in NMDAR mediated currents, most likely due to internalisation of the receptor from the cell surface. In addition, the amplitude and frequency of the currents were unaffected, suggesting that the patient's antibodies do not alter presynaptic release of neurotransmitters, and that this effect is due to a selective loss of NMDAR function. The application of the patient CSF was specific for the NDMAR and did not affect overall levels of GluA2/3, and by extension, the AMPAR mediated currents (Hughes *et al*., 2010).

4.7.3.2: AMPAR antibodies cause internalisation

The reactivity of AMPAR and $GABA_BR$ antibodies to the surface of live transfected HEK cells and primary cultures was also utilised to investigate the effect of these antibodies on receptor levels both qualitatively by looking at changes in intensity using immunofluorescence, and quantitatively via biotinylation of extracellular proteins and western blot analysis. When IgG from a GluA2 antibody patient was applied to the

surface of GluA2 transfected HEK cells or the surface of live hippocampal neurons for an initial one hour incubation at 37°C, a reduction in immunofluorescent intensity was noted within 24 hours suggestive of a reduction in GluA2 receptor level. In addition, western blot analysis showed that the surface expressed GluA2 levels dropped (93% reduction in comparison to TFR intensity) following a 3-day incubation of cortical neurons with IgG purified from a patient with GluA2 antibodies. These findings confirmed that any loss of surface IgG stain was not simply due to dissociation of the antibody-antigen complex. IgG purified from a HC patient resulted in no overall changes in the surface expressed GluA2 protein levels. A visual reduction in the surface binding of AMPAR antibodies after 24 hours was much quicker than was noted in previous reports whereby the reduction in synaptic GluA2/3 clusters in live hippocampal neurons took far longer to achieve 6 days (AMPAR CSF was added 20 µl/day at a dilution of 1:15.

The internalisation is only thought to take place because of the divalent nature of the IgG molecule. Future experiments should investigate whether this is true with AMPAR antibodies using experiments similar to those that have been carried out with AChR antibodies as in Drachman *et al.,* 1978. Here, divalency was shown to be integral, as cleavage of AChR antibodies into monovalent Fab fragments did not result in internalisation. However, when crosslinking between Fab fragments was restored using anti-Fab antibodies, internalisation was observed (Drachman *et al.,* 1978*).*

A loss of AMPAR function could result in the development of many of the symptoms the patients present with during the course of the disease. AMPAR are internalised during synaptic weakening such as LTD (Shepherd *et al.,* 2007). As such, these antibodies could be causing a weakening of the synapse, and disrupting the trafficking and insertion of AMPAR at the synapse. Deficits in AMPAR function could lead to the cognitive deficits, seizures and other symptoms noted in the patients.

4.7.3.3: $GABA_BR$ antibodies do not cause internalisation

$GABA_BR$ IgG did not appear to affect the surface expression of $GABA_BR$ in either the CBA or neuronal experiments, suggesting that this is not a mechanism of action of these antibodies. The fact that like AMPAR antibodies, $GABA_BR$ antibodies are also predominately of the IgG1 subclass (albeit the CBA scores were lower), it is puzzling how these antibodies may not be acting through the same pathological mechanisms as other IgG1 antibodies such as AChR, NMDAR, LGI1, and CASPR2, whereby internalisation and complement activation are documented. The lack of internalisation could be due to the inability of the IgG molecules to cross link due to spatial stoichiometry. That is, the epitopes the patient antibodies recognise are located on a region of the $GABA_BR$ subunits that spatially the IgG molecules are not able to crosslink. The regional reactivity of patient antibodies could be studied by creating constructs where specific regions of the extracellular domain of these receptors are deleted and patient binding analysed as was explored by Gleichman *et al.* (2014) with AMPAR antibodies. It is possible that these antibodies are not pathogenic, but are bystander antibodies caused by the expression $GABA_BR$ on underlying tumours as has been shown by Lancaster *et al.* (2010). The existence of additional antibodies to surface expressed neuronal antigens (co-immunogens), which are primary contributors to the disease cannot be overlooked. However, as many of these patients with high $GABA_BR$ antibody levels respond well to immunomodulatory treatment, and co-immunogens are not present in all samples, these antibodies are likely to be pathogenic and screening for them is of diagnostic and clinical relevance.

4.7.4: Limitation and summary

While useful, these *in vitro* techniques for investigating complement activation and internalisation are an over-simplification of the antibody mechanisms *in vivo.* As previously mentioned, despite the ability of NMDAR antibodies to fix complement on transfected cells and neuronal cultures, complement deposition is not noted in post mortem and biopsy tissue (Martinez-Hernandez *et al.,* 2011 and Bien *et al.,* 2012). Furthermore, while previous *in vitro* work using AQP4 transfected cells suggested that internalisation of AQP4 was a key component of NMO autoantibody pathogenesis, *in vivo* studies have shown that following injection of NMO-IgG into mouse brain, internalisation over 24 hours is not noted (Ratelade *et al.,* 2011).

The findings in this chapter show that while similar IgG subclasses are present in both AMPAR and $GABA_BR$ antibody sera, the same pathogenic mechanisms of action are not shared. Both AMPAR and $GABA_BR$ antibodies have similar subclass specificities, and so theoretically have an equal ability to fix complement. However, only the antibodies to the AMPAR appear to be able to cross-link and internalise the AMPAR. A different mechanism may be involved in the case of patients with $GABA_BR$ antibodies. This may not be a characteristic of the antibodies themselves but of the stoichiometric distribution of the different epitopes or on the distribution of the receptor subtypes themselves. This finding may even be an artifact of the systems (transfected HEK cells) used to investigate the effects of the antibodies themselves. However, the reproduction of the effects on isolated neurons are reassuring that the effects observed are representative of what is occurring *in vivo*.

The ability of antibodies, namely anti-AChR and anti-NMDAR to behave in an agonist or antagonistic fashion has been documented (Riemersma *et al.,* 1996 and Zhang *et al.,* 2012). Before ruling out whether $GABA_BR$ antibodies were directly

pathogenic or not, the direct role of these antibodies on the receptor were explored in the next chapter.

CHAPTER 5: Direct modulation of $GABA_BR$ antibodies on Up and Down states (UDS) of the entorhinal cortex *in vitro*

In the last chapter, activation of the complement cascade and receptor internalisation were assessed as potential pathogenic mechanisms of AMPAR and $GABA_BR$ antibody action. The findings suggest that while complement fixation or internalisation may be mechanisms by which the AMPAR antibodies mediate their effects, this does not appear to be the case for $GABA_BR$ antibodies. As a majority of the $GABA_BR$ antibody positive patients have an underlying malignancy, it is possible that the expression of $GABA_BR$ by tumour cells triggers the production of these antibodies, but it is unclear if the $GABA_BR$ antibodies produce a pathogenic effect and if they do, how this is achieved remains inconclusive. In this chapter, we explored whether there is the possibility that these antibodies are in fact pathogenic, having a direct modulatory effect on the $GABA_BR$. That is, these antibodies are diagnostically relevant, but with a mechanism of action that differs from the AMPAR antibodies.

We aimed to investigate the direct effect IgG purified from a patient with $GABA_BR$ antibodies had on cortical activity in the form of Up and Down states (UDS) in entorhinal cortex (EC) brain slices. The use of brain slices allows for many cell-cell interactions to be maintained, mitigating the problems faced when recording from cultured HEK or primary neurons, and allows for the investigation of the effect of these antibodies on the circuitry of the brain. In addition, the effects of $GABA_{B2}R$ antibodies on the receptor are better observed in brain slices where the two $GABA_BR$ subunits are natively expressed together, as $GABA_{B2}R$ does not function in isolation (Kaupmann *et al.,* 1998).

5.1 Clinical details and reactivity to CBA and primary cultures

5.1.1: Patient clinical details

The patient selected was a 50-year old man who presented with confusion, unsteadiness and proximal leg weakness. After the patient suffered from respiratory failure and generalized weakness, he was admitted to the intensive care unit and EEG revealed he was encephalopathic. The neurophysiology of the patient was consistent with LEMS and a CT scan revealed the patient had SCLC. The patient was treated with PEX and underwent chemotherapy for his tumour. The patient had a significant response to the treatment and while proximal leg weakness persisted, he is independently mobile. This patient was of particular interest as he presented with both peripheral and central neurological impairments. In addition, while the patient had symptoms and a neurophysiology that was typical of LEMS, and an associated tumour, the patient did not have P/Q-type VGCC antibodies, which are the predominant antibodies found in the approximately 40% of LEMS patients (Titulaar *et al.,* 2011). IgG was purified from the patient's plasma (see section 2.7,) by affinity purification on Sepharose G was filtered and stored at -20°C until use.

5.1.2: Reactivity to transfected HEK cells and primary cultures

The patient serum showed strong reactivity to live HEK cells transfected with $GABA_{B1+2}R$ (Figure 5.1A). Incubation on individual assays and preadsorption experiments revealed that this patient was exclusively $GABA_{B2}R$ antibody positive (Figure 5.1B). Furthermore, this patient was tested for other neuronal surface antigens and was negative on the NMDAR, AMPAR, LGI1, CASPR2 and $GABA_AR$ CBAs. The patient had high antibody levels (IgG end point titre; 1:6400). Consistent with the other high antibody titre $GABA_BR$ patients, the IgG from the patient showed strong reactivity to

primary hippocampal and cortical neurons (staining with cortical cultures is shown in Figure 5.1C). IgG purified from a HC patient showed no reactivity to transfected HEK cells or neuronal cultures (Figure 5.1D).

Due to limited sera and CSF availability, the study was limited to just one patient, and the effects of $GABA_{B1}R$ antibodies or IgG purified from patients with clinically defined LE were not investigated.

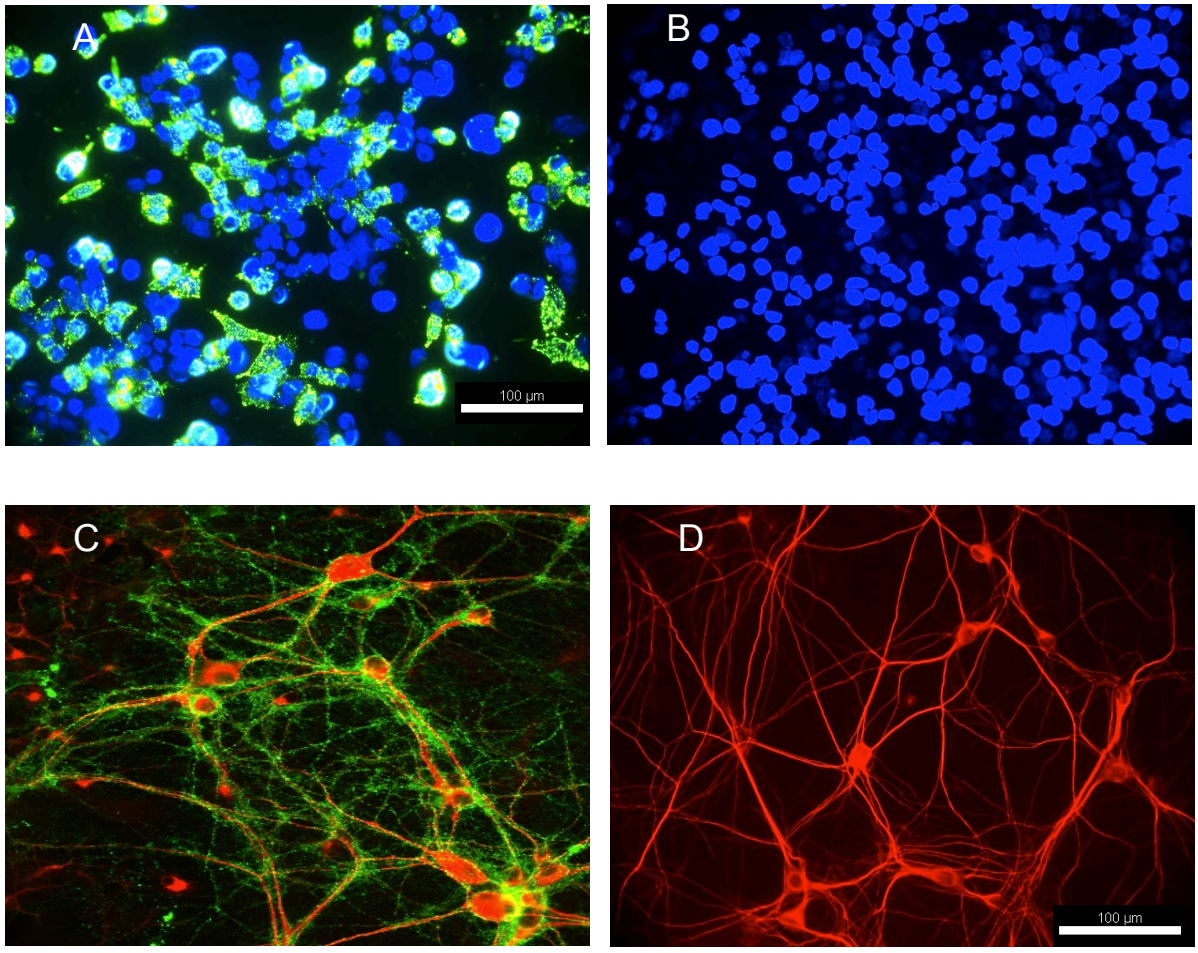

Figure 5.1: IgG purified from a $GABA_BR$ antibody patient showed strong reactivity to transfected HEK cells and primary neuronal cultures

IgG (10 mg/ml; 1:100) purified from a $GABA_BR$ antibody positive patient showed strong reactivity to HEK cells transfected with $GABA_{B1+2}R$. Image of $GABA_BR$ antibody IgG surface binding to transfected cells colocalized with DAPI (A). Following preadsorption with $GABA_{B2}R$ transfected HEK cells, binding was lost, showing exclusivity for $GABA_{B2}R$ antibodies (B). The $GABA_BR$ antibody IgG (1:100) showed strong reactivity to the surface of live cortical neurons (10 div). IgG staining detected using a goat anti-human IgG secondary antibody Alex Fluor 488 (green), and neurons visualized following fixation, permeabilsation and incubation with MAP2 (red; C). IgG purified from a HC (10 mg/ml; 1:100 dilution) showed no reactivity to primary cultures (D). 400x magnification. Scale bar= 100 µm.

5.2: Presence of Up states in slices containing the EC

The EC has been used in various studies to investigate overall cortical networking and analysis of UDS (Cunningham *et al.,* 2006, Mann *et al.,* 2009), as cortical activity is maintained in this region *in vitro.* In addition, because the EC lies in close proximity to the hippocampus and together these regions are important in memory and learning, understanding cortical connectivity in this region is important.

Up states were investigated in cortical neurons of layer III (LIII) in the medial entorhinal cortex (MEC). Up states can be evoked in the principal cells of LIII MEC by LIII stimulation and the response in neurons patched approximately 200 µm away from the stimulating electrode can be recorded (Mann *et al.,* 2009). The electrode used to patch is referred to as the recording electrode from here on. As previously shown (Mann *et al.,* 2009), spontaneous Up state events (without evoking LIII) were noted, though the duration of recordings and the presence of spiking and frequency were variable. Figure 5.2 shows representative images of the Up states observed.

In order to investigate the effects IgG had on various Up state characteristics, the following protocol was adopted (Figure 5.3). The optimal dilution for screening serum samples on the $GABA_BR$ CBA was found to be 1:100. As such, 100 µg/ml (approximately a hundredth of the total IgG content found in the serum) was applied to the slices. IgG was diluted in aCSF (see section 2.11) and acutely applied following initial recordings in aCSF without IgG (baseline recording). The time duration that the diluted IgG was applied to slices was matched to the baseline recordings to ensure that enough time was allowed for the IgG to diffuse through the slice. Immediately following IgG application, slices were superfused with aCSF (wash). Whether or not there was a "washout" effect of the IgG (the IgG that has bound to the receptors is washed away following application of aCSF) was investigated. If a washout was noted and Up states returned, IgG was reapplied. A second reapplication of HC IgG was not explored. All

analysis was carried out using recordings from evoked slices. However, spontaneous Up states were still detected using the Igor Pro program (see section 2.11 and Mann *et al.,* 2009). While the stimulations are mimicking bursts of cortical activity, frequent stimulations were avoided as this could disrupt cell-cell interactions, and overall cortical networking. Stimulations of 1.5pA were applied every 40 seconds.

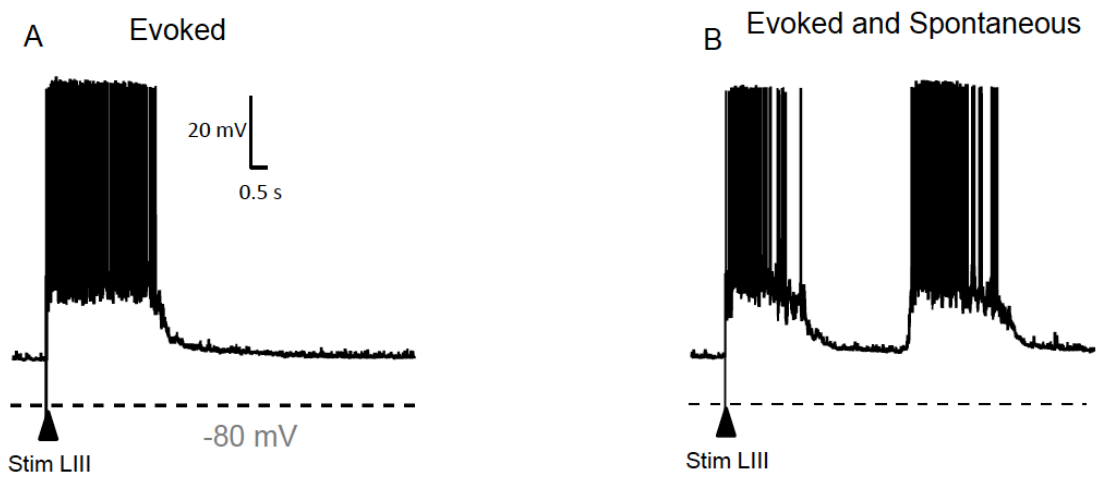

Figure 5.2: Up and Down state transitions are noted in LIII MEC neurons

Recordings were taken from neurons located approximately 200 µm away from the stimulation electrode in LIII of the MEC. Stimulation resulted in evoked Up states (A). In certain cases, evoked and spontaneous Up states were also noted (B). The arrow points to the stimulation. LIII; Layer III, Stim; Stimulation. Dashed line= -80mV

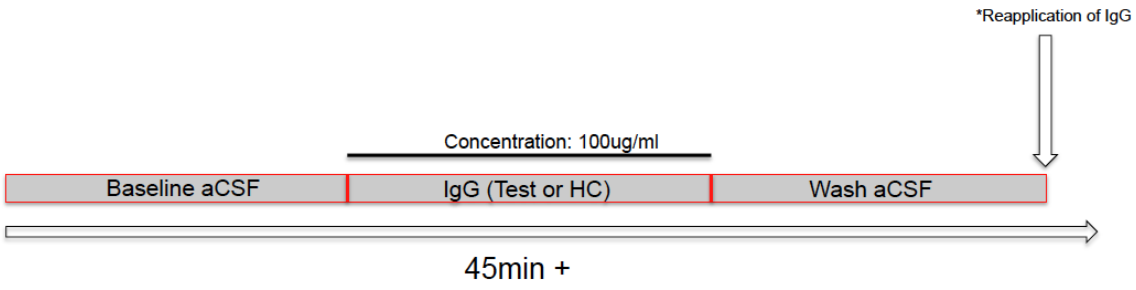

Figure 5.3: Effects of IgG on various Up state characteristics were analysed using the following protocol, approximately 45 minutes in length

Recordings were measured in the EC using horizontal mouse brain slices. Baseline Up states were recorded in aCSF for at least 15 minutes. IgG (Test or HC) at approximately 100 µg/ml was acutely applied to slices and recordings continued in the presence of IgG for approximately 15 minutes (matching baseline), followed by recordings when the slice is being washed in aCSF.

****If recovery of Up states was noted, IgG was reapplied.***

5.3: Effects of HC IgG on Up state duration and spike rate

Whole-cell recordings were made from LIII pyramidal cells. The effects of HC and Test IgG (100 µg/ml) on Up state duration and spike rate were compared.

5.3.1: Effect of IgG on Up state duration

No changes in Up state duration were noted when HC IgG was applied to the slices, in comparison to baseline recordings, or wash (baseline: 2.44 +/-0.45s, HC IgG: 2.55 +/- 0.41s, wash: 2.81 +/- 0.334s, n= 5 slices). The change in Up state duration (shown as percentage of the baseline) following application of IgG and wash was not significant as shown in Figure 5.4A.

In contrast, following the application of $GABA_BR$ antibody IgG (Test) a 23% reduction in Up state duration was noted in comparison to baseline recordings (baseline: 3.75 +/- 0.38s, Test IgG: 2.90 +/- 0.44s, p= 0.0028, Dunn's multiple comparisons test). Following wash of IgG, Up state duration increased (wash: 3.35+/-0.37s) and a washout of the IgG did not show significant changes in duration in comparison to the baseline (Figure 5.4B), suggesting that the effects are reversible. As an effect was noted immediately upon application, incubation of slices with IgG prior to recording was not felt necessary.

Interestingly, it was observed that in some slices (2/7) a washout effect did not occur, and Up state duration was not restored to what was observed during the baseline recordings. Why in certain cases a washout effect was not observed remains to be elucidated.

5.3.2: Effect of IgG on spike rate

To be classified as a spike for analysis, Up states spikes had to cross a threshold of -20 mV. Spike rate was defined as spikes occurring only during Up state events to exclude any random excitatory activity. As previously noted, spikes were not present during Up states in all slices. Spike rate was not significantly altered following the application of HC IgG on the slices (pooled data shown in Figure 5.4C).

Following application of Test IgG on the slices, a 92% reduction in spike rate was noted ($p=0.0185$). Pooled data from these experiments are shown in Figure 5.4D. While no statistical significance existed between the baseline and the wash recordings, more variability between spikes was observed, and spike rate did not always return to baseline levels. The same slices (2/7) that showed a complete reduction in duration during washout also had a complete absence of spikes during Up state events.

A representative trace of the effects of Test and HC IgG on Up state duration and spikes is shown in Figure 5.5.

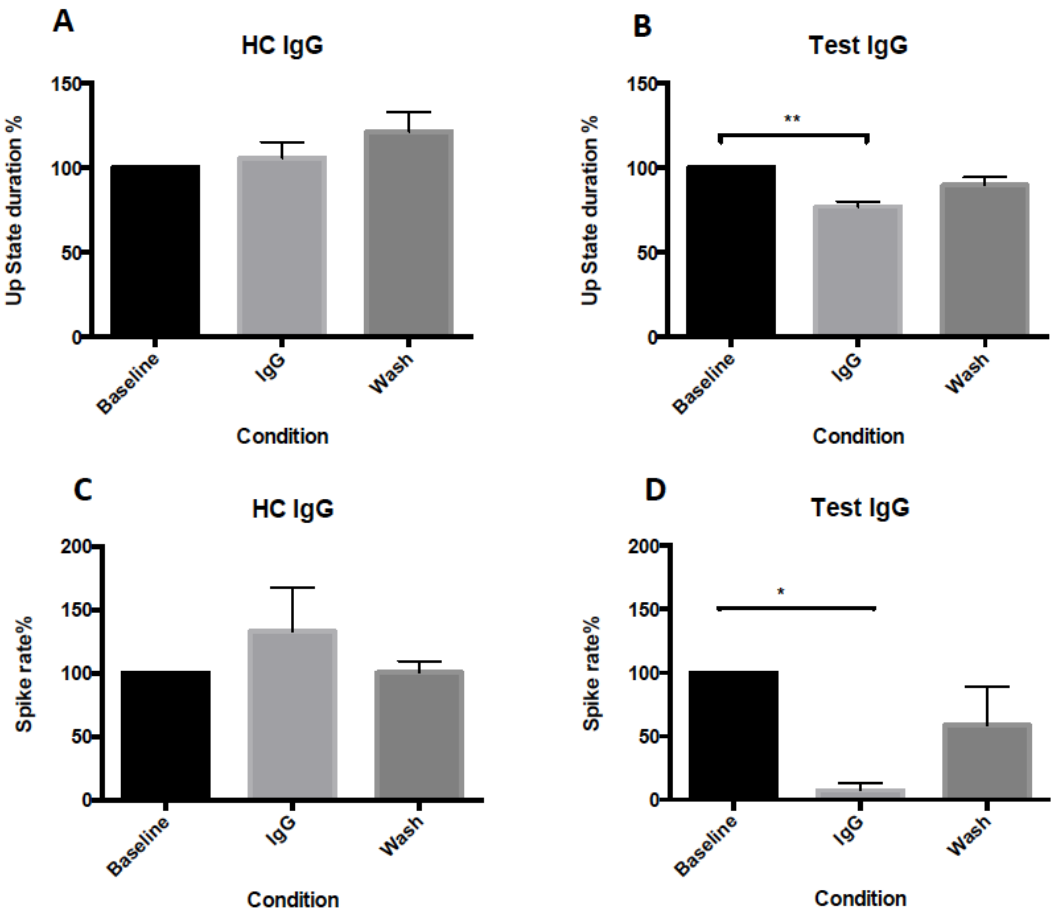

Figure 5.4: The effect of HC and Test IgG on Up state duration % and spike rate %

Baseline normalized to 100%. Changes in Up state duration and spike rate (spikes/s) are shown as a percentage of baseline.

No difference was noted between Up state duration between baseline and HC IgG conditions. Similarly, washing in aCSF following HC IgG application did not result in any changes in Up state duration (A, pooled data from n=5 slices). In contrast, Up state duration was significantly reduced following the application of Test IgG (B, **p=0.0028, pooled data n=6). In slices where spikes were present, no changes in spike rate during Up states was noted in comparison to baseline when HC IgG was applied to slices (C, pooled data from n=4). A significant reduction was noted in spikes present during Up state events following application of Test IgG (D, *p=0.0185, pooled data n=5). Statistical analysis completed using repeated measures ANOVA followed by Dunn's multiple comparison test.

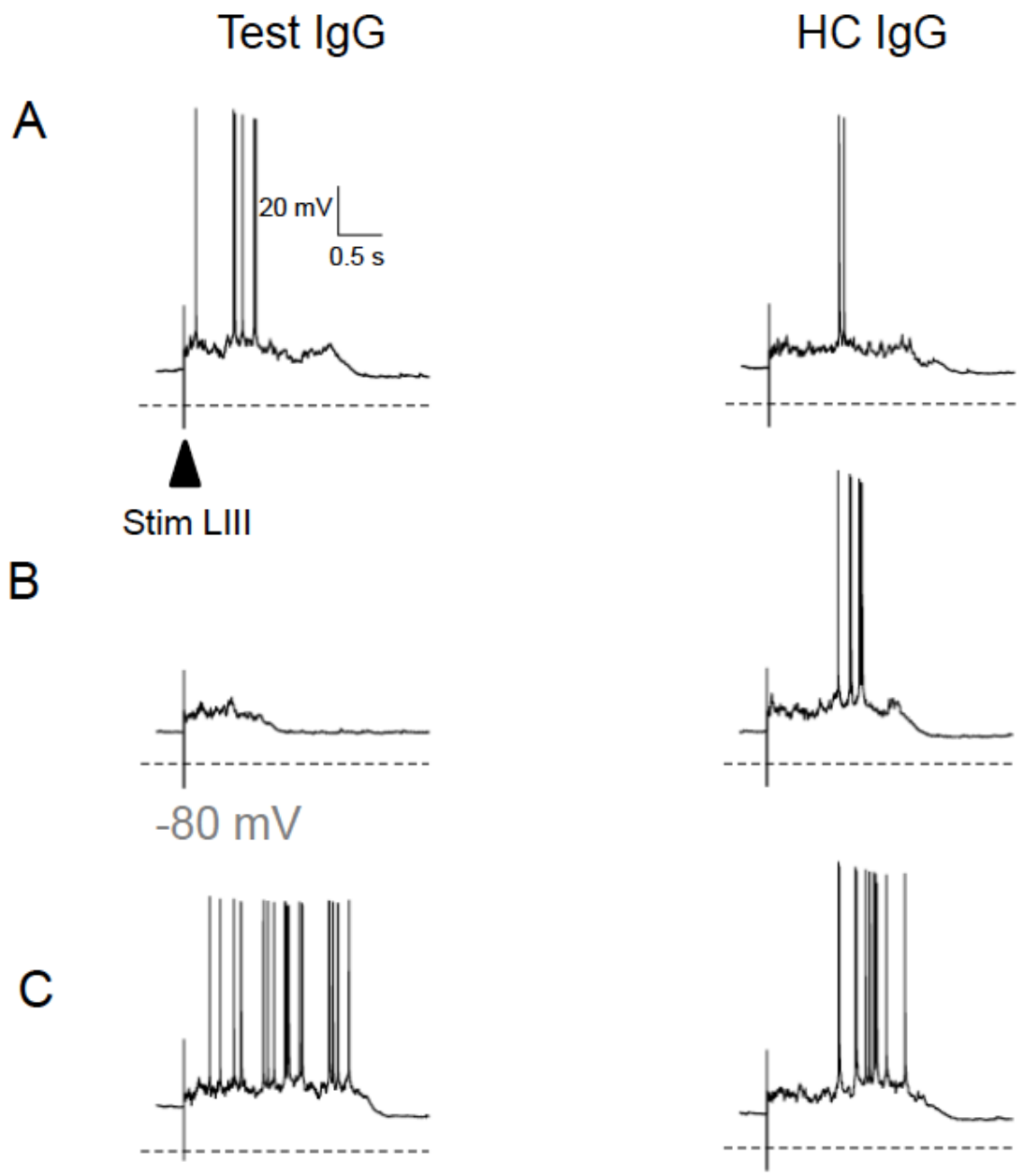

Figure 5.5: Representative image of the effect of Test and HC IgG on Up states

Up state recordings taken during A) baseline recordings in aCSF B) Test or HC IgG (100 µg/ml) and C) aCSF (wash). Both Up state duration and the spike rate during Up events were significantly reduced following the application of Test IgG. Up state duration and spike rate was unaffected following the application of HC IgG. LIII; Layer III, Stim; Stimulation. Dashed line represents -80 mV

5.4: Effects of preadsorbed IgG on Up states

One of the limitations of the experiments above is the use of purified IgG. While the CBA and staining to primary cultures shows that the patient's IgG has high $GABA_{B2}R$ antibody levels, this IgG fraction contains all of the patient's antibodies, not just those directed against the $GABA_BR$. Whilst the IgG tested negative on assays against other surface proteins, it is possible that other components of the IgG fraction are responsible for the observed Up state effect.

To ensure that the effects were indeed due to the $GABA_{B2}R$ antibodies present in the purified IgG, Up state recording were assessed in slices superfused with IgG that had been preadsorbed against HEK cells expressing $GABA_{B2}R$ to remove all anti-$GABA_{B2}R$ antibodies. As can be seen in Figure 5.6, complete abolition of binding to transfected HEK cells and neuronal cultures was noted following the preadsorption. The incubation with blank HEK cells did not result in a change in reactivity when tested on the CBA or neurons. The preadsorbed material was subsequently diluted and applied to the slices at the maximum concentration (100 µg/ml). Figure 5.7A/B shows the representative traces noted when IgG was preadsorbed against transfected HEK cells. The application of the IgG that had been preadsorbed against $GABA_BR$-transfected HEK cells had no effect on Up state duration or spike rate (n=5). On the other hand, when preadsorbed against untransfected HEK cells, there was a reduction in Up states and spike rate, similar to that seen in the Test IgG preparation (data not shown). These findings suggest that modulation in Up state activity noted can be explained by the presence of $GABA_{B2}R$ antibodies and not due to other components present in the patient's IgG.

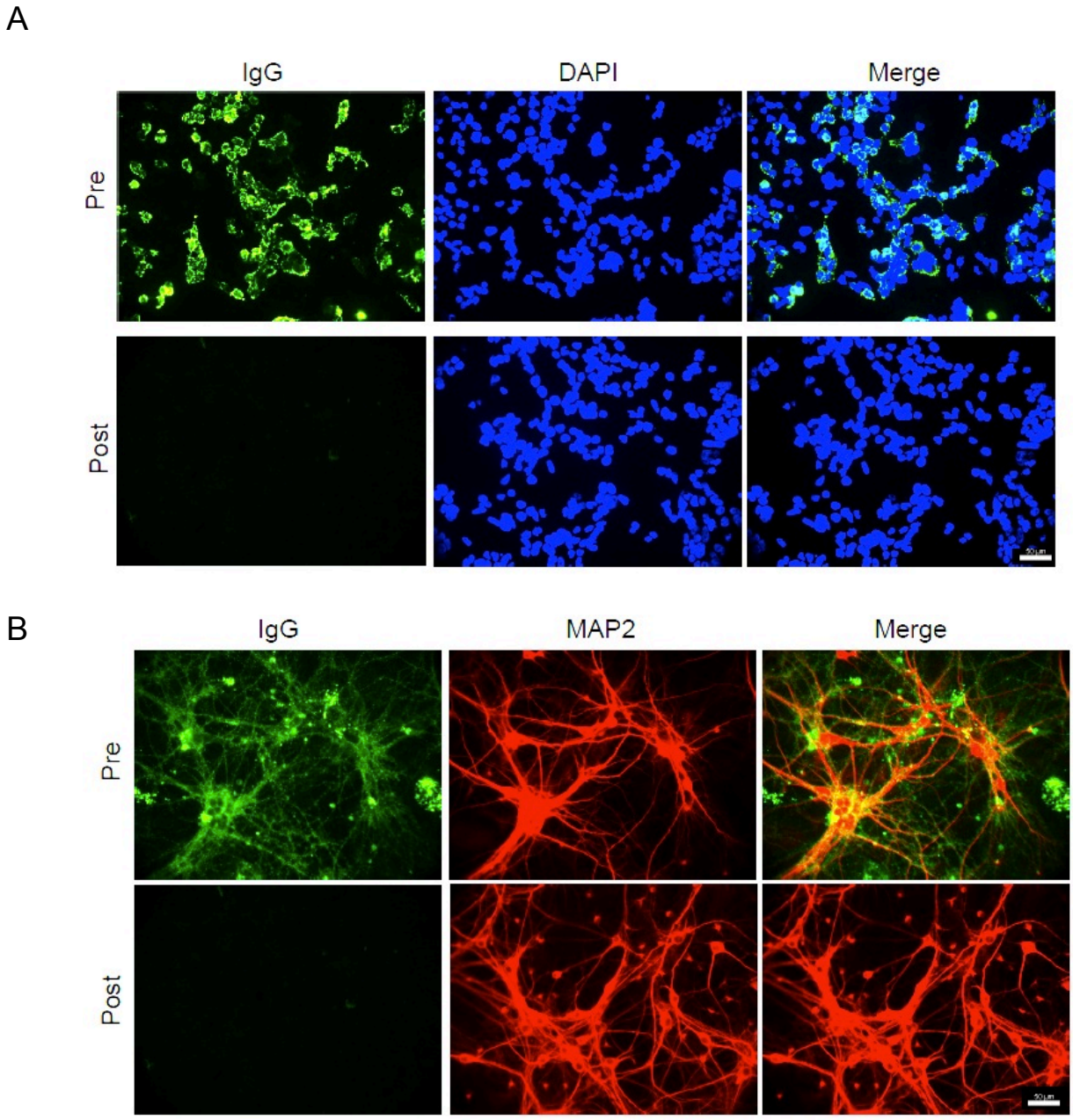

Figure 5.6: Preadsorption of $GABA_BR$ positive Test IgG abolishes binding to transfected HEK cells and primary neuronal cultures

IgG was incubated with a suspension of $GABA_{B2}R$ transfected HEK cells (see methods 2.3.4) and then applied to the $GABA_BR$ CBA and to primary neuronal cultures at a 1:100 dilution. IgG binding detected using a goat anti-human IgG Alexa Fluor 488. Neurons visualised with MAP2. $GABA_BR$ antibody binding to transfected HEK cells (A) and neuronal cultures (B) pre and post absorption with HEK cells transfected with $GABA_BR$. Images 400x magnification. Scale bar=50 µm.

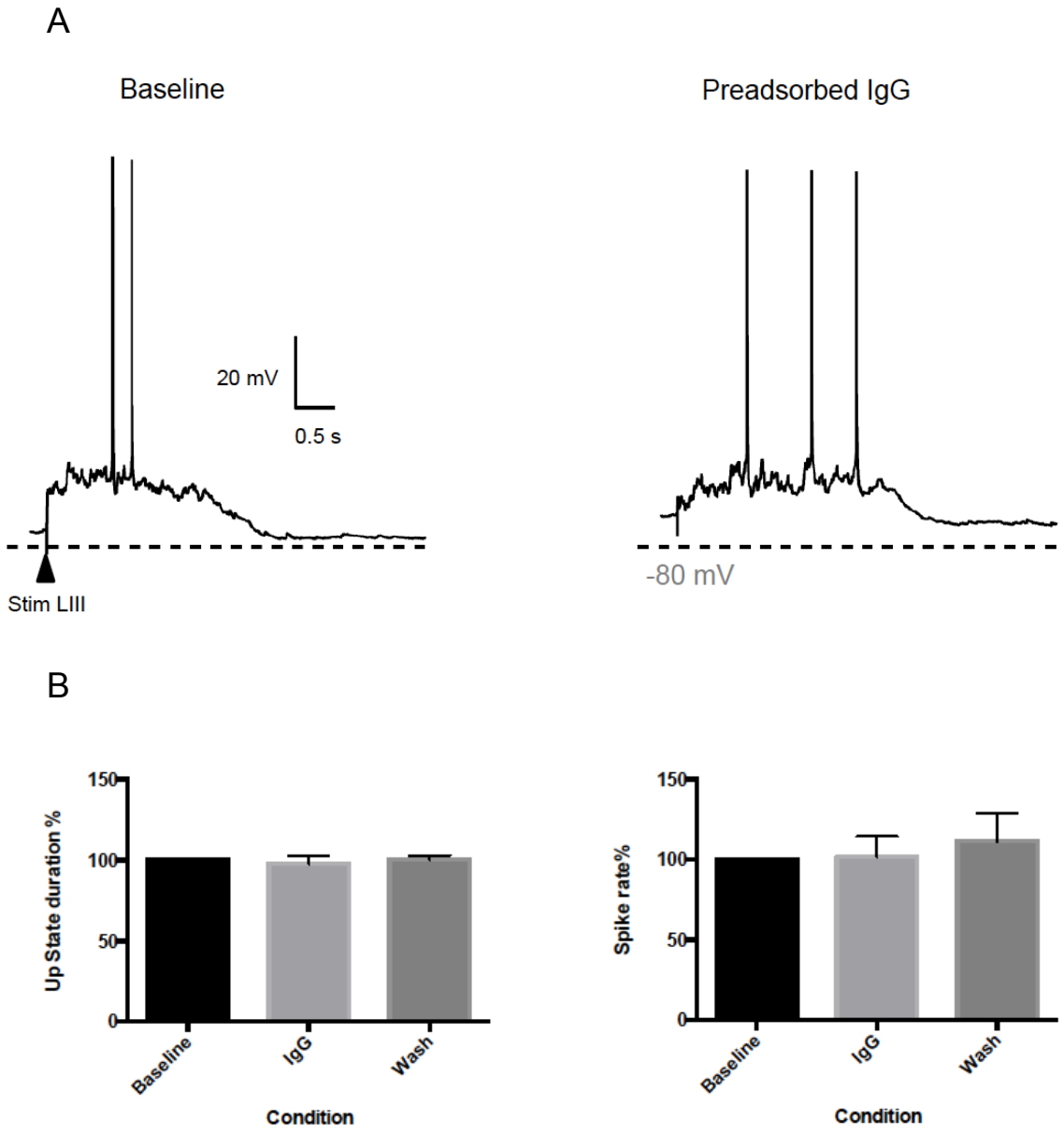

Figure 5.7: Representative images of the effects of $GABA_BR$-IgG on Up states in the EC following antibody absorption with $GABA_BR$ transfected HEK cells

Baseline Up states were comparable to the Up states noted when preadsorbed IgG was applied to slices (A). Pooled data from all experiments (n=5 slices), showing no changes in Up state duration or spike rate, shown as a percentage to baseline. Baseline normalized to 100%. Changes in Up state duration and spike rate (spikes/s) are shown as a percentage of baseline (B). LIII; Layer III, Stim; Stimulation. Statistical analysis completed using repeated measures ANOVA followed by Dunn's multiple comparison test

5.5: $GABA_{B2}R$ antibodies and $GABA_{B1}R$ agonist binding

In order to investigate whether patient IgG was having an agonist or antagonist like effect, we next studied the effects of the $GABA_BR$ agonist baclofen on Up state events. In addition, while the $GABA_BR$ antibodies in this patient were directed against the $GABA_{B2}R$ subunit, these antibodies could be mediating the effects through modulation of the $GABA_{B1}R$ subunit (the subunit that binds the agonists and antagonists).

Superfusing brain slices with baclofen diluted in aCSF (10 μM or 1 μM) resulted in a complete abolition of Up states as shown in Figure 5.8A. Unlike the effects noted with the Test IgG, a washout of the drug was not noted at any dilution, and cells remained in a hyperpolarized state, indicating irreversible binding within the time duration of the experiment.

To determine whether or not binding of IgG to the receptor resulted in an alteration of baclofen's effects, brain slices were first superfused with diluted IgG (100 μg/ml) and when a consistent reduction in Up state duration and spiking was noted as in pervious experiments, baclofen (1 μM) was applied. A complete abolition of Up states was noted in all slices (n=6). In addition, the cells in every slice were hyperpolarized even when varying concentrations of the drug were added. The effects of baclofen were noted to be the same as when applied with or without the IgG, suggesting that IgG does not alter the affects of baclofen.

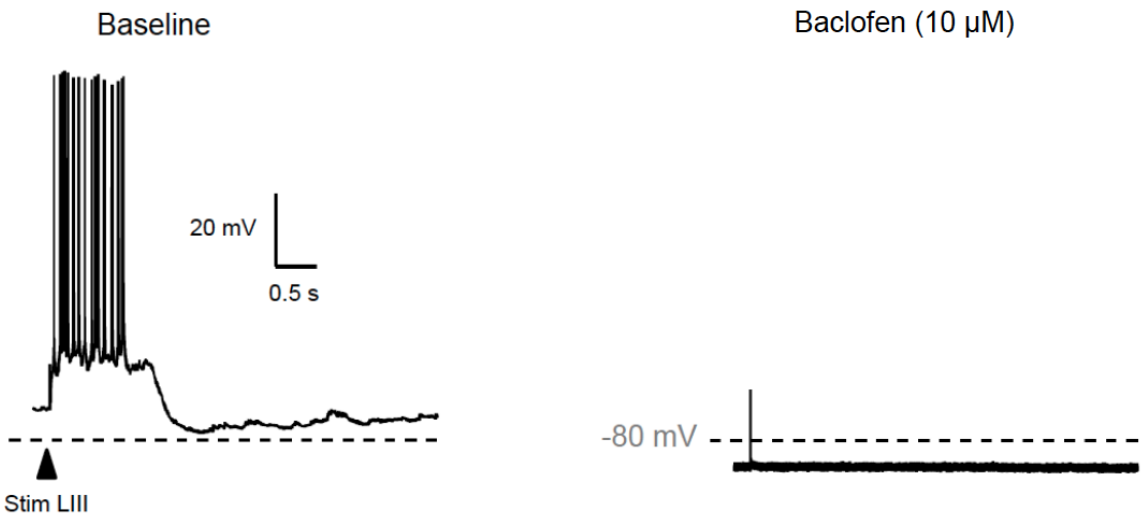

Figure 5.8: Representative image of the effect of baclofen on Up states in the EC

Following application of baclofen (10µM shown above, similar results when 1 µM, 0.1 µM used), a complete abolition of Up state and cortical activity was noted. Baseline recording (A), and following application of baclofen (B). A washout effect was not noted (n=5 slices.) LIII; Layer III, Stim; Stimulation. Dashed line represents -80 mV

5.6: $GABA_{B2}R$ antibodies and $GABA_{B1}R$ antagonist binding

The previous experiments showed the Test IgG did not occlude the effect of $GABA_BR$ agonists. However, the "all or nothing" response noted when baclofen was applied made it difficult to ascertain whether or not the $GABA_{B2}R$ antibodies were having an effect on the $GABA_{B1}R$ subunit. As Up state duration has been shown to be increased in the presence of $GABA_BR$ antagonists (Mann *et al.,* 2009), whether or not the antibodies could exhibit effects in the presence of a $GABA_BR$ antagonist was investigated next.

Application of CGP caused an increase in Up state duration. Figure 5.9A/B, shows the increased Up state duration following the application of CGP55845, at a 1 μM concentration ($p=0.041$, $n=4$), as has previously been used (Mann *et al.,* 2009, Craig *et al.,* 2013). Application of Test IgG resulted in a reduction in Up state duration, showing that the effects of Test IgG do not mimic that of $GABA_BR$ antagonists. The effect of test IgG on Up states was investigated following the application of CGP55845. For these experiments, CGP55845 (1 μM) was first applied to the slices, after which diluted IgG (100 μg/ml) was added to the aCSF containing CGP55845 (1 μM). In comparison to the baseline, the application of CGP55846 increased Up state duration. Duration was not decreased when the Test IgG was added, with the duration continuing to increase, suggesting that blocking $GABA_BR$ with CGP occludes the effects of the Test IgG. Following superfusion of the slice with wash, the duration continued to increase, indicating that CGP5584 is not washed out (Figure 5.9C).

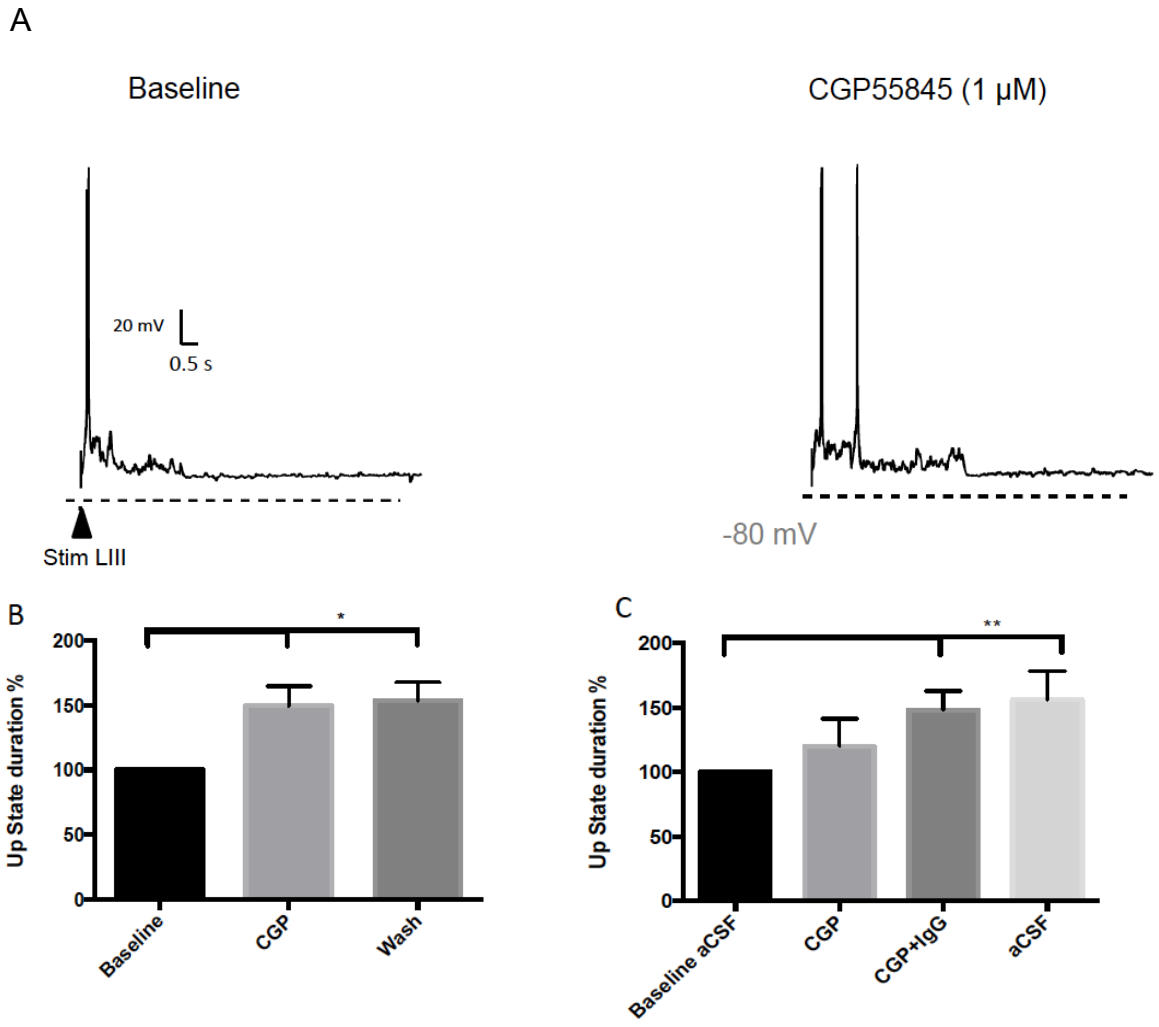

Figure 5.9: Application of the $GABA_BR$ antagonist CGP55845 increases Up state duration. IgG does not affect $GABA_{B1}R$ function

Baseline normalized to 100%. Changes in Up state duration and spike rate (spikes/s) are shown as a percentage of baseline.

The duration of evoked Up states following stimulation of LIII increased after CGP55845 (1µM) was applied (A). CGP (1 µM) increases up state duration in comparison to baseline (p=0.041, n=4 slices) (B). Application of Test IgG at a concentration that showed a reduction in Up state duration (100µg/ml) no longer had an effect suggesting that the CGP55845 outcompetes the IgG. Up state duration continued to show an increase when slices were superfused with aCSF suggesting that this antagonist is not washed out (C; p= 0.002 and 0.005, n=5 slices). LIII; Layer III, Stim; Stimulation. Dashed line represents -80 mV. Statistical analysis completed using repeated measures ANOVA followed by Dunn's multiple comparison test.

Table 5.1 summarises the effects Test IgG, HC IgG, CGP55845, and baclofen had on different Up state parameters. The Test IgG caused a reduction in Up state duration and spike rate during Up states. Preadsorption against $GABA_BR$ HEK cells (removal of the $GABA_BR$ antibodies) did not cause a change in Up state events in comparison to baseline or identically treated HC superfused slices. CGP55845 caused an increased duration of Up states as previously noted (Mann *et al.,* 2009 and Craig *et al.,* 2013). Baclofen caused a complete abolition of Up states, whereas the application of HC IgG had no effect.

Serum from the same patient the IgG was purified from was filtered and diluted in aCSF and applied to slices. However, the effects that were noted with the IgG could not be reproduced in the serum, and in general the cells tended to die soon after patching. To confirm that these were not due to the $GABA_BR$ antibodies, HC serum was also applied to slices and similar results were noted. This is suggestive that something within the sera that cannot be filtered is having a damaging effect on the cells. As such, IgG was deemed the most appropriate material to use.

Table 5.1: Summary of the effects different material superfused on slices had on Up state characteristics

Factor	Test IgG (100µg/ml)	Preadsorbed IgG (100µg/ml)	HC IgG (100µg/ml)	CGP 1µM	Baclofen 1-10µM
UP state duration	Reduced (mean; 23%)	No effect	No effect	Increased (mean; 28.5%)	Abolished
Spike rate	Reduced (mean; 92%)	No effect	No effect	No effect	Abolished
Washout	5/7	-	-	No	No

5.7: Summary and Discussion

As has been outlined in previous chapters, $GABA_BR$ antibodies do not appear to have the potential to activate the complement cascade (despite being predominantly IgG1 and IgG3). In addition, application of these antibodies to transfected HEK cells and primary neuronal cultures did not cause a reduction in the surface expression of the receptor. These patients often have additional antibodies (due to the presence of an underlying tumour), but it is unknown how each of these antibodies contributes to the immunopathology. However, before $GABA_BR$ antibodies were ruled out as a contributing factor to the disease, the direct modulation of the antibodies on the receptor was investigated. In this chapter, the direct effects of $GABA_BR$ IgG on an important GABAR dependent mechanism were explored.

Persistent cortical activity, which consists of fluctuations between active Up states and quiescent Down states (UDS), is imperative for normal cortical functioning. The UDS are noted to be maintained in horizontal mouse brain slices containing the EC (Cunningham *et al.,* 2006). GABA receptors are critical for controlling the proper regulation of this activity. In particular, $GABA_BR$ are necessary for the conversion of Up states into Down states (Mann *et al.,* 2009), and disruption of this transition can result in modulation of the normal activity.

5.7.1: $GABA_BR$ antibodies are having a hypoexcitable effect

It was shown in this chapter that IgG purified from a $GABA_{B2}R$ antibody positive patient resulted in shortening of Up state duration time (23% reduction) in comparison to aCSF alone (baseline). In addition, spikes noted during Up state events were decreased following application of the IgG (92.6% reduction). The reduction in Up state duration and spike rate could be indicative of faster recruitment of activity-dependent K^+

conductance. Conversely, HC IgG had no significant effect on Up state duration or spike rate.

The effects of the Test IgG differed significantly from those of the $GABA_BR$ antagonist CGP, which caused an increased Up state duration. The hypoexcitable effects of the Test IgG were more comparative to baclofen, though application of the agonist caused a complete abolition of Up state events. In the presence of baclofen, duration and spike rate could not be determined even at dilute concentrations as an "all or nothing" effect was noted. This was an interesting finding, as a dose-response was not observed. It is likely that even a weak activation of $GABA_BR$ is sufficient to shut down the network. Nevertheless, the IgG seems to be having an agonist like effect. Of particular interest was the rapid time frame in which the antibodies diffused through the tissue and an effect was noted (approximately 4 minutes). IgG purified from a HC patient had no effect on cortical network activity.

The binding site of $GABA_BR$ agonists and antagonists is the ECD domain located on the $GABA_{B1}R$ subunit (Malitschek *et al.,* 1999). Pre-application of IgG did not alter the effects of baclofen, which could be suggestive that these antibodies do not interfere with the ability of baclofen to bind to the receptor and cause an abolition of Up states. Furthermore, the $GABA_BR$ antagonist CGP55485 occluded the effects of the Test IgG showing that the antibodies are unlikely to be mediating their effects through modulation of $GABA_{B1}R$ activity. Instead Up state events may be altered through modulation of downstream signaling, perhaps via presynaptic VGCC. Again, despite this patient having LEMS, the patient did not have VGCC antibodies. As such, modulation which may be VGCC mediated would be due to the specific pathogenic role of $GABA_BR$ antibodies present in the patient serum.

The Test IgG did not produce results that completely mimicked either the $GABA_BR$ agonist baclofen, or the antagonist CGP55485. However, this was unsurprising as

numerous reports showing varying results of these $GABA_BR$ agonists and antagonists suggest that the mechanism of action of these drugs are diverse. Both baclofen and CGP55485 have been described as both proconvulsant and anti convulsant (Mott *et al.,* 1989 and Ault *et al.,* 1983). In addition, the effects of pharmacological drugs are indistinguishable between $GABA_BR$ autoreceptor (GABAergic synapses) and $GABA_BR$ heteroreceptors (glutamatergic synapses) subtypes (Waldmeier *et al.,* 1994), reinforcing a diverse role of these drugs.

Why it is that some $GABA_BR$ patients present with a clear limbic encephalitis phenotype with seizures whilst other patients have more expanded symptoms such as ataxia and OMS could not be answered in this thesis. The limited amount of sera available for IgG purification, allowed for only one encephalopathic patient with LEMS to be investigated. In addition, while it was demonstrated that the antibodies are having a specific effect on a $GABA_BR$ dependent mechanism, the downstream effects on other brain regions, namely the hippocampus were not investigated. The antibodies purified from the Test patient are having a hypoexcitable effect opposite to that produced by CGP55845, which could explain the overall brain slowing in the encephalopathic patient. However, the widespread distribution of these receptors in the brain and on both inhibitory interneurons and excitatory pyramidal cells leaves ample room for speculation of the actual effects seen in the whole brain. For example, the agonist like effect of this patient's antibodies on $GABA_BR$ located on interneurons would result in increased inhibition on excitatory neurons and could explain the encephalopathy of this patient. Similarly, an agonist like effect on $GABA_BR$ heteroreceptors on glutamatergic synapses would prevent the release of glutamate, counteracting excitatory effects of the neurotransmitter. Indeed downstream effects of the antibodies or antibody binding to different neurons could lead to epileptiform activity, noted in a majority of patients with these antibodies and LE. The excitatory actions of $GABA_BR$ agonists following brain

injury have been well-documented (Van den Pol *et al.,* 1996). It is possible that following seizures, the role of antibodies shift to excitatory leading to epileptiform activity in some LE patients.

5.7.2 Antibodies and direct modulation of receptors

Direct modulation of receptors by antibodies has been documented before. AChR antibodies have been shown to directly block the foetal form (y-subunit) AChR through binding to the agonist site causing a reduction in sodium ion influx (Riemersma *et al.,* 1996). Direct blocking of AChR is thought to cause arthrogryposis (joint contractures leading to foetal paralysis whilst in utero), though these antibodies do not have the same effect on adult AChR.

There have been several reports that have investigated the effects autoimmune antibodies have on brain activity using brain slices. Zhang *et al.* (2012) found the incubating mice brain slices with CSF from a NMDAR-encephalitis patients resulted in a suppressed LTP in Schaffer collateral CA1 synapses. These effects were not noted when CSF from other encephalitis patients (herpes simplex) was applied. Similarly to the results in this chapter, this effect was noted very quickly (approximately 5 minutes following application), suggesting that NMDAR act through direct short-term modulation as well as more long-term effects such as internalisation. Acute effects of NMDAR antibodies in patient CSF on NMDAR transfected HEK cells have also been shown (Gleichman *et al.*, 2012). In these experiments, the duration of the channel opening was prolonged after seven minutes of incubation.

In addition, Lalic *et al.* (2011) investigated the effects of IgG purified from a patient with severe LE with LGI1 antibodies on brain slices. Following incubation of slices with diluted patient IgG (100 µg/ml), extracellular field recordings were taken and its was noted that the LE IgG evoked epileptiform activity in the CA3 region of the

hippocampus. In addition, tonic firing was increased. As seizures can be a main feature of patients with LE, the *in vitro* findings correlated quite closely with the clinical phenotype. LE IgG effects closely mimicked the effects of the VGKC antagonist α-dendrotoxin.

5.7.3 Limitations and future directions

Although there are numerous advantages for the use of brain slices for whole-cell recordings, the superfusion of IgG onto slices, is an over-simplification of the $GABA_BR$ mechanism *in vivo.* Through cell recordings, only the humoral factors from a purified IgG sample are being considered and investigated for effects. Other components of the serum and other inducing factors for the overall encephalitis are overlooked. Animal models based on passive transfer of $GABA_BR$ antibodies into the brain may allow for a more accurate representation of this autoimmune encephalitis. This would allow for Witebsky's criteria of the presentation of the injected animal developing symptoms that mimic the disease in humans to be examined, though the *in vivo* model comes with its own caveats. Again, other contributing factors to the encephalitis besides antibodies, which may play a role in susceptibility to the disease, are not examined. While passive transfer experiments have been very important in understanding diseases such as MG and other PNS autoimmune diseases, the presence of an intact BBB in healthy laboratory mice may make interpretation difficult, and may not be an accurate model for the susceptibility of patients to these diseases.

Due to limited sera and CSF availability, we were unable to record the effects on Up states from IgG purified from a patient with $GABA_{B1}R$ antibodies. As patients with antibodies to this subunit predominately have LE, it would have been interesting to note if IgG had any effects in the hippocampus using extracellular recordings of the CA3 region as in Lalic *et al.* (2011). Furthermore, it would have been interesting to

investigate whether or not LE patients with seizures, versus patients with an encephalopathy but no seizures (our patient) differed on their effects on a cortical network. Furthermore, details on the IgG mechanism, such as differing effects on pyramidal versus inhibitory interneurons needs to be explored in greater detail. How the binding of $GABA_BR$ antibodies to the $GABA_BR$ receptor causes an alteration of Up states, whether that is through modulation of VGCC or inward rectifying potassium channels also needs to be explored in greater detail.

Section 2: Identification of novel antigens in Japanese encephalitis virus (JEV) samples

CHAPTER 6: Screening of Japanese viral encephalitis (JEV) cohort and identification of novel antigen targets

The number of recognised neurological conditions with an autoimmune aetiology is expanding. The identification of integral membrane neuronal antigens in these diseases is crucial for the characterisation of their potential pathogenicity and treatment. What causes the production of these antibodies is a question of great interest. In some cases, for example $GABA_BR$ antibody mediated encephalitis, the expression of neuronal surface proteins on the surface of the SCLC tumour cells may elicit an immune response causing the development of these antibodies; but what triggers the production of these antibodies in patients without a tumour? Infection, specifically viral infection may be one such factor, and a number of recent publications identifying antibodies to CNS proteins following herpes-simplex encephalitis (HSE) relapse support this theory and will be discussed in further detail below.

6.1: Introduction

6.1.1 Autoimmune and infectious encephalitis

Although regional variability makes the precise incidence of encephalitis unknown, it is estimated that 3.5 to 7.4 per 100,000 people are diagnosed per year (Granerod *et al.,* 2007). While encephalitis is a significant cause of morbidity and mortality worldwide, in approximately 40-60% of cases, the etiology remains unknown (Glaser *et al.,* 2006). In a multicenter, population based prospective study of 203 patients, it was found that viruses, such as herpes simplex virus (HSV) and varicella

zoster virus were the most common cause (42%) of encephalitis. In comparison, autoantibody-mediated encephalitis comprised 21% of encephalitis cases (Granerod *et al.,* 2010). Key differences can be noted between autoimmune and viral mediated encephalitis, and in depth comparisons in the literature to date have focused on NMDAR encephalitis and HSE patients (Gable *et al.,* 2009, Pruss *et al.,* 2012). NMDAR encephalitis patients often present with psychiatric symptoms and during the course of the disease go on to develop other neurological symptoms such as dystonia, orofacial movement, choreoathetosis and seizures. Gable *et al*. (2009) reported that HSE patients are less likely to have psychiatric disturbances, seizures, autonomic instability, and movement disorders. CSF investigations also reveal that white blood cell (WBC) count in HSE patients are often higher than in NMDAR encephalitis patients (Gable *et al.,* 2009). Furthermore, patients with autoimmune encephalitis may present with a variety of symptoms during the course of their disease, posing a diagnostic challenge for clinicians.

MRI can be used in the differential diagnosis, especially in the case of LE with AMPAR, $GABA_BR$ and LGI1 antibodies as patients show uni- or bilateral increased FLAIR signal in the medial temporal lobe (Lai *et al.,* 2009, Lai *et al.,* 2010, Lancaster *et al,* 2010). Asymmetric medial temporal lobe necrosis is often noted on MRI of HSE patients (Elbers et al., 2007) but may not be particularly useful in NMDAR encephalitis, where approximately 60% of patients show relatively normal imaging (Titulaer *et al.,* 2013). Of course polymerase chain reaction (PCR) testing can be used to diagnose patients with viral infections, though reports have shown false negatives in HSV cases in early samples (Elbers *et al.,* 2007). Therefore, repeat PCR on samples collected during the course of the patient's disease may be required.

However, the similarities that exist between these two groups of encephalitis could be critical in answering and understanding the question of what triggers the

development of these autoantibodies. Many of these diseases are preceded by a prodromal stage whereby the patients develop flu-like symptoms, which may point towards an infectious etiology. Irani *et al.* (2010) reported 20% of patients as having headaches and fever prior to the onset of neuropsychiatric features, seizures and other neurological symptoms. It is estimated that approximately 35% of patients with HSE go on to suffer from neurological symptoms, some of which lead to eventual death (Raschilas *et al.,* 2002). Although early administration of acyclovir has been suggested as the parameter that can be modified, viral cytotoxicity may not be the only factor in HSE relapses, and additional treatment may be necessary. In fact, when many of the patients relapse, viruses may not be detected via PCR and are referred to as non-viral related relapse (Armangue *et al.,* 2013). The link between HSE and NMDAR encephalitis has come to light in more recent publications and has provided evidence of an infectious aetiology theory in these autoimmune diseases.

6.1.2: HSV infection and NMDAR antibodies

Pruss *et al.* (2012) described 44 patients with PCR proven HSE, whereby paired serum and CSF was tested for IgG, IgA and IgM NMDAR antibodies using commercial slides (Euroimmun). NMDAR antibodies were detected in 13 (30%) patients of which IgA and IgM antibodies were detected in 9 cases and IgG in 5. No significant differences in clinical symptoms between antibody positive HSE and antibody negative HSE patients were noted. Interestingly, the application of IgM antibodies from these patients to the surface of primary hippocampal cultures caused a down regulation of the NMDAR after 3 days in an identical method reported for IgG antibodies in NMDAR-encephalitis (Hughes *et al.,* 2010), suggesting that IgM-antibodies may also be

pathogenic. The obvious limitation to this study was the use of commercial (Euroimmun) slides where the transfected cells are permeabilised.

The presence of both IgG and IgM NMDAR antibodies was also reported in 5 HSE cases, 4 of which were children (Armangue *et al.,* 2014). At initial HSE presentation (PCR confirmed) these patients had no detectable NMDAR antibodies in their serum or CSF, but interestingly high NMDAR antibodies in both the sera and CSF were noted upon HSE-relapse (1-4 weeks after HSE). One patient improved spontaneously, with 3 of the 4 remaining patients showing a return to their pre-relapse neurological level once treated with typical immunomodulatory therapy given in antibody-mediated diseases (corticosteroids, additionally IVIg in two cases). Thirty-four retrospective HSE cases were also investigated in this study, revealing two further NMDAR antibody positive patients and a further 9 patients with antibodies to unknown neuronal surface proteins, further enforcing an association with previous viral infection and a subsequent antibody-mediated encephalitis (Armangue *et al.,* 2014).

A positive response to immunotherapy has been documented in 3 of 7 HSE relapsing children, two of which were NMDAR antibody positive (Hacohen *et al.,* 2013). The patients relapsed with some, but not all symptoms of NMDAR encephalitis, such as movement disorders, seizures and cognitive regression. Of particular interest was one case in which after 10 years of good recovery from HSE, the patient suffered from recurrent episodes of cognitive and behavioral decline until started on IVIG treatment. When HSE-patients are not started on early aggressive immunotherapy, response following relapse tends to be poor (Mohammed *et al.,* 2013). Furthermore, a 37-year-old female who presented with altered memory and also previously had HSE, and later developed AMPAR (GluA2) antibodies has also been documented (Gleichman *et al.,* 2014).

As such, the relapse of patients following HSV infection could be a secondary autoimmune mediated response, particularly in the absence of viral re-activation. The relationship between viral infection and autoimmunity can be linked back to Paul Elhrich and Robert Koch. It has been postulated that a preceding infection may result in the virus causing a modulation of self-antigens, making these autoantigens susceptible to attack, as they are now perceived as foreign by the host's immune system. This is referred to as molecular mimicry. Alternatively, following infection of neurons by the virus and subsequent neuronal lysis, there may be a release of self-antigens, which could trigger the development of autoantibodies (Rose and Bona, 1993).

6.1.3: Japanese Encephalitis Virus (JEV)

What other viral mediated diseases could have an autoimmune component at some stage during the disease? Could these diseases have novel antigen targets? Many of the publications investigating infection followed by the development of autoantibodies are very recent, and the potential role of other viruses and autoimmune antibodies needs to be explored. One such disease that could be used to further our understanding of the viral and antibody link is Japanese encephalitis (JE).

JE is caused by a virus in the Flaviviridae family and is the most common form of viral encephalitis in Asia (Kaur and Vrati, 2003). It is thought to primarily be a tropical disease with very few cases reported in Western countries. Humans become infected with the disease following a bite from an infected mosquito. It has been estimated that in Asia approximately 50,000 new patients are diagnosed each year, though numbers may be higher due to poor surveillance and reporting in remote regions. Of those affected by the disease, approximately 30% die (Kaur and Vrati, 2003).

6.1.4: Clinical Manifestations

The disease generally manifests in children, with symptoms of nonspecific febrile illness. As the disease progresses patients can experience poliomyelitis-like flaccid paralysis and can develop tremor, unblinking eyes, generalized hypertonia and movement abnormalities, which can be Parkinsonian in nature. Reduced consciousness, photophobia and seizures may all develop in later stages (Solomon *et al.,* 1998). Movement abnormalities and epileptiform characteristics can be observed on EEG recordings (Solomon *et al.,* 2000). Approximately 70% of patients survive the disease, though 50 % of patients are reported as having permanent neurological sequelae, including cognitive and language impairment (Kaur and Vrati, 2003).

The development of neurological symptoms during the course of the disease (many of which can persist) is an interesting finding, which have been hypothesised to be attributed to cell death. It is possible that cell death and neurological dysfunction are caused by the pathogenic effects of antibodies generated in response to the Japanese encephalitis virus (JEV).

6.1.5: Pathogenesis

JEV titres are often found to be high in both the sera and CSF (Kaur *et al.,* 2003). How the virus gains access to the CNS remains to be elucidated. A commonly proposed mechanism is the infection of leukocytes (during the incubation period, but prior to the clinical development of JE), which carry the virus to the BBB, where it can bind to the endothelial cells and be internalised. Following JEV infection, microglial infiltration is increased and both neuronal and astrocytic cells are killed. Studies have shown that an increase in levels of pro-inflammatory factors (IL-6, IL-1B, inducible nitric oxide synthase- iNOS) contributes to neuronal death (Goshal *et al.,* 2007). In particular, the increase in iNOS, leads to an increase in the development of nitric oxide (NO). NO is a strong antimicrobial agent and has been shown to inhibit viral RNA synthesis, thereby

having an important role in the innate immunity and preventing early JEV infection. However, reports of dysregulation of NO secretion have been shown to be highly toxic and could play a role in neuronal degradation (Lin *et al.,* 1997). In the study by Goshal *et al.* (2008) mice injected intra-cerebrally with a strain of JEV developed JE symptoms, namely limb paralysis and whole body tremor, 3 days post injection. It was found that the increased release of proinflammatory cytokines following injection was brain region specific, with the hippocampus being the most commonly affected area. Increased levels of lectin positive (marker of activated microglial) microglia in damaged regions were also observed. Neuronal loss in the hippocampus could explain the cognitive impairment and other neurological features that many JE patients with long standing disease suffer from.

The pathogenic role of JEV on astrocytic cells also remains to be fully understood. It has been shown that infection of astrocytic cell lines with JEV results in a modulation of free radicals (Mishra *et al.,* 2008). Neuronal cell death via tumour necrosis factor (TNF) has also been documented (Swarup *et al.,* 2008) and this apoptosis could result in further astrocytic and microglial activation, self- perpetuating the system.

An increase in T-lymphocyte numbers and IgM antibodies are noted early on in the disease course, and testing for IgM antibodies in the sera and CSF via ELISA is the most commonly used diagnostic tool for JE (Ravi *et al.,* 2008).

6.1.6: JEV as an antibody mediated disease

There have been no reports investigating whether or not antibodies play a role in JE. However, recent publications describing the link between HSE and the development of NMDAR antibodies and other potential targets to neuronal surface antigens (Armangue *et al.,* 2014) highlight a potential autoimmune contributing component. Furthermore, reports suggesting that JE may be a biphasic illness make the disease a

good choice for future investigation. Prabhan *et al.* (2002) described 6 cases in India (4 children and 2 adults) that tested positive for JEV during the initial presentation of the disease. Initially symptoms included fever, headaches, altered consciousness, rigidity and tremors. Following recovery from this first stage of illness (a timescale of days to a few weeks), patients had a relapse of symptoms that included behavioral changes, dystonia, pen-oral dyskinesia, mutism and muscle wasting. While these symptoms differ from the first stage of JEV infection they still conform to the symptoms of the disease. MRI imaging of JEV patients shows lesions in thalami, hippocampus, cerebral cortex, the cerebellum and brain stem. These biphasic patients developed fresh lesions, which resembled the acute lesions that developed during the first stage, with older lesions resolving on MRI (Handique *et al.,* 2008). It has not been reported whether patients with biphasic illness who develop neurological symptoms later, also develop lesions in specific regions. The overall recovery of patients with biphasic illness did not differ to cases with the monophasic disease. In one case with biphasic JE, the IgM levels in the CSF were raised, suggesting the JE virus persisted, though the biphasic form of JE is rare, and it is inconclusive whether or not it is the secondary increase in IgM levels that cause the relapse.

6.1.7: Objectives

The aims of this chapter were:

1). To determine whether a viral mediated disease (JE) has autoantibodies to known antigens by screening samples on diagnostic CBAs and RIAs available in the lab

2). To determine whether patients with JEV have autoantibodies to novel antigen targets. This was investigated by screening the samples on primary neuronal cultures and immunoreactivity was assessed.

3). To establish a system for novel antigen identification

6.2: Methods

All CBAs and VGKC RIA were carried out as described in Section 2.3 and 2.4. Neurons were cultured and stained as in section 2.8. All CBAs and neuron staining was scored by two independent observers. The strategy adopted for the identification of novel antigens have been reported previously (Lai *et al.,* 2009, Lancaster *et al.,* 2010). The immunoprecipitation and mass spectrometry protocols are outlined in section 2.12 and 2.13 and discussed in further detail below.

6.3: Results

6.3.1: Screening of JEV samples on CBAs

6.3.1.1: JEV cohort

A total of 93 serum samples and 16 CSF samples were available for testing from 44 children. Original samples were available from 44 patients; 12 patients (taken at onset) with no follow up samples, and 32 patients had follow up samples (1-4 per patient). A summary of the entire cohort is shown in Table 6.1. Eighty percent of samples (35/44) were JEV positive. A further 9 samples were suspected JEV and disease control (DC) samples (two possible dengue).

Age range for the JEV proven samples was between 2 and 14 years (median 6). Males accounted for 66% of samples. Parkinsonism was found in 17/30 (56.7%) patients. Abnormal behaviour was observed in 12/30 (40%) patients. Three-month outcomes were available from 31/35, as 3 patients died and one patient was not followed up. None of the patients that survived relapsed or deteriorated after discharge.

Age range for the suspected JEV and DC samples was between 6 and 14 years (median 12). Males accounted for 77.7% of the patients in this group. Two of 9 patients (22.2%) had Parkinsonism. No patients in this group exhibited abnormal behavior.

Table 6.1: Summary of JEV cohort

Patient Group	Patients (N)	Male:Female	Age range yrs (median)	Parkinsonism	Abnormal behaviour
Confirmed	35	22:13	2-14 (6)	56.7%	40%
Suspected	9	7:2	6-14 (12)	22.2%	0%

6.3.1.2: Testing on available CBAs

All 93 serum samples were initially tested for antibodies against known antibody targets; NMDAR, LGI1, CASPR2, AMPAR, $GABA_AR$ and $GABA_BR$ by CBA. In total 10/35 (28.6%) of confirmed JEV patients were positive for antibodies directed against one of the known antibody targets. NMDAR and LGI1 antibodies were detected in 2/9 (22.2%) of suspected JEV samples. A summary of all the autoantibodies found in the cohort is shown in Figure 6.1. In addition, using the diagnostic VGKC RIA, 15 samples from 9 patients were found to have detectable antibody levels (median; 377 pM), ranging between 119 pM-1767 pM (>100 pM was used as the positivity cut off as previously described, Vincent *et al.,* 2004). Interestingly, none of the 9 positive patients on the VGKC RIA were positive for LGI1 or CASPR2 antibodies, as determined by CBA. However, two VGKC-RIA positive patients also had NMDAR antibodies.

Of importance was that observation that CBA and VGKC RIA positivity was not noted in all serial samples of patients with >1 sequential samples. As such, 19/44 (43.2%) of samples were positive as determined by CBA and VGKC RIA, with 27.2% of the patients in the cohort (12/44) having antibodies to a known neuronal surface antigen, at some point in the disease. Summary of positive samples is found in Table 6.2.

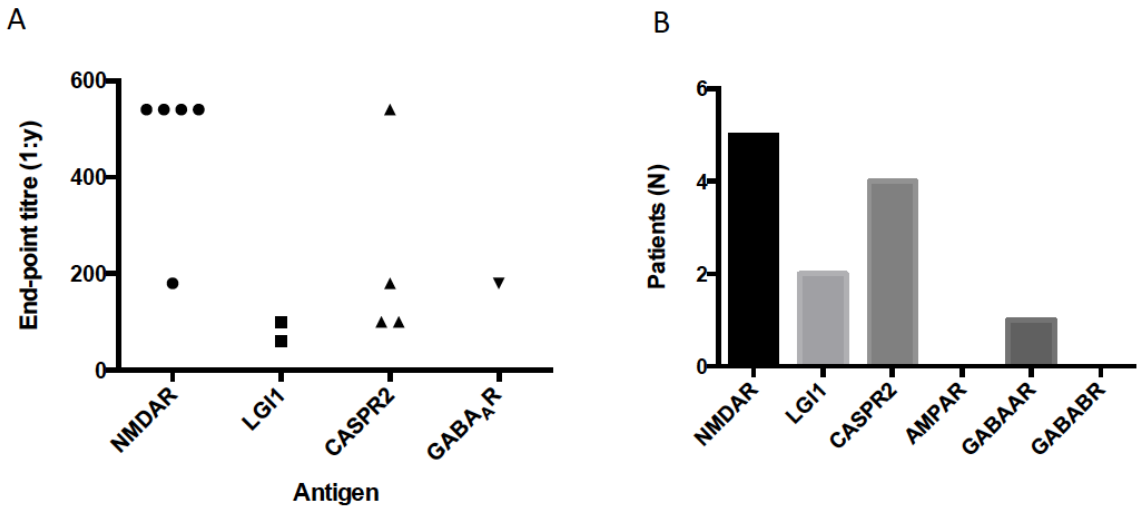

Figure 6.1: Twelve patients in the JEV cohort were positive to a known antigen target, as determined via CBA

Serum samples (1:20 or 1:100) were incubated with HEK cells transfected with NMDAR, LGI1, CASP2, AMPAR, GABA$_A$R and GABA$_B$R DNA as previously described (*Irani *et al.*, 2010a, Irani *et al.,* 2010b and Pettingill *et al.,* 2014 under submission).

12 of 44 serum samples had autoantibodies to known antigenic targets; NMDAR (n=5), LGI1 (n=2), CASPR2 (n=4) and GABA$_A$R (n=1) CBAs. None of the samples showed reactivity on more than one assay. End-point titres of the patients according to the antigen (A). Breakdown of the antibody positive samples according to the antigen (B).

Table 6.2: Summary of the JEV positive samples as determined by CBA and VGKC RIA

Patient Serum	CBA reactivity	CBA Score	CBA end-point titre	VGKC RIA (pM)
JEV 1	NMDAR	1.5	1:180	289
JEV 2	NMDAR	2	1:540	Neg
JEV 3	NMDAR	2.5	1:540	119
JEV 4	NMDAR	2.5	1:540	Neg
JEV 5	NMDAR	3	1:540	Neg
JEV 6	LGI1	1	1:60	Neg
JEV 7	LGI1	1	1:100	Neg
JEV 8	CASPR2	1	1:100	Neg
JEV 9	CASPR2	1	1:100	Neg
JEV 10	CASPR2	1.5	1:180	Neg
JEV 11	CASPR2	2.5	1:540	Neg
JEV 12	$GABA_AR$	1.5	1:180	Neg
JEV 13	Neg			130
JEV 14	Neg			233
JEV 15	Neg			372
JEV 16	Neg			408
JEV 17	Neg			435
JEV 18	Neg			1086
JEV 19	Neg			1767

Representative binding of a NMDAR antibody positive (JEV 4) and CASPR2 antibody positive (JEV 11) are shown in Figure 6.2. None of the samples were positive on more than one CBA, excluding the possibility of non-specific binding to transfected cells. All the positive samples were serial diluted until binding to transfected cells could no longer be visualized (end-point titration). The samples with higher end-point titres had consistently higher CBA scores (Table 6.2). The end-point titre for each antibody positive sample for each antigen is plotted in Figure 6.3A. The mean end-point titrations of the NMDAR-antibody positive samples, was higher than the mean antibody titres of patients positive on the other CBAs (Figure 6.3B $p=0.0241$, Mann-Whitney). The VGKC RIA titres of the 9 positive patients are shown in Figure 6.4.

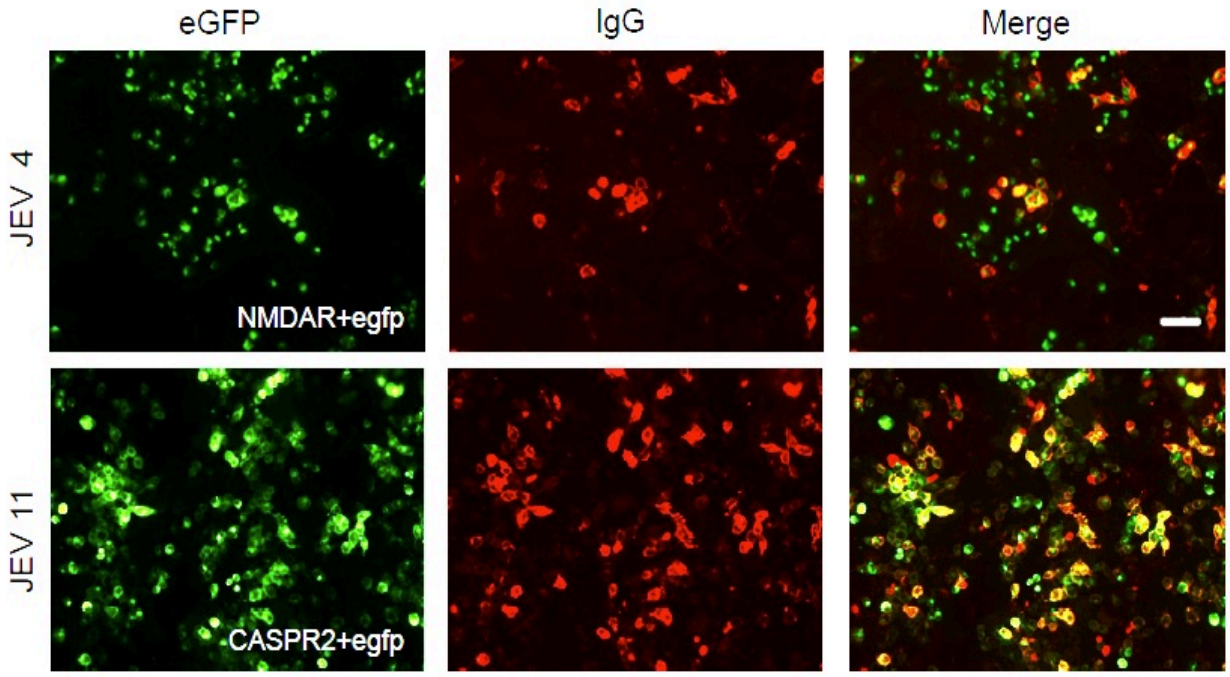

Figure 6.2: Binding of JEV sera to NMDAR and CASPR2 transfected HEK cells

An example of NMDAR antibody patient (JEV 4, 1:20) and CASPR2 antibody patient (JEV 11, 1:100) binding to HEK cells transfected with NMDAR (upper panel) and CASPR2 (bottom panel), respectively. As both constructs were eGFP tagged, transfection could be detected (left column). Co-localisation of IgG binding (goat anti-human IgG (red), middle column) to transfected cells was observed. Merge image shown in far right column. Magnification x200. Scale bar= 100µm.

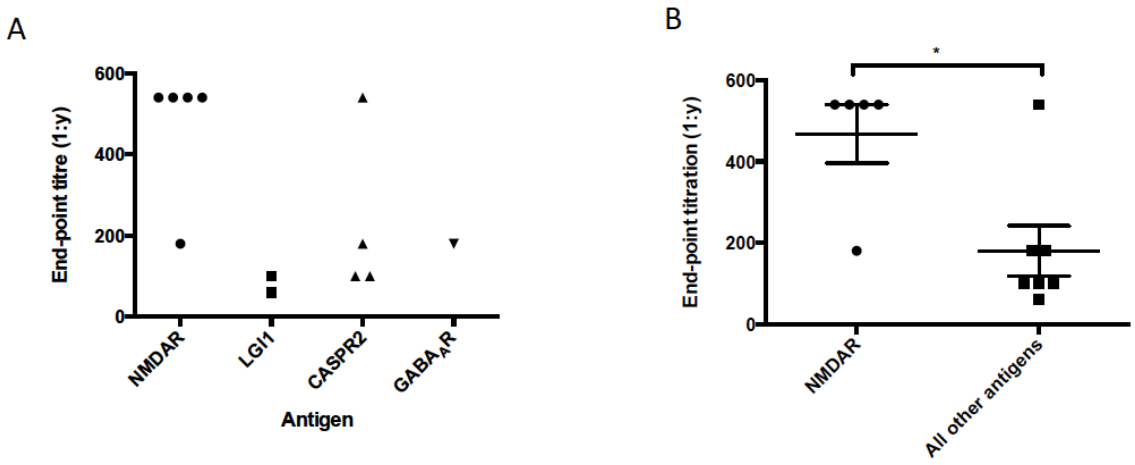

Figure 6.3: Relationship between antibody end-point titre and antigen specificity

End-point titres (dilution; 1:y) were greater for samples with higher CBA scores (A). The NMDAR antibody positive patients had higher CBA scores and end-point titres than the other antibody positive samples (B; p=0.035, Mann-Whitney).

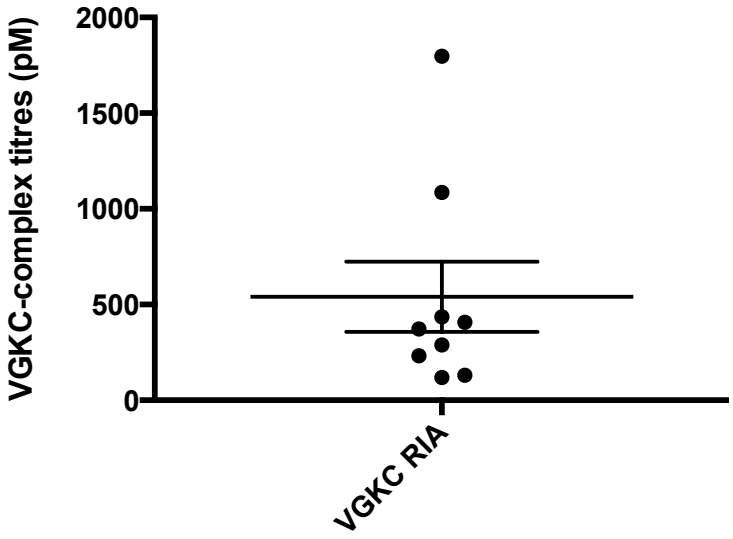

Figure 6.4: VGKC RIA titres for the 9 positive patients

Nine of 44 samples were positive on the VGKC RIA. Range (119-1767 pM).

6.3.1.3: Testing for IgM antibodies

As detection of IgM antibodies in the sera and CSF, is used as a standard test for diagnosing JEV (Ravi *et al.,* 2008), all antibody positive samples were re-tested for IgM antibodies on the respective CBAs. Using a goat-anti human IgM secondary antibody (Alexa Fluor 488), no reactivity was noted with HEK cells transfected with NMDAR, LGI1, or CASPR2. Only the $GABA_AR$ antibody positive sample (JEV 12) had both IgM and IgG antibodies (Figure 6.5). The intensity of binding detected with the IgM antibody was higher than the IgG antibody (with a CBA score of 2.5 vs. 1.5 as scored by two independent observers). The presence of IgM antibodies in low $GABA_AR$ antibody titres has been described (Pettingill *et al.,* 2014 (under submission)).

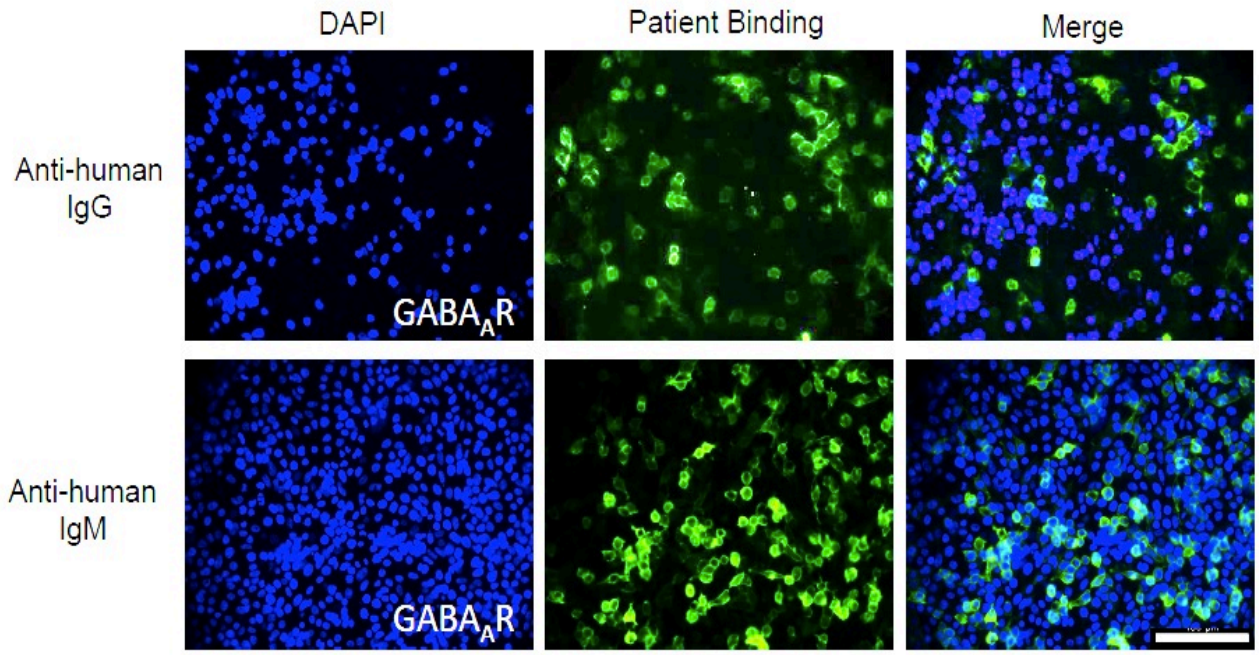

Figure 6.5: Detection of both IgG and IgM antibodies in GABA$_A$R antibody positive serum JEV 12

IgG and IgM antibodies present in JEV 12 serum bound to GABA$_A$R (1:20) transfected HEK cells. Secondary antibodies specific to IgG (goat anti-human IgG 488; upper panel) and IgM (goat anti-human IgM 488; bottom panel) were used to visualize binding. Merge with DAPI positive cells is shown (right column). Images 400x magnification. Scale bar= 100 µm

6.3.2: Reactivity of JEV samples to primary neuronal cultures

6.3.2.1: Binding to primary hippocampal cultures

To investigate binding to protein expressed in a more physiological system, the cohort was screened on primary hippocampal neuronal cultures, selected specifically as previous reports have shown the hippocampus as the region with the most extensive neuronal loss is JEV patients (Goshner *et al.,* 2008).

Interestingly 29/44 (65.9%) sera bound to the surface of live hippocampal neurons (confirmed JEV 23/35 (65.7%) and suspected JEV 6/9 (66.7%)). Of the patients with an antibody confirmed via CBA or by the VGKC RIA, 11/19 (57.9.1%) showed reactivity to hippocampal neurons at some stage of their disease. That is, some but not all sequential samples taken from patients with a positive CBA or VGKC result were positive on the neurons. Six out of 12 samples positive on the CBA (n=6, NMDAR 5; $GABA_AR$ 1), showed staining to neurons. Representative staining of antibody positive samples are shown in Figure 6.6. It was observed that in a majority of samples the staining pattern was quite similar, and large puncta were noted, though the intensity of the stain varied. However, some variability in staining pattern was noted. For example, the NMDAR antibody positive sample JEV 4 showed a more diffuse stain, with the size of the puncta being smaller than what was observed in another NMDAR antibody positive patient, JEV 5 (Figure 6.6; middle and bottom panel).

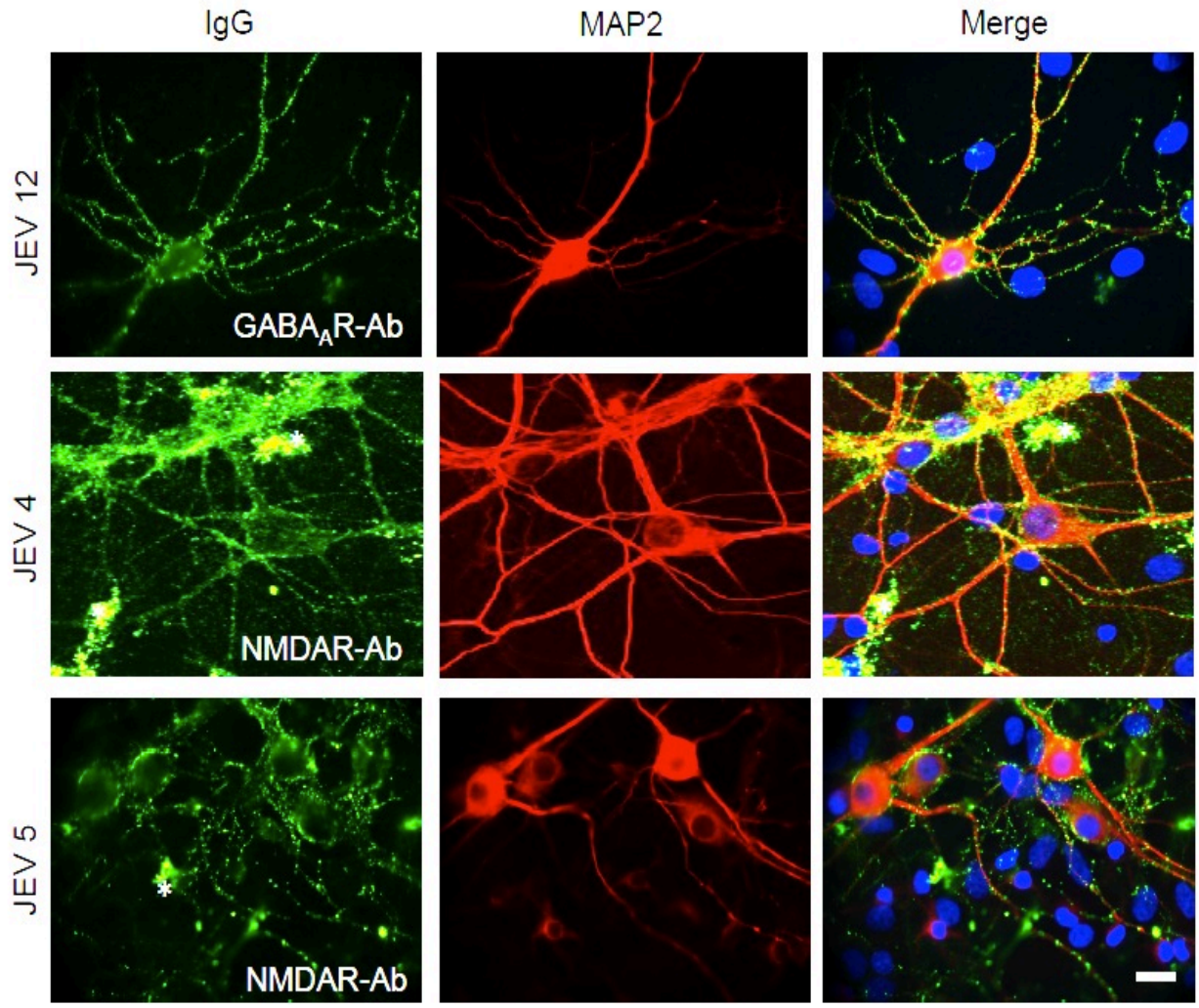

Figure 6.6: JEV sera with GABA$_A$R and NMDAR antibodies bound to the surface of hippocampal neurons

Hippocampal neurons (14 div) were incubated with sera (1:100). JEV 12 is a GABA$_A$R antibody positive patient, and JEV 4 and JEV 5 are both NMDAR antibody positive patients respectively. Patients showed strong binding to the surface of neuronal cultures. IgG binding was visualised with anti-human IgG Alexa Fluor 488 (green). Neurons were visualized with the neuronal marker MAP2 (anti-mouse Alex Fluor 568-red). Magnification x1000. Scale bar= 20 µm.

A comparison between CBA score antibody titre (15 samples from 12 patients) and staining on hippocampal neurons is shown in Figure 6.7A. Samples that were tested on the CBAs and had a higher score were more likely to show immunoreacitivity to cultures ($p=0.0186$, Mann-Whitney). More interestingly, 10/15 (66.7%) of samples positive on the VGKC RIA (from 9 patients) also bound to neurons. This was an interesting finding, as these sera were negative for known VGKC-complex antigens LGI1 and CASPR2, suggesting these sera were binding to a novel antigen target that is a component of the VGKC complex. However, no significant difference in VGKC-RIA antibody titre was noted between those patients that did and did not show reactivity to neurons (Figure 6.7B).

Sixty-two percent (18/29) of patients that showed reactivity to hippocampal neurons were negative on all of the CBAs and VGKC RIA. Representative staining of seronegative JEV samples binding to the surface of hippocampal neurons is shown in Figure 6.8. Taken together, the findings suggest there are autoantibodies to a novel cell surface antigen in some JEV patients. As indicated by the different patterns described in two NMDAR positive patients, and by the VGKC RIA results, there could also be additional antibodies present in samples where a known antigen was identified. Interestingly, none of the CSFs showed immunoreacitivity to neuronal cultures.

As IgM antibodies is a hallmark of the disease and often used as the first line of testing for JEV, reactivity to hippocampal cultures using a secondary antibody specific for IgM antibody detection was carried out. Nine (9.7%) samples were positive for IgM; however, the IgM antibody staining was weak and less intense than the IgG.

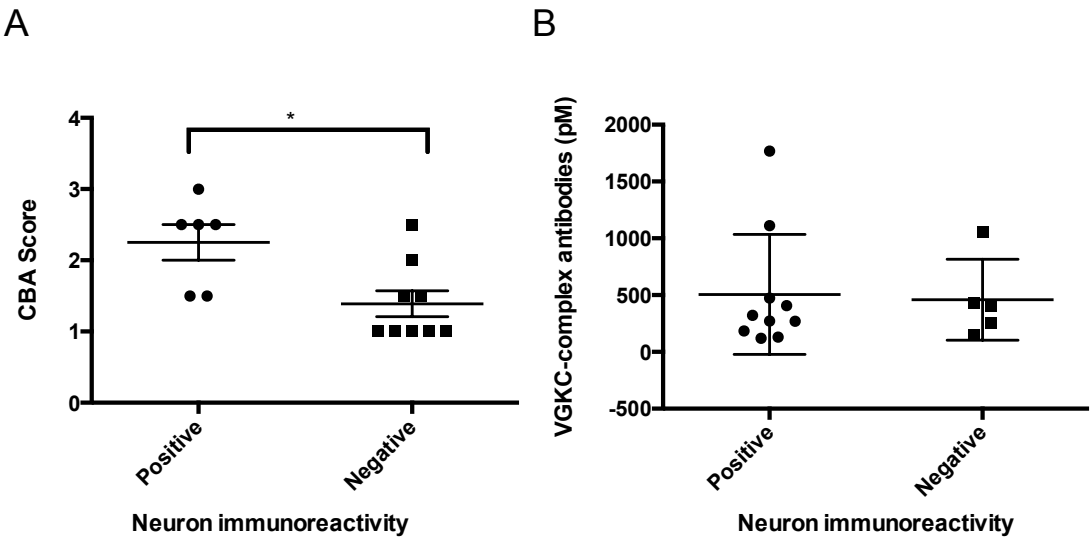

Figure 6.7: Samples from patients with positive CBA or VGKC RIA and neuron immunoreactivity

Not unexpectedly, there was a significant difference in the CBA score between samples that showed positive and negative immunoreactivity to neuronal cultures (p=0.0186, Mann-Whitney). Samples with higher scores on the CBAs were more likely to show positive immunoreactivity (A). No significant difference in the VGKC-complex antibody titres was observed in samples that bound to the surface of neuronal cultures versus those that did not (p=0.2857, Mann-Whitney; B).

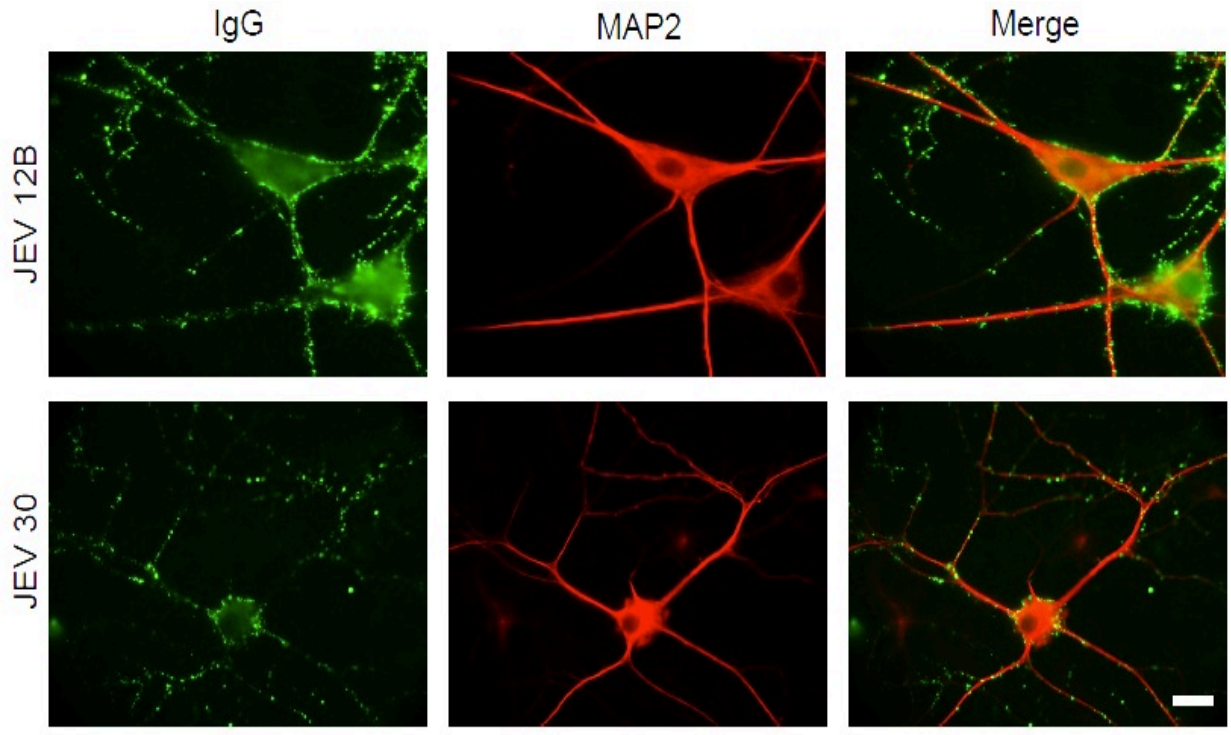

Figure 6.8: JEV samples bound to the surface of live hippocampal neurons

Representative staining of two JEV patients with an unknown antigen (JEV 12B, JEV 30) that *showed strong binding to the surface of neuronal cultures. IgG binding was visualised with anti-human IgG Alexa Fluor 488 (green). Neurons were visualized with the neuronal marker MAP2 (red). Magnification x1000. Scale bar=20 µm.*

6.3.2.2: Binding to cortical and cerebellar granular neurons

As mentioned previously, some of the antibody positive samples did not bind to the surface of live hippocampal neurons. While low antibody levels may explain this, it is possible that the patient sera may be targeting additional brain regions, where the antigen target is expressed at higher levels. Some JEV patients have motor impairment, which could be suggestive of antibodies affecting the cortex, cerebellum and brain stem areas. As such binding of patient sera to neurons cultured from other brain regions was also explored. None of the samples bound to cerebellar granular neurons, whilst only 3 patients, all of which also bound to hippocampal cultures showed very weak IgG-immunoreactivity when screened on cortical neurons. Therefore this path was not pursued.

6.3.3: Clinical details of the JEV cohort

While only a small-unselected group, we sought out to determine whether or not there was a link between antibodies to known or novel surface antibodies and patient symptoms. Perhaps the most interesting finding of our study was the high number of patients (65.9% of children with JEV) that had at some stage shown reactivity to the extracellular surface of neurons. Whilst patients with antibodies to known surface proteins (NMDAR, LGI1, CASPR2 and $GABA_AR$) were present in the cohort, not all of the neuron positive samples had autoantibodies to a known antigen, suggesting the presence of a novel antigen target.

Table 6.3 summarises the clinical details of the antibody positive samples. Eleven of 12 samples where clinical details were available, all showed parkinsonian, extrapyramidal of behavioural features. These features are commonly associated with LE and anti-NMDAR encephalitis. Six of the 9 patients (66.7%) where 3-month outcome

was available from showed improvement (3 patients described as normal upon discharge). Clinically, patients with CBA positive and negative results did not differ from one another, with 66.7% of the CBA positive samples showing improvement at 3 months versus 60% of the CBA negative patients showing improvement. However, as many patients were not followed up, or a detailed clinical report was not available, a more thorough clinical analysis is required. A comparison between the CBA positive and CBA negative samples is shown in Appendix Table 4.

Table 6.3: Summary of the CBA confirmed antibody positive samples

Patient Serum	CBA reactivity	JEV (confirmed or suspected	Parkinsonian	Extrapyramidal features	Behaviour abnormalities	Outcome
JEV 1	NMDAR	Confirmed	Yes	Yes	Yes	Apparently normal
JEV 2	NMDAR	Confirmed	Probable	Yes	Yes	Apparently normal
JEV 3	NMDAR	Confirmed	No	Yes	Yes	Limited improvement in hospital. Severe behavioural abnormalities persist.
JEV 4	NMDAR	Suspected	No	No	No	Not seen
JEV 5	NMDAR	Confirmed	No	Yes	Yes	Brisk reflexes
JEV 6	LGI1	Suspected	No	No	No	Not seen
JEV 7	LGI1	Confirmed	Probable	Yes	No	Tremor persists
JEV 8	CASPR2	Confirmed	Probable	Yes	Yes	Limited speech, improved from seizures
JEV 9	CASPR2	Confirmed	Probable	Yes	No	Apparently normal
JEV 10	CASPR2	Confirmed	Yes	Yes	Yes	Improved but tremor persists
JEV 11	CASPR2	Confirmed	N/K	N/K	N/K	Not seen
JEV 12	$GABA_AR$	Confirmed	No	Yes	Yes	Improved by discharge

We also focused on the clinical outcome based on hippocampal reactivity results. Using the scoring scale for patient clinical outcome (Whitley et al., 1986), no differences in the overall hippocampal reactivity between sequential samples taken from JEV patients was noted. That is, positive and negative samples were noted in the first and follow up samples in equal proportions (Figure 6.9A). Similarly there was no significant difference between positive and negative samples depending on the days post onset the samples were taken (Figure 6.9B). Finally, 3 month clinical outcome was also independent of neuron immunoreactivity ($p=0.5185$, Figure 6.9C).

Unfortunately, JEV (IgM) titres were not available and therefore we were unable to explore the relationship between samples that showed CBA or neuron immunoreactivity to overall titre.

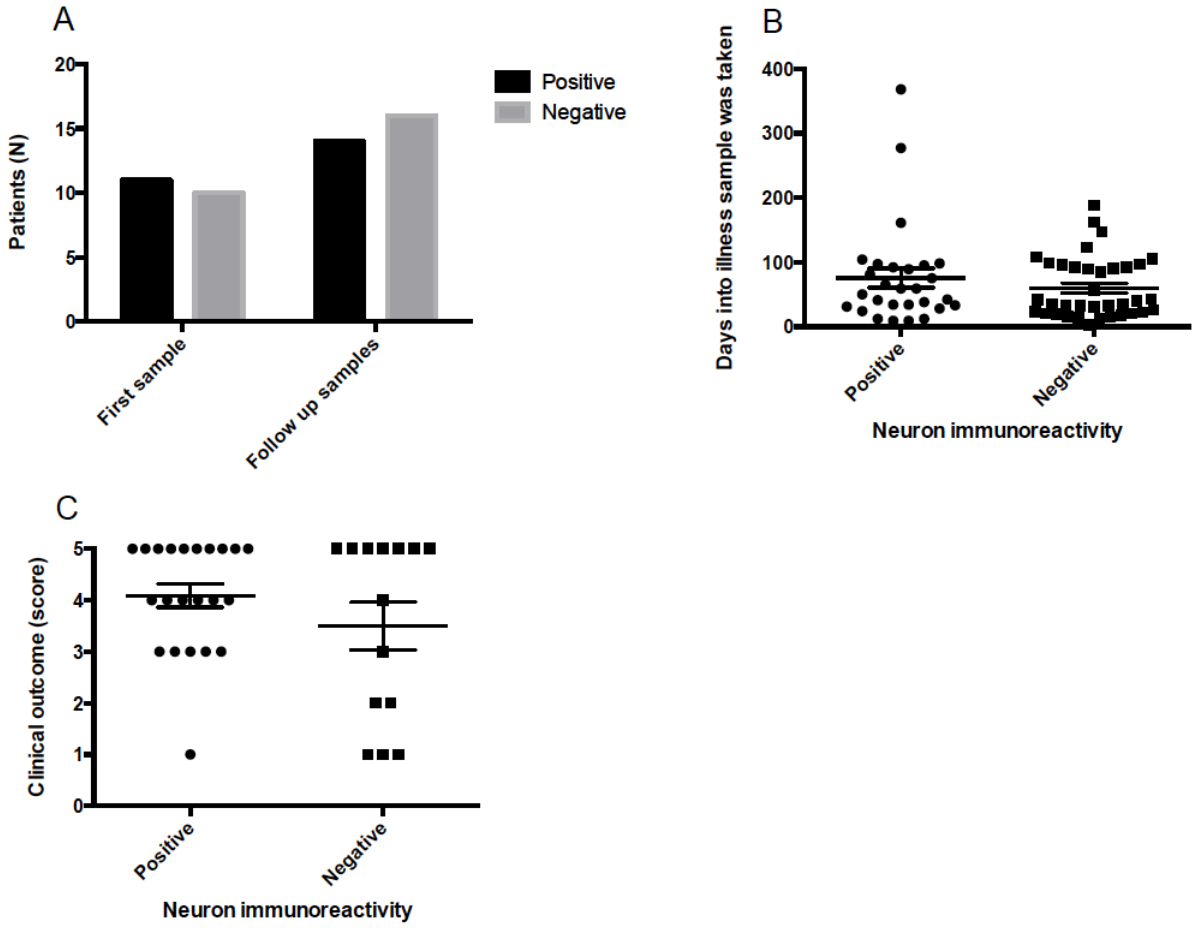

Figure 6.9 Clinical outcome of JEV patients based on neuron immunoreactivity

Positive immunoreactivity was noted in first and follow up samples taken from patients with JEV. No significant differences were noted between the groups (A; p=0.7950, two-way ANOVA). No significant differences were noted between positive and negative neuron immunoreactivity with regards to days from disease onset (B, p=0.5698, Mann-Whitney). The was no difference in 3 month clinical outcome between patients that had a positive or negative neuron immunoreactivity result (C, p=0.5188, Mann-Whitney).

Three-month outcomes using scale from Whitley et al., 1986. 1 = Dead, 2 = Severe sequelae requiring full time support/care, 3 = Obvious sequelae, but able to walk/function independently appropriate to age, 4 = Minor sequelae, usually, 5 = Apparently normal.

6.3.4: Antigen discovery using a positive control model system

In order to identify the cell surface antigen targets of the autoantibodies present in the JEV sera, we used an immunoprecipitation and mass spectrometry strategy as has previously been described (Littleton *et al.,* 2009, Lai *et al.,* 2009, Lancaster *et al.,* 2010). We first sought to optimise the immunoprecipitation and mass spectrometry protocol using patients with known antibody targets (CASPR2 and $GABA_BR$).

6.3.4.1: Selection of positive control patient sera for system optimisation

For this "model system", serum samples were chosen from typical antibody positive patients with high titre IgG-antibodies directed against CASPR2 (end-point titre 1:15000) and $GABA_BR$ (end-point titre 1:6400) as determined by CBA (see Table 6.4 for patient clinical details and antibody titre). Importantly, these patient's sera bound strongly to primary cortical neuronal cultures (Figure 6.10) and therefore represented promising candidate positive control sera to optimise the immunoprecipitation protocol. No reactivity was seen using HC sera.

Table 6.4: Summary of the patients used for the positive control "model system" immunoprecipitation experiments

Patient	Titre	Age/Sex	Clinical Symptoms
CASPR2 Ab	1:15000	76/M	Morvan's Syndrome; SCLC
$GABA_{B2}R$ Ab	1:6400	50/M	Encephalitis/LEMS; SCLC
HC	-	40/M	-

6.3.4.2: Confirmation of appropriate antibody concentration for immunoprecipitation

To confirm that saturating amounts of antibody were present for successful immunoprecipitation, flasks of primary cortical cultures were incubated (1:100) with positive control sera (CASPR2 or $GABA_{B2}R$ antibodies) or HC sera for 30 minutes at 37°C. Following incubation, the supernatant was collected and tested for reactivity on coverslips containing cortical neurons. As shown in Figure 6.10, these supernatants maintained strong neuronal immunoreactivity indicative of excess antibody concentrations applied to the immunoprecipitation preparation. We were therefore confident to proceed with the immunoprecipitation protocol (see section 2.12).

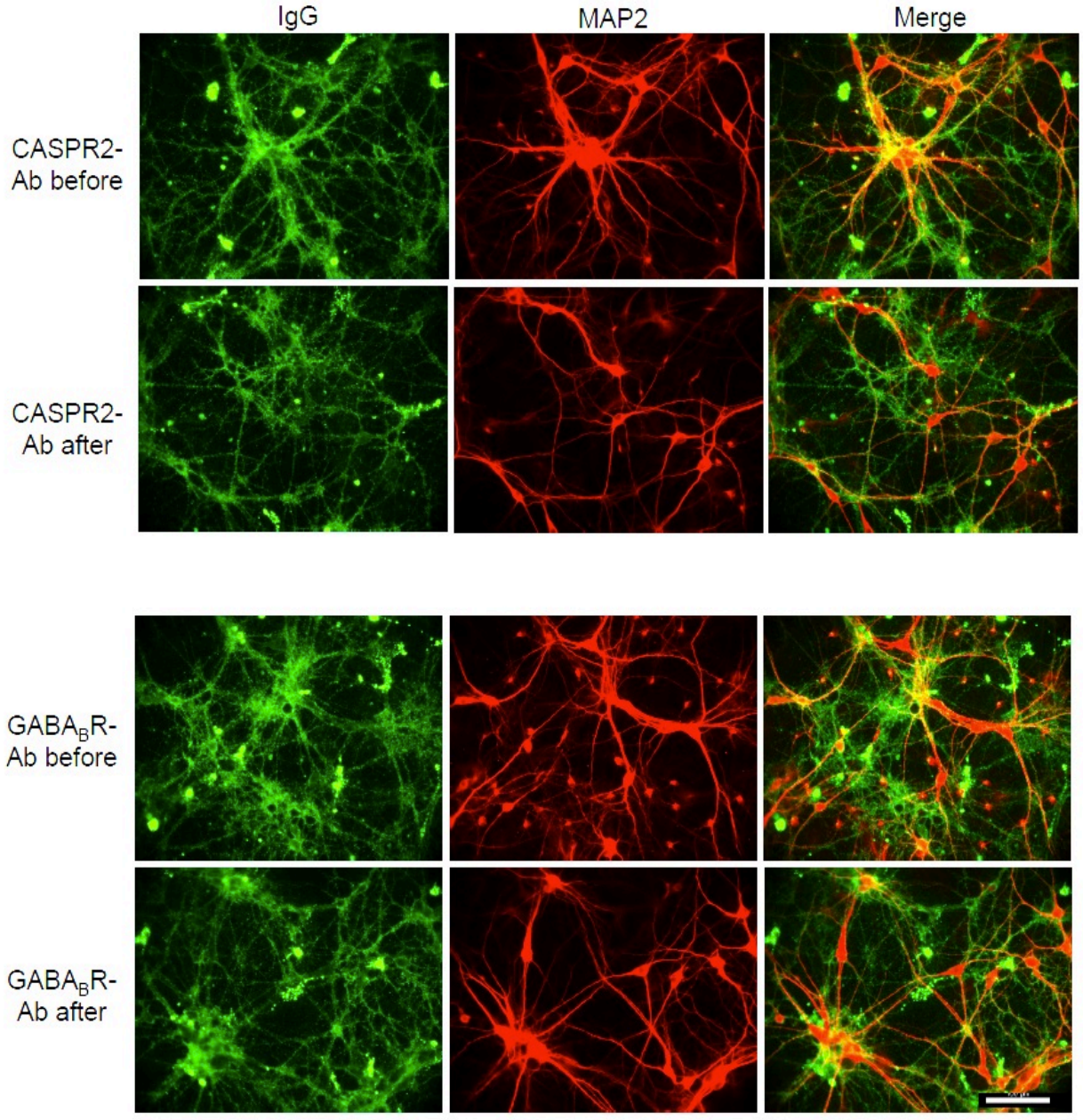

Figure 6.10: CASPR2 and GABA$_B$R antibody positive samples used for the establishment of a positive control "model system" show strong reactivity to primary neurons before and after incubation

Patients showed strong reactivity with neurons (Before). Following incubation with neurons (1:100), supernatants were removed and re-tested. Strong binding to cultures was still observed (After). These results confirm that saturating amount of patient antibodies were incubated with the neurons. Patient IgG detected using a secondary goat anti-human IgG Alexa Fluor 488 (green) Neurons were subsequently fixed, permeabilised and incubated with MAP2 (red). Images 400x magnification. Scale bar=100 µm.

6.3.4.3 Confirmation of successful immunoprecipitation via immunoblot detection

Immunoprecipitated material was loaded on 3-8% Tris-Acetate gel and transferred onto nitrocellulose membrane. Membranes were probed with antibodies specific for CASPR2 and $GABA_{B2}R$ (ab33394 and AB5394 respectively; see Appendix Table 2). Western blot analysis revealed the patient sera immunoprecipitated bands specific for CASPR2 and the $GABA_{B2}R$ subunit at the correct molecular weights (Figure 6.11A and B) indicative of successful immunoprecipitation using human sera. HC sera did not precipitate these bands. Preparing primary neuronal material for immunoprecipitation from cortical tissue is advantageous as a high number of neurons can be cultured. However, as a majority of the JEV samples bound strongly to hippocampal neurons only, the immunoprecipitation technique was also optimized in parallel using primary hippocampal neurons. These hippocampal cultures were incubated with JEV 4, a NMDAR antibody positive patient (see Table 6.1). Again, western blot analysis revealed that using this method, we were able to precipitate the NR1 subunit of the NMDAR (Figure 6.11C) confirming successful optimisation of the method using hippocampal cultures for western blot analysis.

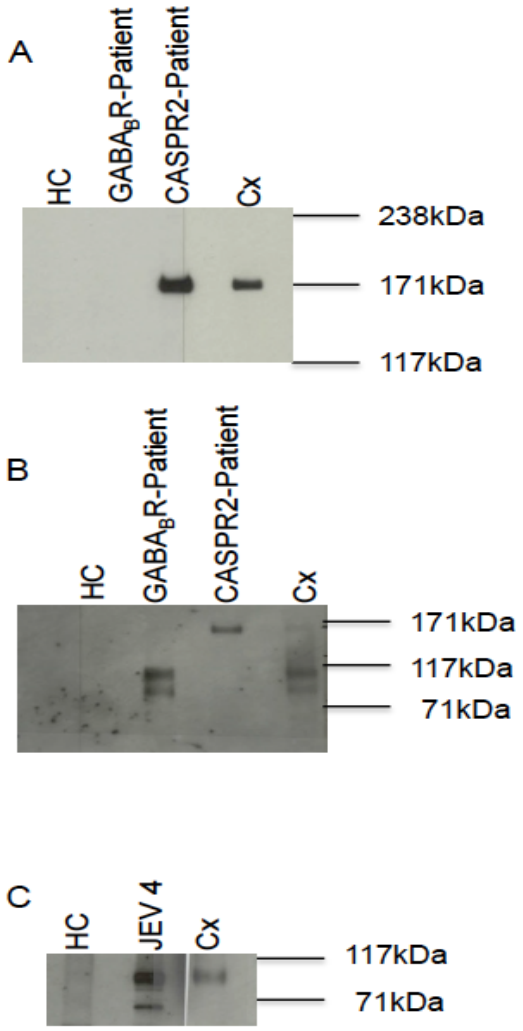

Figure 6.11: Western blot of the immunoprecipitated material from cortical and hippocampal neurons confirmed the presence of the CASPR2 (A), GABA$_{B2}$R (B) and the NR1 subunit of the NMDAR (C)

CASPR2 (165kDa) was detected in the CASPR2 patient fraction but not in the GABA$_B$R patient fraction when probed with a specific rabbit anti-CASPR2 antibody (1:500) (A). GABA$_{B2}$R (98kDa) was detected using a mouse anti-GABA$_{B2}$R commercial antibody (1:500) only in the GABA$_B$R patient fraction (B). Finally, the NR1 subunit was detected using an anti-NR1 antibody (1:200) in the NMDAR patient fraction at 105kDa (C). These proteins were not observed with the HC fractions. All fractions were loaded on Tris-Acetate 3-8% gels, and a HiMark ladder was used to detect protein size. Mouse cortex (Cx) was used as a positive loading control.

6.3.4.4 Preparation of positive controls samples for proteomics

Given that we successfully identified the known antigenic targets with western blot, we next sought to determine if the positive control samples could be identified using mass spectrometry. Samples were separated on a gel and Coomassie stain was used for protein visualization. Bands at the molecular weights specific for CASPR2 and $GABA_BR$ were not apparent in the respective gel lanes. In addition, the patient and HC lanes contained protein bands that were indistinguishable from one another (Figure 6.12). Although the Coomassie dye can detect as low as 9 ng of protein this may not being sensitive enough to detect low concentration of the immunoprecipitated antigens, even when the molecular weight is known. Furthermore, immunoprecipitation of a novel antigen target, where the molecular weight is unknown, could potentially be masked by other protein bands (numerous proteins of a similar molecular weight could be present in the sample and as such would appear as a single band). Nevertheless, identification of the antigens via mass spectrometry was attempted as previous experiments in our laboratory have resulted in successful antigen discovery even when a specific protein band is absent. Therefore the full gel lanes were digested in small pieces for mass spectrometry (Figure 6.12).

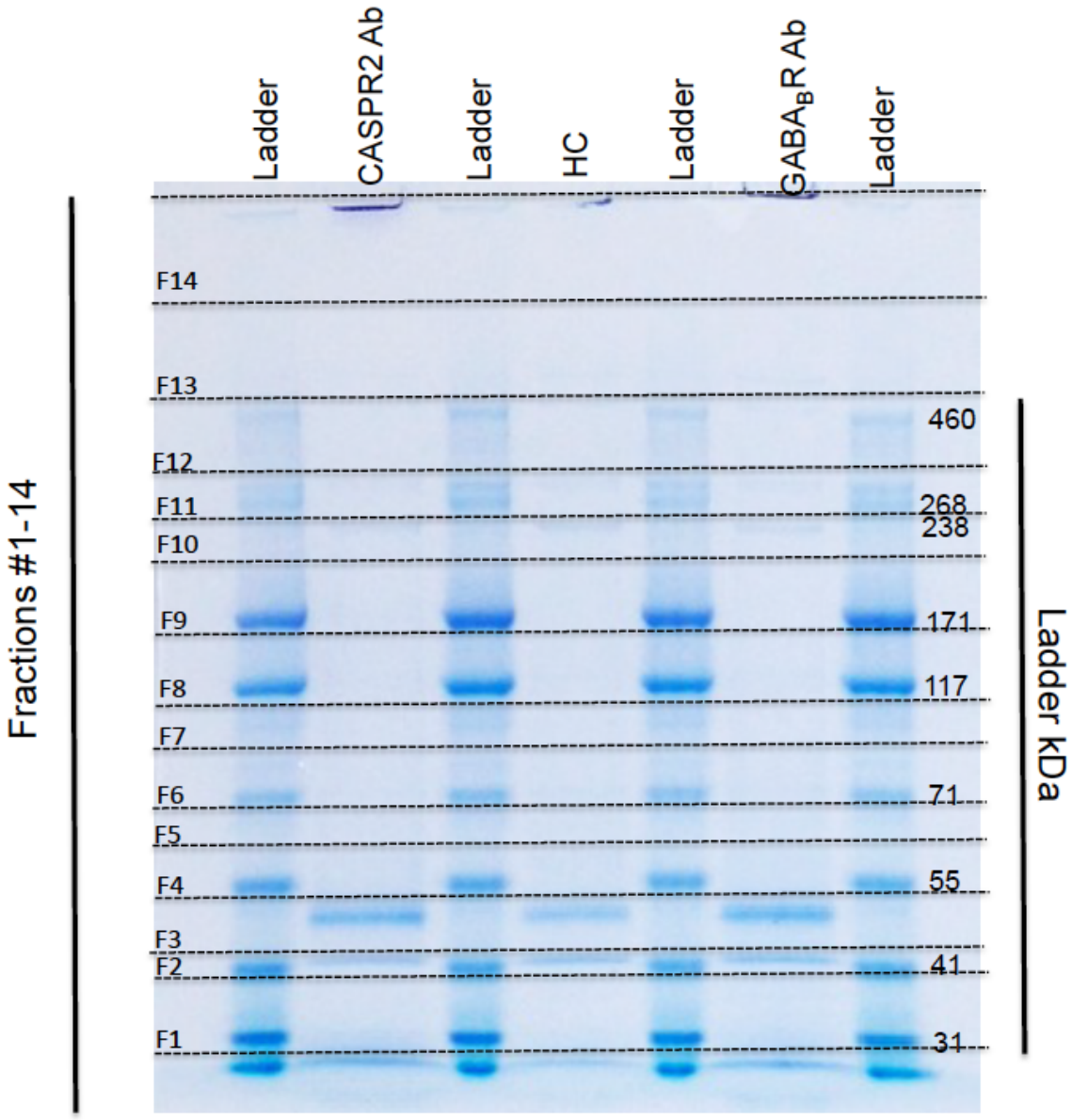

Figure 6.12: Fractionation of immunoprecipitates on Tris Acetate Gels: "model system"

Precipitate fractions from each patient sample were loaded on a 3-8% Tris-Acetate gel. A HiMark ladder was loaded next to every gel lane in order to visualize molecular weights and ease the cutting/digest process. Each lane was divided into 14 pieces (dashed lines). No apparent differences in protein bands were noted between the CASPR2 antibody and the GABA$_B$R antibody positive patients in comparison to each other or a HC when the gel was stained with Coomassie.

6.3.4.5: Mass spectrometry hits from positive control model system

As outlined in 2.12, Raw LC-MS/MS data were processed and Mascot compatible files, with the option to search taxonomies using the UniProt SwissProt database were generated. Both rat (as the neurons used in the immunoprecipitation were cultured from rat embryonic E18 pups) and a broader mammalia taxonomy searches were carried out. In addition, database searches performed using the Mascot algorithm (version 2.4) were able to compile hits based on merged files from the specific fraction (bands) that were cut. An overall "protein score" was generated, and could be used as an inclusion criterion for further analysis. The merged database yielded 127, 123 and 121 protein hits for the CASP2 antibody positive, $GABA_BR$ antibody positive, and HC patients, respectively. Despite the solubilisation steps only occurring after the patient serum was incubated with live primary cultures, the majority of the hits (e.g. 92% of the CASPR2 antibody immunoprecipitate) were intracellular proteins. However, this has been reported in other publications using a similar methodology (see Littleton *et al.,* 2009) and these proteins were subsequently excluded from analysis. In addition, known contaminants such as keratin, which were common to both patient and control fractions were also excluded.

Upon examination of files of the mammalian taxonomies, peptides corresponding to CASPR2 were detected in fraction 9, an area of the gel corresponding to the predicted molecular weight of CASPR2. The score was high (80) and upon examination of the peptides and a comparison of the CASPR2 protein sequence, 6% sequence coverage was noted (Figure 6.13).

However, upon examination of the $GABA_BR$ fractions, only the $GABA_{B1}R$ was identified, despite this patient having $GABA_{B2}R$ subunit specific antibodies. The peptides had a sequence identity of 2%. As the $GABA_{B1}R$ and $GABA_{B2}R$ subunits are generally expressed together *in vivo* as a heterodimer, the identification of $GABA_{B1}R$ is not

particularly surprising. It is possible that the detergent did not break the $GABA_BR$ complex, causing the $GABA_{B1}R$ to also be captured (Figure 6.14). The results highlight that fact that the mass spectrometry analysis system requires additional optimisation.

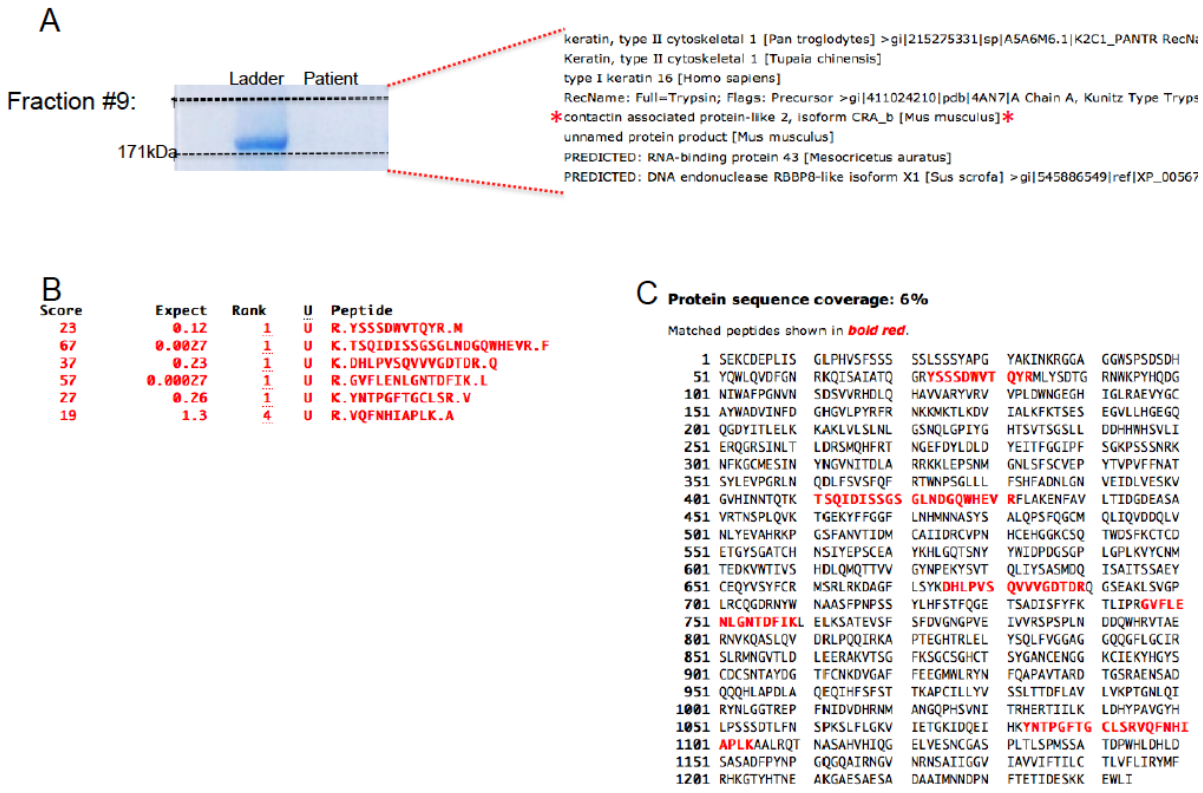

Figure 6.13: Protein hits when looking at individual fractions for the CASPR2 antibody positive immunoprecipitates obtained via mass spectrometry

Fraction #9 which corresponded to an area of the gel compatible with the molecular weight (165KDa) of the CASPR2 protein was analysed (cross referencing with a mammalian database). The top protein hits from this fraction are shown in (A). As can be seen, CASPR2 is present in the fraction. A list of the peptides sequences of the CASPR2 protein isolated from the patient (B). The peptide sequences corresponded to 6% of the protein coverage (Protein Score 80) (C).

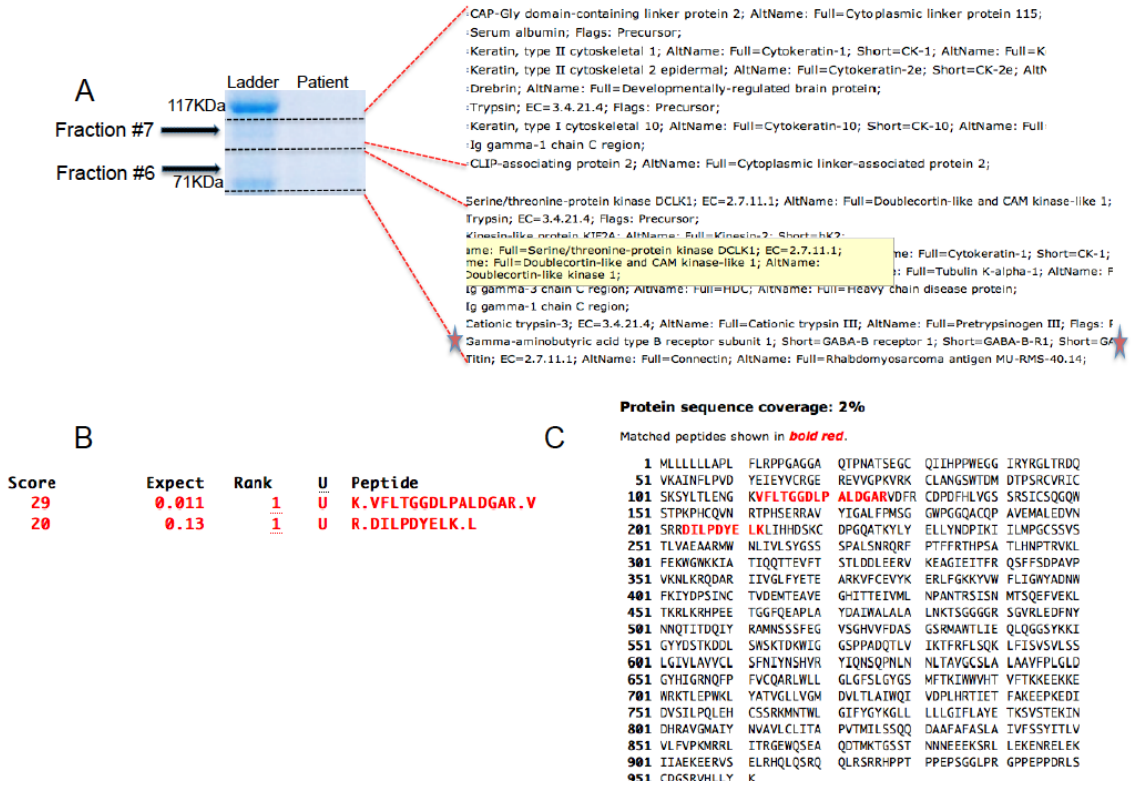

Figure 6.14: Protein hits when looking at individual fractions for the GABABR antibody positive immunoprecipitates obtained via mass spectrometry

$GABA_BR$ has a molecular weight of approximately 100 kDa. As such, two gel fractions (#6 and #7), which cover a molecular mass of 71kDa-117kDa were analysed. The top hits from this fraction are shown in (A). As can be seen, only the $GABA_{B1}R$ protein was identified in fraction #6. A list of the peptides sequences of the $GABA_{B1}R$ protein isolated from the patient as shown in (B). The peptide sequences corresponded to only 2% of the protein coverage (Protein Score 29) (C).

6.3.5: Novel antigen targets in JEV samples

As the protocol for known antigenic targets was at least partly successful we next sought to determine if unknown antigenic targets could be identified following immunoprecipitation by the JEV sera.

6.3.5.1: Antibody status of JEV patients selected for immunoprecipitation

Patients were selected for analysis based on their binding to primary hippocampal cultures. JEV 4 bound intensely to neurons (Figure 6.7), was antibody positive for anti-NMDAR (CBA score 2.5, 1:540) but negative on all other CBAs and the VGKC RIA. As such, JEV 4 acted as a good positive control as the antigen target was at least partially known. Furthermore, the presence of peptide sequences to NMDAR would act as a control for the adapted protocol for hippocampal neurons, with the possibility of additional antigen targets being detected as well. Patient JEV 12B also bound intensely to hippocampal neurons. Interestingly, this patient was the second follow up sample of JEV 12, a $GABA_AR$ positive, though JEV 12B was negative on the assay. The punctate but similar stain between the two (See Figure 6.7 and 6.9) suggests that there may have also been an additional antigen in JEV 12.

6.3.5.2: Mass spectrometry of antigen unknown JEV samples

The immunoprecipitation was completed with hippocampal neurons, where the binding to unknown antigens was strongest. However, the neurons were cultured in 6 well plates, as hippocampal neurons do not grow well on T175 cm^2 flask, which were used in the "model system". No apparent protein band differences were noted between the two samples following Coomassie stain (Figure 6.15). As was noted in the "model system", it was difficult to discern whether a specific band corresponding to the molecular weight of NMDAR was present in the JEV 4 sample gel lane. Again, this may

be a sensitivity issue of the Coomassie stain. Blank protein G-sepharose beads were boiled in SDS-Loading buffer with reducing agent and loaded as a negative control. No protein was detected in the lane with the blank protein G-sepharose beads. Following Coomassie stain, gel fractions, 14 in total, were made from each of the lanes, as outlined for the “model system”.

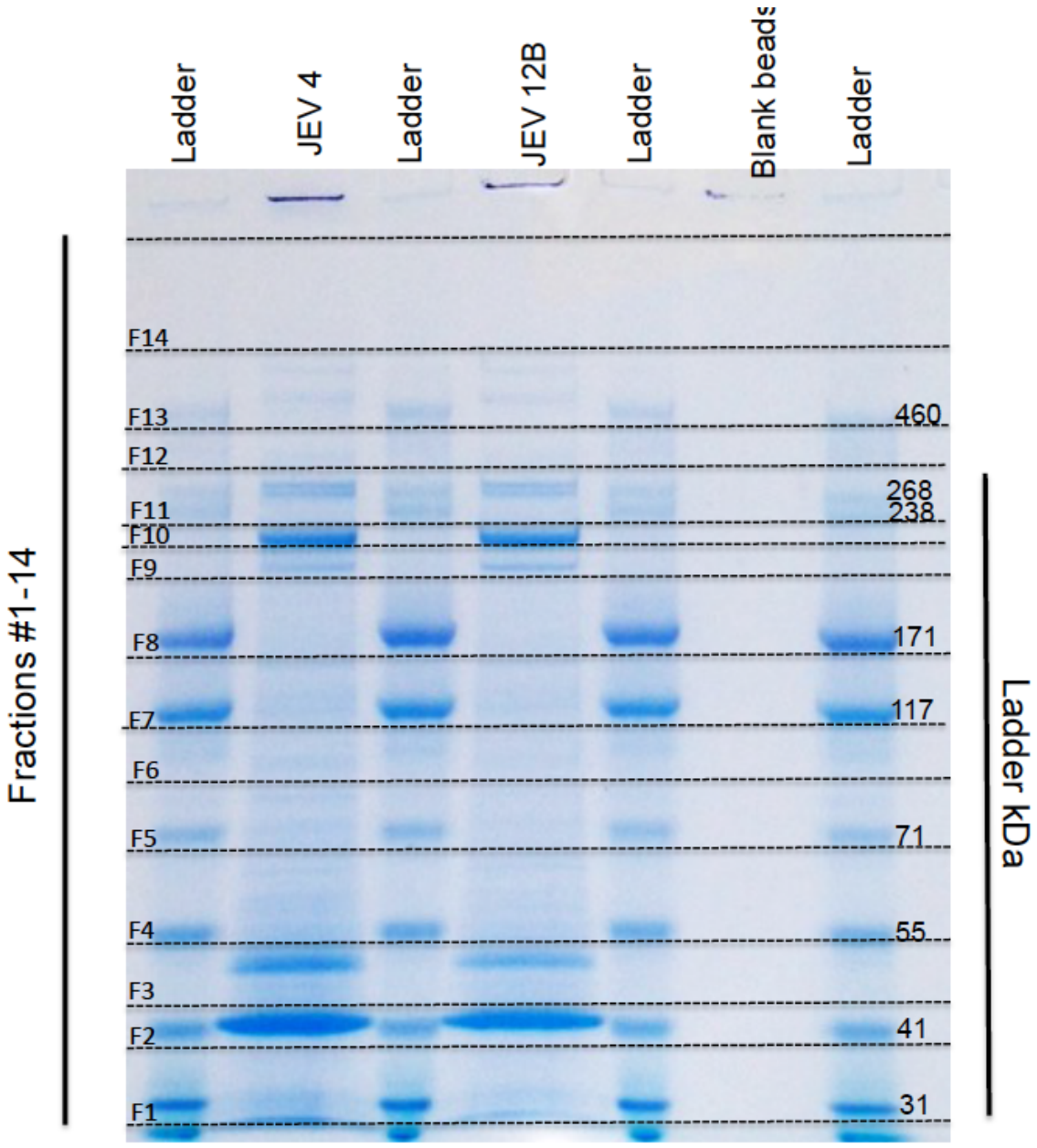

Figure 6.15: Fractionation of immunoprecipitates on Tris Acetate Gels: IP from JEV patient sera

Precipitate fractions from each patient sample were loaded on a 3-8% Tris-Acetate gel. A HiMark ladder was loaded next to every gel lane in order to visualize molecular weights and ease the cutting/digest process. Each lane was divided into 14 pieces (dashed lines). No apparent differences in protein bands were noted between the JEV patient samples. Blank beads were loaded as a negative control, and no protein was detected in this lane.

Disappointingly, the NMDAR was not identified by mass spectrometry despite this sample being positive on the NMDAR CBA and testing positive on the western blot when probed with an anti-NMDAR antibody (Figure 6.16). This finding raises the possibility that the protocol is not sufficiently sensitive. As such, whether or not to pick up specific proteins immunoprecipitated from a hippocampal preparation using mass spectrometry remains to be optimised.

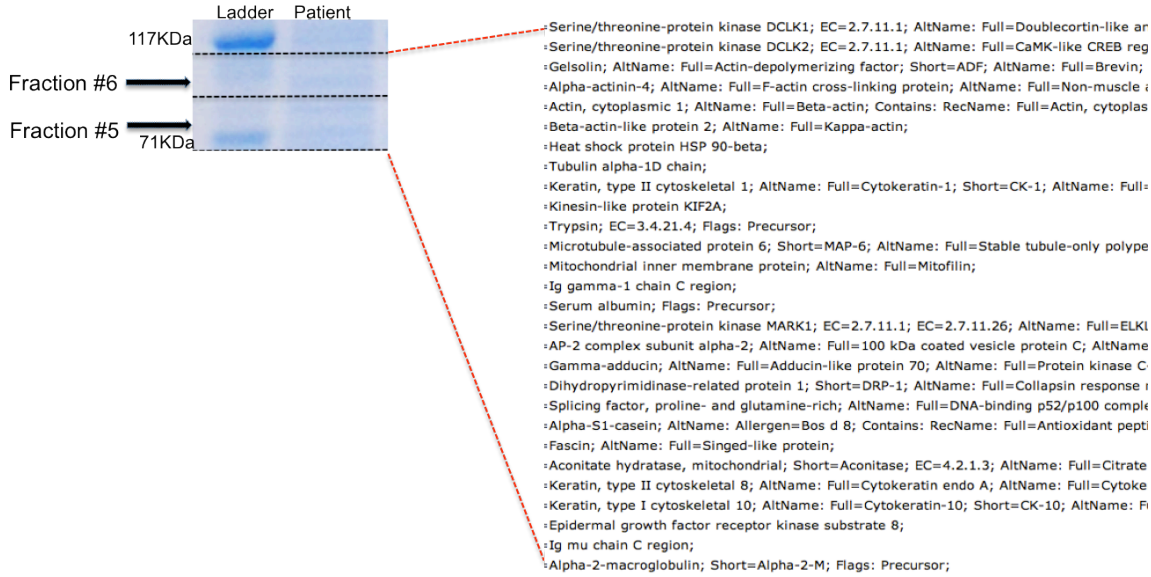

Figure 6.16: Mass Spectrometry hits when looking at individual fractions 5 and 6 for the JEV4 (NMDAR antibody positive) immunoprecipitate

NMDAR has a molecular weight of approximately 100kDa. As such, two gel fractions (#5 and #6), which cover a molecular mass of 71kDa-117kDa were analysed individually. The top protein hits from this fraction are shown. NMDAR subunits were not detected in these fractions.

The individual protein fractions for each of the patients, JEV 12B, JEV 4, and HC were all used as points of comparison. Similar protein targets in both JEV 12B and JEV 4 could be discerned and either rejected or analysed further based on whether or not the protein hit was also present in the HC files. Peptide hits from the "model system" files were also used to include or exclude proteins. After excluding intracellular proteins, four proteins of interest were identified (Table 6.4).

Table 6.4: List of proteins with extracellular regions, identified using mass spectrometry following immunoprecipitation of hippocampal neurons with JEV sera

Protein	Score	Description	Sequence coverage/ Protein size	Function
1	35	Plexin-A2	9% (1894)	• Important in axon guidance, invasive growth
2	32	Melatonin-related receptor	2% (617)	• Alters function of melatonin receptor subunits
3	28	Alpha-2-macroglobulin receptor-associated protein	3% (357)	• Binds LRP1
4	24	Teneurin-4	5% (2769)	• Important in establishing neuronal connectivity

JEV 12B

JEV 4

6.3.6: Potential antigen targets

In total, four neuronal proteins with extracellular regions, which were not present in the equivalent HC or model system fractions, were identified (1 from JEV 12B and 3 from JEV 4). Some proteins had a higher score, and a higher peptide sequence coverage than others (Table 6.4), making certain proteins a more likely antigen target (discussed in further detail below). Very little published material is available for some of the proteins. Brief details of each of the proteins are outlined below.

6.3.6.1: Plexin-A2

This protein is a member of the plexin-A family of semaphorin (Sema6a) co-receptors, which are secreted or membrane bound proteins that are important in axonal growth, migration and "path finding" during nervous system development. More recently, plexin-A2 has been implicated in cell migration of granule cells by controlling centrosome positioning (Renaud *et al.,* 2008).

Peptide hits from the JEV 12B immunoprecipitate corresponded to a 9 % sequence coverage of the plexin-A2 protein. The protein contains a 1203 amino acid large extracellular domain (63% of the protein), a single transmembrane domain and a 636 amino acid cytoplasmic C-terminal domain region. The extracellular domains of two plexin-A2 proteins and two Sema6a proteins interact extracellularly to form heterotetramers. The Sema6A/Plexin-A2 complex is important for signaling and the structure is shown in Figure 6.17A. The topological domain (derived from a transmembrane domain predictor) is shown in Figure 6.17B. The large extracellular domain of this protein makes it a probable target for circulating antibodies.

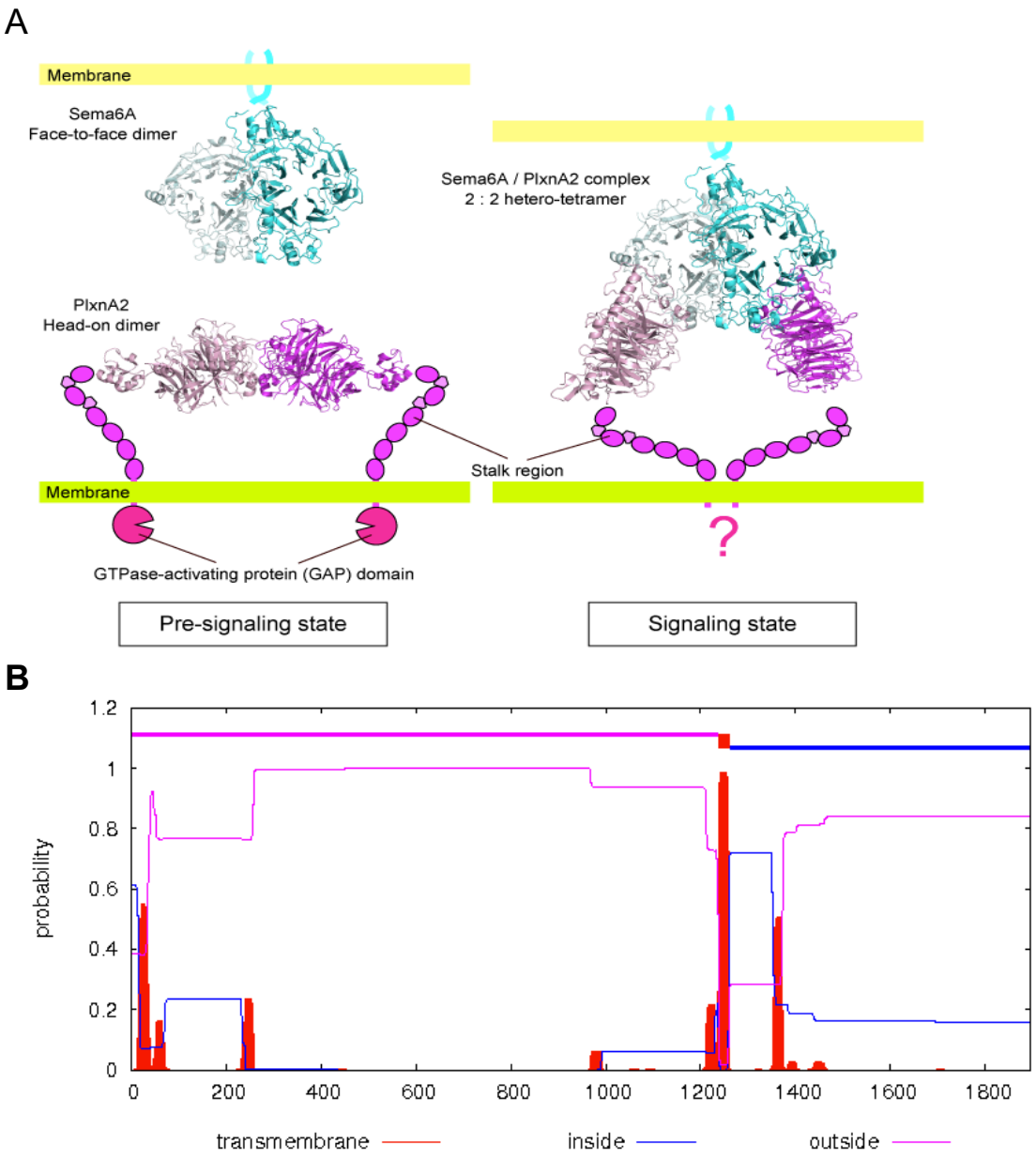

Figure 6.17: The structure of Plexin-A2

Plexin-A2 (PlxnA2) proteins form homodimers through interactions of their large amino terminal extracellular domain in the pre-signaling state. In the signaling state, the PlxnA2 homodimer interacts with a semaphorin (Sema6A) homodimer forming the Sema6A/ PlexnA2 complex, a 2:2 heterotetramer. Image from Protein Data Bank: 3A3al8 (A). Topological domains of the Plexin-A2 derived from a transmembrane domain predictor (TMHMM Server v. 2.0), showing a large amino terminal extracellular domain (pink), a single transmembrane domain (red), and an intracellular C-terminal domain (blue). Red bars indicate probability of a transmembrane domain present in that region of the sequence (with a probability of 1 indicating the presence of a TMD) (B).

6.3.6.2: Melatonin-related receptor

Despite its name, the melatonin-related receptors do not bind melatonin. Most reports show that this receptor is found predominately in the hypothalamus and pituitary, and less commonly in the hippocampus. Reports linking this receptor to neurological diseases have not been published. Mass spectroscopy of immunoprecipitates of hippocampal neuron proteins with JEV 4 serum resulted in peptide hits corresponding to 2% sequence coverage of the melatonin-related receptor. This G-coupled protein receptor is 617 amino acids in length and is cell membrane bound receptor. The topological domain (derived from a transmembrane domain predictor) is shown in Figure 6.18. In total there are 7 transmembrane domains. The extracellular regions comprise only 10.5% of the protein (65/617 amino acids). The relatively small extracellular region, and the low expression in the hippocampus make this protein a less likely target.

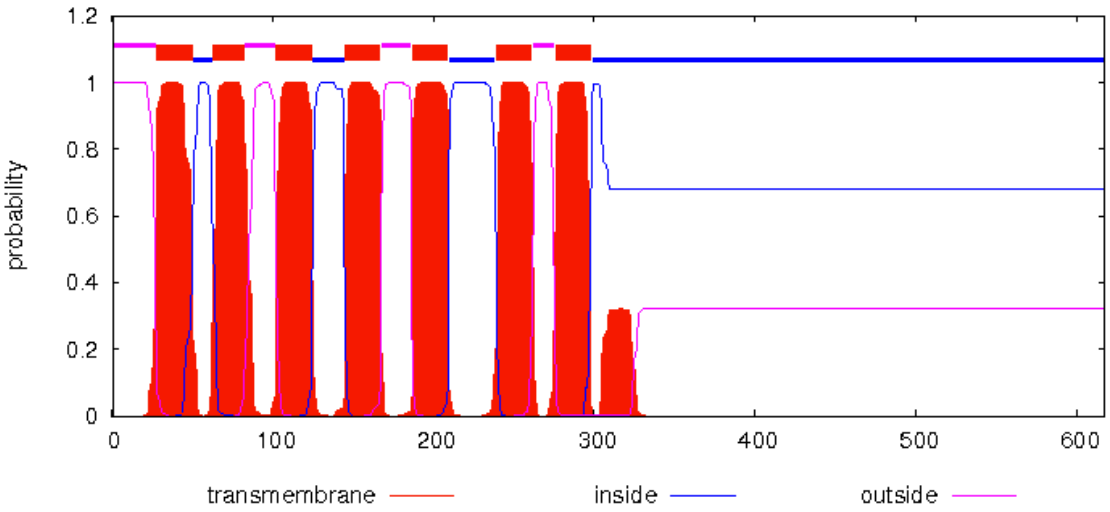

Figure 6.18: Predictor of intracellular, extracellular and transmembrane regions of the melatonin-related receptor protein

Topological domains of the melatonin-related receptor derived from a transmembrane domain predictor (TMHMM Server v. 2.0), showing very small extracellular regions (pink), seven transmembrane domains (red), and a large intracellular C-terminal domain (blue). Red bars indicate probability of a transmembrane domain (TMD) present in that region of the sequence (with a probability of 1 indicating the presence of a TMD).

6.3.6.3: Alpha-2-macroglobulin receptor-associated protein (alpha-2-MRAP)

Alpha-2-MRAP is a 367 amino acid protein, present on the cell surface and endoplasmic reticulum of cells. Very little is known about its function other than its interaction with low-density lipoprotein receptor related protein (LRP1), which is involved in a variety of cell membrane processes such as lipid homeostasis and clearance of apoptotic cells. Mutations of this gene have been implicated in a form of myopia (Aldahmesh *et al.,* 2013).

Peptide hits, which corresponded to 3% sequence coverage of the protein, were found in the JEV 4 immunoprecipitate. Following a very small intracellular amino terminal domain (only a few amino acids in length) is a single transmembrane domain. A majority of the protein (approximately 91%) is extracellularly located, again making this a good target for circulating antibodies (Figure 6.19).

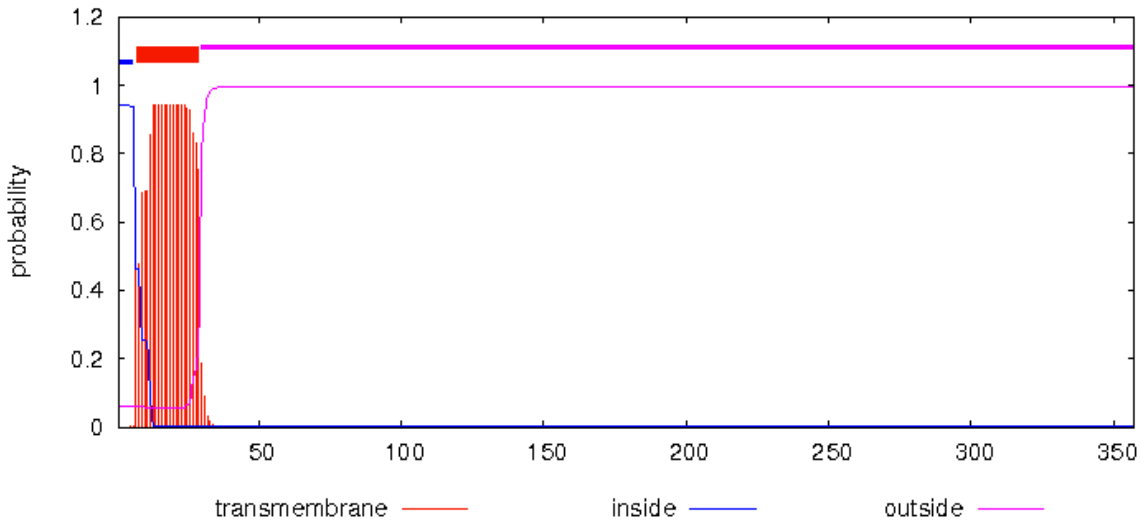

Figure 6.19: Predictor of intracellular, extracellular and transmembrane regions of Alpha-2-MRAP

Topological domains of Alpha-2-MRAP derived from a transmembrane domain predictor (TMHMM Server v. 2.0), showing a very small intracellular amino terminal domain (blue), followed by a single transmembrane domain (red), and a large extracellular C-terminal domain (pink). Red bars indicate probability of a transmembrane domain (TMD) present in that region of the sequence (with a probability of 1 indicating the presence of a TMD).

6.3.6.4: Teneurin-4

Teneurin-4 is highly expressed throughout the CNS and is involved in neural development and is critical for regulating the establishment of proper connectivity within the nervous system (Suzuki *et al.,* 2013). A transgene insertion in the Teneurin-1 gene (called *furue)* in mice results in the absence of Teneurin-4 expression, and lack of myelination of small diameter axons and oligodendocyte differentiation in P6 pups (Suzuki *et al.,* 2012). Interestingly, because of hypomyelination, these *furue* mice present with tremor, a symptom often noted in JEV patients (Solomon *et al.,* 1998).

Peptide hits, which corresponded to 5% sequence coverage of the protein, were found in the JEV 4 immunoprecipitate. Teneruin-4 is 2769 amino acids in length and exists at the cell surface as a homodimer. The amino terminal of the domain is cytoplasmically located and constitutes approximately 366 amino acids. Following a singly transmembrane domain is a very large 2402 amino acid extracellular region (Figure 6.20).

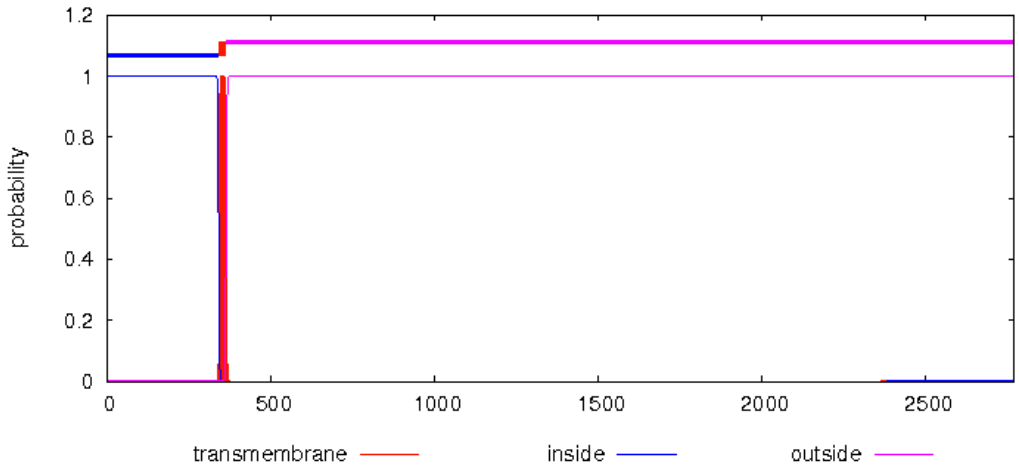

Figure 6.20: Predictor of intracellular, extracellular and transmembrane regions of Teneurin-4

Topological domains of Teneurin-4 derived from a transmembrane domain predictor (TMHMM Server v. 2.0), showing a very small intracellular amino terminal domain (blue), followed by a single transmembrane domain (red), and a large extracellular C-terminal domain (pink). Red bars indicate probability of a transmembrane domain (TMD) present in that region of the sequence (with a probability of 1 indicating the presence of a TMD).

6.4 Summary and Discussion

6.4.1 Viral encephalitis and autoimmune mediated encephalitis

Autoimmune neurological conditions with antibodies directed against neuronal surface proteins comprise an expanding group of CNS diseases. The identification of the antigenic target in a group of patients with clinical defined symptoms is important in understanding the relevance and pathogenic potential of these antibodies. Many of these diseases have a prodromal period whereby symptoms such as headache, and fever are common and suggestive of a viral infection. Pradhan *et al.* (1996) reported 6 patients with JE that presented with fever, headaches, rigidity and tremors during the first phase of the illness, and after a partial recovery relapsed and went on to develop behavioral changes, dystonia, mutism and muscle wasting. The aim of this chapter was to analyse whether JE could have an autoimmune mediated component using a variety of *in vitro* techniques.

6.4.2: Antibodies in JEV

This biphasic illness pattern of JE is similar to the HSE relapse some patients experience, and it is possible that neurological symptoms seen in JE patients are the result of an autoimmune attack. Initially, the JEV sera were tested for known antibodies using standard techniques. In total 19/44 patients were positive on either the CBA (NMDAR 5, LGI1 2, CASPR2 4, $GABA_AR$ 1), or VGKC RIA (additional 7 patients). None of the samples showed reactivity to the AMPAR or $GABA_BR$ transfected cells.

Previously it has been reported that an increase in T-lymphocyte numbers and IgM antibodies are noted early on in the disease course. Testing for IgM antibodies in JE patient sera and CSF via ELISA is the most commonly used diagnostic tool (Ravi *et al.,* 2008). As such, the positive samples were tested for IgM antibodies against their respective targets and with the exception of the $GABA_AR$ antibody patient, the samples

were negative. Clinically, the patients with antibodies to a known antigen did not differ from patients that did not have a known antibody. One explanation for this finding was that the antibodies are secondary to infection and are themselves not directly pathogenic. The lack of significant clinical differences between antibody positive and antibody negative viral encephalitis patients has also been noted by Pruss *et al.* (2012) in his study of HSV infected patients, though he showed that NMDAR IgM antibodies were pathogenic and were able to cause internalisation. However, as many patients were not followed up, or a detailed clinical report was not available, a more thorough clinical analysis is required before conclusions can be drawn regarding antibody pathogenicity in different patient subgroups. Clinicians in this study did not note a biphasic illness in any of these patients. Furthermore, unlike HSE patients, whereby antibodies were not detected in HSV positive samples taken at onset (Armangue *et al.,* 2014), we noted the presence of antibodies to neuronal surface proteins in some patient samples taken at onset. Unfortunately, as JEV titres for serial samples were unavailable, we were unable to explore the link between JEV titres and neuron immunoreactivity.

6.4.3: Presence of novel targets in JEV sera

Armangue *et al.* (2014) reported 9 patients that showed reactivity to hippocampal neurons but were not positive for antibodies to any currently known antigen. In our study, 7 patients with positive VGKC RIA titres were negative on the CBA to CASPR2 and LGI1, thus suggesting the sera is binding to an additional unknown antibody targets associated with the VGKC complex. As such, all samples were screened on primary neuronal cultures. Furthermore, this study has also demonstrated that a majority (65.9%) of the JEV children bound to neurons, suggesting additional antibodies may be present in these patients. Interestingly, CSF from these patients (including two samples that were paired with the antibody positive sera) did not bind. It is possible that the

CSFs were taken too close to onset of the disease, and antibodies synthesized peripherally due to molecular mimicry have not gained access to the CNS. Alternatively, the CSF antibodies may be too low to detect via hippocampal screening.

6.4.4: Preliminary investigations identifying a novel target

It is advantageous to know what the antigen target is, to better understand the potential pathogenic mechanism of action. A number of antigen targets have been discovered using proteomic methods such as, AMPAR, $GABA_BR$, LGI1, and more recently DPPX and $GABA_AR$ (Lai *et al*., 2009, Lancaster *et al.,* 2010, Boronat *et al.,* 2013 and Petit-Pedrol *et al*., 2014). All of these protein targets were identified using hippocampal neurons as starting material, though depending on the volume of material available CSF (1:10-1:15) or sera (1:500) were used.

A "model system" involving the identification of antigen targets from patients with known antibodies was carried out prior to the search for novel targets, using CASPR2 and $GABA_{B2}R$ patients. The protein stain Coomassie, was not sensitive enough to distinguish protein bands between control and test immunoprecipitates. However, using immunoblotting and mass-spectrometry analysis of digested protein bands, both the CASPR2 and $GABA_BR$ proteins were identified.

The immunoprecipitation of JEV samples was carried out using an antibody unknown JEV sample (JEV 12B), and a NMDAR antibody positive suspected JEV sample (JEV 4). Both sera bound strongly to the surface of hippocampal neurons, and the immunoprecipitation was carried out using these cultures. Immunoblotting of the precipitated material revealed that the NR1 subunit was present in the sample. Disappointingly the NR1 subunit of the NMDAR in the JEV 4 immunoprecipitates was not identified by mass spectrometry analysis. Taken together, these findings suggest that although the NMDAR was present in the immunoprecipitate confirmed with western

blot analysis, the analysis step using the mass-spectrometry system may not be optimised or sensitive enough to pick up surface expressed antigen targets from hippocampal neuronal cultures.

However, four novel extracellular proteins present in the CNS were identified from the two JEV samples, each with varying protein sequence coverage and protein score. While there may be more than one antigen target in this disease, many of the sera showed a staining pattern similar to one another. Despite this, the same extracellular proteins were not identified in each precipitate independently. The protein sequences that were identified were located on the intracellular and extracellular regions of the proteins in question. Plexin-A2 is a likely target as it has a very large extracellular domain (approximately 1200 amino acids), had the highest sequence coverage (9%) and protein score (35) from the mass spectrometry hits. However, each of these proteins should be explored in more detail. In addition, comparisons between the protein hits and JEV sequence should be investigated to characterise if there is any cross reactivity between the targets, which would be indicative of molecular mimicry. While numerous intracellular proteins were picked up using this method, few extracellular proteins were detected and should be tested via CBA before being excluded as an artifact.

6.4.5: Limitations and future experiments

More detailed clinical data is required to fully understand the disease and the role both viral and autoimmune components play. The following questions need to be addressed for a better understanding of the disease:

1). What were the JEV titres at the time the samples were collected? Were these different between follow up samples taken from the same patient?

2). Do the JEV and antibody titres to known antigenic targets correlate, and is there any relationship to response to treatment?

3). Do the JEV antibody titres correlate to patients with positive neuronal immunoreactivity and is there any relationship to the treatment regime used in these patients?

The status of the 9 suspected JEV or DC patients remains unknown, as few clinical details were available from these patients. As such, the lack of a greater number of control viral samples (patients with a confirmed virus that is not JEV) is a major limitation to the study. In the future more control viral samples need to be screened on neurons, and the percentage of positive samples compared to the JEV cohort.

There are also a variety of issues that need to be explored in greater detail for future antigen searching experiments. First, the presence of intracellular proteins in both control and test patient immunoprecipitates needs to be explored further. Antibodies to many of these intracellular proteins have been implicated in a variety of diseases. Actin and heat shock protein antibodies have been suggested as autoantigens in patients with chronic hepatitis (Fukuda *et al.,* 2004), and tubulin antibodies have been suggested to play a role in relapsing polychondritis, a systemic inflammatory disease (Tanaka *et al.,* 2006). However, as these proteins were also present in the immunoprecipitation from sera from HC patients, it is unlikely that they play a role in the disease. In addition, their localisation makes them and unlikely target as the antigen target must be extracellular expressed in order for antibodies to mediate pathogenic effects. The presence of intracellular components in immunoprecipitates that involved the capture of surface expressed proteins prior to precipitation has been described (Littleton, *et al* 2009). It is possible that the integrity of the neurons is compromised during the incubation or solubilisation steps, and as a result intracellular proteins nonspecifically bind. The use of stronger detergents (higher percentage of digitonin or Triton) also needs to be investigated in greater detail. However, this needs to be carefully optimised as it is

possible that solubilisation with a stronger detergent may break up complexes that could be important in the identification of the autoantigen.

Finally, the mass spectrometry analysis of protein hits needs to be optimised. While we showed that NMDAR was present in the immunoprecipitation fractions, these were not identified in the analysis.

The detection of four possible antigenic targets needs to be investigated. Other patients with similar staining patterns to neurons should be used in future immunoprecipitation and mass spectrometry experiments to attempt to reproduce the results. The binding of commercial antibodies to the four target proteins on neurons should be studied. If these studies can reproduce the findings in any of the four cases, then the DNA of that protein could be cloned and inserted into a vector to transfect cell lines and a CBA could be developed. The detection of pathogenic autoantibodies in the sera and CSF of patients with infectious encephalitis would not only gives us vital information of how the disease evolves, but also gives the clinician a therapeutic window of opportunity in which to alleviate and diminish the progression of the disease.

6.4.6: Conclusions

In conclusion, 65.9% of children with JEV had antibodies to known and novel antigen targets, strongly indicating an autoimmune component in this disease. A number of possible antigen targets exist and need to be explored further. These experiments provide further evidence that viral infection could be a likely trigger for the development of autoantibodies.

Chapter 7: General discussion

7.1: Introduction

Autoimmune neurological conditions with antibodies directed against neuronal surface proteins were first recognised in the PNS, where disorders such as MG and LEMS were identified as antibody-mediated and the pathological mechanisms established (Buckley, 2008). In the last few years autoantibodies directed against proteins expressed in the brain and spinal cord have been identified in a number of neurological disorders including various forms of encephalopathy, and in some patients with seizures or psychiatric disorders. These disorders comprise an expanding group of CNS diseases. The identification of the antigenic target in a group of patients with clinical defined symptoms is important in understanding the relevance and pathogenic potential of these antibodies.

7.2: Section 1 general discussion

AMPAR and $GABA_BR$ antibodies have been described in patients, of which a majority are diagnosed with LE. During the preparation of this thesis only 12 AMPAR antibody and 32 $GABA_BR$ antibody patients had been described. *In vitro* studies have shown that AMPAR antibodies cause a reversible reduction of the surface expression of AMPAR when AMPAR IgG is incubated with cultured live hippocampal neurons for 6 days (Lai *et al.,* 2009). The potential pathogenic effects of $GABA_BR$ antibodies however, have not previously been described, although others have suggested that receptor internalisation is not the pathogenic mechanism (Lancaster *et al.,* 2010). In the first part of this thesis we developed a cell-based assay for the detection of antibodies to both the AMPAR and $GABA_BR$ and used this to study the prevalence of these autoantibodies in

samples sent for diagnostic testing and various clinically defined cohorts. Once patients with these autoantibodies were identified, the pathogenic effects of AMPAR antibodies were validated and the potential pathogenic mechanisms of $GABA_BR$ antibodies were explored.

Antibodies to the AMPAR were first tested in a cohort of RE patients. Interestingly, antibodies to a conformational epitope present when the GluA2 and GluA3 subunits are co-expressed were identified in 2/63 patients with RE. These patients did not clinically differ from those patients without these antibodies, though the presence of antibodies to an unknown antigen target in 8 additional patients, suggests that a subset of RE patients have an autoimmune component. It remains unknown whether or not these antibodies are pathogenic and contributing to the disease, or whether they are developed in response to T-cell mediated neuronal damage. Due to limited sera availability, the novel antigen target(s) could not be identified, and the pathogenic potential of these antibodies could not be evaluated.

Using the newly established AMPAR and $GABA_BR$ CBAs, 13/1298 (1%) patients with AMPAR antibodies, and 14/964 (1.45%) patients with $GABA_BR$ antibodies were identified from diagnostic testing. Ten $GABA_BR$ antibody patients were also identified in a cohort 4.2% of SCLC patients. Patients in both groups presented with symptoms not limited to LE. We found that the patients with higher titres appeared to have symptoms more typical of LE, and the expanded spectrum was observed mostly in patients with lower antibody titres. This phenomenon has also been noted in patients with low $GABA_AR$ antibodies in the serum (Petit-Pedrol *et al*., 2013). Whereas the high titre patients had LE and were identified using at least 3 methods of detection (CBA, primary cultures and IHC), low titre patients (<1:160) were all positive on the CBA, but not all bound to sections or neurons. As such, whether or not these low level antibodies are sufficient to account for the clinical symptoms noted in these patients, needs to be

explored more thoroughly. Follow up samples may reveal whether or not these low antibody titre patients go on to develop higher antibody levels and by extension symptoms more typical with LE, highlighting the importance of collecting longitudinal samples.

Consistent with previous reports, we were able to demonstrate that AMPAR antibodies cause a reduction of surface AMPAR levels *in vitro*. While the direct effects of AMPAR were not shown in this thesis, a recent study by Gleichman *et al*. (2014) showed that following incubation of cultured cortical neurons with AMPAR antibodies for one day mEPSP were reduced, suggesting that AMPAR levels were down regulated during the incubation and excitatory transmission is therefore disrupted. However, whether or not AMPAR can mediate direct short-term effects needs to be explored in greater detail.

The fact that like AMPAR antibodies, $GABA_BR$ antibodies are also predominately of the IgG1 subclass, it is puzzling how these antibodies do not appear to be acting through the same pathological mechanisms as other IgG1 antibodies such as AChR, NMDAR, LGI1, and CASPR2, whereby internalisation and complement activation are documented. The antigenic epitope region needs to be investigated to determine whether or not spatial stoichiometry prevents these antibodies from cross-linking clustered antigens. Nevertheless, investigating the short-term direct effects of these antibodies, we found that application of IgG from a $GABA_{B2}R$ antibody positive patient on brain slices resulted in a reduction of the time that cortical neurons of the EC spent in an active Up state. In addition, spike rate was reduced, suggesting these antibodies are having a direct hypoexcitable agonist-like effect. Future investigations of the effects of $GABA_{B1}R$ antibodies on cortical networking are required to determine whether or not antibodies directed against different $GABA_BR$ subunits behave differently. Furthermore, the specific effects of these antibodies on the pre- or post-synapse as well as on select subgroups of excitatory and inhibitory neurons needs to be explored in greater detail. It

is likely that the shortening of the Up state duration is due to increased recruitment of post-synaptic potassium inward rectifying channels (Mann *et al*., 2009). However, these antibodies may also be mediating their effects through pre-synaptic VGCC. As the mechanism of action of different $GABA_BR$ agonists and antagonists has shown to be diverse (Mott *et al.,* 1989 and Ault *et al*., 1983), the widespread distribution of $GABA_BRs$ leaves ample room for speculation of the actual effects seen in the whole brain, and as such, the downstream effects of $GABA_BR$ antibodies needs to be carefully explored. However, an increased hypoexcitable effect on both GABAergic and glutamatergic synapses can explain the encephalopathy noted in the specific patient used in our study.

As seizures and cognitive impairment are common features associated with AMPAR and $GABA_BR$ mediated LE, in the future, passive transfer experiments should be conducted. In these experiments, ICV injections using purified AMPAR or $GABA_BR$ IgG could be carried out. The development of seizures (analysed using EEG telemetry) and performance on behavioural tasks could be compared to mice injected with HC IgG. To investigate how peripherally produced antibodies gain access to the CNS, antibodies should be injected intraperitoneally into mice. Following this initial injection, mice could be given lipopolysaccharide, which induces a neuroinflammatory response, disrupting the intact BBB, and allowing antibodies to gain access to the CNS (Banks and Robinson, 2010).

7.3 Section 2 general discussion

The expression of neuronal surface antigens on the surface of tumor cells has been well described (Benetar *et al.,* 2001, Dalmau *et al*., 2007, Lai *et a*l., 2009, Lancaster *et a*l., 2010) and this expression is known to elicit an immune response and the development of autoantibodies in some cases. Perhaps the most convincing description of this is the association of LEMS with SCLC (Titulaer *et al*., 2011, 2013).

However, in the absence of a tumor, what triggers autoantibody production remains unknown. This is not to say that autoimmune disorders develop due to one factor. Indeed, the “mosaic of autoimmunity” is caused by a combination of immunologic, environmental, hormonal and genetic factors. It has been postulated that the cumulative effect of a “burden of infections” can cause autoimmunity, and the mechanisms of antibody development, namely molecular mimicry and polyclonal antibody development due to neuronal lysis can be a contributing factor to the development of autoimmune diseases (Kivity *et al.,* 2009).

A number of groups have reported the development of autoantibodies to CNS antigens following viral infection or HSE relapse (Pruss *et al.,* 2012, Hacohen *et al.,* 2013, Armangue *et al.,* 2014). In this thesis we attempted to study this in greater detail by investigating autoantibodies in a JEV cohort.

Forty-four patients were assessed and 27% of patients had antibodies to known neuronal surface proteins during some point in their disease. Furthermore, sera from approximately two thirds of the JEV patients had the capability to bind hippocampal neurons. These findings reinforce the putative role of an autoimmune mediated component at some stage of the disease. These results also strongly indicate the presence of antibodies to novel antigen targets in the sera of some patients with JEV. The identification of unknown antigen targets was attempted from a seronegative JEV patient, and from a disease control that had NMDAR antibodies. Despite clear limitations with the immunoprecipitation and mass spectrometry techniques, a total of 4 potential targets were identified. Molecular biological techniques including cloning of these proteins and the subsequent expression in human cell lines in order to carry out a CBA would be required to validate these protein hits as potential targets in this cohort. All CSFs were negative, suggesting these antibodies are not intrathecally produced, or that at the time of CSF collection, the antibodies that are peripherally produced have not yet

gained access to the CNS. It is possible that the detection system may not be sensitive enough to detect the antibodies under these conditions and/or low levels of antibodies may quickly be sequestered onto their target antigens, taking them out of CSF circulation and rendering them undetectable.

The pathogenic effect of IgM NMDAR antibodies from patients post HSE has been described (Pruss *et a*l., 2012). Future studies investigating the pathogenic effects using *in vitro* experiments as described in section 1 of this thesis should be carried out to determine whether antibodies in JEV patients are causing the disease, or are markers of neuronal damage.

Autoantibodies to neuronal proteins in JEV have not been previously described. The results shown in this thesis, along with those in the literature that have looked at other viral infections, show that known and novel antigen targets are present in diseases that develop following infection.

7.4: Global questions and conclusion

While the diagnostic relevance and pathogenic role of antibodies directed against neuronal surface proteins are becoming increasing recognised in a variety of CNS disorders, there are many areas that need to be explored further. More global questions pertaining to specific areas include:

1). Antibody production:

What triggers antibody production in patients without tumours? Are infections (viral, bacterial, parasites and fungi) one such trigger? As infections are common, what additional factors (genetic, environmental, hormonal etc.) determine whether patients are

susceptible to autoantibody development and by extension disease? How common are these antibodies in patients with viral infection but no neurological symptoms?

2). Antibody access to the CNS:

How and where do these antibodies gain access to the CNS? Is a primary insult to the BBB (infection/trauma/stress) necessary for autoantibodies to gain access the CNS? Is disruption of the BBB region specific?

3). Antibody titres:

While many of these autoantigens are ubiquitously expressed, why is it that high antibody titre patients have clinical features associated with specific areas of the brain, and lower titre patients have a more expanded phenotype? Are low-titre antibodies clinically meaningful?

4). Possible treatment regimes:

Should high and low antibody titre patients be treated similarly? How relevant are low-antibody titres when deciding on a treatment course?

The discovery of these autoantibodies has allowed us to diagnose and treat patients, which was not previously available. Although there is still much to discover in these diverse conditions, defining which patients have an autoimmune component to their disease will in the longer-term aid the treatment, diagnosis and classification of these disorders and result in a greater benefit to these patients.

References:

Angus-Leppan H, Rudge P, Mead S, et al. Autoantibodies in sporadic Creutzfeldt-Jakob disease. JAMA neurology 2013; 70(7):919-22

Aldahmesh MA, Alshammari MJ, Khan AO, et al. The syndrome of microcornea, myopic chorioretinal atrophy, and telecanthus (MMCAT) is caused by mutations in ADAMTS18. Hum Mutat 2013; 34(9):1195-9

Alvarez-Baron E, Bien CG, Schramm J, et al. Autoantibodies to Munc18, cerebral plasma cells and B-lymphocytes in Rasmussen encephalitis. Epilepsy Res 2008; 80:93–97

Anggono V, Hunganir RL. Regulation of AMPA receptor trafficking and synaptic plasticity. Curr Opin Neurol 2012; 22(3):461-469

Antozzi C, Granata T, Aurisano N, et al. Long-term selective IgG immuno-adsorption improves Rasmussen's encephalitis. Neurology 1998; 51: 302–05

Armangue T, Leypoldt F, Malaga I, et al. Herpes simplex virus encephalitis is a trigger of brain autoimmunity. Ann Neurol 2014; 75:317–323.

Armangue T, Leypoldt F, Dalmau J. Autoimmune encephalitis as differential diagnosis of infectious encephalitis. Curr Opin Neurol 2014; 27(3):361-8

Ault B, Nadler JV. Anticonvulsant-like actions of baclofen in the rat hippocampal slice. Br. J. Pharmacol 1983; 78:701-708

Balint B, Jaruys S, Nagel S, et al. Progressive encephalomyelitis with rigidity and myoclonus: a new variant with DPPX antibodies. Neurology 2014; 82(17): 1521-1528

Banks WA, Robinson SM. Minimal penentration of lipopolysaccharide across the murine blood-brain barrier. Brain, Behav Immun. 2010; 24(1):102-109

Bataller L, Galiano R, Garcia-Escrig M. Reversible paraneoplastic limbic encephalitis associated with antibodies to the AMPA receptor. Neurology 2010; 74(3):265-267

Bauer J, Elger CE, Hans VH, et al. Astrocytes are a specific immunological target in Rasmussen's encephalitis. Ann Neurol 2007;62:67–80

Benarroch EE. $GABA_B$ receptors: Structure, functions, and clinical implications. Neurology 2012;78:578-584

Benarroch EE. ADAM proteins, their ligands and clinical implications. Neurology 2012;78:914-920

Benchenane K, Castel H, Boulouard M, et al. Anti-nr1 n-terminal-domain vaccination unmasks the crucial action of tpa on nmda-receptor mediated toxicity and spatial memory. J Cell Sci 2007;120(Pt 4):578-585

Benetar M, Blaes F, Johnston I, et al. Presynaptic neuronal antigens expressed by a small cell lung carcinoma cell line. J Neuroimmunol 2001;113(1):153-162

Berman P W, Patrick J. Experimental myasthenia gravis: a murine system. J Exp Med 1980;151(1):204-223.

Beyer B, Deleuze C, Letts VA, et al. Absence seizures in C3H/HeJ and knockout mice caused by mutation of the AMPA receptor subunit Gria4. Hum Mol Genet 2008; 17(12):1738-1749

Bien CG, Bauer J, Deckwerth TL, et al. Destruction of neurons by cytotoxic T cells: a new pathogenic mechanism in Rasmussen's encephalitis. Ann Neurol 2002;51:311–318

Bien CG, Granata T, Antozzi JH, et al. Pathogenesis, diagnosis and treatment of Rasmussen encephalitis. Brain 2005; 128:454-471

Bien CG, Vincent A, Barnett MH, et al. Immunopathology of autoantibody-associated encephalitides: clues for pathogenesis. Brain 2012; 135:1622-1638

Bien CG, Tiemeier H, Sassen R, et al. Rasmussen encephalitis: Incidence and course under randomized therapy with tacrolimus or intravenous immunoglobulins. Epilepsia 2013; 54:543–50

Boronat A, Sabater L, Saiz A, et al. GABA(B) receptor antibodies in limbic encephalitis and anti-GAD-assocaited neurologic disorders. Neurology 2011; 76(9):795-800

Boronat A, Gelfand JM, Gresa-Arribas N, et al. Encepahlitis and antibodies to dipeptidyl-peptidase-like protein-6, a subunit of Kv4.2 potassium channels. Ann Neurol 2013; 73(1): 120-128

Brusa R, Zimmermann F, Koh DS, et al. Early-onset epilepsy and postnatal lethality associated with an editing-deficient GluR-B allele in mice. Science 1995; 270:1677–1680

Buckley C. Autoimmune neurological diseases. Medicine 2008; 36(12): 653-657

Burke DS, Nisalak A. Detection of Japanese encephalitis virus immunoglobulin M antibodies in serum by antibody capture radioimmunoassay.J Clin Microbiol 1982; 15:353–361.

Burton AR, Vincent E, Arnold PY, et al. On the pathogenicity of autoantigen-specific T-cell receptors. Diabetes. 2008; 57:1321–1330.

Burton AR, Baquet Z, Eisenbarth GS, et al. Central nervous system destruction mediated by glutamic acid decarboxylase-specific CD4+ T cells. J. Immunol. 2010; 184:4863–4870

Carvajal-Gonzalez A, Leite MI, Water P, et al. Glycine receptor antibodies in PERM and related syndromes: characteristics, clinical features and outcomes. Brain 2014; 137(8): 2178-2192

Coesmans M, Smitt PA, Linden DJ, et al. Mechanisms underlying cerebellar motor deficits due to mGluR1-autoantibodies. Ann. Neurol 2003; 53:325–336

Cokić B. Stein V. Stargazin modulates AMPA receptor antagonism. Neuropharmacology. 2008; 54:1062–1070

Costa M, Saiz A, Casamitjana R, et al. T-cell reactivity to glutamic acid decarboxylase in stiff-man syndrome and cerebellar ataxia associated with polyendocrine autoimmunity. Clin Exp Immunol 2002; 129:471–478

Craig MT, Mayne EW, Bettler B, et al. Distinct roles of GABAB1a- and GABAB1b-containing GABAB receptors in spontaneous and evoked termination of persistent cortical activity. J Physiol 2013; 15(59):835-43

Dale RC, Irani SR, Brilot F, et al. N-methyl-D-aspartate receptor antibodies in pediatric dyskinetic encephalitis lethargica. Ann Neurol 2009;66(5):704-709

Dalmau J, Furneaux HM, Rosenblum MK, et al. Detection of the anti-Hu antibody in specific regions of the nervous system and tumour from patients with paraneoplastic encephalomyelitis/sensory neuronopathy. Neurology 1991; 41(11):1757-64

Dalmau J, Tuzun E, Wu H, et al. Paraneoplastic Anti-N-methyl-D-aspartate Receptor Encephalitis Associated with Ovarian Teratoma. Ann Neurol 2007; 61(1):25-36

Dalmau J, Rosenfeld MR. Paraneoplastic syndromes of the CNS. Lancet Neurol 2008; 7(4): 327-40.

Dalmau J, Gleichman AJ, Hughes EG, et al. Anti-NMDA receptor encephalitis: case series and analysis of the effects of antibodies. Lancet Neurol 2008; 7(12) :1091-1098

Díaz E. Regulation of AMPA receptors by transmembrane accessory proteins. Eur J Neurosci. 2010; 32:261–268.

Drachman DB, Angus CW, Adams RN, et al. Myasthenic antibodies cross-link acetylcholine receptors to accelerate degradation. N Engl J Med 1978; 298(20):1116-1122

Elbers JM, Bitnun A, Richardson SE, et al. A 12-year prospective study of childhood herpes simplex encephalitis: is there a broader spectrum of disease? Pediatrics 2007; 119:399–407

Engel A, Lambert E, Howard F. Immune complexes (IgG and C3) at the motor end-plate in myasthenia gravis: ultrastructural and light microscopic localisation and electrophysiologic correlations. Mayo Clin Proc 1977; 52(5):267-80

Faas GC, Adwanikar H, Gereau RW. Modulation of presynaptic calcium transients by metabotropic glutamate receptor activation: a differential role in acute depression of synaptic transmission and long-term depression. J Neurosci 2002; 22:6885–6890

Fambrough DM, Drachman DB, Satyamurti S, et al. Neuromuscular Junction in Myasthenia Gravis: Decreased Acetylcholine Receptors. Science 1973; 182(4109):293-295

Farrell MA, Droogan O, Secor DL, et al. Chronic encephalitis associated with epilepsy: immunohistochemical and ultrastructural studies. Acta Neuropathol Berl 1995; 89: 313–21

Frank MM. Complement disorders and hereditary angioedema. J Allergy Clin Immunol 2010;125(2 Suppl 2):S262-271

Frassoni C, Spreafico R, Franceschetti S, et al. Labeling of rat neurons by anti-GluR3 IgG from patients with Rasmussen's encephalitis. Neurology 2001;57:324–327

Fukata Y, et al. (2010) Disruption of LGI1-linked synaptic complex causes abnormal synaptic transmission and epilepsy. Proc. Natl Acad. Sci. USA.;107:3799–3804

Fukuda T, Motomura M, Nakao Y, et al. Reduction of P/Q-type calcium channels in the postmortem cerebellum of paraneoplastic cerebellar degeneration with Lambert–Eaton myasthenic syndrome. Ann. Neurol 2003 ;53:21–28

Fukuda Y, Yotsuyanagi H, Ooka S, et al. Identification of a new autoantibody in patients with chronic hepatitis. Hum. Immunol 2004;65,1530– 1538

Fukunaga H, Engel AG, Lang B, et al. Passive transfer of lambert-eaton myasthenic syndrome with igg from man to mouse depletes the presynaptic membrane active zones. Proc Natl Acad Sci USA 1983;80(24):7636-7640

Gable MS, Gavali S, Radner A, et al. Anti-NMDA receptor encephalitis: report of ten cases and comparison with viral encephalitis. Eur J Clin Microbiol Infect Dis 2009; 28:1421–1429

Gahring LC, Rogers SW. Autoimmunity to Glutamate Receptors in Rasmussen's Encephalitis: A Rare Finding or The Tip of an Iceberg? The Neuroscientist 1998; 4:373

Gahring LC, Carlson NG, Meyer EL,et al. Cutting edge: Granzyme B proteolysis of a neuronal glutamate receptor generates an autoantigen and is modulated by glycosylation. J Immunol 2001; 166:1433–8

Geis C, Weishaupt A, Hallermann S, et al. Stiff person syndrome-associated autoantibodies to amphiphysin mediate reduced GABAergic inhibition. Brain 2010; 133(11):3166-80

Ghoshal A, Das S, Ghosh S, et al. Proinflammatory mediators released by activated microglia induces neuronal death in Japanese encephalitis. Glia 2007; 55: 483–496.

Giometto B, Marchiori GC, Nicolao P, et al. Sub acute cerebellar degeneration with anti Yo autoantibodies: immunohistochemical analysis of the immune reaction in the central nervous syste. Neuropathol Appl Neurobiol 1997; 23(6):468-74

Glaser CA, Honarmand S, Anderson LJ, et al. Beyond viruses: clinical profiles and etiologies associated with encephalitis. Clin Infect Dis 2006; 43:1565– 1577

Gleichman AJ, Spruce LA, Dalmau J, et al. Anti-NMDA Receptor Encephalitis Antibody Binding Is Dependent on Amino Acid Identity of a Small Region within the GluN1 Amino Terminal Domain. J Neurosci 2012; 32(32):11082-11094

Gleichman AJ, Panzer JA, Baumann BH, et al. Antigenic and mechanistic characterization of anti-AMPA receptor encephalitis. Annals of Clinical and Translational Neurology 2014; 1(3): 180-189

Gonzalez MI. The possible role of GABAA receptors and gephyrin in epileptogenesis. Front Cell Neurosci 2013; 7:1–7

Granerod J. The epidemiology of acute encephalitis. Neuropsychol Rehabil 2007; 17(4-5): 406-428

Granerod J, Ambrose HE, Davies NW, et al. Causes of encephalitis and differences in their clinical presentations in England: a multicentre, population-based prospective study. Lancet Infect Dis 2010; 10:835–844.

Graus F, Illa I, Agusti M, et al. Effect of intraventricular injection of an anti-Purkinje cell antibody (anti-Yo) in a guinea pig model. J Neurol Sci 1991;106(1):82-7.

Graus F, Boronat A, Xifró X. et al. The expanding clinical profile of anti-AMPA receptor encephalitis. Neurology 2010; 74(10):857-859

Gregor A, Albrecht B, Bader I, et al. Expanding the clinical spectrum associated with defects in CNTNAP2 and NRXN1. BMC Med. Genet 2011;12:106

Greiner H, Leach JL, Lee KH, Krueger DA. Anti-NMDA receptor encephalitis presenting with imaging fi ndings and clinical features mimicking Rasmussen syndrome. Seizure 2011; 20:266–70.

Gresa-Arribas N, Titulaer MJ, Torrents A, et al. Antibody titres at diagnosis and during follow-up of anti-NMDA receptor encephalitis: a retrospective study. Lancet Neurol 2014;13:167-77

Gronseth GS, Barohn RJ. Practice parameter: thymectomy for autoimmune myasthenia gravis (an evidence-based review): report of the quality standards subcommittee of the american academy of neurology. Neurology 2001; 55(1):7-15.

Hacohen Y, Deiva K, Pettingill P, et al. N-Methyl-D-Aspartate Receptor Antibodies in Post-Herpes Simplex Virus Encephalitis Neurological Relapse. Movement Disorders 2013; 29(1): 90-96.

Hollmann M, Heinemann S. Cloned glutamate receptors. Annu. Rev. Neurosci 1994;17 31–108

Höftberger R, Titulaer MJ, Sabater L, et al. Encephalitis and GABAB receptor antibodies: novel findings in a new case series of 20 patients. Neurology 2013; 81(17):1500-6

Hughes EG, Peng X, Gleichman AJ, et al. Cellular and Synaptic Mechanisms of Anti-NMDA Receptor Encephalitis. J Neurosci 2010; 30(17):5866-75.

Illa I. IVIg in myasthenia gravis, Lambert Eaton myasthenic syndrome and inflammatory myopathies: current status. J Neurol 2005; 252 Suppl 1:I14-8

Irani S, Lang B. Autoantibody-mediated disorders of the central nervous system. Autoimmunity 2008;41(1):55-65

Irani SR, Alexander S, Waters P, et al. Antibodies to Kv1 potasssium channel-complex proteins leucine-rich, glioma inactivated 1 protein and contactin-associated protein-2 in limbic encephalitis, Morvan's syndrome and acquired neuromyotonia. Brain 2010a;133:2734-2748

Irani SR, Bera K, Waters P, et al. N-methyl-D-aspartate antibody encephalitis: temporal progression of clinical and paraclinical observations in a predominantly non-paraneoplastic disorder of both sexes. Brain 2010b; 133:1655-1667

Irani SR, Michell A, Lang B, et al. Faciobrachial dystonic seizures precede Lgi1 antibody limbic encephalitis. Ann Neurol 2011;69(5):892-900

Irani SR, Pettingill P, Kleopa KA, et al. Morvan syndrome: Clinical and serological observations in 29 cases. Ann Neurol 2012; 72(2):241-255.

Jeffery OJ, Lennon VA, Pittock SJ, et al. $GABA_B$ receptor autoantibody frequency in service serological evaluation. Neurology 2013; 81:882-887

Kaulin YA, De Santiago-Castillo JA, Rocha CA, et al. The dipeptidyl-peptidase-like protein DPP6 determines the unitary conductance of neuronal Kv4.2 channels. J Neurosci 2009; 29:3242-3251

Kaupmann K, Schuler V, Mosbacher J, et al. Human gamma-aminobutyric acid type B receptors are differentially expressed and regulate inwardly rectifying K+ channels. Proc. Natl. Acad. Sci. 1998; 95:14991-14996

Kaur R, Vrati S. Development of a recombinant vaccine against Japanese encephalitis. J Neurovirol 2003; 9:421–431.

Kivity S, Agmon-Levin N, Blank M, et al. Infections and autoimmunity- friends or foes? Trends in Immunology 2009; 30(8): 409-414

Koneczny I, Cossins J, Waters P, et al. MuSK Myasthenia Gravis IgG4 Disrupts the Interaction of LRP4 with MuSK but Both IgG4 and IgG1-3 Can Disperse Preformed Agrin-Independent AChR Clusters. PLoS ONE 2013; 8(11): e80695

Lai M, Hughes EG, Peng X, et al. AMPA receptor antibodies in limbic encephalitis alter synaptic receptor location. Ann Neurol 2009; 65(4):424-434

Lai M, Huijbers MG, Lancaster E, et al. Investigation of LGI1 as the antigen in limbic encephalitis previously attributed to potassium channels: a case series. Lancet Neurol 2010; 9:776–785

Lalic T, Pettingill P, Vincent A, et al. Human limbic encephalitis serum enhances hippocampal mossy fiber-CA3 pyramidal cell synaptic transmission. Epilepsia 2011; 52(1):121-31

Lamb K, Scott WJ, Mensah A, et al. Prevalence and clinical outcome of Rasmussen encephalitis in children from the United Kingdom. Dev Med Child Neurol 2013; 55 (suppl 1): 14

Lambert EH, Eaton LM, Rooke ED. Defect of neuromuscular conduction associated with malignant neoplasms. Am J Physiol 1956;187: 612–13

Lancaster E, Lai M, Peng X, et al. Antibodies to the $GABA_B$ receptor in limbic encephalitis with seizures: case series and characterisation of the antigen. Lancet Neurol 2010; 9:67-76

Lancaster E, Maartje GM, Vered B, et al. Investigations of Caspr2, an autoantigen of encephalitis and neuromyotonia. Ann. Neurol 2011a; 69:303–311

Lancaster E, Martinez-Hernandez E, Titulaer MJ, et al. Antibodies to metabotropic glutamate receptor 5 in the Ophelia syndrome. Neurology 2011; 77:1698–1701

Lancaster E, Dalmau J. Neuronal autoantigens—pathogenesis, associated disorders and antibody testing. Nat Rev Neurol 2012c; 8(7):380-90

Lang B, Molenaar PC, Newsom-Davis J, et al. Passive transfer of lambert-eaton myasthenic syndrome in mice: decreased rates of resting and evoked release of acetylcholine from skeletal muscle. J Neurochem, 1984; 42(3):658-662.

Lang B, Ashwin P, Giovannini F, et al. Pathogenic Autoantibodies in Lambert-Eaton Myasthenic Syndrome. Annals 2003; 998:187-195

Leite MI, Jacob S, Viegas S, et al. IgG1 antibodies to acetylcholine receptors in 'seronegative' myasthenia gravis. Brain 2008; 131(7):1940-52

Lennon VA, Kryzer TJ, Griesmann GE, et al. Calcium-channel antibodies in the Lambert-Eaton syndrome and other paraneoplastic syndromes. N Engl J Med 1995; 332: 1467–74

Li Y, Uccelli A, Laxer KD, et al.Local-clonal expansion of infiltrating T lymphocytes in chronic encephalitis of Rasmussen. J Immunol 1997; 158:1428–37

Lin YL, Huang YL, Ma SH, et al. Inhibition of Japanese encephalitis virus infection by nitric oxide: antiviral effect of nitric oxide on RNA virus replication. J Virol 1997; 71: 5227–5235

Lindstrom JM, Lennon VA, Seybold ME, et al. Experimental autoimmune myasthenia gravis and myasthenia gravis: biochemical and immunochemical aspects. Ann N Y Acad Sci 1976; 274:254-74

Littleton E, Dreger M, Palace J, et al. Immunocapture and Identification of Cell Membrane Protein Antigenic Targets of Serum Autoantibodies. Mol Cell Proteomics 2009; 8(7):1688-1696

Mackay G, Ahmad K, Stone J, et al. NMDA receptor autoantibodies in sporadic Creutzfeldt-Jakob disease. J Neurol. 2012; 259(9):1979-81

Maddison P, Newsom-Davis J, Mills KR, et al. Favourable prognosis in lambert-eaton myasthenic syndrome and small-cell lung carcinoma. Lancet 1999; 353(9147):117-118

Major G, Tank D. Persistent neural activity: prevalence and mechanisms. Curr Opin Neurobiol 2004; 14:675– 684

Malitschek B, Schweizer C, Keir M, et al. The N-terminal domain of gamma-aminobutyric acid-B receptors is sufficient to specify agonist and antagonist binding. Mol Pharmacol 1999; 56: 448–454

Mann EO, Kohl MM, Paulsen O. Distinct roles of GABA(A) and GABA(B) receptors in balancing and terminating persistent cortical activity. J Neurosci 2009; 29:7513–7518

Mantegazza R, Bernaconi P, Baggi F, et al. Antibodies against GluR3 peptides are no specific for Rasmussen's encephalitis but are also present in epilepsy patients with severe, early onset disease and intractable seizures. J Neuroimmunol 2012; 131(1-2):179-85

Marignier R, Chenevier F, Rogemond V, et al. Metabotropic glutamate receptor type 1 autoantibody-associated cerebellitis: a primary autoimmune disease? Arch. Neurol 2010; 67:627–630

Martinez-Hernandez E, Horvath J, Shiloh-Malawsky Y, et al. Analysis of complement and plasma cells in the brain of patients with anti-NMDAR encephalitis. Neurology 2011;77(6):589-93

Massimini, M. Huber, R. Ferrarelli, F. et al. The Sleep Slow Oscillation as a traveling Wave. J Neurosci 2004;24(31):6862-6870

McNamara RK, Skelton RW. Baclofen, a selective GABAB receptor agonist, dose-dependently impairs spatial learning in rats. Pharmacol Biochem Behav 1996;53:303–08

Mishra MK, Kumawat KL, Basu A. Japanese encephalitis virus differentially modulates the induction of multiple pro-inflammatory mediators
in human astrocytoma and astroglioma cell-lines. Cell Biol Int 2008;32:1506–1513

Mikasova L, De Rossi P, Bouchet D. et al. Disrupted surface cross-talk between NMDA and Ephrin-B2 receptors in anti-NMDA encephalitis. Brain 2012;135(5):1606-21.

Mohammad SS, Sinclair K, Pillai S, Herpes simplex encephalitis relapse with chorea is associated with autoantibodies to N-Methyl-D-aspartate receptor or dopamine-2 recepor. Mov Disorder 2014; 29:117-122

Motomura M, Lang B, Johnston I, et al. Incidence of serum anti-P/Q-type and anti-N-type calsium channel autoantibodies in the Lambert-Eaton myasthenic syndrome. Jounral of Neurological Sciences 1997;147:35-42

Mott DD, Bragdon AC, Lewis DV, et al. Baclofen has a proepileptic effect in the rat dentate gyrus. J. Pharmacol. Exp. Ther 1989; 249:721-725

Murinson BB, Guarnaccia JB. Stiff-person syndrome with amphiphysin antibodies. Neurology 2008; 71(24):1955-1958

Nakao YK, Motomura M, Fukudome T, et al. Seronegative Lambert-Eaton myasthenic syndrome: study of 110 Japanese patients. Neurology 2002; 59(11):1773-1775

Newsom-Davis J, Mills KR. Immunological associations of acquired neuromyotonia (Isaacs' syndrome). Report of five cases and literature review. Brain 1993; 116 (2):453-69

Nutt SL, Kamboj RK. Differential RNA editing efficiency of AMPA receptor GluR-2 in human brain. Neuroreport 1994; 5:1679–1683

Oguni H, Andermann F, Rasmussen TB. The natural history of the syndrome of chronic encephalitis and epilepsy: a study of the MNI series of forty-eight cases. In: Andermann F, ed. Chronic encephalitis and epilepsy–Rasmussen's syndrome. Boston: Butterworth-Heinemann, 1991:7–35

Ohkawa T, Fukata Y, Yamasaki M. Autoantibodies to Epilepsy-Related LGI1 in Limbic Encephalitis Neutralize LGI1-ADAM22 Interaction and Reduce Synaptic AMPA Receptors. J Neurosci 2013; 33(46):18161-18174

Onugoren, MD. Rauschka, H. Bien, CG. Conjoint occurrence of GABA-B receptor antibodies in Lambert Eaton myasthenic syndrome with antibodies to the voltage gated calcium channel. J Neuroimmunol 2014;15;273(1-2):115-6

O'Neill JH, Murray NMF, Newsom-Davis J. The Lambert-Eaton Myasthenic Syndrome - A Review of 50 Cases. Brain 1988;111:577-596

Ottman R, Rosenberger L, Bagic A, et al. Altered language processing in autosomal dominant partial epilepsy with auditory features. Mol Cell Neurosci 2008; 42(4):448-57

Pardo CA, Vining EP, Guo L, et al. The pathology of Rasmussen syndrome: stages of cortical involvement and neuropathological studies in 45 hemispherectomies. Epilepsia 2004; 45: 516–26

Patrick J, Lindstrom J, Culp B. et al. Studies on Purified Eel Acetylcholine Receptor and Anti-Acetylcholine Receptor Antibody. Proc Natl Acad Sci U S A 1973; 70(12):3334-3338

Peng PL, Zhong X, Tu W, et al. ADAR2-dependent RNA editing of AMPA receptor sub-unit GluR2 determines vulnerability of neurons in forebrain ischemia. Neuron 2006 ;49:719–733

Petit-Pedrol M, Armangue T, Peng X, et al. Encephalitis with refractory seizures, status epilepticus, and antibodies to the $GABA_A$ receptor: a case series, characterisation of the antigen, and analysis of the effects of antibodies. Lancet Neurol 2014; 13(3):276-286

Pettigrew HD, Teuber SS, Gershwin ME. Clinical significance of complement deficiencies. Ann. NY Acad. Sci 2009; 1173:108–123

Piletz JE, Halaris A, Ernsberger PR. Psychopharmacology of imidazoline and alpha 2-adrenergic receptors: implications for drepression. Crit Rev Neurobiol 1994; 9(1):29-66.

Pinto A, Iwasa K, Newland C, et al. The action of Lambert–Eaton myasthenic syndrome immunoglobulin G on cloned human voltage-gated calcium channels. Muscle Nerve 2002; 25:715–724

Pittock SJ, Lucchinetti CF, Parisi JE, et al. Amphiphysin autoimmunity: paraneoplastic accompaniments. Ann. Neurol. 2005; 58:96–107

Poliak S, Salomon D, Elhanany H, et al. Juxtaparanodal clustering of Shaker-like K+ channels in myelinated axons depends on Caspr2 and TAG-1. J Cell Biol 2003; 162(6):1149-60

Pradhan S, Gupta RK, Singh MB, et al. Biphasic illness pattern due to early relapse in Japanese-B virus encephalitis. J Neurol Sci 2001; 183:13-18

Prosser, HM. Gill, CH. Hirst, WD. et al. Epileptogenesis and Enhanced Prepulse Inhibition in $GABA_{B1}$- Deficient Mice. Molecular and Cellular Neuroscience 2001; 17:1059-1070

Prüss H, Dalmau J, Harms L, et al. Retrospective analysis of NMDA receptor antibodies in encephalitis of unknown origin. Neurology 2010; 75(19):1735-1739

Rajasekaran K, Todorovic M, Kapur J. Calcium-permeable AMPA receptors are expressed in a rodent model of status epilepticus. Ann Neurol 2012; 72(1):91-102

Raschilas F, Wolff M, Delatou F. Outcome of an prognostic factors for herpes simplex encephalitis in adult patients:results of a multicenter study. Clin. Infect Dis 2002; 35(3):254-60

Rasmussen T, Olszewski J, Lloyd-Smith D. Focal Seizures due to chronic localizaed encephalitis. Neurology 1958; 8:435-445

Ratelade J, Bennet JL, Verkman AS. Evidence against cellular internalisation in vivo of NMO-IgG, aquaporin-4, and excitatory amino acid transporter 2 in neuromyelitis optica. J Biol Chem 2011; 286(25):45156-45164

Ravi V, Desai A, Balaji M, Apte MP, et al. Development and evaluation of a rapid IgM capture ELISA (JEV-Chex) for the diagnosis of Japanese encephalitis. J Clin Virol 2006; 35:429–434

Renaud J, Kerjan G, Sumita I, et al. Plexin-A2 and its ligand, Sema6A, control nucleus-centrosome coupling in migrating granule cells. Nature Neurosciences 2008;11:440 – 449

Ricklin D, Hajishengallis G, Yang K, et al. Complement:a key system for immune surveillance and homeostasis. Nature Immunology 2010; 11(9): 785-797

Riemersma S, Vincent A, Beeson D. et al. Association of arthrogryposis multiplex congenita with maternal antibodies inhibiting fetal acetylcholine receptor function. Journal of Clinical Investigation 1996; 98(10):2358-2363

Rogers SW, Andrews PI, Gahring LC, et al. Autoantibodies to glutamate receptor GluR3 in Rasmussen's encephalitis. Science 1994; 265:648-651

Rose NR, Bona C. Defining criteria for autoimmune diseases (Witebsky's postulates revisited). Immunol Today 1993; 4(9):426-30

Sanderson DJ, Hindley E, Smeaton E, et al. Deletion of the GluA1 AMPA receptor subunit impairs recency-dependent object recognition memory. Neuropsychologia 2010; 48(8):2302-2315

Sakussolia CL, Gan Q, Kazi R, et al. A Eukaryotic Specific Transmembrane Segment is Required for Tetramerization in AMPA Receptors. J Neurosci 2013;33(23):9840 –9845

Shillito P, Molenaar PC, Vincent A, et al. Acquired neuromyotonia: Evidence for autoantibodies directed against Kfl channels of peripheral nerves. Ann Neurol 1995; 38:701–702

Schroeder HW, Cavancini L. Structure and function of immunoglobulins. J Alergyl Clin Immunol 2010; 125(2):S41-S52

Schuler V, Luscher C, Blanchet C, et al. Epilepsy, Hyperalgesia, Impaired Memory, and Loss of Pre and Postsynaptic $GABA_B$ Responses in Mice Lacking $GABA_{B(1)}$. Neuron 2001; 31:47-58

Schwab N, Bien CG, Waschbisch A, et al. CD8+ T cell clones dominate brain infiltrates in Rasmussen encephalitis and persist in the periphery. Brain 2009; 132: 1236–46

Shepherd JD, Huganir RL. The cell biology of synapticplasticity: AMPA receptor trafficking. Annu Rev Cell Dev Biol 2007; 23:613– 643

Shigemoto K, Kubo S, Jie C, et al. Myasthenia gravis experimentally induced with muscle-specific kinase. AnnN Y Acad Sci, 2008; 1132:93-98

Shillito P, Molenaar PC, Vincent A, et al. Acquired neuromyotonia: evidence for autoantibodies directed against k+ channels of peripheral nerves. Ann Neurol, 1995; 38(5):714-722

Sinha S, Newsom-Davis J, Mills K, et al. Autoimmune aetiology for acquired neuromyotonia (Isaacs' syndrome). Lancet 1991; 338(8759):75-7

Smitt PS, Kinoshita A, Leeuw BD, et al. Paraneoplastic cerebellar ataxia due to autoantibodies against a glutamate receptor. N. Engl. J. Med 2000;342:21–27

Sobolevsky A, Rosconi M, Gouaux E. X-ray structure, symmetry and mechanism of an AMPA-subtype glutamate receptor. Nature 2009;462:745–756.

Solomon T, Kneen R, Dung NM, Khanh VC, Thuy TT, et al. Poliomyelitis-like illness due to Japanese encephalitis virus. Lancet 1998; 351:1094–1097.

Solomon T, Dung NM, Kneen R, et al. Japanese encephalitis. J Neurol Neurosurg Psychiatry 2000; 68: 405–415

Sommer B, Keiniinen K, Verdoom TA, et al. Flip and flop: a cell-specific functional switch in glutamate-operated channels of the CNS. Science 1990; 249:158G-85

Sprengel R. Role of AMPA receptors in synaptic plasticity. Cell Tissue Res 2006; 326:447– 455

Suzuki N, Fukushi M, Kosak K, et al. Teneurin-4 is a novel regulator of oligodendrocyte differentiation and myselination of small-diameter axons in the CNS. J Neurosci 2012;32(34):11586-99

Suzuki N, Numakawa T, Chou J, et al. Teneurin-4 promoted cellular protrusion formation and neurite outgrowth through focal adhesion kinase signaling. FASEB J 2013; 28(3):1386-97

Swarup V, Ghosh J, Das S, et al. Tumour necrosis factor receptor associated death domain mediated neuronal death contributes to the glial activation and subsequent neuroinflammation in Japanese encephalitis. Neurochem Int 2008; 52: 1310–1321

Tanaka K, Tanaka M, Onodera O, et al. Passive transfer and active immunisation with the recombinant leucine-zipper (Yo) protein as an attempt to establish an animal model of paraneoplastic cerebellar degeneration. J Neurol Sci. 1994; 127(2):153-158

Tanaka M, Tanaka K, Onodera O, et al. Trial to establish an animal model of paraneoplastic cerebellar degeneration with anti-Yo antibody. 1. Mouse strains bearing different MHC molecules produce antibodies on immunisation with recombinant Yo protein, but do not cause Purkinje cell loss. Clin Neurol Neurosurg 1995; 97(1):101-105

Tanaka K, Tanaka M, Igarashi S, et al. Trial to establish an animal model of paraneoplastic cerebellar degeneration with anti-Yo antibody. 2. Passive transfer of murine mononuclear cells activated with recombinant Yo protein to paraneoplastic cerebellar degeneration lymphoctyes in severe combined immunodeficiency mice. Clin Neurol Neurosurg. 1995; 97(1):101-5

Tanaka Y, Nakamura M, Matsui T, et al Proteomic surveillance of autoantigens in relapsing polychondritis. Microbiol. Immunol 2006; 50:117– 126

Tao MH, Smith RI, Morrison SL. Structural features of human immunoglobulin G that determine isotype- specific differences in complement activation. J Exp Med 1993; 178(2):661-667

Timofeev I, Grenier F, Bazhenov M, et al. Origin of slow cortical oscillations in deafferented cortical slabs. Cereb Cortex 2000; 10:1185–1199

Titulaer MJ, Maddison P, Sont JK, et al. Clinical Dutch-English Lambert-Eaton myasthenic syndrome (LEMS) tumour association prediction score accurately predicts small-cell lung cancer in the LEMS. J Clin Oncol 2011; 29:902–08

Titulaer MJ, McCracken L, Gabilondo I, et al. Treatment and prognostic factors for long-term outcome in patients with anti-NMDA receptor encephalitis: an observational cohort study. Lancet Neurol 2013; 12:157-165

Tobias SM, Robitaille Y, Hickey WF, et al. Bilateral Rasmussen encephalitis: postmortem documentation in a five-year-old. Epilepsia 2003; 44:127–30

Toyka KV, Drachman DB, Pestronk A, et al. Myasthenia gravis: passive transfer from man to mouse. Science 1975;190(4212):397-399

Toyka KV, Drachman DB, Grin DE, et al. Myasthenia gravis. study of humoral immune mechanisms by passive transfer to mice. N Engl J Med 1977; 296(3):125-131

Tuzun E, Zhou L, Baehring JM, et al. Evidence for antibody-mediated pathogenesis in anti-NMDAR encephalitis associated with ovarian teratoma. Acta Neuropathol 2009; 118:737–74

Twyman RE, Gahnng LC, Speiss J, et al. Glutamate receptor antibodies activate a subset of receptors and reveal an agonist binding site. Neuron 1995; 14:755-762

Varadkar S, Bien CG, Kruse CA, et al. Rasmussen's encephalitis: clinical features, pathobiology and treatment advances. Lancet Neurolo 2014;13:195-205.

Vincent A, Palace J, Hilton-Jones D. Myasthenia Gravis. The Lancet 2001; 357: 2122-2128

Vincent A, Buckley C, Schott JM, et al. Potassium channel antibody-associated encephalopathy: a potentially immunotherapy-responsive form of limbic encephalitis. Brain 2004; 127(3):701-712

Vincent A, Bien CG, Irani SR, et al. Autoantibodies associated with diseases of the CNS: new developments and future challenges. Lancet Neurol 2011; 10(8):759-72

Waldmeier PC, Wicki P, Feldtrauer JJ, et al. GABA and glutamate release affected by $GABA_B$ receptor antagonists with similar potency: no evidence for pharmacologically different presynaptic receptors. Br. J. Pharamcol 1994; 113:1515-1521

Wang X, Lambert NA. $GABA_B$ Receptors Couple to Potassium and Calcium Channels on Identified Lateral Perforant Pathway Projection Neurons. J Neurophysiol 2000; 83:1073-1078

Watson R, Jiang Y, Bermudez I, et al. Absence of antibodies to glutamate receptor type 3 (GluR3) in Rasmussen encephalitis. Neurology 2004; 63(43):43-50

Watson R, Jepson JE, Bermudez I, et al. Alpha7-acetylcholine receptor antibodies in two patients with Rasmussen encephalitis. Neurology 2005; 65:1802–04

Wenthold RJ, Petralia RS, Bla-hos JI, et al. Evidence for multiple AMPA receptor complexes in hippocampal CA1/CA2 neurons. J. Neurosci. 1996; 16:1982–1989

Wei YC, Liu CH, Lin JJ, et al. Rapid progression and brain atrophy in anti-AMPA receptor encephalitis. J Neuroimmunol 2013; 261:129–133

Whitley RJ, Alford CA, Hirsch MS et al. Vidarabine versus acyclovir therapy in herpes simplex encephalitis. N Engl J Med 1986; 314:144-149

Whitney KD, McNamara JO. GluR3 autoantibodies destroy neural cells in a complement-dependent manner modulated by complement regulatory proteins. J Neurosci 2000; 20:7307–7316

Wiendl HM, Bien CB, Bernasconi PP, et al. GluR3 antibodies: prevalence in focal epilepsy but no specificity for Rasmussen's encephalitis. Neurology 2001; 57:1511–14

Wirtz PW, Nijnuis MG, Sotodeh M, et al. The epidemiology of myasthenia gravis, Lambert-Eaton myasthenic syndrome and their associated tumours in the northern part of the province of South Holland. J Neurol 2003; 250:698–701

Witebsky E, Rose NR, Terplan K, et al. Chronic thyroiditis and autoimmunisation. J Am Med Assoc 1957; 164(13):1439-47

Yang R, Puranam RS, Butler LS, et al. Autoimmunity to munc-18 in Rasmussen's encephalitis. Neuron 2000; 28: 375–83

Zamanillo D, Sprengel R, Hvalby O, et al. Importance of AMPA receptors for hippocampal synaptic plasticity but not for spatial learning. Science 1999; 284(5421):1805-1811

Zhang Q, Tanaka K, Sun P, Nakata M, et al. Suppression of synaptic plasticity by cerebrospinal fluid from anti-NMDA receptor encephalitis patients. Neurobiol Dis 2012; 45(1):610-5.

Appendices:

Table 1: List of AMPAR and $GABA_BR$ constructs (cDNA and the vectors) used in the establishment of new CBAs

cDNA	Vector	Antibiotic resistance
GluA1	pTriEx-1	Ampicillin
GluA2	pcDNA-DEST40	Ampicillin
GluA3	pcDNA3.1	Ampicillin
$GABA_{B1}R$	pcDNA-DEST40	Ampicillin
$GABA_{B2}R$	pTriEx-1	Ampicillin

Table 2: List of primary antibodies used

Primary antibody	Raised in	Company	Intra/extracellular binding	Uses (dilution)
Anti-GluA1 ab1504	Rabbit	Millipore	Intracellular	WB (1:1000), ICC (1:250)
Anti-GluA1 AGC-004	Rabbit	Alomone	Extracellular	ICC (1:50)
Anti-GluA2 N-19	Goat	Santa Cruz	Extracellular	ICC (1:50)
Anti-GluA2/3 ab1506	Rabbit	Millipore	Intracellular	WB (1:1000), ICC (1:100)
Anti-GluA3 sc-7613	Rabbit	Santa Cruz	Extracellular	WB (1:100)
Anti-$GABA_{B1}R$ ab55051	Mouse	Abcam	Intracellular	WB (1:1000)
Anti-$GABA_{B2}R$ AB5394	Mouse	Millipore	Intracellular	WB (1:1000), ICC (1:100)
Anti NR1 mab363	Mouse	Millipore	Extracellular	WB (1:200)
Anti-CASPR2 ab33394	Rabbit	Abcam	Extracellular	WB (1:1000)
Anti actin A2066	Rabbit	Sigma	Intracellular	WB (1:5000)
Anti-transferrin receptor H68.4	Mouse	Sigma	Extracellular	WB (1:1000)
Anti-C3c A0062	Rabbit	Dako	-	ICC (1:200)

Table 3: List of secondary antibodies used

Secondary antibody	Raised in	Company	Fluorescence	Usage	Typical concentration
Anti-rabbit (P0448)	Goat	DAKO	None	WB	1:2000
Anti-mouse (P0161)	Rabbit	DAKO	None	WB	1:2000
Anti-rabbit IgG (A11008)	Goat	Invitrogen	488	ICC	1:750
Anti mouse (A11004)	Goat	Invitrogen	568	ICC	1:750
Anti-human (A21090)	Goat	Invitrogen	568	ICC	1:750
Anti-human (A11013)	Goat	Invitrogen	488	ICC	1:750
Anti-human IgG	Goat	Binding site	None	iP	1:10

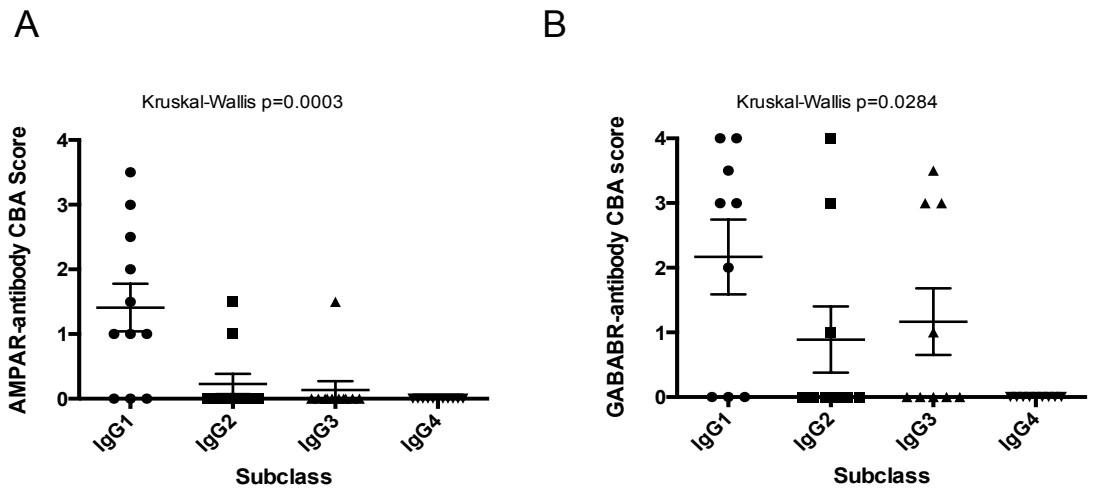

Figure 1: AMPAR and $GABA_BR$ antibody subclasses CBA scores

Serum samples were incubated on AMPAR transfected HEK cells (1:20) or $GABA_{B1+2}R$ transfected HEK cells (1:100). Mouse anti-IgG1-4 commercial antibodies (1:20) were incubated with the cells and binding was visualised using a goat anti-mouse IgG Alexa Fluor 568.
Patients had antibodies that were predominantly IgG1. CBA score >1 was used as a cutoff. Comparisons between subclasses were made using a one-way ANOVA. A). AMPAR antibodies (n=11) were predominantly IgG1. IgG1> IgG2, IgG3 & IgG4 ($p < 0.05$, $p<0.01$, $p<0.001$). B). $GABA_BR$ patients (n=9) are predominantly IgG1. IgG1> IgG4 ($p<0.05$). No statistical difference between IgG1, IgG2 and IgG3.

Table 4: Clinical summary of the CBA positive and CBA negative JEV samples

Patient (N)	Parkinsonian (Scores)	Extrapyramidal features (Score)	Behaviour abnormalities (Score)	Outcome
CBA positive (12)	55% (2.75)	82% (1.83)	63% (1.67)	66% (6/9)
CBA negative (32)	50% (2.75)	60% (1.88)	30% (2.658)	60% (16/27)

Patients were each given a value depending if they had the specific feature (Yes=1), did not have the feature (No=2), probably had the feature (Probable=3) or the status was unknown (Not Known=9). The mean score of each group was calculated. Differences between the two patient groups were not statistically significant (t-test, unpaired. Behaviour abnormalities p= 0.37).